frontiers | Research Topics

The cellular stress response and physiological adaptations of corals subjected to environmental stressors and pollutants, volume II

Edited by
Davide Seveso, Ranjeet Bhagooli and Craig Downs

Coordinated by
Yohan Dider Louis and Walter Dellisanti

Published in
Frontiers in Physiology
Frontiers in Marine Science

ISSN 1664-8714
ISBN 978-2-8325-5379-4
DOI 10.3389/978-2-8325-5379-4

About Frontiers

Frontiers is more than just an open access publisher of scholarly articles: it is a pioneering approach to the world of academia, radically improving the way scholarly research is managed. The grand vision of Frontiers is a world where all people have an equal opportunity to seek, share and generate knowledge. Frontiers provides immediate and permanent online open access to all its publications, but this alone is not enough to realize our grand goals.

Frontiers journal series

The Frontiers journal series is a multi-tier and interdisciplinary set of open-access, online journals, promising a paradigm shift from the current review, selection and dissemination processes in academic publishing. All Frontiers journals are driven by researchers for researchers; therefore, they constitute a service to the scholarly community. At the same time, the *Frontiers journal series* operates on a revolutionary invention, the tiered publishing system, initially addressing specific communities of scholars, and gradually climbing up to broader public understanding, thus serving the interests of the lay society, too.

Dedication to quality

Each Frontiers article is a landmark of the highest quality, thanks to genuinely collaborative interactions between authors and review editors, who include some of the world's best academicians. Research must be certified by peers before entering a stream of knowledge that may eventually reach the public - and shape society; therefore, Frontiers only applies the most rigorous and unbiased reviews. Frontiers revolutionizes research publishing by freely delivering the most outstanding research, evaluated with no bias from both the academic and social point of view. By applying the most advanced information technologies, Frontiers is catapulting scholarly publishing into a new generation.

What are Frontiers Research Topics?

Frontiers Research Topics are very popular trademarks of the *Frontiers journals series*: they are collections of at least ten articles, all centered on a particular subject. With their unique mix of varied contributions from Original Research to Review Articles, Frontiers Research Topics unify the most influential researchers, the latest key findings and historical advances in a hot research area.

Find out more on how to host your own Frontiers Research Topic or contribute to one as an author by contacting the Frontiers editorial office: frontiersin.org/about/contact

The cellular stress response and physiological adaptations of corals subjected to environmental stressors and pollutants, volume II

Topic editors
Davide Seveso — University of Milano-Bicocca, Italy
Ranjeet Bhagooli — University of Mauritius, Mauritius
Craig Downs — Haereticus Environmental Laboratory, United States

Topic coordinators
Yohan Dider Louis — University of Mauritius, Mauritius
Walter Dellisanti — University of Copenhagen, Denmark

Citation
Seveso, D., Bhagooli, R., Downs, C., Louis, Y. D., Dellisanti, W., eds. (2024). *The cellular stress response and physiological adaptations of corals subjected to environmental stressors and pollutants, volume II*. Lausanne: Frontiers Media SA. doi: 10.3389/978-2-8325-5379-4

Topic editor Craig Downs is the Co-Founder of MarineSafe and the Executive Director of the Haereticus Environmental Laboratory. All other Topic Editors declare no competing interests with regards to the Research Topic subject.

*We would like to acknowledge **Dr. Yohan Didier Louis** and **Dr. Walter Dellisanti** who acted as Topic Coordinators and contributed to the preparation of this Research Topic.*

Table of contents

frontiers | Frontiers in Physiology

TYPE Editorial
PUBLISHED 19 August 2024
DOI 10.3389/fphys.2024.1473792

OPEN ACCESS

EDITED AND REVIEWED BY
Pung Pung Hwang,
Academia Sinica, Taiwan

*CORRESPONDENCE
Davide Seveso,
davide.seveso@unimib.it

RECEIVED 31 July 2024
ACCEPTED 09 August 2024
PUBLISHED 19 August 2024

CITATION
Seveso D, Louis YD, Bhagooli R, Downs CA and Dellisanti W (2024) Editorial: The cellular stress response and physiological adaptations of corals subjected to environmental stressors and pollutants, volume II.
Front. Physiol. 15:1473792.
doi: 10.3389/fphys.2024.1473792

Editorial: The cellular stress response and physiological adaptations of corals subjected to environmental stressors and pollutants, volume II

Davide Seveso[1,2]*, Yohan D. Louis[1,2], Ranjeet Bhagooli[3,4,5,6,7], Craig A. Downs[8] and Walter Dellisanti[9]

[1]Department of Earth and Environmental Science, University of Milano Bicocca, Milano, Italy, [2]MaRHE Center (Marine Reseacrh and High Education Center), Magoodhoo, Faafu, Maldives, [3]Department of Biosciences and Ocean Studies, Faculty of Science and Pole of Research Excellence in Sustainable Marine Biodiversity, University of Mauritius, Réduit, Mauritius, [4]The Biodiversity and Environment Institute, Réduit, Mauritius, [5]Institute of Oceanography and Environment (INOS), University Malaysia Terengganu, Kuala Terengganu, Terengganu, Malaysia, [6]Department of Marine Science, Faculty of Fisheries and Marine Science, Diponegoro University, Semarang, Indonesia, [7]The Society of Biology (Mauritius), Réduit, Mauritius, [8]Haereticus Environmental Laboratory, Clifford, VA, United States, [9]Marine Biology Section, Department of Biology, University of Copenhagen, Helsingør, Denmark

KEYWORDS

cellular stress, corals, biomarkers, climate change, anthropogenic impact

Editorial on the Research Topic
The cellular stress response and physiological adaptations of corals subjected to environmental stressors and pollutants, volume II

There is substantial evidence that coral reefs are suffering worldwide due to global climate change, anthropogenic pressures, and local stressors, which led to their rapid decline over the last few decades with bleaching causing most of this loss (Hughes et al., 2017; Hughes et al., 2018). In order to more accurately predict the impacts of global changes and develop conservation and stress mitigation strategies, efforts have recently increased in elucidating the cellular and molecular mechanisms underlying coral bleaching and other coral responses to environmental stressors (Helgoe et al., 2024). As sessile and long-lived animals that experience variable conditions, corals rely mainly on their cellular stress responses for acclimatization and adaptation (Drury, 2020). Moreover, since changes at the cellular level are the first detectable responses to environmental perturbations, the analysis of cellular biomarkers represents a useful diagnostic tool reflecting variations in cellular integrity and pathways before larger-scale processes are affected (Downs, 2005; Louis et al., 2020; Montalbetti et al., 2021).

Although recent and substantial advances in omics technologies have made the study of coral molecular processes more efficient, rapid, and accessible (Weis, 2019; Cziesielski et al., 2020), our understanding of coral cell biology remains inadequate (Oakley and Davy, 2018; Weis, 2019). This Research Topic aimed to expand this knowledge and bridge existing gaps. The articles presented here demonstrate how various physiological and molecular approaches and techniques can be adopted to understand the responses of coral holobionts to a multitude of stressors.

Sea surface temperature increase and heat waves are the primary drivers of coral bleaching and reef degradation worldwide (Hughes et al., 2018; Eakin et al., 2019). Therefore, mesophotic habitats often represent potential refugia for corals (Bongaerts et al., 2010; Muir et al., 2017). In their study, Tavakoli-Kolour et al. analyzed the photosynthetic efficiency (maximum quantum yield at photosystem II) and the bleaching conditions, via symbiotic microalgal density and chlorophyll concentrations, of mesophotic and shallow coral species subjected to different temperature scenarios reproducing different Degree Heating Weeks (DHWs). Their results indicated that mesophotic corals have a threshold temperature slightly lower or equal to that of shallow corals, suggesting that, although they can survive thermal stress below 4 DHWs, mass bleaching can occur above this threshold. Coral reefs at relatively high latitudes could also be potential refuges for corals (Camp et al., 2018; Dellisanti et al., 2023). However, corals living in such habitat could suffer from low-temperature stress, inducing bleaching (Tracey et al., 2003; Marangoni et al., 2021). Wei et al. explore the response of *Porites lutea* from a high-latitude coral reef in the South China Sea under acute (1–2 weeks) and chronic (6–12 weeks) low-temperature stress, by analyzing maximum quantum yields and transcriptomic profiles. Low temperatures inhibited photosynthetic efficiency and reduced energy production and calcification by down-regulating sugar metabolism and calcification-related genes. However, this was particularly observed during a short acute treatment, suggesting a possible coral acclimation to chronic low temperature.

Although thermal stress is recognized as the main cause of coral bleaching, high solar irradiance can also play a central role in this process by exacerbating the production of reactive oxygen species (ROS) (Roth, 2014; Courtial et al., 2018). Shading-based management interventions could therefore reduce coral bleaching risk. Butcherine et al. examined the effectiveness of intermittent shade on two coral species held at either optimum or high temperatures. The analysis of coral health condition through the bleaching assessment (chlorophyll *a*, and symbiont density), the photochemistry, and the use of antioxidant enzymes (SOD and CAT) as cellular stress biomarkers, suggested that intermittently shading corals for 4 h can mitigate the impact of thermal stress.

However, even extremely low light levels, mainly related to high sedimentation rate and turbidity, can induce coral bleaching and negatively impact coral metabolism (DeSalvo et al., 2012; Bollati et al., 2021; Tuttle and Donahue, 2022). Using transcriptomics, Lock et al. identified gene expression patterns and molecular pathways that may allow the massive coral *Porites lobata* to tolerate and persist to chronic and severe sedimentation in the turbid Fouha Bay (Guam), providing important insights into coral metabolic plasticity and acclimation to this stressor. In particular, alternative energy generation pathways may help to counteract low light and oxygen levels, the upregulation of apoptosis genes may maintain colony integrity, and increased expression of cellular communication genes may help corals respond to sediment-associated pathogens.

Molecular biomarkers are also used as a proxy for water quality and anthropogenic pollution. Tisthammer et al. employed enzyme-linked immunosorbent assays to evaluate stress responses in *P. lobata* along an environmental gradient in Maunalua Bay (Hawaii), revealing distinct protein expression patterns, especially those of ubiquitin and Hsp70, which correlate with anthropogenic stressor levels across the bay. Nardi et al. analyzed the ecotoxicological response of the Mediterranean coral *Madracis pharensis* to polycyclic aromatic hydrocarbons (PAHs) bioaccumulated from chronic oil leakage from a shipwreck in Cyprus. The high ROS scavenging capacity and the low functionality of detoxification processes associated with the glutathione-S-transferase enzyme suggested that *M. pharensis* has the capability to develop cellular and physiological adaptations to chemical-mediated stress. Morgan et al. focused on the synergistic, antagonistic, or additive effect of oxybenzone BP-3, the active ingredient in sunscreen, and ocean acidification (OA), on the expression profiles of 22 genes of interest (GOIs) in sea the anemone *Exaiptasia diaphana*. The collective antagonistic responses of GOIs associated with collagen synthesis suggested their role as candidate biomarkers of stress, while GOIs with synergistic and additive responses, such as serotransferrin-like (TF) and monocarboxylate transporters (MCTs) genes, respectively, were also identified.

Finally, cellular stress mechanisms are also known to be involved in coral response to biotic interactions (Seveso et al., 2012; Seveso et al., 2017). For example, using gel-filtration chromatography and liquid chromatography-tandem mass spectrometry, Suzuki et al. identified and characterized red fluorescent proteins (RFPs) and chromoproteins (CPs) in inflammatory pink lesions of *Porites* colonies subjected to the pink pigmentation response (PPR). The results suggested a possible differential role of these proteins in coral immunity despite their coexistence. Additionally, CPs, which are specifically expressed in PPR lesions, may serve as an antioxidant protection, providing new insights into the role of CPs in the coral immune response.

Considering that understanding how corals can genetically or physiologically adapt to environmental changes has become a global research priority, we believe that this Research Topic provides a more comprehensive view of the cellular mechanisms involved. It may encourage future advancements in this field and support strategies and tools to potentially reduce or mitigate the impacts of cellular stress in corals.

Author contributions

DS: Writing–original draft. YL: Writing–review and editing. RB: Writing–review and editing. CD: Writing–review and editing. WD: Writing–review and editing.

Funding

The author(s) declare that no financial support was received for the research, authorship, and/or publication of this article.

Conflict of interest

The authors declare that the research was conducted in the absence of any commercial or financial relationships that could be construed as a potential conflict of interest.

Publisher's note

References

Bollati, E., Rosenberg, Y., Simon-Blecher, N., Tamir, R., Levy, O., and Huang, D. (2021). Untangling the molecular basis of coral response to sedimentation. *Mol. Ecol.* 2021, 884–901. doi:10.1111/mec.16263

Bongaerts, P., Ridgway, T., Sampayo, E. M., and Hoegh-Guldberg, O. (2010). Assessing the 'deep reef refugia' hypothesis: focus on Caribbean reefs. *Coral Reefs* 29, 309–327. doi:10.1007/s00338-009-0581-x

Camp, E. F., Schoepf, V., Mumby, P. J., Hardtke, L. A., Rodolfo-Metalpa, R., Smith, D. J., et al. (2018). The future of coral reefs subject to rapid climate change: lessons from natural extreme environments. *Front. Mar. Sci.* 5. doi:10.3389/fmars.2018.00004

Courtial, L., Planas Bielsa, V., Houlbreque, F., and Ferrier-Pagès, C. (2018). Effects of ultraviolet radiation and nutrient level on the physiological response and organic matter release of the scleractinian coral *Pocillopora damicornis* following thermal stress. *PLoS One* 13 (10), e0205261. doi:10.1371/journal.pone.0205261

Cziesielski, M. J., Schmidt-Roach, S., and Aranda, M. (2020). The past, present, and future of coral heat stress studies. *Ecol. Evol.* 9, 10055–10066. doi:10.1002/ece3.5576

Dellisanti, W., Chung, J. T., Yiu, S. K., Tsang, R. H. L., Ang, J. P., Yeung, Y. H., et al. (2023). Seasonal drivers of productivity and calcification in the coral *Platygyra carnosa* in a subtropical reef. *Front. Mar. Sci.* 10, 994591. doi:10.3389/fmars.2023.994591

DeSalvo, M. K., Estrada, A., Sunagawa, S., and Medina, S. M. (2012). Transcriptomic responses to darkness stress point to common coral bleaching mechanisms. *Coral Reefs* 31, 215–228. doi:10.1007/s00338-011-0833-4

Downs, C. A. (2005). "Cellular diagnostics and its application to aquatic and marine toxicology," in *Techniques in aquatic toxicology*. Editor G. K. Ostrander (Boca Raton: CRC Press), Vol. 2, 181–208. doi:10.1201/9780203501597.sec2

Drury, C. (2020). Resilience in reef-building corals: the ecological and evolutionary importance of the host response to thermal stress. *Mol. Ecol.* 29, 448–465. doi:10.1111/mec.15337

Eakin, C. M., Sweatman, H. P., and Brainard, R. E. (2019). The 2014–2017 global-scale coral bleaching event: insights and impacts. *Coral Reefs* 38 (4), 539–545. doi:10.1007/s00338-019-01844-2

Helgoe, J., Davy, S. K., Weis, V. M., and Rodriguez-Lanetty, M. (2024). Triggers, cascades, and endpoints: connecting the dots of coral bleaching mechanisms. *Biol. Rev.* 99, 715–752. doi:10.1111/brv.13042

Hughes, T. P., Kerry, J., Álvarez-Noriega, M., Álvarez-Romero, J. G., Anderson, K. D., Baird, A. H., et al. (2017). Global warming and recurrent mass bleaching of corals. *Nature* 543, 373–377. doi:10.1038/nature21707

Hughes, T. P., Anderson, K. D., Connolly, S. R., Heron, S. F., Kerry, J. T., Lough, J. M., et al. (2018). Spatial and temporal patterns of mass bleaching of corals in the Anthropocene. *Science* 359, 80–83. doi:10.1126/science.aan8048

Louis, Y. D., Bhagooli, R., Seveso, D., Maggioni, D., Galli, P., Vai, M., et al. (2020). Local acclimatisation-driven differential gene and protein expression patterns of Hsp70 in *Acropora muricata*: implications for coral tolerance to bleaching. *Mol. Ecol.* 29, 4382–4394. doi:10.1111/mec.15642

Marangoni, L., Rottier, C., and Ferrier-Pagès, C. (2021). Symbiont regulation in *Stylophora pistillata* during cold stress: an acclimation mechanism against oxidative stress and severe bleaching. *J. Exp. Biol.* 224, jeb235275. doi:10.1242/jeb.235275

Montalbetti, E., Biscéré, T., Ferrier-Pagès, C., Houlbrèque, F., Orlandi, I., Forcella, M., et al. (2021). Manganese benefits heat-stressed corals at the cellular level. *Front. Mar. Sci.* 8, 681119. doi:10.3389/fmars.2021.681119

Muir, P. R., Marshall, P. A., Abdulla, A., and Aguirre, J. D. (2017). Species identity and depth predict bleaching severity in reef-building corals: shall the deep inherit the reef? *Proc. R. Soc. B* 284, 20171551. doi:10.1098/rspb.2017.1551

Oakley, C. A., and Davy, S. K. (2018). "Cell biology of coral bleaching," in *Coral bleaching. Ecological studies (analysis and synthesis)*. Editors M. van Oppen and J. Lough (Cham: Springer), 233, 189–211. doi:10.1007/978-3-319-75393-5_8

Roth, M. S. (2014). The engine of the reef: photobiology of the coral-algal symbiosis. *Front. Microbiol.* 5, 422. doi:10.3389/fmicb.2014.00422

Seveso, D., Montano, S., Reggente, M. A. L., Maggioni, D., Orlandi, I., Galli, P., et al. (2017). The cellular stress response of the scleractinian coral *Goniopora columna* during the progression of the black band disease. *Cell Stress Chap* 22 (2), 225–236. doi:10.1007/s12192-016-0756-7

Seveso, D., Montano, S., Strona, G., Orlandi, I., Vai, M., and Galli, P. (2012). Up-regulation of Hsp60 in response to skeleton eroding band disease but not by algal overgrowth in the scleractinian coral *Acropora muricata*. *Mar. Environ. Res.* 78, 34–39. doi:10.1016/j.marenvres.2012.03.008

Tracey, S., William, C. D., and Ove, H.-G. (2003). Photosynthetic responses of the coral *Montipora digitata* to cold temperature stress. *Mar. Ecol. Prog. Ser.* 248, 85–97. doi:10.3354/meps248085

Tuttle, L. J., and Donahue, M. J. (2022). Effects of sediment exposure on corals: a systematic review of experimental studies. *Environ. Evid.* 11 (1), 4–33. doi:10.1186/s13750-022-00256-0

Weis, V. M. (2019). Cell biology of coral symbiosis: foundational study can inform solutions to the coral reef crisis. *Integr. Comp. Biol.* 59, 845–855. doi:10.1093/icb/icz067

frontiers | Frontiers in Marine Science

TYPE Original Research
PUBLISHED 14 September 2023
DOI 10.3389/fmars.2023.1210662

OPEN ACCESS

EDITED BY
Aldo Cróquer,
The Nature Conservancy
Dominican Republic

REVIEWED BY
Shashank Keshavmurthy,
Academia Sinica, Taiwan
Daniel J. Barshis,
Old Dominion University, United States

*CORRESPONDENCE
Saki Harii
sharii@lab.u-ryukyu.ac.jp

RECEIVED 23 April 2023
ACCEPTED 21 August 2023
PUBLISHED 14 September 2023

CITATION
Tavakoli-Kolour P, Sinniger F, Morita M, Nakamura T and Harii S (2023) Variability in thermal stress thresholds of corals across depths.
Front. Mar. Sci. 10:1210662.
doi: 10.3389/fmars.2023.1210662

Variability in thermal stress thresholds of corals across depths

Parviz Tavakoli-Kolour[1], Frederic Sinniger[2], Masaya Morita[2], Takashi Nakamura[1,2] and Saki Harii[2]*

[1]Graduate School of Engineering and Science, University of the Ryukyus, Okinawa, Japan, [2]Sesoko Station, Tropical Biosphere Research Center, University of the Ryukyus, Okinawa, Japan

Mesophotic habitats are potential refugia for corals in the context of climate change. The seawater temperature in a mesophotic habitat is generally lower than in a shallow habitat. However, the susceptibility and threshold temperatures of mesophotic corals are not well understood. We compared 11 mesophotic and shallow species to understand their thermal stress thresholds using physiological parameters. Coral fragments were exposed to two thermal stress treatments, with temperatures set at ~30°C and ~31°C, and a low-temperature treatment set at ~28°C as the "no stress" condition for 14 days. We found that the threshold temperature of coral species at mesophotic depths is slightly lower or equal to that of corals in shallow depths. The results suggest that species in the mesophotic coral ecosystems can survive low (<4 degree heating weeks) thermal stress. However, mass bleaching and high mortality can be expected when temperatures rise above 4 degree heating weeks.

KEYWORDS

mesophotic coral ecosystems (MCEs), stress response, resilience, threshold, temperatures, heat stress, bleaching

Introduction

Coral reefs are ecosystems threatened by anthropogenic activities and consequent extensive coral bleaching events (Hoegh-Guldberg et al., 2007; Spalding and Brown, 2015; Hughes et al., 2017). Shallow coral reefs are facing unprecedented bleaching events and subsequent degradation (Hughes et al., 2018b; Lough et al., 2018). The severity and frequency of the bleaching events may increase in the near future (McClanahan et al., 2015). Coral bleaching begins when a sea surface temperature anomaly exceeds 1°C above the maximum monthly mean recorded temperature (Glynn and D'Croz, 1990). The threshold temperature for coral bleaching substantially varies geographically based on the habitat temperature (Hughes et al., 2003; Jokiel, 2004; Hughes et al., 2017). The degree heating week (DHW) index is used to estimate the severity and duration of thermal stress (Kayanne, 2017; Skirving et al., 2020). DHWs indicate the accumulation of temperature anomalies exceeding the historical maximum monthly mean (MMM) temperature, and

bleaching potentially occurs at more than 4 DHWs (Liu et al., 2013; Kayanne, 2017). Temperature stress strongly influences the physiological function of reef-building corals (Hoadley et al., 2016), and consequently can affect the integrity of the ecosystem (Baker et al., 2008). However, numerous studies have confirmed that thermally variable environments have led to more thermally tolerant species/colonies than those inhabiting moderate habitats (Oliver and Palumbi, 2011; Mayfield et al., 2013; Klepac and Barshis, 2020).

In contrast to shallow reefs, mesophotic coral ecosystems (MCEs; coral reefs below 30 m depth) are subjected to lower light intensity, lower wave disturbance, and exhibit variable temperature regimes that can range from moderate (Lesser et al., 2009; Kahng et al., 2010) to extreme variations (Schramek et al., 2019; Wyatt et al., 2020; Pérez-Rosales et al., 2021; Wyatt et al., 2023). While seawater temperatures in MCEs are generally considered cooler compared to their shallower counterparts (Lesser et al., 2009; Shlesinger et al., 2018; Turner et al., 2019; Tavakoli-Kolour et al., 2023), the extent of this thermal variability raises questions about the thermal tolerance of corals inhabiting these ecosystems. MCEs are considered potential refugia for coral reefs (Riegl and Piller, 2003; Bongaerts et al., 2010; Muir et al., 2017), and may safeguard reef biodiversity and ecological function in the face of climate change in the near future. Therefore, the "deep reef refugia" hypothesis (DRRH) has been postulated (Glynn, 1996; Bongaerts et al., 2010). However, there is limited empirical data thus far to support the DRRH (Bongaerts and Smith, 2019). Studies investigating the effectiveness of the DRRH have found that it is only applicable in certain cases (Bongaerts et al., 2017; Frade et al., 2018). Furthermore, it is unclear whether MCEs serve as refugia for both shallow and mesophotic species or only for shallow species.

Stress responses, such as bleaching, differ among species (Bieri et al., 2016; Traylor-Knowles, 2019). The thermal tolerance threshold of coral species depends on the temperature regime of their habitat and their acclimation/adaptation (Logan et al., 2014; Kleypas et al., 2016). Therefore, given the variability of the thermal regime in mesophotic ecosystems, it is important to consider the implications for the thermal tolerance of corals in these ecosystems. While there is growing interest in the study of the thermal tolerance of mesophotic corals (Nir et al., 2014; Smith et al., 2016; Schramek et al., 2018; Skutnik et al., 2020; Gould et al., 2021; Pérez-Rosales et al., 2021; Godefroid et al., 2023; Wyatt et al., 2023), there is still a significant gap in knowledge pertaining to MCEs.

Elucidating the physiological functions that respond to environmental stress can help understand the tolerance and acclimatization levels of corals in the unique ecological settings of MCEs. Temperature is a factor that affects the physiological functions of corals (Hoadley et al., 2016). For example, responses to thermal stress, which are involved in bleaching, have been examined in terms of physiological aspects, such as symbiotic algal density, algal chlorophyll content, and maximum photosynthetic efficiency (Nielsen et al., 2018; Ben-Zvi et al., 2020). Furthermore, mortality after bleaching and the degree of bleaching have been examined (Pratchett et al., 2020). These stress responses occur in genera- and species-specific manner (Abrego et al., 2008; Diaz et al., 2016; Dias et al., 2019), and the susceptibility of corals to thermal stress has been considered as a critical factor affecting the community structure of coral reef ecosystems (Marshall and Baird, 2000; Dias et al., 2018). While some studies have compared the thermal tolerance of corals from different depths (Skutnik et al., 2020; Gould et al., 2021), our current knowledge remains limited, providing an incomplete understanding of the physiological function and thermal thresholds across a wide range of species, from shallow coral ecosystems to MCEs. Published studies have found contradicting patterns of lower thresholds versus equal or potentially higher thresholds in mesophotic corals compared to shallow water corals. Consequently, further investigation is necessary to compare the thermal thresholds and physiological responses between corals from mesophotic and shallow depths.

In this study, we aimed to examine the response of eleven coral species from both mesophotic and shallow depths to thermal stress in terms of survivorship, bleaching, and photosynthetic activity. Furthermore, we discuss the acclimatization potential of these species to global warming.

Materials and methods

Coral collection and experimental design

This study was performed on five coral species, including *Acropora valida*, *Galaxea fascicularis*, *Porites* sp., *Porites cylindrica*, and *Turbinaria mesenterina*, from shallow depth (5–7 m) and five species, including *Acropora* cf. *horrida*, *Galaxea* cf. *astreata*, *Porites* sp., *Seriatopora hystrix*, and *Leptoseris papyracea*, from upper mesophotic depth (40 m), with one species, *Pachyseris speciosa*, collected at both depths (Figure 1). Three healthy colonies with roughly equal-sized (approximately 20-25 cm^2) of each species were collected by SCUBA divers with hammer and chisel from shallow (26° 39' N, 127° 52' E) and mesophotic (26° 40' N 127° 51' E) depths north of Sesoko Island, Okinawa, Japan, in August 2018 and transferred to the Sesoko Station of the Tropical Biosphere Research Center of the University of the Ryukyus. The coral species were identified based on Wallace (1999) and Nishihira and Veron (1995). Twelve fragments of similar sizes were collected from each colony and mounted on plastic screws using super jelly glue. They were placed in seawater flow-through tanks at 28°C and maintained under experimental light conditions (as described below) for two weeks before starting the experiment to facilitate wound healing.

We exposed shallow and mesophotic fragments to different light and temperature conditions for two weeks. Light conditions were set based on the light (photosynthetically active radiation, PAR) measured at shallow and mesophotic site (Prasetia et al., 2016). Due to the limitation of LED lamps, data from cloudy day were used as a reference for shallow reef (5m depth). The fragments were placed under a 12:12-h light/dark cycle, in two different light conditions corresponding to their original depths. LED lights (AI Hydra FiftyTwo HD LED, Aqua Illumination, USA) were used with shallow light irradiance (~200 µmol m^{-2} s^{-1}) for the shallow coral fragments and mesophotic light irradiance (~25 µmol m^{-2} s^{-1}) for the mesophotic coral fragments. To achieve this intensity for the mesophotic depth, the lamp was set to 20% of its maximum capacity.

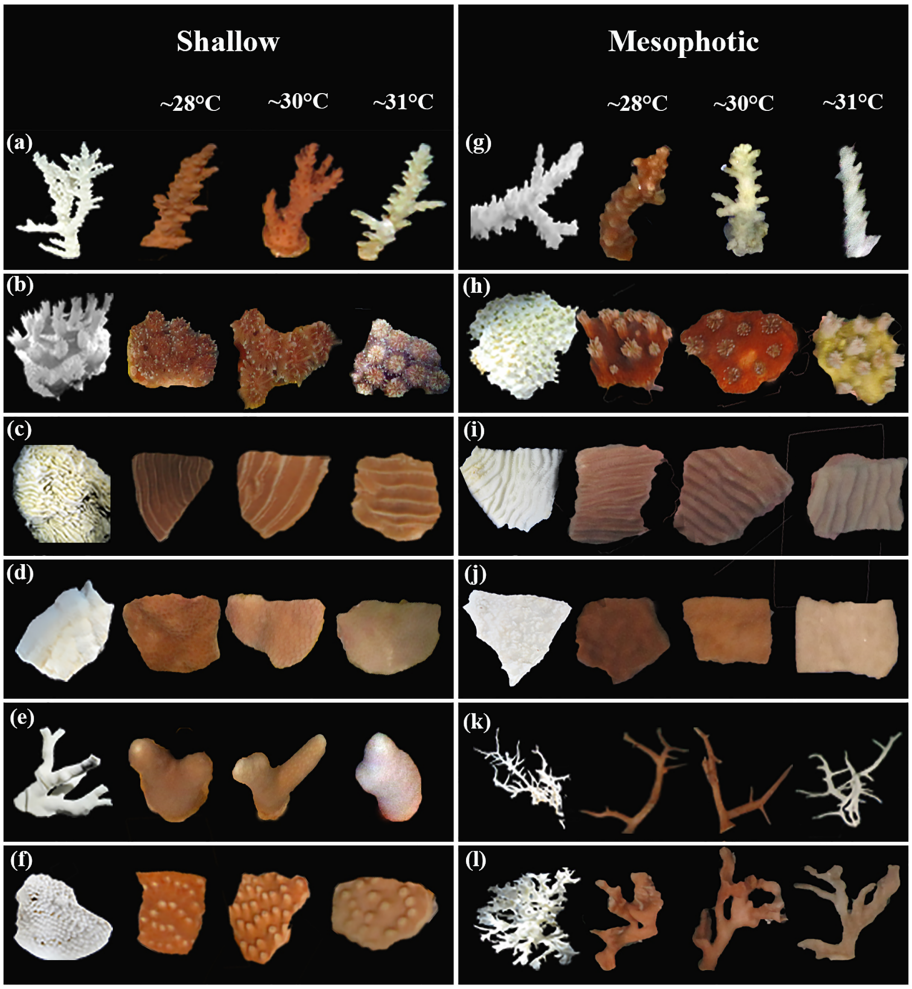

FIGURE 1
Images of 11 coral species fragments from shallow and mesophotic depths exposed to different temperature regimes to indicate interspecific responses of the species. The left column display the bleached skeleton of coral species. **(A)** *Acropora valida*; **(B)** *Galaxea fascicularis*; **(C)** *Pachyseris speciosa*; **(D)** *Porites* sp.; **(E)** *Porites cylindrica*; **(F)** *Turbinaria mesenterina*; **(G)** *Acropora* cf. *horrida*; **(H)** *Galaxea* cf. *astreata*; **(I)** *Pachyseris speciosa*; **(J)** *Porites* sp.; **(K)** *Seriatopora hystrix*; and **(L)** *Leptoseris papyracea*.

Three temperature treatments were designated based on the determination of maximum monthly mean (MMM) temperatures at different depths. Due to temperature anomalies and coral bleaching observed at shallow depths of the study sites during 2016 and 2017, MMM values for the shallow depths at the study sites were obtained from the National Oceanic and Atmospheric Administration (NOAA) Coral Reef Watch (CRW) satellite products for the Northern Ryukyus Island 5 km Regional Virtual Station (Liu et al., 2014; Liu et al., 2017). The MMM for the 40m depth was calculated by averaging the highest monthly temperatures during the warmest months (June 21st to September 21st) of each year, based on *in-situ* water temperatures measured at hourly intervals from 2015 to 2018 at the mesophotic study site (Prasetia et al., 2022) using underwater temperature loggers (HOBO Water Temp Pro v2, Onset, USA) (Liu et al., 2003). The climatological MMM values were calculated for each depth: 28.4°C for the shallow depths and 27.9°C for the mesophotic depths. The solar calendar was used to accurately determine the corresponding seasons.

We conducted an experiment with three temperature treatments to induce moderate-duration thermal stress for 14 days. The temperature treatments were ~28°C, ~30°C, and ~31°C. The ~28°C temperature was set at 27.8 ± 0.9°C, which corresponds to the average maximum daily temperature at mesophotic depth during the experiment (Figures 2, S1). The thermal stress temperature of ~30°C was set at 29.8 ± 0.4°C, which corresponds to 4 > eDHWs in mesophotic and shallow depths for two weeks. The thermal stress temperature of ~31°C was set at 31.3 ± 0.5°C, which corresponds to 5~7 eDHWs in shallow and mesophotic depths. To achieve the desired temperatures and start the experiment, the temperature in the thermal stress conditions was ramped up by 0.5°C every 6 hours. Chillers were used to regulate the temperature conditions at ~28°C, while separate heaters controlled the thermal temperature conditions. Temperature loggers (HOBO Water Temp Pro v2) were used to monitor the temperatures (Figure S2A).

A total of 18 aquariums were utilized in this study. Three replicates of 26-L flow-through (0.02 L s^{-1}) aquaria were established

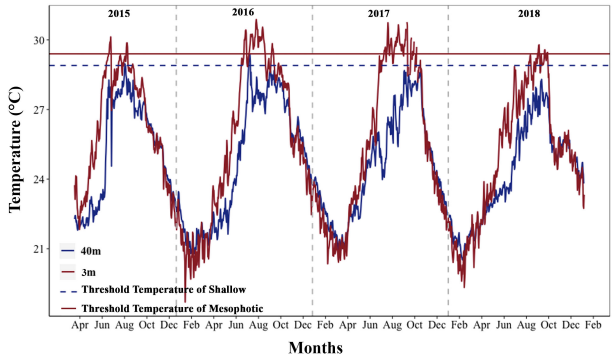

FIGURE 2
Annual temperature fluctuations in shallow and mesophotic depths of the study area (2015–2018). The horizontal dark red line (TTS) and the dark blue dashed line (TTM) represent the threshold temperature for shallow depth (29.4°C) and mesophotic depth (28.9°C), respectively. The vertical gray dashed lines separate the years.

for each temperature treatment under each light condition (Figure S2B). In each temperature treatment, twelve fragments of each species (with four replicates per colony) were randomly placed in three aquaria, resulting in a total of four fragments from each species per aquarium. At least one fragment of each colony was placed in an aquarium (Figure S2C).

Overall, each aquarium contained 24 fragments from six species, which were placed with a 4 cm distance between fragments. Finally, three fragments from each species were randomly collected from each temperature treatment and each species (one fragment per colony/aquarium) to measure physiological parameters on days seven and 14 of the experiment. The collected fragments were stored at -80°C until measurement.

Monitoring coral health and color

The health status of fragments (healthy and dead fragments with no live tissue) was visually assessed daily, and color was monitored every other day during the experiment. All the fragments in each aquarium were photographed using a digital camera (Canon Powershot G10; Canon, Japan) with constant white balance under identical illumination, and Coral Health Chart (Coral Watch) was used to assess bleaching intensity (Siebeck et al., 2006).

The coral images were analyzed using Adobe Photoshop CC 2015. The coral reflection color was recorded using the histogram function with the RGB channel and matched with the Coral Health Chart color category (Siebeck et al., 2006).

Photosynthetic efficiency

The maximum quantum yield of the photosystem II (F_v/F_m) was used as a sensitive indicator of symbiotic microalgal cells and monitored every other day for each fragment after 20 min of dark adaptation (after sunset) using a pulse-amplitude modulated fluorometer (Diving PAM; Walz, Effeltrich, Germany). Minimum fluorescence (Fo) was determined using 3µs pulses of a light emitting diode (blue LED, peak emission at 470 nm; MEAS-INT: 6, DAMP:1, GAIN:3), and the maximum fluorescence (Fm) of each dark-adapted sample was measured by a 0.8 s saturation light pulses (8000 µmol photons $m^{-2}s^{-1}$;SAT-INT: 12).

Symbiotic microalgal density and chlorophyll concentrations

To determine symbiotic microalgal density and chlorophyll content, samples stored at −80°C were used. Coral tissues were collected from each fragment (n = 3 per treatment) using an air pick and transferred to filtered (0.22 µm) seawater. Subsequently, the coral tissue slurry was homogenized using a Potter–Elvehjem tissue grinder and centrifuged at 5000 × *g* for 20 min at 4°C. Following this, the supernatant was discarded, and the pellet of symbiotic microalgae cells was resuspended in fresh filtered seawater. The cell density of the fragments (n = 3 for each species in each treatment) was counted with a hemocytometer under a light microscope.

One milliliter of the slurry was centrifuged for 20 min, and the supernatant was discarded for each fragment. The pellet was resuspended in 1 mL acetone and stored in darkness for 24 h at 4°C to extract chlorophyll. The absorbance of the samples was measured using a spectrophotometer (Shimadzu UV-1800 spectrophotometer; Shimadzu Inc., Kyoto, Japan), and chlorophyll *a* and c_2 concentrations (n = 3 for each species in each treatment) were calculated using the equations of Jeffrey and Humphrey (1975). The symbiotic microalgae density and chlorophyll content were normalized and estimated to the surface area of each fragment by the wax dipping technique (Veal et al., 2010).

Assessment of thermal stress accumulation levels in treatments

The level of accumulated thermal stress within each treatment during the 14-day experiment was monitored using two metrics: experimental degree heating weeks (eDHW) (Leggat et al., 2022) and experimental degree heating days (eDHD) as described in Wyatt et al. (2020). These metrics were calculated based on the recorded temperature data in the treatments and provide an indication of the intensity and duration of thermal stress accumulation commonly associated with coral bleaching responses (Skirving et al., 2020; Wyatt et al., 2023). Briefly, to calculate the eDHW values, we sum of the recorded water temperatures anomalies that exceeded 1°C above the maximum monthly means (MMM; shallow treatment: 28.4°C; mesophotic treatment: 27.9°C) in each treatment over the 14-day period. We then divide this sum by seven to obtain weekly units. For the eDHD values, we sum of the recorded water temperature anomalies in 10-minute intervals that exceeded 1°C above the maximum monthly means (MMM) of each treatment. We then divide the sum by the

number of recorded temperatures in each day (n=144, 10-minute intervals) to achieve daily units.

Statistical analyses

The survival of species in different treatments was estimated using the log-rank test on the Kaplan–Meier curves (Kaplan and Meier, 1958) using the "survfit" function from the "survival" package on R (Therneau, 2015). Normality and homogeneity of variances were assessed using Shapiro–Wilk test and Levene's test, respectively (Queen et al., 2002). Spearman correlation coefficients were used to analyze the relationships between the daily mean *in situ* seawater temperatures at depths of 3 and 40 meters during 2015 and 2018. Wilcoxon rank test was used to test the differences in maximum and mean daily temperatures between shallow and mesophotic depths. Generalized linear models (GLM) using the package "lme4" were used to evaluate the effect of temperature treatments on brightness and F_v/F_m for each species and depth. Temperature treatments and days were considered as fixed effect factors. A generalized linear model (GLM) was also used to test the effect of temperature on symbiotic algal density and chlorophyll concentration. Tukey's test was performed using the "emmeans" package on R (Lenth, 2019).

To investigate inter-specific and depth-dependent variation in the thermal tolerance of corals to different treatments, the standardized mean differences of the data were obtained using Hedges' G method (Hedges, 1981), and the effect size was calculated using the "metacont" function of "meta" package in R (Schwarzer et al., 2015). Forest plots were used to generate the effect size with 95% confidence intervals using the "ggplot" package. Statistical significance was set at $p < 0.05$. R v4.0.4 (R Core Team, 2021) was used for all statistical analyses.

Results

Temperatures in shallow and mesophotic reefs

Maximum monthly mean (MMM) climatological temperatures obtained were 28.4°C and 27.9°C in the shallow and mesophotic habitats, respectively, during three months of the high-temperature season. The thermal thresholds in the shallow and mesophotic habitats were predicted to be one degree higher than the MMM temperatures at each depth (shallow: 29.4, mesophotic: 28.9) (Figure 2). To obtain a comprehensive understanding of the thermal conditions at various depths, we analyzed the maximum and average daily temperatures at different depths using temperature data recorded over a five-year period from 2015 to 2020. Additionally, we examined the daily temperature fluctuations during both high-temperature seasons (summer: June 21st to September 21st) and low-temperature seasons (winter: December 21st to March 21st). The analysis of temperature data from different depths revealed that the maximum and mean daily temperatures in the mesophotic depth were lower than those in the shallow depth at the study sites (Wilcoxon rank test, $p < 0.0001$). However, temperature fluctuations increased with depth during the summer (GLM, $p < 0.0001$). In the winter, the mesophotic depth showed lower daily temperature fluctuations than the shallow depth (GLM, $p < 0.0001$; Figures 2, S1). Furthermore, a strong correlation was found between seawater temperatures at depths of 3 and 40 m (Spearman's correlation, $p < 0.0001$, $\rho = 0.908$).

Survivorship of different species

All shallow and mesophotic species fragments survived in the ~28°C temperature until the end of the 14-day experiment. Among species from shallow depths, mortality was observed only at ~31°C temperatures (5.6 eDHWs in shallow), with the highest mortality rates observed in *Porites cylindrica* (22%), *Porites* sp. (11%), and *Acropora valida* (11%). In contrast, among species from mesophotic depths, high mortality was observed in ~30°C and ~31°C temperature treatments (3.7 and 6.7 eDHWs in mesophotic) for *Acropora* cf. *horrida* (100%) and ~ 31°C temperature treatments (6.7 eDHWs) for *Seriatopora hystrix* (100%), *Galaxea* cf. *astreata* (44%), and *Porites* sp. (11%).

Other species, such as *Pachyseris speciosa*, *Turbinaria mesenterina*, and *Galaxea fascicularis* from shallow depths and *Pachyseris speciosa* and *Leptoseris papyracea* from mesophotic depths, survived under all temperature conditions. The log-rank test showed significant differences in survival rates between colonies subjected to ~30°C and ~31°C temperatures compared to ~28°C, as well as between the depths (Figure 3; Table S1).

Coral brightness and bleaching

The color of shallow and mesophotic fragments exposed to higher temperatures turned pale (brighter color caused by bleaching) compared with those in the ~28°C treatment, and the brightness of the fragments gradually increased over the experimental period (Figure 4; Table S2). A significant increase in brightness was observed in all species at shallow and mesophotic depths at ~31°C treatment (GLM, $p < 0.0001$). In the ~30°C treatment, three out of six species showed a significant change in brightness: *Acropora valida* (GLM, $p < 0.0001$), *Porites cylindrica* (GLM, $p < 0.0001$), and *Pachyseris speciosa* (GLM, $p = 0.0001$). In contrast, four out of six mesophotic species exhibited a significant increase in brightness in the ~30°C treatment: *Acropora* cf. *horrida* ($p < 0.0001$), *Pachyseris speciosa* ($p = 0.01$), *Leptoseris papyracea* ($p = 0.007$), and *Seriatopora hystrix* ($p = 0.003$) (Figures 1, 4; Table S2).

Photosynthetic efficiency

In most species, the maximum quantum efficiency of photosystem II (F_v/F_m) was highest at ~28°C and decreased in corals exposed to temperature treatments at ~30°C and ~31°C (Figure 5; Table S3). Among the shallow species, four out of six

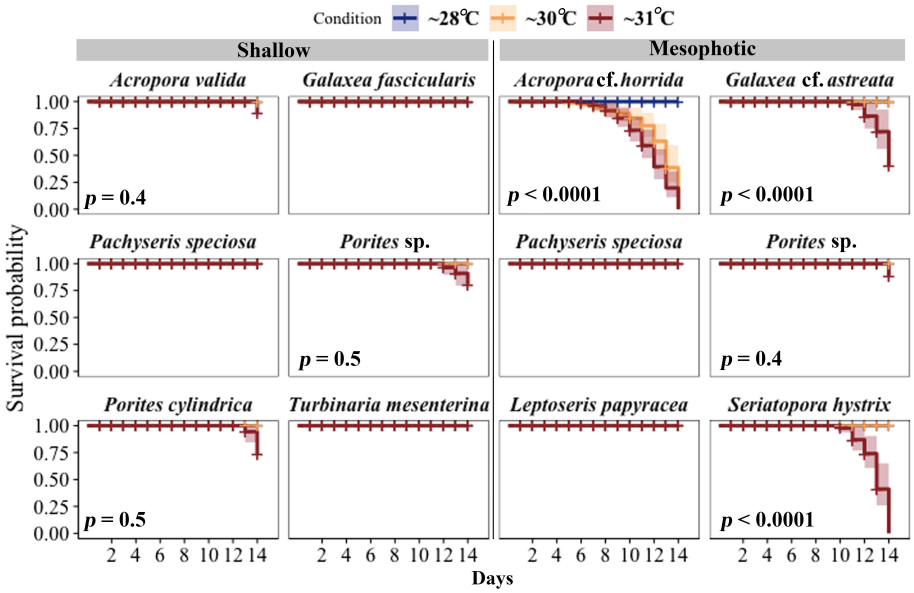

FIGURE 3
Survival probabilities of corals from mesophotic and shallow reefs over a period of 14 days under three different temperature conditions. Kaplan–Meier log-rank test *p*-values are shown for comparing survival curves in three different temperature treatments. All fragments of *Pachyseris speciosa*, *Turbinaria mesenterina*, and *Galaxea fascicularis* from shallow areas and *P. speciosa* and *Leptoseris papyracea* from mesophotic depths, exhibited 100% survivorship under all temperature conditions throughout the experimental period.

species showed a significant decrease in F_v/F_m at ~31°C (*Acropora valida*, $p < 0.0001$; *Porites* sp., $p = 0.01$; *Porites cylindrica*, $p < 0.0001$; *Turbinaria mesenterina*, $p < 0.0001$), while no significant reduction was observed at ~30°C. Among the mesophotic species, all species exhibited a significant reduction in F_v/F_m at ~31°C (GLM, $p < 0.05$), and only *Acropora* cf. *horrida* showed a significant reduction at ~30°C (GLM, $p = 0.0003$).

Pachyseris speciosa displayed different responses in shallow and mesophotic habitats. In mesophotic fragments, a significant reduction of 67.61% was observed at ~31°C (GLM, $p < 0.0001$),

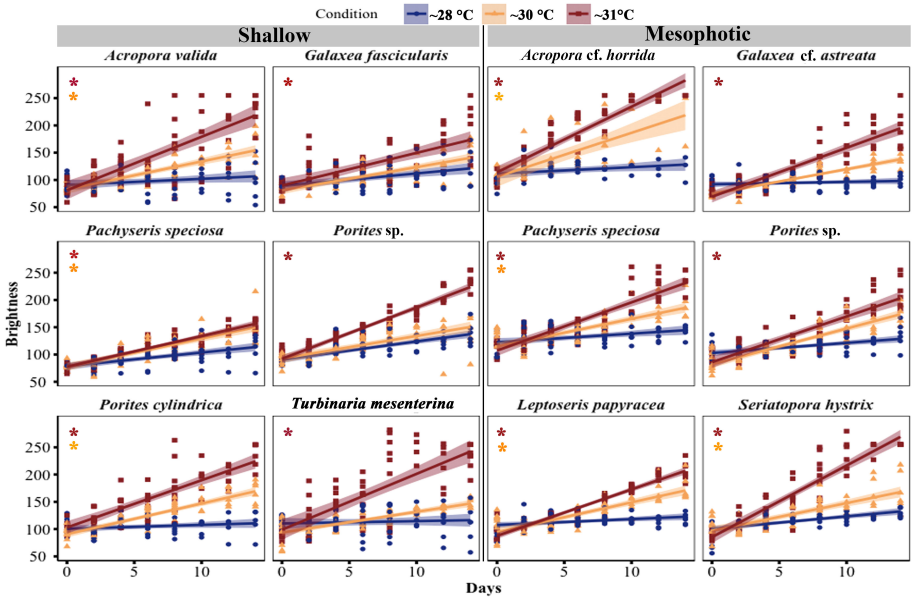

FIGURE 4
Changes in brightness of corals from mesophotic and shallow reefs under three different temperature treatments over a period of 14 days. The brightness was determined based on the hue value measured from photos. The brightness range varied from 55 to 255, with a value of 55 corresponding to healthy fragments, and a value of 255 indicating bleached fragments (Siebeck et al., 2006). An asterisk on the left side of the plots indicates a significant difference between treatments: orange represents a significant difference between ~28°C and ~30°C treatments, while red represents a significant difference between ~28°C and ~31°C treatments.

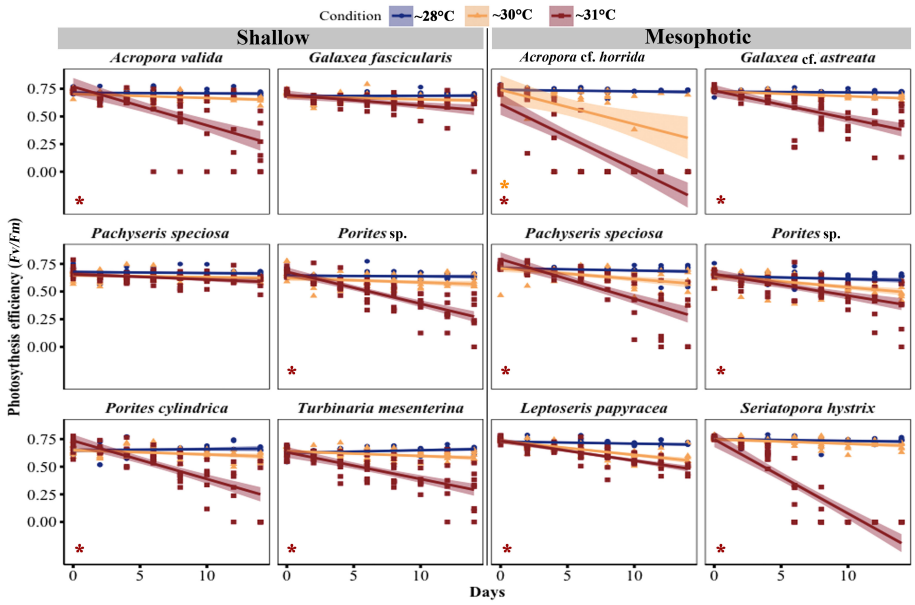

FIGURE 5
Changes in maximal quantum yield of photosystem II (F_v/F_m) in corals from mesophotic and shallow reefs under three temperature conditions over 14 days. An asterisk on the left side of the plots indicates a significant difference between treatments: orange represents a significant difference between ~28°C and ~30°C treatments, while red represents a significant difference between ~28°C and ~31°C treatments.

while at ~30°C, there was a non-significant reduction of 18.03% (GLM, $p = 0.4$) during the experimental period. In contrast, in the F_v/F_m of shallow *Pachyseris speciosa* fragments, there was no significant reduction (GLM, $p > 0.5$) at ~31°C, with a decrease of 14.7%, and at ~30°C, there was a 7.15% reduction during the experimental period.

Symbiotic algal density and chlorophyll

Throughout the experiment, the symbiont density in the fragments decreased in the ~30°C and ~31°C temperature treatments compared with the ~28°C treatments. A significant reduction in symbiotic algal density was observed in three out of six shallow species at ~31°C temperature treatments, including *A. valida* (GLM, $p = 0.005$), *Porites cylindrica* (GLM, $p < 0.0001$), and *T. mesenterina* (GLM, $p = 0.0006$), while there was no significant difference at ~30°C. In contrast, four out of six mesophotic species showed a significant decrease in symbiotic algal density in the 31-degree treatment, including *Acropora* cf. *horrida* (GLM, $p = 0.0001$), *Pachyseris speciosa* (GLM, $p = 0.005$), *S. hystrix* (GLM, p = 0.0001), and *Galaxea* cf. *astreata* (GLM, $p = 0.01$). Additionally, *Acropora* cf. *horrida* showed a significant reduction at ~30°C (GLM, $p = 0.01$) (Figure 6; Table S4)."

Chlorophyll (*a* and c_2) content per surface area showed a significant decrease in three out of six species from shallow depths, namely *Pachyseris speciosa*, *Porites cylindrica*, and *T. mesenterina*, at ~31°C temperature treatments. Additionally, *Pachyseris speciosa* exhibited a significant reduction in chlorophyll content at ~30°C treatment. In contrast, among coral fragments from mesophotic depth, five out of six species, including *Acropora* cf. *horrida*, *Galaxea* cf. *astreata*, *Pachyseris speciosa*, *Porites* sp., and *S. hystrix*, showed a significant decrease in chlorophyll content at ~31°C temperature treatments. Among these mesophotic species, only *Pachyseris speciosa* also displayed a significant reduction in chlorophyll content at ~30°C temperature treatments. It is worth noting that the total chlorophyll content in the other species did not differ between the temperature treatments (see Figure 7; Table S5).

Thermal responses, eDHWs and eDHD

We examined coral fragments from shallow and mesophotic depths in response to water temperature using two metrics: eDHW and eDHD. The accumulation of thermal stress exposure over the 14-day experimental period reached an eDHW (Degree Heating Weeks) of 2.6°C-weeks for shallow fragments and 3.7°C-weeks for mesophotic fragments under moderate conditions (~30°C treatments). Under higher stress conditions (~31°C treatments), the eDHW was 5.6°C-weeks for shallow fragments and 6.7°C-weeks for mesophotic fragments. The accumulation of thermal stress exposure in terms of Degree Heating Days (eDHD) over the experimental period was 18.8°C-days for shallow fragments and 26.5°C-days for mesophotic fragments under moderate conditions. Under higher stress conditions, the eDHD was 39.6°C-days for shallow fragments and 47.3°C-days for mesophotic fragments.

The results indicated variable reactions (Table 1). In terms of brightness, bleaching was observed in *Acropora* cf. *horrida* among mesophotic species, while among shallow species, slight bleaching was observed in a few fragments of *Acropora valida*, *Porites* sp., and *Galaxea fascicularis*. Additionally, at 5 < eDHWs, the brightness in mesophotic fragments of *Pachyseris speciosa* was significantly

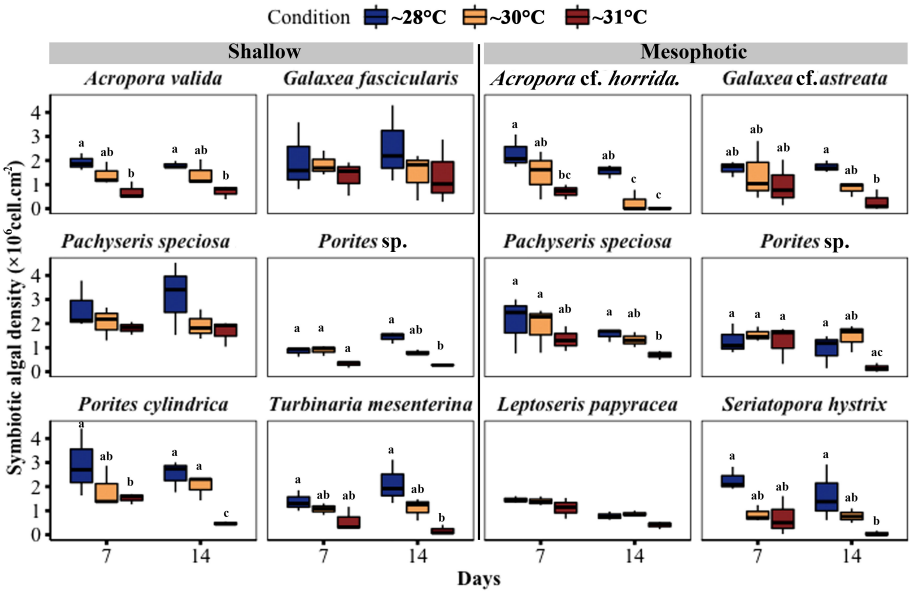

FIGURE 6
Changes in symbiotic algal density in corals from mesophotic and shallow reefs under three temperature conditions over 14 days. Boxes show the upper (75th percentile) and lower (25th percentile) quartiles, center lines represent medians, and whiskers extend to less than 1.5 × interquartile range measured data away from the first/third quartile. Letters indicate a significant difference between treatments each day and between days.

higher than in shallow fragments (LMM, $p < 0.0001$). In terms of survival, among the mesophotic species, only *Acropora* cf. *horrida* showed low survivorship at 5 < eDHWs and all other species survived through the treatment, while among the shallow species slight mortality was observed in *Acropora valida*, *Porites* sp. and *Porites cylindrica* at 4DHWs although it was not significant (Figure 3, Table 1). Interestingly, F_v/F_m for *Pachyseris speciosa* was not significantly different between the mesophotic and shallow depths (LMM, $p = 0.29$) but was different in brightness (LMM, $p < 0.0001$).

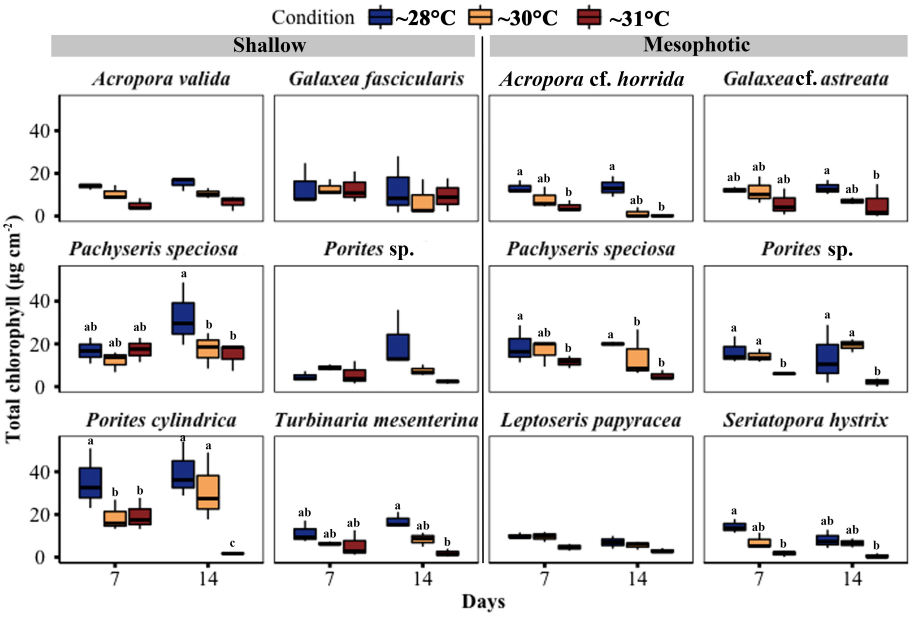

FIGURE 7
Changes in total chlorophyll (Chl *a* + c_2) concentration per cm^2 in corals from mesophotic and shallow reefs under three temperature conditions over 14 days. Boxes show the upper (75th percentile) and lower (25th percentile) quartile, center lines represent medians, and whiskers extend to less than 1.5×interquartile range measured data away from the first/third quartile. Letters indicate a significant difference between treatments each day and between days.

TABLE 1 Comparison between +4DHWs in moderate temperature for mesophotic- and higher temperature for shallow species.

Interaction	F_v/F_m (LMM)					Brightness (LMM)					Survival (Kaplan-Meyer)	
Mesophotic moderate temp. – Shallow high temp.	estimate	SE	df	t.ratio	*p*.value	estimate	SE	df	t.ratio	*p*.value	Chisq	p.value
Acropora cf. *horrida* – *Acropora valida*	-0.00834	0.082	14	-0.102	0.9204	16.6	16.1	14	1.03	0.097	38.9	**4.00E-10**
Porites sp. (mesophotic) – *Porites* sp. (shallow)	0.0782	0.029	16	2.642	**0.0178**	-27.8	3.82	16	-7.286	**<0.0001**	3	0.08
Galaxea cf. *astreata* – *Galaxea fascicularis*	0.0647	0.020	16	3.225	**0.0053**	-25	7.57	16	-3.298	**<0.0001**	N.D.	
Pachyseris (mesophotic) – *Pachyseris* (shallow)	-0.0232	0.021	16	-1.072	0.2995	-33.3	3.81	16	-8.735	**<0.0001**	N.D.	

N.D. indicates 'no data,' and significant values are in bold.

Discussion

The present study indicates that the thermal threshold of mesophotic corals is slightly lower or equal to that of corals distributed in shallow water. Organisms in colder environments show lower thermal tolerance and higher sensitivity than those in warmer climates (Jokiel and Coles, 1990; Jokiel, 2004). Since the thermal tolerance of corals may be linked to the temperature of their habitats (Oliver and Palumbi, 2011; Schoepf et al., 2015; Safaie et al., 2018), it is reasonable to expect depth-dependent differences in their thermal tolerance. Species inhabiting highly variable shallow habitats often possess higher thermal tolerance and better resistance to bleaching compared to those inhabiting stable habitats (Schoepf et al., 2015; Smith et al., 2016; Schoepf et al., 2019).

The thermal threshold may be associated with species and temperature in their habitat; thus, the thresholds differ among species and locations. Previous studies have also indicated lower thermal tolerance among colonies from mesophotic depths compared to shallow depths (Smith et al., 2016; Skutnik et al., 2020; Frates et al., 2021). However, some regions have had contrasting results, such as the Great Barrier Reef (Frade et al., 2018) and Moorea in French Polynesia (Pérez-Rosales et al., 2021). In these areas, mesophotic coral communities have shown a decreased incidence of bleaching across depths, particularly from shallow to upper mesophotic depths (40 m). Furthermore, lower mesophotic communities (> 60 m) in Polynesia have been observed to escape the detrimental effects caused by thermal bleaching events (Pérez-Rosales et al., 2021). This could be attributed to the relatively stable and constant temperatures experienced by shallow and upper mesophotic depths in Polynesia during the high-temperature season (Pérez-Rosales et al., 2021), which might affect the thermal tolerance of corals in upper mesophotic depths. Nevertheless, in the present study site in Okinawa, mesophotic depths generally experienced lower temperatures than shallow depths. Additionally, the high-temperature fluctuations caused by short-term cooling events induced by internal waves further contribute to maintaining a cooler environment in deeper coral ecosystems (Wyatt et al., 2020; Godefroid et al., 2023; Wyatt et al., 2023). Consequently, this leads to a lower thermal threshold for mesophotic corals than their shallow counterparts.

Bleaching responses were highly variable but more severe in most of the examined species from mesophotic depths. The bleaching responses, represented as a decrease in algal density and an increase in color brightness in the studied species, were observed in both shallow and mesophotic areas, but their rates of change were not consistent (Figures 3, 6). Bleaching was prominently observed in the mesophotic species *Acropora* cf. *horrida*, *Seriatopora hystrix*, and *Galaxea* cf. *astreata* (Figures 3, 6). The variable responses in the examined species were congruent with those in previous reports; susceptibility to thermal stress varied among genera, species, and populations (Loya et al., 2001; Hongo and Yamano, 2013; Palumbi et al., 2014). The corals with high bleaching prevalence were physiologically damaged and suffered increased mortality (Glynn, 1984; Berkelmans et al., 2004; Hughes et al., 2018a).

Low thermal tolerance of *S. hystrix* has been documented in shallow reefs (Marshall and Baird, 2000; Loya et al., 2001; van Woesik et al., 2011; Seveso et al., 2014; Hoey et al., 2016). Notably, the disappearance of *S. hystrix* in shallow reefs around Sesoko Island followed a mass coral bleaching event in 1998 (van Woesik et al., 2011). Subsequently, a dense population of the species was found in the upper mesophotic depth north of Sesoko Island (Sinniger et al., 2013). This surviving population was likely protected from the extreme heat stress on shallow reefs because of the depth, underscoring the relationship between their habitat and susceptibility to environmental stressors. However, considering rising seawater temperature (0.2–1°C per decade) and the predicted annual coral bleaching phenomenon in the next decades (Donner et al., 2005), the mesophotic coral population may not be able to persist in the future due to the strong correlation with depth-dependent temperatures (Figures 3, 4, 8). Given the rising temperature, the duration, and magnitude of heatwaves, they will surpass the threshold temperature of the coral species, particularly at mesophotic depths where the corals live in cooler habitats and experience more stable thermal regimes. Indeed, coral bleaching due to high temperatures has been documented in some MCEs (Nir et al., 2014; Smith et al., 2016; Frade et al., 2018; Pérez-Rosales et al.,

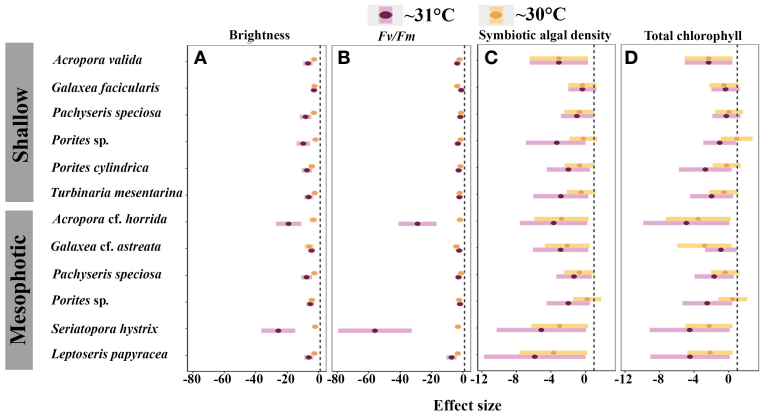

FIGURE 8
Inter-specific effect of medium- and high-temperature treatments on: **(A)** brightness; **(B)** F_v/F_m; **(C)** symbiotic algal density; and **(D)** total chlorophyll. The black dashed line indicates zero effect, and negative points indicate the negative impact of thermal treatments on the physiological function of species.

2021; Eyal et al., 2022). Owing to the discrepancy between a rapidly changing environment and phenotypic adaptation, the acclimatization/adaptation of corals to changing environments can be considered a major challenge (Putnam, 2021). Furthermore, even if the mesophotic population has the potential to replenish its shallow counterpart for a relatively long period as has been hypothesized in DRRH, the rising temperature and lower thermal threshold of this population limit the success of such regeneration.

The heat tolerance of the species from both mesophotic and shallow reefs is essential for reef persistence. For example, despite differences in the thermal tolerance between *A.* cf. *horrida* from mesophotic depths and *A. valida* from shallow depths, both species were found to be susceptible to and physiologically damaged by high water temperature. In contrast, *Porites* sp. from both depth ranges and *L. papyracea* exhibited lower susceptibility to high water temperatures. Moreover, the laminar species *Pachyseris speciosa* demonstrated the highest heat tolerance (Figures 7, 8). However, mesophotic fragments of this species displayed significantly higher brightness levels than those shallow fragments at > 5 eDHWs. Previous studies have also shown that other laminar species exhibit higher heat tolerance than branching species (Loya et al., 2001; van Woesik et al., 2011). *Pachyseris speciosa* is widely distributed in mesophotic depths, including the Ryukyu archipelago (Sinniger and Harii, 2018). If water temperature increases by 2°C, heat-tolerant species such as *Pachyseris speciosa* may dominate the reef ecosystem. The acclimatization and adaptation potential of other species need to be clarified.

The responses to heat stress were highly variable among the examined species. In terms of DHWs, up to 4 eDHWs did not cause a critical negative effect on the survivorship of most species, except for *Acropora* cf. *horrida*, from mesophotic depths (Figure 3). In terms of brightness, bleaching was observed in only one fragments of *Pachyseris speciosa* and *S. hystrix* (Figures 4–7). In corals from shallow depths, a value of 5.71 eDHW, indicating a state of high-stress conditions, significantly impacted most of the examined parameters (Figures 3–7). However, the impact of temperature on species from mesophotic depths was most severe, and most of the examined species from this depth in the high thermal stress treatment (6.81 eDHWs) showed high levels of brightness and mortality. Regarding the DHWs index, DHWs from +4 to 8, considered moderate thermal stress, were expected to cause medium bleaching (Liu et al., 2018).

In this study, except for *Acropora* cf. *horrida* from mesophotic depth, other coral species from shallow and mesophotic habitats showed heat tolerance up to 4 eDHW. Therefore, we conclude that the upper-mesophotic habitats could act as refugia for coral species if the accumulation of thermal stress in mesophotic depth does not exceed 4 DHW. Some mesophotic ecosystems are protected from temperature anomalies because of the thermocline depth (Bridge et al., 2013), which could serve as potential thermal refugia. Otherwise, corals in mesophotic habitats should tolerate a similar temperature threshold as their shallow counterparts to withstand rising temperatures (Gould et al., 2021). Similar responses have been proposed for mesophotic and shallow colonies of *Montastraea cavernosa* (Skutnik et al., 2020) and *Orbicella faveolata* (Frates et al., 2021) against thermal stress. However, the temperature in mesophotic depth in the present study was considerably correlated with shallow depth temperature. Changes in shallow-depth temperature alter mesophotic depth temperature. Owing to rising sea surface temperature and annual consecutive thermal stress, which have been predicted (van Hooidonk et al., 2013), the water temperature in the mesophotic reef will eventually rise. Therefore, considering our findings, the mesophotic reef could act as a refugium for the species which could tolerate heat stress up to 4 DHW. However, the corals that inhabit mesophotic depths have significantly limited capacity for thermal tolerance when faced with high levels of thermal stress (>6 DHWs), which could have serious implications for the health and survival of these important ecosystems. On the other hand, the thresholds of the thermal tolerance in the corals are diverse and not essentially different in several species inhabiting mesophotic to shallow areas.

Data availability statement

The raw data supporting the conclusions of this article will be made available by the authors, without undue reservation.

Author contributions

PT-K, FS, and SH conceived and designed the experiments and conducted fieldwork. PT-K performed laboratory experiments. TN supported photo-physiological measurements. PT-K and MM analyzed the data and wrote the original draft of the manuscript. All authors contributed to the article and approved the submitted version.

Funding

This study was supported by Grants-in-Aid for Scientific Research (KAKENHI) from Japan Society for the Promotion of Science to SH (grant numbers 16H02490, 16KK0164, and 21H04943), FS (20K06210), and MM (21H05304 and 22H02369).

Acknowledgments

We thank Dr. H. Rouzé, E. D. S. Sitorus, S. Kadena, and M. Jinza for field assistance and Dr. S. Hazraty-Kari for laboratory assistance. The English language in this document has been checked by at least two professional editors, both native speakers of English.

Conflict of interest

The authors declare that the research was conducted in the absence of any commercial or financial relationships that could be construed as a potential conflict of interest.

Publisher's note

All claims expressed in this article are solely those of the authors and do not necessarily represent those of their affiliated organizations, or those of the publisher, the editors and the reviewers. Any product that may be evaluated in this article, or claim that may be made by its manufacturer, is not guaranteed or endorsed by the publisher.

Supplementary material

The Supplementary Material for this article can be found online at: https://www.frontiersin.org/articles/10.3389/fmars.2023.1210662/full#supplementary-material

References

Abrego, D., Ulstrup, K. E., Willis, B. L., and van Oppen, M. J. H. (2008). Species-specific interactions between algal endosymbionts and coral hosts define their bleaching response to heat and light stress. *Proc. R. Soc B* 275, 2273–2282. doi: 10.1098/rspb.2008.0180

Baker, A. C., Glynn, P. W., and Riegl, B. (2008). Climate change and coral reef bleaching: An ecological assessment of long-term impacts, recovery trends and future outlook. *Estuar. Coast. Shelf Sci.* 80, 435–471. doi: 10.1016/j.ecss.2008.09.003

Ben-Zvi, O., Tamir, R., Keren, N., Tchernov, D., Berman-Frank, I., Kolodny, Y., et al. (2020). Photophysiology of a mesophotic coral 3 years after transplantation to a shallow environment. *Coral Reefs* 39, 903–913. doi: 10.1007/s00338-020-01910-0

Berkelmans, R., De'ath, G., Kininmonth, S., and Skirving, W. J. (2004). A comparison of the 1998 and 2002 coral bleaching events on the Great Barrier Reef: spatial correlation, patterns, and predictions. *Coral Reefs* 23, 74–83. doi: 10.1007/s00338-003-0353-y

Bieri, T., Onishi, M., Xiang, T. T., Grossman, A. R., and Pringle, J. R. (2016). Relative contributions of various cellular mechanisms to loss of algae during cnidarian bleaching. *PloS One* 11. doi: 10.1371/journal.pone.0152693

Bongaerts, P., Ridgway, T., Sampayo, E. M., and Hoegh-Guldberg, O. (2010). Assessing the 'deep reef refugia' hypothesis: focus on Caribbean reefs. *Coral Reefs* 29, 309–327. doi: 10.1007/s00338-009-0581-x

Bongaerts, P., Riginos, C., Brunner, R., Englebert, N., Smith, S. R., and Hoegh-Guldberg, O. (2017). Deep reefs are not universal refuges: reseeding potential varies among coral species. *Sci. Adv.* 3, e1602373. doi: 10.1126/sciadv.1602373

Bongaerts, P., and Smith, T. B. (2019). "Beyond the "Deep Reef Refuge" hypothesis: a conceptual framework to characterize persistence at depth," in *Mesophotic Coral Ecosystems* (Springer Cham), 881–895.

Bridge, T. C., Hoey, A. S., Campbell, S. J., Muttaqin, E., Rudi, E., Fadli, N., and Baird, A. H. (2013). Depth-dependent mortality of reef corals following a severe bleaching event: implications for thermal refuges and population recovery. *F1000Res* 16(2), 187. doi: 10.12688/f1000research.2-187.v3

Dias, M., Ferreira, A., Gouveia, R., Cereja, R., and Vinagre, C. (2018). Mortality, growth and regeneration following fragmentation of reef-forming corals under thermal stress. *J. Sea Res.* 141, 71–82. doi: 10.1016/j.seares.2018.08.008

Dias, M., Madeira, C., Jogee, N., Ferreira, A., Gouveia, R., Cabral, H., et al. (2019). Oxidative stress on scleractinian coral fragments following exposure to high temperature and low salinity. *Ecol. Indic.* 107. doi: 10.1016/j.ecolind.2019.105586

Diaz, J. M., Hansel, C. M., Apprill, A., Brighi, C., Zhang, T., Weber, L., et al. (2016). Species-specific control of external superoxide levels by the coral holobiont during a natural bleaching event. *Nat. commu* 7. doi: 10.1038/ncomms13801

Donner, S. D., Skirving, W. J., Little, C. M., Oppenheimer, M., and Hoegh-Guldberg, O. (2005). Global assessment of coral bleaching and required rates of adaptation under climate change. *Glob. Change Bio.* 11, 2251–2265. doi: 10.1111/j.1365-2486.2005.01073.x

Eyal, G., Laverick, J. H., Ben-Zvi, O., Brown, K. T., Kramer, N., Tamir, R., et al. (2022). Selective deep water coral bleaching occurs through depth isolation. *Sci. Total Environ.* 844, 157180. doi: 10.1016/j.scitotenv.2022.157180

Frade, P. R., Bongaerts, P., Englebert, N., Rogers, A., Gonzalez-Rivero, M., and Hoegh-Guldberg, O. (2018). Deep reefs of the Great Barrier Reef offer limited thermal refuge during mass coral bleaching. *Nat. commu* 9. doi: 10.1038/s41467-018-05741-0

Frates, E., Hughes, A., and Randall, A. (2021). *Orbicella faveolata: Shallow versus Mesophotic Coral Responses to Temperature Change*. Boston University 15.

Glynn, P. W. (1984). Widespread coral mortality and the 1982–83 el niño warming event. *Environ. Conserv.* 11, 133–146. doi: 10.1017/S0376892900013825

Glynn, P. W. (1996). Coral reef bleaching: Facts, hypotheses and implications. *Glob. Change Bio.* 2, 495–509. doi: 10.1111/j.1365-2486.1996.tb00063.x

Glynn, P. W., and D'Croz, L. (1990). Experimental evidence for high temperature stress as the cause of El Niño-coincident coral mortality. *Coral Reefs* 8, 181–191. doi: 10.1007/BF00265009

Godefroid, M., Dubois, P.Under The Pole Consortium, , Hédouin, L. (2023). Thermal performance with depth: Comparison of a mesophotic scleractinian and an antipatharian species subjected to internal waves in Mo'orea, French Polynesia. *Mar. Environ. Res.* 184, 105851. doi: 10.1016/j.marenvres.2022.105851

Gould, K., Bruno, J. F., Ju, R., and Goodbody-Gringley, G. (2021). Upper-mesophotic and shallow reef corals exhibit similar thermal tolerance, sensitivity and optima. *Coral Reefs* 40, 907–920. doi: 10.1007/s00338-021-02095-w

Hedges, L. V. (1981). Distribution theory for Glass's estimator of effect size and related estimators. *J. Educ. Stat.* 6, 107–128. doi: 10.3102/10769986006002107

Hoadley, K. D., Pettay, D. T., Grottoli, A. G., Cai, W. J., Melman, T. F., Levas, S., et al. (2016). High-temperature acclimation strategies within the thermally tolerant endosymbiont *Symbiodinium trenchii* and its coral host, *Turbinaria reniformis*, differ with changing pCO(2) and nutrients. *Mar. Biol.* 163. doi: 10.1007/s00227-016-2909-8

Hoegh-Guldberg, O., Mumby, P. J., Hooten, A. J., Steneck, R. S., Greenfield, P., Gomez, E., et al. (2007). Coral reefs under rapid climate change and ocean acidification. *Science* 318, 1737–1742. doi: 10.1126/science.1152509

Hoey, A. S., Howells, E., Johansen, J. L., Hobbs, J. P. A., Messmer, V., McCowan, D. M., et al. (2016). Recent advances in understanding the effects of climate change on coral reefs. *Diversity* 8. doi: 10.3390/d8020012

Hongo, C., and Yamano, H. (2013). Species-specific responses of corals to bleaching events on anthropogenically turbid reefs on okinawa island, Japan, over a 15-year period, (1995-2009). *PloS One* 8. doi: 10.1371/journal.pone.0060952

Hughes, T. P., Anderson, K. D., Connolly, S. R., Heron, S. F., Kerry, J. T., Lough, J. M., et al. (2018a). Spatial and temporal patterns of mass bleaching of corals in the Anthropocene. *Science* 359, 80–8+. doi: 10.1126/science.aan8048

Hughes, T. P., Baird, A. H., Bellwood, D. R., Card, M., Connolly, S. R., Folke, C., et al. (2003). Climate change, human impacts, and the resilience of coral reefs. *Science* 301, 929–933. doi: 10.1126/science.1085046

Hughes, T. P., Barnes, M. L., Bellwood, D. R., Cinner, J. E., Cumming, G. S., Jackson, J. B. C., et al. (2017). Coral reefs in the anthropocene. *Nature* 546, 82–90. doi: 10.1038/nature22901

Hughes, T. P., Kerry, J. T., Baird, A. H., Connolly, S. R., Dietzel, A., Eakin, C. M., et al. (2018b). Global warming transforms coral reef assemblages. *Nature* 556, 492–496. doi: 10.1038/s41586-018-0041-2

Jeffrey, S. W., and Humphrey, G. F. (1975). ew spectrophotometric equations for determining chlorophylls a, b, c1 and c2 in higher plants, algae and natural phytoplankton. *Biochem. Physiol. Pflanz.* 167, 191–194

Jokiel, P. L. (2004). "Temperature stress and coral bleaching, in: Rosenberg," in *Coral health and disease* (Berlin, Germany: Springer), 401–425.

Jokiel, P. L., and Coles, S. L. (1990). Response of Hawaiian and other Indo-Pacific reef corals to elevated temperature. *Coral Reefs* 8, 155–162. doi: 10.1007/BF00265006

Kahng, S. E., Garcia-Sais, J. R., Spalding, H. L., Brokovich, E., Wagner, D., Weil, E., et al. (2010). Community ecology of mesophotic coral reef ecosystems. *Coral Reefs* 29, 255–275. doi: 10.1007/s00338-010-0593-6

Kaplan, E. L., and Meier, P. (1958). Nonparametric estimation from incomplete observations. *J. Am. Stat. Assoc.* 53, 457–481. doi: 10.1080/01621459.1958.10501452

Kayanne, H. (2017). Validation of degree heating weeks as a coral bleaching index in the northwestern Pacific. *Coral Reefs* 36, 63–70. doi: 10.1007/s00338-016-1524-y

Klepac, C. N., and Barshis, D. J. (2020). Reduced thermal tolerance of massive coral species in a highly variable environment. *Proc. R. Soc B* 287. doi: 10.1098/rspb.2020.1379

Kleypas, J. A., Thompson, D. M., Castruccio, F. S., Curchitser, E. N., Pinsky, M., and Watson, J. R. (2016). Larval connectivity across temperature gradients and its potential effect on heat tolerance in coral populations. *Glob. Change Bio.* 22, 3539–3549. doi: 10.1111/gcb.13347

Leggat, W., Heron, S. F., Fordyce, A., Suggett, D. J., and Ainsworth, T. D. (2022). Experiment Degree Heating Week (eDHW) as a novel metric to reconcile and validate past and future global coral bleaching studies. *J. Environ. Manage.* 301, 113919. doi: 10.1016/j.jenvman.2021.113919

Lenth, R. (2019). *Emmeans: Estimated marginal means, aka least squares means.* (R package version 1.4.1). Available online at: https://cran.r-project.org/package=emmeans

Lesser, M. P., Slattery, M., and Leichter, J. J. (2009). Ecology of mesophotic coral reefs. *J. Exp. Mar. Biol. Ecol.* 375, 1–8. doi: 10.1016/j.jembe.2009.05.009

Liu, G., Eakin, C. M., Chen, M., Kumar, A., de la Cour, J. L., Heron, S. F., et al. (2018). Predicting heat stress to inform reef management: NOAA coral reef watch's 4-month coral bleaching outlook. *Front. Mar. Sci.* 5, 57. doi: 10.3389/fmars.2018.00057

Liu, G., Heron, S., Eakin, C., Muller-Karger, F., Vega-Rodriguez, M., Guild, L., et al. (2014). Reef-scale thermal stress monitoring of coral ecosystems: New 5-km global products from NOAA coral reef watch. *Remote Sens.* 6 (11), 11,579–11,606. doi: 10.3390/rs61111579

Liu, G., Rauenzahn, J. L., Heron, S. F., Eakin, C. M., Skirving, W. J., Christensen, T., et al. (2013). NOAA coral reef watch 50 km satellite sea surface temperature-based decision support system for coral bleaching management. *NOAA Tech. Rep. Nesdis* 143:33.

Liu, G., Skirving, W. J., Geiger, E. F., and La, J. L. D. (2017). *NOAA coral reef watch's 5-km satellite coral bleaching heat stress monitoring product suite version 3 and four-month outlook version 4*, Vol. 32. 7.

Liu, G., Strong, A. E., and Skirving, W. (2003). Remote sensing of sea surface temperature during 2002 Barrier Reef coral bleaching. *EOS* 84 (15), 137–144. doi: 10.1029/2003EO150001

Logan, C. A., Dunne, J. P., Eakin, C. M., and Donner, S. D. (2014). Incorporating adaptive responses into future projections of coral bleaching. *Glob. Chang Biol.* 20, 125–139. doi: 10.1111/gcb.12390

Lough, J. M., Anderson, K. D., and Hughes, T. P. (2018). Increasing thermal stress for tropical coral reefs: 1871-2017. *Sci. Rep.* 8, 6079. doi: 10.1038/s41598-018-24530-9

Loya, Y., Sakai, K., Yamazato, K., Nakano, Y., Sambali, H., and van Woesik, R. (2001). Coral bleaching: the winners and the losers. *Ecol. Lett.* 4, 122–131. doi: 10.1046/j.1461-0248.2001.00203.x

Marshall, P. A., and Baird, A. H. (2000). Bleaching of corals on the Great Barrier Reef: differential susceptibilities among taxa. *Coral Reefs* 19, 155–163. doi: 10.1007/s003380000086

Mayfield, A. B., Chen, M. N., Meng, P. J., Lin, H. J., Chen, C. S., and Liu, P. J. (2013). The physiological response of the reef coral *Pocillopora damicornis* to elevated temperature: results from coral reef mesocosm experiments in Southern Taiwan. *Mar. Environ. Res.* 86, 1–11. doi: 10.1016/j.marenvres.2013.01.004

McClanahan, T. R., Maina, J., and Ateweberhan, M. (2015). Regional coral responses to climate disturbances and warming is predicted by multivariate stress model and not temperature threshold metrics. *Clim. Change* 131, 607–620. doi: 10.1007/s10584-015-1399-x

Muir, P. R., Marshall, P. A., Abdulla, A., and Aguirre, J. D. (2017). Species identity and depth predict bleaching severity in reef-building corals: shall the deep inherit the reef? *Proc. R. Soc B* 284. doi: 10.1098/rspb.2017.1551

Nielsen, D. A., Petrou, K., and Gates, R. D. (2018). Coral bleaching from a single cell perspective. *ISME J.* 12, 1558–1567. doi: 10.1038/s41396-018-0080-6

Nir, O., Gruber, D. F., Shemesh, E., Glasser, E., and Tchernov, D. (2014). Seasonal mesophotic coral bleaching of *Stylophora Pistillata* in the Northern Red Sea. *PloS One* 9. doi: 10.1371/journal.pone.0084968

Nishihira, M., and Veron, J. (1995). *Hermatypic corals of Japan* (Kaiyusha, Tokyo).

Oliver, T. A., and Palumbi, S. R. (2011). Do fluctuating temperature environments elevate coral thermal tolerance? *Coral Reefs* 30, 429–440. doi: 10.1007/s00338-011-0721-y

Palumbi, S. R., Barshis, D. J., Traylor-Knowles, N., and Bay, R. A. (2014). Mechanisms of reef coral resistance to future climate change. *Science* 344, 895–898. doi: 10.1126/science.1251336

Pérez-Rosales, G., Rouze, H., Torda, G., Bongaerts, P., Pichon, M., Parravicini, V., et al. (2021). Mesophotic coral communities escape thermal coral bleaching in French Polynesia. *R. Soc Open Sci.* 8. doi: 10.1098/rsos.210139

Prasetia, R., Sinniger, F., and Harii, S. (2016). Gametogenesis and fecundity of *Acropora tenella* (Brook 1892) in a mesophotic coral ecosystem in Okinawa, Japan. *Coral Reefs* 35, 53–62. doi: 10.1007/s00338-015-1348-1

Prasetia, R., Sinniger, F., Nakamura, T., and Harii, S. (2022). Limited acclimation of early life stages of the coral *Seriatopora hystrix* from mesophotic depth to shallow reefs. *Sci. Rep.* 12, 12836. doi: 10.1038/s41598-022-16024-6

Pratchett, M. S., Caballes, C. F., Newman, S. J., Wilson, S. K., Messmer, V., and Pratchett, D. J. (2020). Bleaching susceptibility of aquarium corals collected across northern Australia. *Coral Reefs* 39, 663–673. doi: 10.1007/s00338-020-01939-1

Putnam, H. M. (2021). Avenues of reef-building coral acclimatization in response to rapid environmental change. *J. Exp. Biol.* 224. doi: 10.1242/jeb.239319

Queen, J. P., Quinn, G. P., and Keough, M. J. (2002). *Experimental design and data analysis for biologists* (Cambridge university press, United Kingdom).

R Core Team (2021). *R: A Language and Environment for Statistical Computing* (Vienna, Austria: R Foundation for Statistical Computing). Available at: https://www.R-project.org/.

Riegl, B., and Piller, W. E. (2003). Possible refugia for reefs in times of environmental stress. *Int. J. Earth Sci.* 92, 520–531. doi: 10.1007/s00531-003-0328-9

Safaie, A., Silbiger, N. J., McClanahan, T. R., Pawlak, G., Barshis, D. J., Hench, J. L., et al. (2018). High frequency temperature variability reduces the risk of coral bleaching. *Nat. commu.* 9. doi: 10.1038/s41467-018-04074-2

Schoepf, V., Carrion, S. A., Pfeifer, S. M., Naugle, M., Dugal, L., Bruyn, J., et al. (2019). Stress-resistant corals may not acclimatize to ocean warming but maintain heat tolerance under cooler temperatures. *Nat. commu* 10, 4031. doi: 10.1038/s41467-019-12065-0

Schoepf, V., Stat, M., Falter, J. L., and McCulloch, M. T. (2015). Limits to the thermal tolerance of corals adapted to a highly fluctuating, naturally extreme temperature environment. *Sci. Rep.* 5. doi: 10.1038/srep17639

Schramek, T. A., Colin, P. L., Merrifield, M. A., and Terrill, E. J. (2018). Depth-dependent thermal stress around corals in the tropical Pacific Ocean. *Geophys. Res. Lett.* 45, 9739–9747. doi: 10.1029/2018GL078782

Schramek, T. A., Cornuelle, B. D., Gopalakrishnan, G., Colin, P. L., Rowley, S. J., Merrifield, M. A., et al. (2019). Tropical western Pacific thermal structure and its relationship to ocean surface variables: A numerical state estimate and forereef temperature records. *Oceanography* 32, 156–163. doi: 10.5670/oceanog.2019.421

Schwarzer, G., Carpenter, J. R., and Rücker, G. (2015). *Meta-analysis with R* (Springer Cham). doi: 10.1007/978-3-319-21416-0

Seveso, D., Montano, S., Strona, G., Orlandi, I., Galli, P., and Vai, M. (2014). The susceptibility of corals to thermal stress by analyzing Hsp60 expression. *Mar. Environ. Res.* 99, 69–75. doi: 10.1016/j.marenvres.2014.06.008

Shlesinger, T., Grinblat, M., Rapuano, H., Amit, T., and Loya, Y. (2018). Can mesophotic reefs replenish shallow reefs? Reduced coral reproductive performance casts a doubt. *Ecology* 99, 421–437. doi: 10.1002/ecy.2098

Siebeck, U. E., Marshall, N. J., Kluter, A., and Hoegh-Guldberg, O. (2006). Monitoring coral bleaching using a colour reference card. *Coral Reefs* 25, 453–460. doi: 10.1007/s00338-006-0123-8

Sinniger, F., and Harii, S. (2018). "Studies on mesophotic coral ecosystems in Japan," in *Coral Reef Studies of Japan* (Singapore: Springer), 149–162.

Sinniger, F., Morita, M., and Harii, S. (2013). "Locally extinct" coral species *Seriatopora hystrix* found at upper mesophotic depths in Okinawa. *Coral Reefs* 32, 153–153. doi: 10.1007/s00338-012-0973-1

Skirving, W., Marsh, B., de la Cour, J., Liu, G., Harris, A., Maturi, E., et al. (2020). CoralTemp and the coral reef watch coral bleaching heat stress product suite version 3.1. *Remote Sens.* 12, 3856. doi: 10.3390/rs12233856

Skutnik, J. E., Otieno, S., Khoo, S. K., and Strychar, K. B. (2020). Examining the effect of heat stress on *Montastraea cavernosa* (Linnaeus 1767) from a mesophotic coral ecosystem (MCE). *Water* 12. doi: 10.3390/w12051303

Smith, T. B., Gyory, J., Brandt, M. E., Miller, W. J., Jossart, J., and Nemeth, R. S. (2016). Caribbean mesophotic coral ecosystems are unlikely climate change refugia. *Glob. Chang Biol.* 22, 2756–2765. doi: 10.1111/gcb.13175

Spalding, M. D., and Brown, B. E. (2015). Warm-water coral reefs and climate change. *Science* 350, 769–771. doi: 10.1126/science.aad0349

Tavakoli-Kolour, P., Sinniger, F., Morita, M., and Harii, S. (2023). Acclimation potential of *Acropora* to mesophotic environment. *Mar. Pollut. Bull.* 188, 114698. doi: 10.1016/j.marpolbul.2023.114698

Therneau, T. (2015). *A package for survival analysis in S* R package. Available online at: https://CRAN.R-project.org/package=survival

Traylor-Knowles, N. (2019). Heat stress compromises epithelial integrity in the coral, *Acropora hyacinthus*. *Peerj* 7. doi: 10.7717/peerj.6510

Turner, J. A., Andradi-Brown, D. A., Gori, A., Bongaerts, P., Burdett, H. L., Ferrier-Pagès, C., et al. (2019). "Key questions for research and conservation of mesophotic coral ecosystems and temperate mesophotic ecosystems," in *Mesophotic coral ecosystems: Coral reefs of the world*, vol. 12 . Eds. Y. Loya, K. Puglise and T. Bridge (Springer, Cham), 989–1003.

van Hooidonk, R., Maynard, J. A., and Planes, S. (2013). Temporary refugia for coral reefs in a warming world. *Nat. Clim. Change* 3, 508–511. doi: 10.1038/nclimate1829

van Woesik, R., Sakai, K., Ganase, A., and Loya, Y. J. (2011). Revisiting the winners and the losers a decade after coral bleaching. *Mar. Ecol. Prog. Ser.* 434, 67–76. doi: 10.3354/meps09203

Veal, C. J., Carmi, M., Fine, M., and Hoegh-Guldberg, O. (2010). Increasing the accuracy of surface area estimation using single wax dipping of coral fragments. *Coral Reefs* 29, 893–897. doi: 10.1007/s00338-010-0647-9

Wallace, C. C. (1999). *Staghorn Corals of the World: A revision of the genus Acropora* (Collingwood, Australia: CSIRO Publishing).

Wyatt, A. S. J., Leichter, J. J., Toth, L. T., Miyajima, T., Aronson, R. B., and Nagata, T. (2020). Heat accumulation on coral reefs mitigated by internal waves. *Nat. Geosci.* 13, 28–34. doi: 10.1038/s41561-019-0486-4

Wyatt, A. S. J., Leichter, J. J., Washburn, L., Kui, L., Edmunds, P. J., and Burgess, S. C. (2023). Hidden heatwaves and severe coral bleaching linked to mesoscale eddies and thermocline dynamics. *Nat. Commun.* 14, 25. doi: 10.1038/s41467-022-35550-5

frontiers | Frontiers in Marine Science

TYPE Original Research
PUBLISHED 20 September 2023
DOI 10.3389/fmars.2023.1162896

OPEN ACCESS

EDITED BY
Charles Alan Jacoby,
St. Johns River Water Management District, United States

REVIEWED BY
Albert Gabric,
Griffith University, Australia
Keisha D. Bahr,
Texas AandM University Corpus Christi, United States

*CORRESPONDENCE
Peter Butcherine
peter.butcherine@scu.edu.au

RECEIVED 10 February 2023
ACCEPTED 07 August 2023
PUBLISHED 20 September 2023

CITATION
Butcherine P, Tagliafico A, Ellis SL, Kelaher BP, Hendrickson C and Harrison D (2023) Intermittent shading can moderate coral bleaching on shallow reefs. *Front. Mar. Sci.* 10:1162896. doi: 10.3389/fmars.2023.1162896

Intermittent shading can moderate coral bleaching on shallow reefs

Peter Butcherine[1]*, Alejandro Tagliafico[1], Sophia L. Ellis[1], Brendan P. Kelaher[1], Conor Hendrickson[1] and Daniel Harrison[1,2]

[1]National Marine Science Centre, Southern Cross University, Coffs Harbour, NSW, Australia, [2]School of Geosciences, University of Sydney, Sydney, NSW, Australia

The health of coral reefs is declining from the effects of human activity and climate change. Mass coral bleaching is often triggered by elevated water temperature and excessive solar irradiance. Shading can reduce coral bleaching risk. Shading-based management interventions, such as whole-of-reef marine fogging, have been proposed as a conservation tool for periods when coral undergoes excessive thermal stress. This study examined the effect of intermittent shade (30% for 0, 4, or 24 h) on two coral species, *Duncanopsammia axifuga* and *Turbinaria reniformis*, held at either 26.4°C or 32.4°C for 18 days. Coral fragments were assessed for bleaching (relative mean intensity of grey, chlorophyll *a*, and symbiont density), photochemistry (PAM fluorometry), and antioxidant biomarkers (SOD and CAT). Shading responses were species-specific, with *T. reniformis* more responsive to shading than *D. axifuga*. Thirty per cent shading delayed bleaching up to three-degree heat weeks (DHW), and 24 h shade was more protective than 4 h shade. Shading suppressed catalase activity in *T. reniformis*. Overall, our results suggest that intermittently shading corals for 4 h can moderate light stress and slow bleaching in some corals and could improve the efficiency of active solar radiation management in marine ecosystems.

KEYWORDS

irradiance, bleaching, photochemistry, climate change, oxidative stress, solar-radiation management, shading

1 Introduction

The unprecedented decline of coral reefs globally has been robustly documented over the last two decades (De'ath et al., 2012; Hughes et al., 2018a). Coral cover in some iconic ecosystems, such as the Great Barrier Reef, has been reduced by up to 70% (Bell et al., 2014), while at other places, 100% mortality has been reported (Guzman, 1991). Crown-of-thorns predation (De'ath et al., 2012), the severe effects of climate change and ocean acidification, and the increasing frequency and intensity of tropical storms and bleaching

events are considered the main drivers of the current coral crisis (Hughes et al., 2003; Grottoli et al., 2014; Hughes et al., 2018b). Recently, extreme weather events triggered some of the worst mass bleaching events on the Great Barrier Reef during 2016–2017 (Hughes et al., 2017). The aftermath of this third global-scale coral bleaching event showed that the accumulated heat exposure exceeding a critical threshold of 3–4 degree heating weeks (DHW) contributed to bleaching on 91% of reefs, coral cover loss up to 75–100% in some reefs, and an 80% decline in specific species (e.g. staghorn *Acropora*, *Seriatopora hystrix*, *Stylophora pistillata*) (Hughes et al., 2018a; Hughes et al., 2018b).

The most recent Intergovernmental Panel on Climate Change report indicated that global sea surface temperatures would continue to rise even under the lowest emission scenario presented (Cooley et al., 2022). Thus, the frequency and severity of coral bleaching events are expected to increase in the coming decades (Donner, 2009; Jackson et al., 2022). This presents an urgent challenge to develop and implement management interventions that reduce the impacts of environmental stressors on corals and facilitate their recovery following bleaching events (Bay et al., 2019).

It is well known that high irradiance levels coupled with high temperatures can trigger bleaching events (Brown, 1997; Berkelmans, 2002; Courtial et al., 2017; Cropp et al., 2018; Jackson et al., 2018). The possible benefits of coral shading have been demonstrated over several decades of coral research (Wethey and Porter, 1976; Shick et al., 1996; Baker et al., 2008). Previous attempts to shade reefs have been limited and do not operate at a reef scale, i.e., 10's to 100's km^2. In their review of coral shading, Tagliafico et al. (2022) showed several artificial coverings have been used to reduce light intensity and assist coral rehabilitation such as screens (Coles and Jokiel, 1978), aeration and sprinklers (Kramer et al., 2016), awnings (Simpson et al., 2008), shade cloths (Coelho et al., 2017), fabric (Thinesh et al., 2017), and plastic sheeting (Muller and van Woesik, 2009; Muller and van Woesik, 2011). Consequently, shading reefs is a potential solution to reduce irradiance levels reaching corals and may mitigate bleaching, although implementing reef scale solutions remain elusive. Recent projections suggest that by 2040, coral cover on shaded reefs could double that found on unshaded reefs (Condie et al., 2021). Current research attempts to scale shading to the scale of individual reefs or even the entire Great Barrier Reef (e.g. fogging and cloud and sky brightening) (Tollefson, 2021). However, this research is in an early phase, and up-scaling equipment may present a technical and financial challenge (Baker et al., 2021), and the required light attenuation levels and implementation times to reduce the risk of coral bleaching are still unclear (Coelho et al., 2017). Nonetheless, shading the entire Great Barrier Reef is predicted to reduce degree heating weeks (DHW) and could limit coral mortality during severe bleaching events (Harrison et al., 2019).

Some of the shading technologies being trialled on the Great Barrier Reef (i.e., fogging and cloud brightening) require energy (e.g. diesel generator, vessel generator), and improvements in energy consumption and cost-effectiveness are desirable. Satellite imaging and weather models can help to predict when shading technologies may be necessary (Coelho et al., 2017), but variable weather conditions can impact deployment. To assess the effectiveness of intermittent sub-daily shading targeted around peak sunlight, we tested the hypothesis that different levels of shading (4 h and 24 h per day) at two different temperatures [collection site temperature: 26.4°C and four degrees above the maximum monthly mean (28.6°C), reaching 32.6°C] would significantly affect the bleaching response of corals during a high-temperature episode of up to 5 DHW. Coral bleaching is a general stress response of symbiotic corals to a wide variety of environmental stressors that results in the loss of unicellular symbiotic algae in corals (Fitt et al., 2001; Lesser and Farrell, 2004; Ainsworth et al., 2016). Elevated sea temperature and its interaction with excess solar radiation are the key environmental triggers of coral bleaching (Brown, 1997; Fitt et al., 2001; Ainsworth et al., 2016). The interaction between excessive light and water temperature can result in oxidative stress, where excessive generation of reactive oxygen species is the primary cause of coral bleaching (Smith et al., 2005; Suggett et al., 2008; Baird et al., 2009). Superoxide dismutase and catalase are important coral antioxidant defences addressing the products of oxidative stress (Weydert and Cullen, 2010).

We used chlorophyll *a* concentration, symbiont density, and relative mean intensity of grey as bleaching proxies. Pulse amplitude modulation (PAM) fluorometry was used to evaluate symbiont photochemistry. In addition, we used the activity of superoxide dismutase and catalase to assess the antioxidant response to oxidative stress.

2 Materials and methods

2.1 Coral species selection, collection, and preparation

The branching coral, *Duncanopsammia axifuga* was selected due to a demonstrated quick recovery and high survival rate after the fragmentation process, as well as the large coral tissue yield that can be obtained per small fragments of around 3 cm (mean ± SD = 1.01 ± 0.52 g), which allows laboratory analyses of different variables response (Tagliafico et al., 2017; Tagliafico et al., 2018). The plate coral, *Turbinaria reniformis*, was selected as it has been previously used in experiments looking at the effects of different levels of irradiance and other stressors (Courtial et al., 2017; Jones et al., 2020; Dobson et al., 2021).

Colonies of *Duncanopsammia axifuga* and *Turbinaria reniformis* were collected at 10 m depth from Arlington Reef (-16.724°, 146.063°) and Vlasoff Reef (-16.655°, 145.992°), respectively. The water temperature at each collection site was 26.4°C (November 2021), and the maximum monthly mean (MMM) at each collection site was estimated at 28.6°C using eReefs data from the 1 km resolution hydrodynamic model (Steven et al., 2019).

The collected corals were transported to the National Marine Science Centre, Coffs Harbour, New South Wales, Australia (-30.268°, 153.138°), and acclimatised in a 1200 L flow-through filtered seawater tank for one week at 26 ± 0.5°C. Corals were fed

twice with *Artemia salina* (1d old). Afterwards, colonies were fragmented into similar sizes using a Dremel rotary tool with a diamond wheel. No significant differences were found for buoyant weight among fragments of the same species ($p > 0.05$).

A total of 152 fragments (76 per species, 12 replicates per treatment) were acclimatised for an additional week in conditions similar to those described above. Post-acclimation, no supplemental feeding was provided. Each fragment was randomly allocated to one of six treatments (see below). *In-situ* and destructive sampling of coral occurred on four occasions: (i) before starting the experiment [baseline], (ii) after 3.1 DHW [day 13], at 5 DHW [day 19], and (iv) after seven days of recovery [day 26].

2.2 Experimental setup

In the experimental system, 144 x 600 mL experimental tanks were supplied with 100 mL min^{-1} of flow-through, sand-filtered seawater from Charlesworth Bay (-30.267°, 153.141°). The experimental tanks were arranged in orthogonal combinations of temperature (two levels): 1) collection site temperature: 26.4°C, hereafter referred to as lower temperature (LT) and 2) MMM + 4°C: 32.6°C, henceforth higher temperature (HT); and two levels of 30% shade (4h around solar noon and 24 h). Shade cloth that reduced PAR by 30.1 ± 0.85% (mean ± SE, n = 3340) was used for the shaded treatments. For the 4 h shade treatment, the shade cloth was placed over each tank for two hours on either side of solar noon (approximately 10 am to 2 pm), and for the 24 h shade treatment, the shade cloth cover remained in place throughout the experiment. Controls with no shade were established at 26.4°C and 32.6°C. Temperature was maintained at 26 ± 0.5°C and 32.6 ± 0.5°C using heat pumps (2100 Lh^{-1}, EVO-F5, Australia). The higher temperature treatment was increased over a week by 1.1°C per day to reach the experimental temperature of 32.6°C. To minimise possible tank position effects, the experimental tanks were randomly relocated every four days.

2.3 Environmental parameters

Visible light was measured thrice daily (11:00; 13:00 and 15:00) with a LI-250A meter with an attached LI-192 underwater quantum sensor (LI-COR, Nebraska) and over 24 h, with photosynthetic irradiance loggers (Odyssey) placed under direct sunlight and underwater with and without shade, respectively (Supplementary Figure 1). The PAR loggers were calibrated under solar radiation against a recently calibrated LI-250A. A multiplier of –143.68 and –189.66 was applied to calibrate the PAR loggers deployed in air and water, respectively.

Nitrite (0.012 ± 0.008 mg L^{-1} NO_2), phosphate (0.23 ± 0.33 mg L^{-1} PO_4) and alkalinity (163 ± 36 mg L^{-1} $CaCO_3$) were measured from incoming water twice a week with a photometer system (Palintest® model 7100, UK). Dissolved oxygen (HT: 7.78 ± 0.29 mg L^{-1}, LT: 8.03 ± 0.25 mg L^{-1}) and conductivity (HT: 57.61 ± 5.26 mS cm^{-1}, LT: 52.55 ± 5.95 mS cm^{-1}) were recorded thrice daily (11:00, 13:00 and 15:00) with a handheld probe meter (Hach HQ40d).

2.4 In situ sampling

Maximum quantum yield (F_v/F_m) was measured using a diving pulse amplitude modulation (DIVING-PAM©) fluorometer (Heinz Walz GmbH, Germany) from dark-adapted corals after 1 h dark acclimation. Each coral fragment was measured once per sample period. PAM settings were set to avoid low signal or overflow readings (measuring light intensity 8, damping 2, gain 12, actinic light intensity 5, saturation pulse intensity 8, and saturation pulse width 0.8). PAM readings were made with the probe 1 cm from the coral. At the start of the experiment, no significant differences were found in maximum quantum yield among coral fragments within *D. axifuga* ($df = 2, 66$; pseudo-F = 0.28; $p = 0.76$) and *T. reniformis* ($df = 2, 66$; pseudo-F = 1.75; $p = 0.17$).

Each coral was photographed while underwater in their experimental tank from above using a Canon EOS 5D Mark II DSLR camera fitted with a Canon Macro EF 100mm f/2.8L IS USM lens. Camera settings were slightly modified from those suggested by Winters et al. (2009), ISO-100, F = 3.5, 1/60 and white balance manually set to 6000 K. Each image contained a white tile as a true colour reference. The camera was mounted on a video tripod with a centred mid-level spreader (Cayer BV30L, China). A Neewer T120 18W filming light (WB 5600 K, brightness 100%) was mounted on a different tripod (Evo-2 mini tripod, Manfrotto, Italy) 15 cm from the coral angled 30° off-nadir. The camera was manually focused using the two-step expanded focus (10X) function, accounting for differences in fragment shape. The tripod position (camera and light) and distance between the camera lens and coral were consistent for all pictures.

Each photograph was analysed using ImageJ (ver. 1.53k) following Amid et al. (2018) and Mclachlan and Grottoli (2021). Images were converted to 8-bit greyscale and the mean grey value for twenty 60-pixel diameter (~1 mm) areas in each image was collected. These values were normalised to a white reference and then averaged to obtain the mean intensity of grey (MIG). The relative MIG was calculated using the initial and final MIG values (Amid et al., 2018). At the start of the experiment, there was no significant difference in MIG among fragments of *D. axifuga* ($df = 2, 66$; pseudo-F = 0.45; $p = 0.64$) and *T. reniformis* ($df = 2, 66$; pseudo-F = 0.1; $p = 0.90$).

2.5 Tissue collection

Tissue from four coral fragments from each of the six treatments (n = 24 per species) was extracted using an air pistol connected to an electric 1 HP air compressor delivering air at 40 L min^{-1} at 7 bar (Black Ridge, Australia) by adding 0.6 mL or 1.2 mL of 0.1 M phosphate-buffered saline (PBS, Sigma Aldrich: P3813) for *D. axifuga* and *T. reniformis*, respectively. Individual plastic bags were used to maximise tissue recovery which was subsampled into

vials for chlorophyll *a* and symbiont density and for enzymatic analysis and snap frozen (Rangel et al., 2019).

2.6 Laboratory analyses

Tissues for chlorophyll *a* and symbiont density were lysed in 0.8 mL of ice-cold 0.1 M PBS using a TissueLyser LT (Qiagen) at 40 Hz for 120 s. The resulting lysate was centrifuged at 3500 ×*g* (4°C) for 5 min (Beckman Coulter, USA), and the supernatant was discarded. The pellet was resuspended in 0.8 mL PBS and centrifuged with the same settings, and the supernatant was discarded. The pellet was then resuspended in 1.6 mL of PBS, and 0.8 mL was aliquoted for chlorophyll *a* analysis. The remainder of the sample was used to determine symbiont density using a Leica DM750 compound microscope and a Neubauer haemocytometer.

The aliquot for chlorophyll analysis was centrifuged with the same settings as above and the supernatant discarded. Chlorophyll *a* was extracted using 0.8 mL of 100% undenatured ethanol and incubated without light at 4°C overnight (Ritchie, 2006). Chlorophyll *a* concentration was determined by absorbance at 629 and 665 nm following Warren (2008) and quantified using Ritchie (2006). Chlorophyll and symbiont density data were normalised against surface area, obtained using the wax dipping method (Veal et al., 2010) for *D. axifuga* and the aluminium foil technique (Marsh, 1970) for *T. reniformis*.

Tissues for enzyme analysis were homogenised in cold 0.1 M Trizma-HCl (pH 7.4) with 0.5% Triton X-100, 5 nM β-mercaptoethanol and protease inhibitor cocktail (Sigma Aldrich: P2714) for 180s at 50 Hz. The homogenate was centrifuged at 14000 ×*g* at 4°C for 10 min and the supernatant collected for analysis of SOD and CAT activity. Superoxide dismutase (SOD) activity was estimated using the SOD Activity kit (Sigma Aldrich: CS0009). SOD activity was estimated by comparison to an inhibition curve, normalised to protein content, and reported as U mg^{-1} protein, where 1 unit of SOD inhibits the rate of reduction of cytochrome c by 50% in a coupled xanthine and xanthine oxidase system.

Catalase (CAT) activity was estimated following Aebi (1984) and Li and Schellhorn (2007) using 0.01 M H_2O_2 as a substrate in a UV transparent microplate (Merck: CLS3635) at 240 nm. CAT activity was calculated using an extinction coefficient of 43.6 M^{-1} cm^{-1} and expressed as nmol min^{-1} mg^{-1} protein. Soluble protein content was determined at 595 nm following Bradford (1976) and used to normalise enzyme activity. All assays were completed on a BMG FLUOstar® Omega microplate reader (BMG Labtech, Australia) and corrected for path length.

2.7 Statistical analysis

Permutational multivariate analysis of variance (PERMANOVA, Anderson, 2017) was used to test for significant differences in SOD and CAT activity, growth, chlorophyll *a*, and symbiont concentration for each species using PRIMER + PERMANOVA v7 (PRIMER-e). A two-factor PERMANOVA model tested for significant differences within each sample event according to temperature (fixed, 2-levels: 26.4°C and 32.6°C) and shading (fixed, 3-levels: control (no shade), 4 h, and 24 h shade) and their interactions. Univariate PERMANOVA using the same model tested for significant differences in relative mean intensity of grey and maximum quantum yield within each sample event. Pairwise comparisons were run when the main factor or their interaction terms were significant. All analyses were based on a Euclidean distance dissimilarity matrix.

The potential effect of coral genotype was included in tests at each sample event, and no significant difference was found among genotypes within each treatment for any of the tests. Therefore, the coral genotype was not a significant factor in the bleaching responses detected.

3 Results

There was a significant temperature and shade effect, but no interaction for relative MIG in *D. axifuga* and *T. reniformis* on day 13 (Table 1). After 13 days, shading for either 4 or 24 h significantly reduced bleaching compared to the unshaded corals in each species (Figures 1A, D), and less bleaching occurred in the 24 h than the 4 h shaded corals. The colouration of *D. axifuga* shaded for 24 h improved compared to the initial measurement (Figure 1A). A significant temperature effect was found at 19 and 26 days for *D. axifuga* (Table 1). The higher temperature increased bleaching in *D. axifuga* compared to the lower temperature (Figures 1A–C). A significant shade × temperature interaction was detected for relative MIG for *T. reniformis* after 19 and 26 days (Table 1). A similar bleaching trend was found for each day. After 19 and 26 days, less bleaching occurred in *T. reniformis* at the lower compared to the higher temperature (Figures 1E, F). At the lower temperature, less bleaching occurred as shade duration increased in *T. reniformis*. At the higher temperature, *T. reniformis* bleaching was unaffected by shading. Bleaching of unshaded *T. reniformis* was similar at either temperature after 19 days (Figures 1E, F).

Higher temperature significantly reduced the maximum quantum yield (F_v/F_m) of *D. axifuga* and *T. reniformis* at day 13 and day 19 compared to the lower temperature (Table 1; Figure 2). F_v/F_m of *T. reniformis* remained lower in the higher temperature at day 26 (Figure 2E). A significant shading effect was found for F_v/F_m in *T. reniformis* at days 13, 19, and 26 (Table 1). On day 13, F_v/F_m in *T. reniformis* was significantly higher with 24 h shade than with 4 h or no shade (Figure 2C). By day 19, the F_v/F_m of the 4 h shaded *T. reniformis* had recovered slightly to be similar to the 24 h shade treatment, while F_v/F_m of the unshaded coral was significantly lower than the 24 h shaded coral (Figure 2D). By day 26, F_v/F_m in the 24 h shaded *T. reniformis* was significantly higher than the 4 h shaded and unshaded coral (Figure 2E). The maximum quantum yield of *D. axifuga* was unaffected by shading.

Chlorophyll *a* was significantly reduced by higher temperature in *D. axifuga* and *T. reniformis* on days 13 and 19, and in *D. axifuga* on day 26 (Table 1). A significant shade × temperature interaction was detected for chlorophyll *a* in *T. reniformis* on day 19 (Figure 3A). Higher temperature significantly reduced chlorophyll

10.3389/fmars.2023.1162896

TABLE 1 PERMANOVA summaries using a 2-factor model (shading: 3 levels and temperature: 2 levels) for *Duncanopsammia axifuga* and *Turbinaria reniformis* exposed to either a higher (32.6°C) or lower (26.4°C) water temperature and unshaded or shaded for 4 or 24 h per day after 13 and 19 days and after a 7d recovery (Day 26).

	Duncanopsammia axifuga						*Turbinaria reniformis*					
	Shade		Temp		Shade × Temp		Shade		Temp		Shade × Temp	
Day 13	F	p	F	p	F	p	F	p	F	p	F	p
MIG	7.66	< **0.01**	5.91	**0.03**	2.33	0.11	14.89	< **0.01**	10.87	< **0.01**	2.24	0.10
F_v/F_m	0.74	0.48	6.46	**0.02**	0.11	0.90	4.32	**0.02**	12.70	< **0.01**	0.04	0.96
SOD	1.45	0.26	0.88	0.36	2.71	0.10	0.58	0.59	0.73	0.41	0.45	0.68
Catalase	1.30	0.29	0.31	0.61	1.27	0.34	3.54	**0.05**	0.01	0.99	0.01	0.99
Chl *a*	0.37	0.68	6.99	**0.02**	2.32	0.13	1.10	0.35	7.76	**0.02**	3.24	0.06
Symbiont	2.43	0.11	19.72	< **0.01**	2.44	0.113	6.64	< **0.01**	2.48	0.14	0.16	0.88
All biomarkers (multivariate)												
	1.19	0.32	6.99	< **0.01**	1.38	0.22	3.22	<**0.01**	2.07	0.09	1.02	0.42
Day 19												
MIG	0.17	0.84	8.72	**0.01**	0.10	0.90	13.45	< **0.01**	14.12	< **0.01**	7.59	< **0.01**
F_v/F_m	1.01	0.38	10.91	< **0.01**	0.17	0.82	3.86	< **0.01**	10.58	< **0.01**	2.63	0.07
SOD	1.579	0.23	0.232	0.66	0.40	0.73	0.91	0.47	0.55	0.51	0.64	0.55
Catalase	1.22	0.31	0.42	0.50	0.83	0.43	6.97	< **0.01**	5.64	**0.03**	3.03	0.08
Chl *a*	1.30	0.31	38.37	< **0.01**	1.62	0.23	3.12	0.06	5.10	**0.05**	7.429	< **0.01**
Symbiont	1.57	0.22	7.94	**0.01**	0.535	0.61	23.03	< **0.01**	74.75	< **0.01**	2.78	0.09
All biomarkers (multivariate)												
	1.92	0.07	8.47	< **0.01**	0.89	0.53	5.19	<**0.01**	4.61	<**0.01**	2.16	**0.04**
Day 26												
MIG	1.41	0.27	18.49	< **0.01**	0.18	0.81	4.87	**0.01**	10.48	< **0.01**	8.38	< **0.01**
F_v/F_m	1.18	0.35	3.44	0.08	0.05	0.94	4.99	**0.03**	6.35	**0.03**	2.578	0.09
SOD	0.12	0.89	2.72	0.11	1.06	0.39	0.16	0.93	1.90	0.18	0.36	0.81
Catalase	0.88	0.43	0.01	0.94	1.79	0.18	2.94	0.07	2.01	0.17	0.76	0.47
Chl *a*	1.32	0.30	5.61	**0.02**	0.78	0.48	0.37	0.57	0.95	0.37	0.93	0.44
Symbiont	2.38	0.11	18.67	< **0.01**	2.97	0.07	22.28	< **0.01**	26.45	< **0.01**	2.015	0.14
All biomarkers (multivariate)												
	1.57	0.15	9.61	< **0.01**	1.61	0.14	2.74	< **0.01**	3.50	< **0.01**	0.78	0.66

Bold values indicate a significant result ($p < 0.05$).

a in unshaded *T. reniformis*, and shading reduced chlorophyll *a* in the 24 h shade treatment compared to the 4 h shaded and unshaded coral (Figure 3A). Higher temperature significantly reduced symbiont density for *D. axifuga* on days 13, 19, and 26, and for *T. reniformis* on days 19 and 26 (Table 1). A significant shading effect was found for symbiont density in *T. reniformis* on days 13, 19, and 26 (Table 1). Symbiont density was significantly higher in the 24 h shaded *T. reniformis* than the 4 h or unshaded coral (Figure 3B). On day 19, symbiont density was significantly greater in the shaded compared to the unshaded *T. reniformis*. By day 26, symbiont density increased significantly as the shade duration increased (Figure 3B). Shading or temperature did not affect symbiont density in *D. axifuga* (Table 1).

Catalase activity was significantly greater in the unshaded than the shaded *T. reniformis* at days 13 and 19 (Table 1; Figure 4). Higher temperature increased catalase activity in *T. reniformis* on day 19 (Table 1). Neither shade nor temperature affected catalase in *D. axifuga* on days 13, 19, or 26. Superoxide dismutase activity was not significantly affected by temperature or shading in *D. axifuga* or *T. reniformis* (Table 1).

10.3389/fmars.2023.1162896

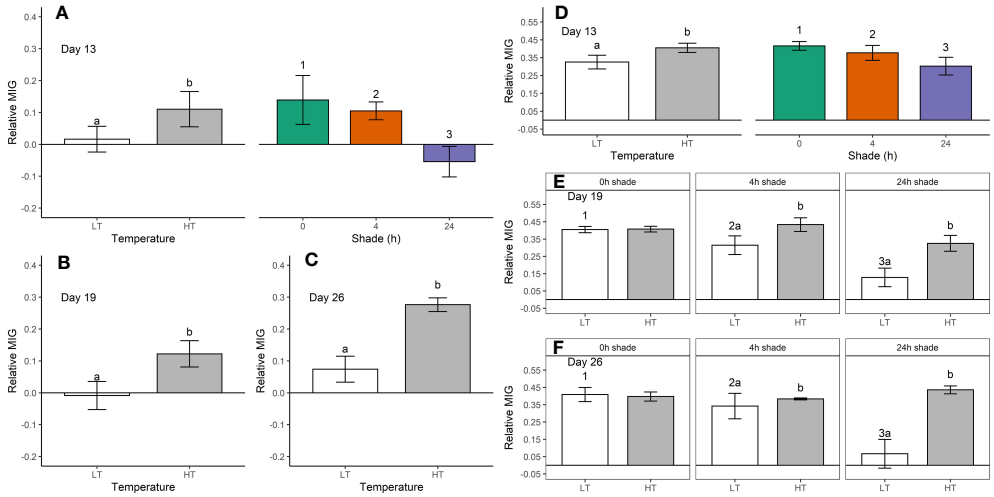

FIGURE 1
Relative mean intensity of grey (MIG, mean ± SE) in *Duncanopsammia axifuga* **(A-C)** and *Turbinaria reniformis* **(D–F)** shaded for 0, 4, or 24 h daily at a higher temperature (HT, 32.6°C) or a lower temperature (LT, 26.4°C) after day 13 **(A, D)**, day 19 **(B, E)**, and day 26 **(C, F)**. Only the significant results are shown where letters indicate a significant difference between temperatures, and numbers indicate significant differences among shade treatments within each day.

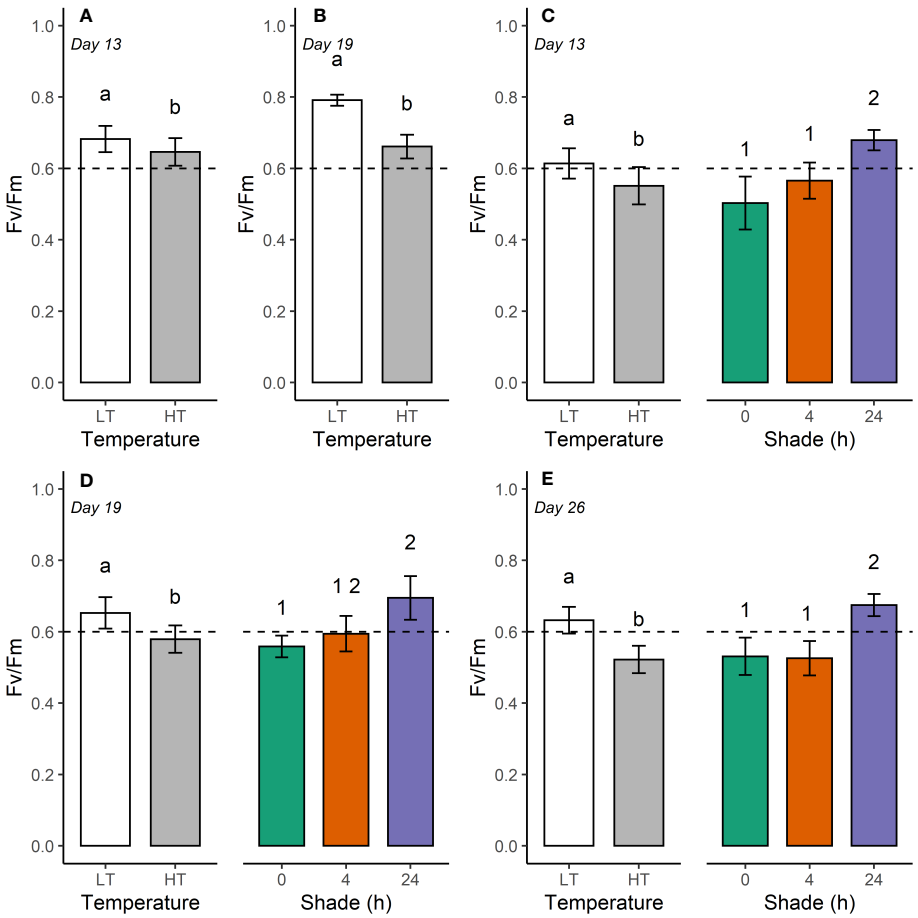

FIGURE 2
Maximum quantum yield (F_v/F_m, mean ± SE) for *Duncanopsammia axifuga* **(A, B)** and *Turbinaria reniformis* **(C–E)** held at 26.4°C (LT) and 32.6°C (HT) at day 13, 19, and 26. The dashed horizontal line indicates a lower threshold for F_v/F_m for healthy coral of 0.6. Letters indicate a significant difference between temperatures, and numbers denote a significant difference among shade treatments.

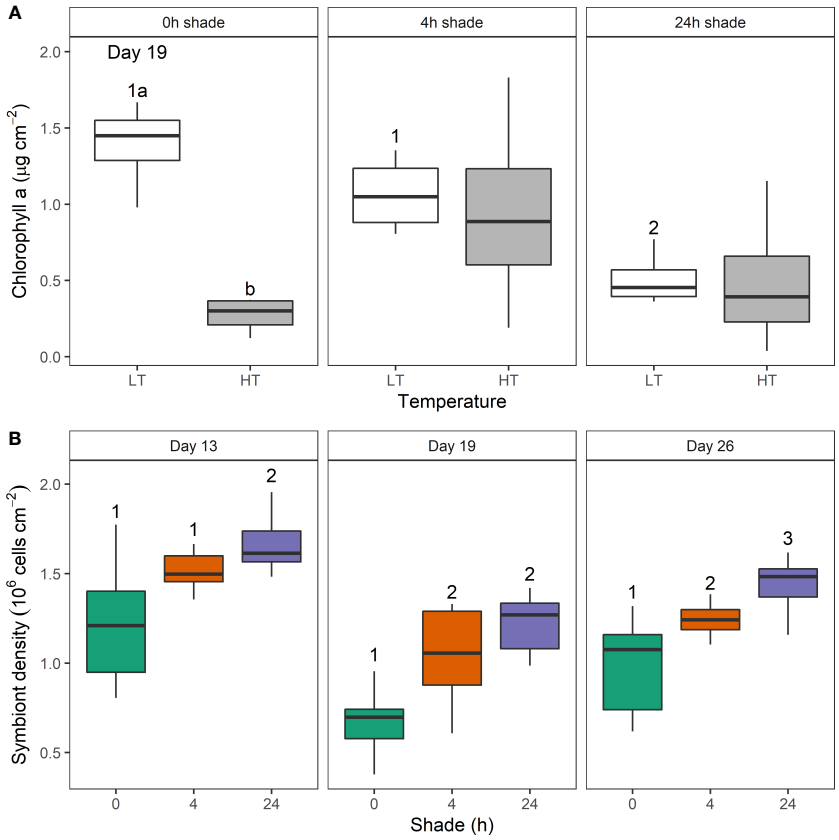

FIGURE 3
The effect of shade duration (0, 4, or 24 h) and higher (HT) and lower temperature (LT) on **(A)** chlorophyll *a* concentration (µg cm^{-2}) from *Turbinaria reniformis* on day 19 and **(B)** symbiont density (10^6 cells cm^{-2}) on day 13, 19, and 26. Box plots show the percentiles (25, 50, and 75%) and range. Letters show a significant temperature difference within shade treatment, and numbers indicate a significant difference among shade treatments each day.

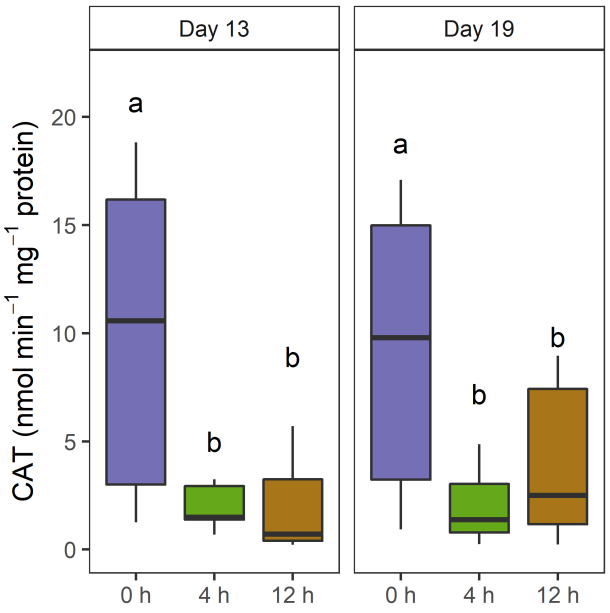

FIGURE 4
Catalase activity (nmol min^{-1} mg^{-1} protein) in *Turbinaria reniformis* tissue at day 13 and 19 when shaded for 0, 4, and 24 h. The letters indicate significant differences within each day.

4 Discussion

Intermittently shading corals by 30% for 4 h per day can delay bleaching in a thermally stressed shallow coral species, *T. reniformis*. Conversely, *D. axifuga* responded to 24 h shading until 3 DHW, but was unresponsive to shading as the degree heat weeks increased. Thermal stress had the most significant effect on bleaching in these two species, and as the thermal stress increased, the beneficial effect of intermittent shading declined. The novel shading regime, of 30% shading for 4 h around solar noon, slowed bleaching, and the decline of chlorophyll *a* and symbiont density and reduced antioxidant activity. Intermittent shading has the potential to moderate the projected impacts of warming oceans on at-risk corals during bleaching events.

Thermal stress had the greatest effect on bleaching of *D. axifuga* and *T. reniformis*. Elevated water temperature is the primary stressor of many bleaching events (Coles et al., 1976; Berkelmans, 2002; Ainsworth et al., 2016; Sully et al., 2019), where heat stress leads to a breakdown of biochemical and physiological pathways (Fitt et al., 2001). Bleaching reduces coral colouration either by ejection of symbionts, shuffling or loss of chlorophyll or symbionts or both (Brown and Dunne, 2015). *Turbinaria reniformis* and *D. axifuga* showed a decrease in chlorophyll *a* and symbiont density at

higher temperatures, resulting in an elevated relative MIG and decreased maximum quantum yield. Coral responses to thermal stress are well known; subsequently, the response to the novel shading regime will be the focus of the remainder of this discussion.

Shading reduced relative MIG and catalase activity, moderating the bleaching of *T. reniformis*, with relative MIG lower when shading corals continuously. Reduced antioxidant activity suggests reactive oxygen species production decreased, limiting a key mechanism of the bleaching response in thermal and/or light-stressed corals (Downs et al., 2002; Higuchi et al., 2008; Krueger et al., 2015; Wietheger et al., 2018). Continual shading of thermally stressed *Acropora muricata*, *Pocillopora damicormis*, and *Porites cylindrica* by either 50 or 75% was very effective at reducing bleaching until 4 DHW and offered some protection up to 8 DHW, and the heavier shading was more effective (Coelho et al., 2017). Here, 30% shade for 4 h reduced bleaching of *T. reniformis* up to 3 DHW, after which the protection decreased up to 5 DHW. Although the protection offered by the 30% shading was less than that shown by Coelho et al. (2017) using higher levels of shade. This is a particularly relevant result as there is a 40% probability of severe mass bleaching on the Great Barrier Reef bleaching at 3 DHW (Hughes et al., 2017), and 30% shade may be more achievable over reef scale areas. However, further work is needed to establish the shading level required for other coral species and the physiological and biological responses to intermittent shading.

Shading delayed the decline of maximum quantum yield indicating reduced physiological stress. The decline in PSII efficiency during bleaching has been well described (Jones et al., 1998; Hill et al., 2012; Roth, 2014) and is likely caused by damage to the D1 protein (Warner et al., 1999). Declining PSII efficiency can lead to the accumulation of reactive oxygen species, damaging cellular membranes and triggering bleaching (Downs et al., 2002). Furthermore, loss of PSII efficiency can significantly impact coral nutritional status where symbiote-derived products can account for up to 30% of total nitrogen (Bythell, 1988) and 95% of carbon for growth, reproduction, and maintenance (Muscatine and Porter, 1977; West and Salm, 2003). Slowing the decline in maximum quantum yield by shading corals, can reduce reactive oxygen species production and maintain coral energy reserves for recovery when stressors decrease. Energy reserves are particularly important in oligotrophic waters where coral reefs abound.

Interspecific differences existed in the bleaching response between *D. axifuga* and *T. reniformis*. *T. reniformis* responded to shading, whereas *D. axifuga* was less responsive to shading. The interaction of light with temperature is subtle and is more pronounced at the thermal limits of a coral (Coles and Jokiel, 1978). Pratchett et al. (2020) showed that a significant bleaching response in *D. axifuga* in warming waters was exacerbated by high light intensity. The limited response of *D. axifuga* to shading in the present study suggests that the coral may not be at its thermal limit, although it is unclear if it is above or below the thermal limit. Furthermore, bleaching susceptibility can vary due to nutritional status (Hoogenboom et al., 2012; Beraud et al., 2013), morphological (Brown and Dunne, 2015), physiological (Dias et al., 2019), or symbiont variation (Hoadley et al., 2016), and acclimation to differing thermal or light conditions (Fitt et al., 2001). Regardless of the cause, a range of responses to shading can be expected and understanding the interactions between environmental conditions and the long-term health of corals is critical for managing potential shading interventions (Bay et al., 2019). Further studies are needed to assess coral responses to short-term localised shading and should include a multifactorial approach with a range of environmental variables, such as ocean acidification and nutrient loading.

Intermittent shading could reduce the costs associated with active marine ecosystem management. Shading corals is an unconventional local strategy to minimise the impacts of temperature and carbon dioxide as global stressors of marine ecosystems (Rau et al., 2012; Tagliafico et al., 2022). The success of many of these shading interventions depends on water and atmospheric conditions (Bay et al., 2019). For example, in-water interventions such as shade cloth deployment (Coelho et al., 2017) depend on wave conditions and currents, while atmospheric conditions affect interventions such as smoke generation (Russell et al., 2013) or marine cloud brightening or fogging (Harrison et al., 2019). Interventions could be targeted in response to bleaching forecasts or, more broadly, over the high-risk summer months (Berkelmans, 2002; Coelho et al., 2017) as weather conditions permit. Targeted intermittent deployment of energy-intensive interventions, such as marine fogging or cloud brightening, shorten operating time, reduce power consumption, and could lower operational and maintenance expenses. The intermittent deployment of in-water shading, such as shade cloths, reduces the risks of invasive species, algal overgrowth, and the potential to shelter more sensitive coral species or symbionts less adapted to the prevailing conditions that may be impacted when shading is removed (Donner, 2009, Hughes 2018a). However, further research is necessary to investigate the indirect effects of these novel shading techniques. The bleaching protection shown here indicates that 30% shading for 4 h is sufficient to delay bleaching and improve the viability of active interventions that depend on variable climatic conditions.

Temperature is the predominant stressor during bleaching events; however, solar radiation management can delay bleaching responses up to 3 DHW, beyond which the protective benefits of intermittent shading diminish. Intermittent shading delayed the decline in relative bleaching and maximum quantum yield, symbiont density, and chlorophyll a concentration. Shading of *T. reniformis* reduced catalase activity, indicating decreased reactive oxygen species production, a key driver of coral bleaching. Shading responses were species-specific, with *T. reniformis* more responsive to shading than *D. axifuga*, possibly due to thermal stress susceptibility. Overall, practical management interventions at appropriate scales (e.g. reef scale marine fogging) could be targeted to periods of maximum coral vulnerability and suitable environmental conditions for deployment, lowering costs and reducing the risk of invasive species while protecting marine ecosystems.

Data availability statement

The raw data supporting the conclusions of this article will be made available by the authors, without undue reservation.

Ethics statement

Ethical approval was not required for the study involving animals in accordance with the local legislation and institutional requirements because it is not required for research involving corals.

Author contributions

PB: Data curation, Formal analysis, Investigation, Visualisation, Writing – original draft. AT: Conceptualisation, Investigation, Methodology, Writing – original draft. SE: Investigation, Writing – review and editing. BK: Methodology, Writing – review and editing. CH: Investigation, Writing – review and editing. DH: Conceptualisation, Methodology, Supervision, Funding acquisition, Writing – review and editing. All authors contributed to the article and approved the submitted version.

Funding

This work was undertaken for the Reef Restoration and Adaptation Program (Cooling and shading sub-program), funded by the partnership between the Australian Government's Reef Trust and the Great Barrier Reef Foundation.

Acknowledgments

We extend our deepest respect and recognition to all Traditional Owners of the Gumbaynggirr country where this study was conducted and to all Traditional Owners of the Great Barrier Reef and its Catchments as First Nations Peoples holding the hopes, dreams, traditions and cultures of the Reef.

Conflict of interest

The authors declare that the research was conducted in the absence of any commercial or financial relationships that could be construed as a potential conflict of interest.

Publisher's note

Supplementary material

The Supplementary Material for this article can be found online at: https://www.frontiersin.org/articles/10.3389/fmars.2023.1162896/full#supplementary-material

References

Aebi, H. (1984). Catalase in *vitro*. *Methods Enzymol.* 105, 121–126. doi: 10.1016/s0076-6879(84)05016-3

Ainsworth, T. D., Heron, S. F., Ortiz, J. C., Mumby, P. J., Grech, A., Ogawa, D., et al. (2016). Climate change disables coral bleaching protection on the Great Barrier Reef. *Science* 352 (6283), 338–342. doi: 10.1126/science.aac7125

Amid, C., Olstedt, M., Gunnarsson, J. S., Le Lan, H., Tran Thi Minh, H., Van den Brink, P. J., et al. (2018). Additive effects of the herbicide glyphosate and elevated temperature on the branched coral *Acropora formosa* in Nha Trang, Vietnam. *Environ. Sci. pollut. Res. Int.* 25 (14), 13360–13372. doi: 10.1007/s11356-016-8320-7

Anderson, M. J. (2017). "Permutational multivariate analysis of variance (PERMANOVA)," in *Wiley statsRef: statistics reference online* (eds. N. Balakrishnan, T. Colton, B. Everitt, W. Piegorsch, F. Ruggeri and J. L. Teugels), 1–15. doi: 10.1002/9781118445112.stat07841

Baird, A. H., Bhagooli, R., Ralph, P. J., and Takahashi, S. (2009). Coral bleaching: the role of the host. *Trends Ecol. Evol.* 24 (1), 16–20. doi: 10.1016/j.tree.2008.09.005

Baker, P., Alroe, J., Tagliafico, A., Ellis, S., Harrison, L., Hernandez, D., et al. (2021). Fogging feasibility stage 1 report, In *A Report Provided to the Australian Government by the Reef Restoration and Adaptation Program* (Townsville: Reef Restoration and Adaptation Program).

Baker, A. C., Glynn, P. W., and Riegl, B. (2008). Climate change and coral reef bleaching: An ecological assessment of long-term impacts, recovery trends and future outlook. *Estuar. Coast. Shelf Sci.* 80 (4), 435–471. doi: 10.1016/j.ecss.2008.09.003

Bay, L. K., Rocker, M., Bostrom-Einarsson, L., Babcock, R. C., Buerger, P., Cleves, P., et al. (2019). *Reef restoration and adaptation program: intervention technical summary. A report provided to the Australian Government by the Reef Restoration and Adaptation Program*. (89pp).

Bell, P. R., Elmetri, I., and Lapointe, B. E. (2014). Evidence of large-scale chronic eutrophication in the Great Barrier Reef: Quantification of chlorophyll a thresholds for sustaining coral reef communities. *AMBIO* 43 (3), 361–376. doi: 10.1007/s13280-013-0443-1

Beraud, E., Gevaert, F., Rottier, C., and Ferrier-Pages, C. (2013). The response of the scleractinian coral *Turbinaria reniformis* to thermal stress depends on the nitrogen status of the coral holobiont. *J. Exp. Biol.* 216 (Pt 14), 2665–2674. doi: 10.1242/jeb.085183

Berkelmans, R. (2002). Time-integrated thermal bleaching thresholds of reefs and their variation on the Great Barrier Reef. *Mar. Ecol. Prog. Ser.* 229, 73–82. doi: 10.3354/meps229073

Bradford, M. M. (1976). A rapid and sensitive method for the quantitiation of microgram quantities of protein utilizing the principle of protein-dye binding. *Anal. Biochem.* 72), 248–254. doi: 10.1016/0003-2697(76)90527-3

Brown, B. E. (1997). Coral bleaching: Causes and consequences. *Coral Reefs* 16 (0), S129–S138. doi: 10.1007/s003380050249

Brown, B. E., and Dunne, R. P. (2015). Coral Bleaching: The roles of sea temperature and solar radiation. *Dis. Coral.* 18, 266–283. doi: 10.1002/9781118828502.ch18

Bythell, J. C. (1988). "A total nitrogen and carbon budget for the elkhorn coral *Acropora palmata* (Lamark)," in *Proceedings of the 6th International Coral Reef Symposium*, Townsville, Australia.

Coelho, V., Fenner, D., Caruso, C., Bayles, B. R., Huang, Y., and Birkeland, C. (2017). Shading as a mitigation tool for coral bleaching in three common Indo-Pacific species. *J. Exp. Mar. Biol. Ecol.* 497, 152–163. doi: 10.1016/j.jembe.2017.09.016

Coles, S. L., and Jokiel, P. L. (1978). Synergistic effects of temperature, salinity and light on the hermatypic coral *Montipora verrucosa*. *Mar. Biol.* 49 (3), 187–195. doi: 10.1007/BF00391130

Coles, S. L., Jokiel, P. L., and Lewis, C. R. (1976). Thermal tolerance in tropical versus subtropical Pacific reef corals. *Pacific Science*. 30 (2), 159–166.

Condie, S. A., Anthony, K. R. N., Babcock, R. C., Baird, M. E., Beeden, R., Fletcher, C. S., et al. (2021). Large-scale interventions may delay decline of the Great Barrier Reef. *R. Soc. Open Sci.* 8 (4), 201296. doi: 10.1098/rsos.201296

Cooley, S., Schoeman, D., Bopp, L., Boyd, P., Donner, S., Ghebrehiwet, D. Y., et al. (2022). "Oceans and coastal ecosystems and their services," in *Climate change 2022: impacts, adaptation and vulnerability*. Eds. H.-O. Pörtner, D. C. Roberts, M. Tignor, E. S. Poloczanska, K. Mintenbeck, A. Alegría, M. Craig, S. Langsdorf, S. Löschke, V. Möller, A. Okem and andB. Rama (UK and New York: Cambridge University Press) pp. 379–550. doi: 10.1017/9781009325844.005

Courtial, L., Roberty, S., Shick, J. M., Houlbrèque, F., and Ferrier-Pagès, C. (2017). Interactive effects of ultraviolet radiation and thermal stress on two reef-building corals. *Limnol. Oceanog.* 62 (3), 1000–1013. doi: 10.1002/lno.10481

Cropp, R., Gabric, A., van Tran, D., Jones, G., Swan, H., and Butler, H. (2018). Coral reef aerosol emissions in response to irradiance stress in the Great Barrier Reef, Australia. *AMBIO* 47 (6), 671–681. doi: 10.1007/s13280-018-1018-y

De'ath, G., Fabricius, K. E., Sweatman, H., and Puotinen, M. (2012). The 27-year decline of coral cover on the Great Barrier Reef and its causes. *Proc. Natl. Acad. Sci. U.S.A.* 109 (44), 17995–17999. doi: 10.1073/pnas.1208909109

Dias, M., Ferreira, A., Gouveia, R., Madeira, C., Jogee, N., Cabral, H., et al. (2019). Long-term exposure to increasing temperatures on scleractinian coral fragments reveals oxidative stress. *Mar. Environ. Res.* 150, 104758. doi: 10.1016/j.marenvres.2019.104758

Dobson, K. L., Ferrier-Pagès, C., Saup, C. M., and Grottoli, A. G. (2021). The effects of temperature, light, and feeding on the physiology of *Pocillopora damicornis*, *Stylophora pistillata*, and *Turbinaria reniformis* corals. *Water* 13 (15), 1–20. doi: 10.3390/w13152048

Donner, S. D. (2009). Coping with commitment: Projected thermal stress on coral reefs under different future scenarios. *PloS One* 4 (6), e5712. doi: 10.1371/journal.pone.0005712

Downs, C. A., Fauth, J. E., Halas, J. C., Dustan, P., Bemiss, J., and Woodley, C. M. (2002). Oxidative stress and seasonal coral bleaching. *Free Radical Biol. Med.* 33 (4), 533–543. doi: 10.1016/S0891-5849(02)00907-3

Fitt, W. K., Brown, B. E., Warner, M. E., and Dunne, R. P. (2001). Coral bleaching: Interpretation of thermal tolerance limits and thermal thresholds in tropical corals. *Coral Reefs* 20 (1), 51–65. doi: 10.1007/s003380100146

Grottoli, A. G., Warner, M. E., Levas, S. J., Aschaffenburg, M. D., Schoepf, V., McGinley, M., et al. (2014). The cumulative impact of annual coral bleaching can turn some coral species winners into losers. *Glob Chang Biol.* 20 (12), 3823–3833. doi: 10.1111/gcb.12658

Guzman, H. M. (1991). Restoration of coral reefs in Pacific Costa Rica. *Conserv. Biol.* 5 (2), 189–194. doi: 10.1111/j.1523-1739.1991.tb00123.x

Harrison, D. P, Baird, M., Harrison, L., Utembe, S., Schofield, R., Escobar Correa, R., et al. (2019). *Reef restoration and adaptation program: Environmental modelling of large scale solar radiation management. A report provided to the Australian Government by the Reef Restoration and Adaptation Program*. (83pp).

Higuchi, T., Fujimura, H., Arakaki, T., and Oomori, T. (2008). "Activities of antioxidant enzymes (SOD and CAT) in the coral *Galaxea fascicularis* against increased hydrogen peroxide concentrations in seawater," in *11th International Coral Reef Symposium*, Ft. Lauderdale, Florida.

Hill, R., Larkum, A. W. D., Prášil, O., Kramer, D. M., Szabó, M., Kumar, V., et al. (2012). Light-induced dissociation of antenna complexes in the symbionts of scleractinian corals correlates with sensitivity to coral bleaching. *Coral Reefs* 31 (4), 963–975. doi: 10.1007/s00338-012-0914-z

Hoadley, K. D., Pettay, D. T., Grottoli, A. G., Cai, W.-J., Melman, T. F., Levas, S., et al. (2016). High-temperature acclimation strategies within the thermally tolerant endosymbiont *Symbiodinium trenchii* and its coral host, *Turbinaria reniformis*, differ with changing pCO_2 and nutrients. *Mar. Biol.* 163 (6), 1–13. doi: 10.1007/s00227-016-2909-8

Hoogenboom, M. O., Campbell, D. A., Beraud, E., Dezeeuw, K., and Ferrier-Pages, C. (2012). Effects of light, food availability and temperature stress on the function of photosystem II and photosystem I of coral symbionts. *PloS One* 7 (1), e30167. doi: 10.1371/journal.pone.0030167

Hughes, T. P., Anderson, K. D., Connolly, S. R., Heron, S. F., Kerry, J. T., Lough, J. M., et al. (2018a). Spatial and temporal patterns of mass bleaching of corals in the Anthropocene. *Science* 359 (6371), 80–83. doi: 10.1126/science.aan8048

Hughes, T. P., Baird, A. H., Bellwood, D. R., Card, M., Connolly, S. R., Folke, C., et al. (2003). Climate change, human impacts, and the resilience of coral reefs. *Science* 301 (5635), 929–933. doi: 10.1126/science.1085046

Hughes, T. P., Kerry, J. T., Alvarez-Noriega, M., Alvarez-Romero, J. G., Anderson, K. D., Baird, A. H., et al. (2017). Global warming and recurrent mass bleaching of corals. *Nature* 543 (7645), 373–377. doi: 10.1038/nature21707

Hughes, T. P., Kerry, J. T., Baird, A. H., Connolly, S. R., Dietzel, A., Eakin, C. M., et al. (2018b). Global warming transforms coral reef assemblages. *Nature* 556 (7702), 492–496. doi: 10.1038/s41586-018-0041-2

Jackson, R., Gabric, A., and Cropp, R. (2018). Effects of ocean warming and coral bleaching on aerosol emissions in the Great Barrier Reef, Australia. *Sci. Rep.* 8 (1), 14048. doi: 10.1038/s41598-018-32470-7

Jackson, R. L., Woodhouse, M. T., Gabric, A. J., and Cropp, R. A. (2022). CMIP6 projections of ocean warming and the impact on dimethylsulfide emissions from the Great Barrier Reef, Australia. *Front. Mar. Sci.* 9. doi: 10.3389/fmars.2022.910420

Jones, R., Giofre, N., Luter, H. M., Neoh, T. L., Fisher, R., and Duckworth, A. (2020). Responses of corals to chronic turbidity. *Sci. Rep.* 10 (1), 4762. doi: 10.1038/s41598-020-61712-w

Jones, R. J., Hoegh-Guldberg, O., Larkum, A. W. D., and Schreiber, U. (1998). Temperature-induced bleaching of corals begins with impairment of the CO_2 fixation mechanism in zooxanthellae. *Plant Cell Environ.* 21 (12), 1219–1230. doi: 10.1046/j.1365-3040.1998.00345.x

Kramer, J., Ripkey, N., Segard, L., Troisi, M., Kramer, P. R., Coraspe, P., et al. (2016). Turn down the heat: An innovative citizen science pilot project to reduce impacts of coral bleaching. *Proc. Gulf Caribb. Fish. Inst.* 69, 231–242.

Krueger, T., Hawkins, T. D., Becker, S., Pontasch, S., Dove, S., Hoegh-Guldberg, O., et al. (2015). Differential coral bleaching - Contrasting the activity and response of enzymatic antioxidants in symbiotic partners under thermal stress. *Comp. Biochem. Physiol. A Mol. Integr. Physiol.* 190, 15–25. doi: 10.1016/j.cbpa.2015.08.012

Lesser, M. P., and Farrell, J. H. (2004). Exposure to solar radiation increases damage to both host tissues and algal symbionts of corals during thermal stress. *Coral Reefs* 23 (3), 367–377. doi: 10.1007/s00338-004-0392-z

Li, Y., and Schellhorn, H. E. (2007). Rapid kinetic microassay for catalase activity. *J. biomol. techniques* 18 (4), 185–187.

Marsh, J. A. (1970). Primary productivity of reef-building calcareous red algae. *Ecology* 51 (2), 255–263. doi: 10.2307/1933661

Mclachlan, R., and Grottoli, A. G. (2021). *Image analysis to quantify coral bleaching using greyscale model*. doi: 10.17504/protocols.io.bx8wprxe

Muller, E. M., and van Woesik, R. (2009). Shading reduces coral-disease progression. *Coral Reefs* 28 (3), 757–760. doi: 10.1007/s00338-009-0504-x

Muller, E. M., and van Woesik, R. (2011). Black-band disease dynamics: Prevalence, incidence, and acclimatization to light. *J. Exp. Mar. Biol. Ecol.* 397 (1), 52–57. doi: 10.1016/j.jembe.2010.11.002

Muscatine, L., and Porter, J. W. (1977). Reef corals: Mutualistic symbioses adapted to nutrient-poor environments. *BioScience* 27 (7), 454–460. doi: 10.2307/1297526

Pratchett, M. S., Caballes, C. F., Newman, S. J., Wilson, S. K., Messmer, V., and Pratchett, D. J. (2020). Bleaching susceptibility of aquarium corals collected across northern Australia. *Coral Reefs* 39 (3), 663–673. doi: 10.1007/s00338-020-01939-1

Rangel, M. S., Erler, D., Tagliafico, A., Cowden, K., Scheffers, S., and Christidis, L. (2019). Quantifying the transfer of prey δ15N signatures into coral holobiont nitrogen pools. *Mar. Ecol. Prog. Ser.* 610, 33–49. doi: 10.3354/meps12847

Rau, G. H., McLeod, E. L., and Hoegh-Guldberg, O. (2012). The need for new ocean conservation strategies in a high-carbon dioxide world. *Nat. Climate Change* 2 (10), 720–724. doi: 10.1038/nclimate1555

Ritchie, R. J. (2006). Consistent sets of spectrophotometric chlorophyll equations for acetone, methanol and ethanol solvents. *Photosynthesis Res.* 89 (1), 27–41. doi: 10.1007/s11120-006-9065-9

Roth, M. S. (2014). The engine of the reef: photobiology of the coral-algal symbiosis. *Front. Microbiol.* 5. doi: 10.3389/fmicb.2014.00422

Russell, L. M., Sorooshian, A., Seinfeld, J. H., Albrecht, B. A., Nenes, A., Ahlm, L., et al. (2013). Eastern Pacific emitted aerosol cloud experiment. *Bull. Am. Meteorol. Soc.* 94 (5), 709–729. doi: 10.1175/BAMS-D-12-00015.1

Shick, J. M., Lesser, M. P., and Jokiel, P. L. (1996). Effects of ultraviolet radiation on corals and other coral reef organisms. *Global Change Biol.* 2 (6), 527–545. doi: 10.1111/j.1365-2486.1996.tb00065.x

Simpson, M. C., Gossling, S., Scott, D., Hall, C. M., and Gladin, E. (2008). "Climate change adaptation and mitigation in the tourism sector: Frameworks, tools and practices," in *Climate change adaptation and mitigation in the tourism sector: Frameworks, tools and practices (CABI)* [(Paris, France: United Nations Environmental Programme (UNEP)].

Smith, D. J., Suggett, D. J., and Baker, N. R. (2005). Is photoinhibition of zooxanthellae photosynthesis the primary cause of thermal bleaching in corals? *Global Change Biol.* 11 (1), 1–11. doi: 10.1111/j.1529-8817.2003.00895.x

Steven, A. D. L., Baird, M. E., Brinkman, R., Car, N. J., Cox, S. J., Herzfeld, M., et al. (2019). eReefs: An operational information system for managing the Great Barrier Reef. *J. Operat. Oceanog.* 12 (sup2), S12–S28. doi: 10.1080/1755876x.2019.1650589

Suggett, D. J., Warner, M. E., Smith, D. J., Davey, P., Hennige, S., and Baker, N. R. (2008). Photosynthesis and production of hydrogen peroxide by *Symbiodinium* (Pyrrhophyta) phylotypes with different thermal tolerances. *J. Phycol.* 44 (4), 948–956. doi: 10.1111/j.1529-8817.2008.00537.x

Sully, S., Burkepile, D. E., Donovan, M. K., Hodgson, G., and van Woesik, R. (2019). A global analysis of coral bleaching over the past two decades. *Nat. Commun.* 10 (1), 1264. doi: 10.1038/s41467-019-09238-2

Tagliafico, A., Baker, P., Kelaher, B., Ellis, S., and Harrison, D. (2022). The effects of shade and light on corals in the context of coral bleaching and shading technologies. *Front. Mar. Sci.* 9. doi: 10.3389/fmars.2022.919382

Tagliafico, A., Rangel, S., Kelaher, B., and Christidis, L. (2018). Optimizing heterotrophic feeding rates of three commercially important scleractinian corals. *Aquaculture* 483, 96–101. doi: 10.1016/j.aquaculture.2017.10.013

Tagliafico, A., Rudd, D., Rangel, M. S., Kelaher, B. P., Christidis, L., Cowden, K., et al. (2017). Lipid-enriched diets reduce the impacts of thermal stress in corals. *Mar. Ecol. Prog. Ser.* 573, 129–141. doi: 10.3354/meps12177

Thinesh, T., Meenatchi, R., Pasiyappazham, R., Jose, P. A., Selvan, M., KIran, G. S., et al. (2017). Short-term in *situ* shading effectively mitigates linear progression of coral-killing sponge Terpios hoshinota. *PloS One* 12 (8), e0182365. doi: 10.1371/journal.pone.0182365

Tollefson, J. (2021). Can clouds save the Great Barrier Reef? *Nature* 596, 476–478. doi: 10.1038/d41586-021-02290-3

Veal, C. J., Carmi, M., Fine, M., and Hoegh-Guldberg, O. (2010). Increasing the accuracy of surface area estimation using single wax dipping of coral fragments. *Coral Reefs* 29 (4), 893–897. doi: 10.1007/s00338-010-0647-9

Warner, M. E., Fitt, W. K., and Schmidt, G. W. (1999). Damage to photosystem II in symbiotic dinoflagellates: A determinant of coral bleaching. *Proc. Natl. Acad. Sci.* 96 (14), 8007–8012. doi: 10.1073/pnas.96.14.8007

Warren, C. R. (2008). Rapid measurement of chlorophylls with a microplate reader. *J. Plant Nutr.* 31 (7), 1321–1332. doi: 10.1080/01904160802135092

West, J. M., and Salm, R. V. (2003). Resistance and resilience to coral bleaching: Implications for coral reef conservation and management. *Conserv. Biol.* 17 (4), 956–967. doi: 10.1046/j.1523-1739.2003.02055.x

Wethey, D. S., and Porter, J. W. (1976). Sun and shade differences in productivity of reef corals. *Nature* 262 (5566), 281–282. doi: 10.1038/262281a0

Weydert, C. J., and Cullen, J. J. (2010). Measurement of superoxide dismutase, catalase and glutathione peroxidase in cultured cells and tissue. *Nat. Protoc.* 5 (1), 51–66. doi: 10.1038/nprot.2009.197

Wietheger, A., Starzak, D. E., Gould, K. S., and Davy, S. K. (2018). Differential ROS Generation in response to stress in Symbiodinium spp. *Biol. Bull.* 234 (1), 11–21. doi: 10.1086/696977

Winters, G., Holzman, R., Blekhman, A., Beer, S., and Loya, Y. (2009). Photographic assessment of coral chlorophyll contents: Implications for ecophysiological studies and coral monitoring. *J. Exp. Mar. Biol. Ecol.* 380 (1-2), 25–35. doi: 10.1016/j.jembe.2009.09.004

frontiers | Frontiers in Physiology

TYPE Original Research
PUBLISHED 07 December 2023
DOI 10.3389/fphys.2023.1308777

OPEN ACCESS

EDITED BY
Davide Seveso,
University of Milano-Bicocca, Italy

REVIEWED BY
Liqiang Zhao,
Guangdong Ocean University, China
Yina Shao,
Ningbo University, China

*CORRESPONDENCE
Yanjie Qin,
qyj_tina@163.com

†These authors have contributed equally to this work

RECEIVED 07 October 2023
ACCEPTED 15 November 2023
PUBLISHED 07 December 2023

CITATION
Zheng Z, Huo Z, Huang K, Jiang M, Yan X, Liu Y and Qin Y (2023), Metabolic adaptation of the clam *Ruditapes philippinarum* during air exposure and the positive effects of sodium nitroprusside pretreatment. *Front. Physiol.* 14:1308777. doi: 10.3389/fphys.2023.1308777

Metabolic adaptation of the clam *Ruditapes philippinarum* during air exposure and the positive effects of sodium nitroprusside pretreatment

Zhilong Zheng†, Zhongming Huo†, Kaiyue Huang, Min Jiang, Xiwu Yan, Yang Liu and Yanjie Qin*

Engineering and Technology Research Center of Shellfish Breeding in Liaoning Province, College of Fisheries and Life Science, Dalian Ocean University, Dalian, China

The Manila clam (*Ruditapes philippinarum*), as one of the shellfish living in the intertidal zone, is known for its strong ability to withstand air exposure. Sodium nitroprusside (SNP), a donor of nitric oxide (NO), has been shown to be useful for antioxidant and immune regulation in aquatic animals. In this study, an untargeted metabolomics (LC–MS/MS) technique was employed for the first time in Manila clam to analyze the metabolic and histological impacts after air exposure and the positive effects of SNP pretreatment. During air exposure, a significant increase in taurine, L-glutamate, and several polyunsaturated fatty acids in clams was detected, which indicates that clams may experience inflammatory reactions, oxidative stress, and an increase in blood ammonia content. When clams were exposed to SNP for 6 h, arginine, spermine, L-glutamic acid, and glutathione content were all upregulated, indicating that the SNP exposure induced NO production and improved antioxidant capacity in clams. When the clams were exposed to air after SNP pretreatment, there were no significant differences in the levels of taurine, L-glutamate, or aliphatic acids between the experimental and control groups. Gill tissue was more severely damaged in clams directly exposed to air than in those that experienced air exposure after SNP pretreatment, especially in clams exposed to air for a long time (72 h). Both metabolomics and tissue section structure indicated that SNP pretreatment decreased the stress responses caused by air exposure in *R. philippinarum*. These findings provided fresh insights and a theoretical foundation for understanding the tolerance to air exposure and physiological functions of SNP (or NO) in *R. philippinarum*.

KEYWORDS

***Ruditapes philippinarum*, air exposure, metabolomics, sodium nitroprusside, gill tissue structure**

1 Introduction

The Manila clam (*Ruditapes philippinarum*) is an economically important marine bivalve species in aquaculture, which has a widespread natural distribution in coastal areas from Europe to Asia. As a mollusc living in the intertidal zone, the Manila clam must deal with hard dynamic environments and environmental changes caused by physical elements such as PH, salinity, temperature, osmotic pressure, and air exposure (Zhang et al.,

2015). Among these physicochemical factors, air exposure is one of the most influential factors. Intertidal organisms exposed to air could cause physiological responses that might lead to deaths in prolonged water-deficient circumstances (Li et al., 2017). The ability to survive in open air is a critical factor in the harvesting and transporting of many shellfish (Gu et al., 2020). During air exposure, clam shells are usually closed to reduce water loss to a minimum and protect the soft tissues (Coleman, 1973; Ali and Nakamura, 1999). However, due to an acidosis caused by anaerobic end-product formation or continuous aerobic metabolism, the prevention of breathing by tightly closing valves increases mortality during air exposure (Byrne et al., 1988; Ali and Nakamura, 2000). It was reported that *Meretrix meretrix* began to die after more than 24 h of air exposure (Wei et al., 2017). Mussels (*Perna perna*) exposed to air for 6, 12, 24, and 48 h showed hypoxia-induced antioxidant and tissue-specific immune systems (Nogueira et al., 2017). Significant oxidative stress can be caused by air exposure, which can result in oxidative damage and antioxidation (Xu et al., 2018). Oxidative stress can produce an increase in reactive oxygen species (ROS), which can cause substantial cell damage (Jia et al., 2019). A series of antioxidant defense mechanisms, including antioxidant enzymes, are produced in the organism to preserve its balance (Halliwell, 1999). Many studies have focused on the influence of air exposure on the molecular, physiological, and biochemical responses in *Crassostrea gigas* (Kawabe and Yokoyama, 2010; Gong et al., 2019), *Haliotis diversicolor* (Zhang et al., 2019), and *Solen grandis* (Nie et al., 2018). Recently, the effects of aerial exposure on the clams have been investigated in many aspects, including gene expression variation, metabolite changes, and physiological responses (Nie et al., 2020; Sun et al., 2021).

Nitric oxide (NO) is a key signaling chemical in marine invertebrates, and its signaling pathway is extremely conserved among species (Palumbo, 2005). NO has been demonstrated to have a wide range of biological roles in marine invertebrates, including eating, defense, and immunological responses (Palumbo, 2005), and to slow down the respiration of gills in bivalve mollusks (Gonzáleze et al., 2019). NO is catalyzed by monoxide synthase (NOS) in the presence of oxygen (O_2), NADPH, and a substrate (L-arginine) (Förstermann and Sessa, 2012). In eukaryotes, there are three forms of NOS: neuronal NOS (nNOS), endothelial NOS (nNOS), and inducible NOS (iNOS). Among them, iNOS is considered to be induced by the stimulation of environmental perturbations (Kraft and Harry, 2011). A small quantity of NO can be produced by structured NOS under normal circumstances in organisms, and it is a chain blocker that can inhibit lipid peroxidation and scavenge oxygen free radicals (Yu et al., 2021). NO has also been proved to inhibit the production of mitochondrial oxygen free radicals in arctic clams (*Arctica islandica*) following chronic hypoxia and hypoxia (Strahl and Abele, 2020). Xian et al. (2013) used flow cytometry to evaluate NO production in *Penaeus monodon*, proving that the SNP (NO donor) could dramatically boost NO production in shrimp hemocytes. It was indicated that the supplementation of exogenous SNP and the synthesis of NO in marine organisms should be an effective way to improve antioxidant or immune capacity.

Metabolomics is a high-throughput molecular method that can quickly identify and quantify small-molecule metabolites (metabolomes) and is frequently considered the closest discipline to phenomics (Guijas et al., 2018). In recent years, this technology has gradually been applied to the study of the environmental adaptability of bivalve mollusks. Different metabolites in response to acute hypoxia in clams have been investigated with the goal of revealing the adaptive mechanism of acute hypoxia tolerance at the metabolic level (Sun et al., 2021). Metabolic profiles revealed that high temperatures caused changes in fatty acid composition, energy metabolism, antioxidant metabolites, hydroxyl compounds, and amino acids in heat-hardened clams compared to non-hardened clams (Zhang et al., 2023). Targeted metabolomics technology revealed the adaptation mechanism to high temperature, low oxygen, and compound stress at the metabolic level in the hard clam (*Mercenaria mercenaria*) (Hu et al., 2022). To our knowledge, the metabolites in response to air exposure in clams are still very lacking. The underlying metabolite mechanisms of air exposure tolerance and exogenous substances to enhance the ability to resist air exposure remain largely unknown in this commercially important species.

In this research, we studied the effects of air exposure and SNP exposure on tissue damage in *R. philippinarum*. The metabolites of clams after air exposure with/without SNP pretreatment were, respectively, analyzed using untargeted metabolomics (LC–MS/MS). Based on the metabolic characteristics analysis of clams in open air and in the presence of SNP, we will explore the changes in metabolic adaptation mechanisms of clams during air exposure after SNP pretreatment. This research provides new insights into the adaptation of the Manila clam to air exposure, as well as revealing the antioxidant protection of nitric oxide (NO).

2 Materials and methods

2.1 Experimental animals

Manila clams (average weight: 11.3 ± 0.5 g; average shell length: 37.5 ± 1.5 mm) were collected from the coastal area of Lvshun, Dalian, China. These clams were temporarily cultured in farming tanks at 15°C ± 1°C for a week. During this period, the seawater was changed and chlorella was fed once a day.

2.2 Air exposure with/without SNP pretreatment and sample collection

Sodium nitroprusside (SNP, NO donor, Biyuntian Biotechnology Co., Ltd., China) was dissolved in ultrapure water to make a 200 mg/mL mother solution, which was then diluted with seawater according to the experimental concentration.

A total of 180 clams were randomly collected and cultured in six separate tanks. Among them, three were experimental groups, and these clams were cultured in seawater with an SNP concentration of 100 μm/L for 6 h (N6) and then exposed to air for 72 h (NE). The other three groups were kept in normal seawater for 6 h (C0) and then in open air for 72 h (CE), which were considered the control groups. The gills were collected from the clams treated with SNP/- for 6 h and air exposure for 24, 48, and 72 h. Three individuals were sampled from each group at each period and promptly preserved with 4% paraformaldehyde for tissue sectioning.

A total of 360 clams were divided into treatment and control groups, with six parallels in each group. The clams in the two groups were cultured in normal seawater (C0) and then treated with 100 μm/L SNP for 6 h (N6). Subsequently, both groups were exposed to air for 72 h (CE and NE). 200–400 μL hemolymph was collected from clams in each group (C0, N6, CE, and NE), quickly frozen in liquid nitrogen, and then, stored at −80°C for metabonomics analysis. A mixture of 100 μL of the sample and 400 μL of an 80% methanol solution was vortexed and stored in ice water for 5 min. The supernatant was extracted via centrifugation at 15,000 g for 20 min at 4°C and diluted with mass spectrometry-grade water until the methanol level was 53%. The obtained solution was transferred to a sterile, enzyme-free EP tube and centrifuged at 15,000 g for 20 min at 4°C. The supernatants were stored at −80°C and transferred for LC–MS/MS analysis (Want et al., 2013).

2.3 Tissue sectioning and metabolite analysis

Gills fixed in 4% paraformaldehyde for histological observations were embedded in paraffin, sectioned into 7-μm slices and stained with hematoxylin–eosin. The slices were observed and photographed using the BX21 microscope and DP73 CCD camera (Olympus), respectively.

The UHPLC–MS/MS analyses were performed using a Vanquish UHPLC system (Thermo Fisher Scientific, Germany) coupled with an Orbitrap Q Exactive™ HF mass spectrometer (Thermo Fisher Scientific, Germany) at Novogene Co., Ltd. (Beijing, China). Samples were injected into a Hypersil GOLD column (100 mm × 2.1 mm, 1.9 μm) using a 17-min linear gradient at a flow rate of 0.2 mL/min. The eluents for the positive polarity mode were eluent A (0.1% FA in water) and eluent B (methanol). The eluents for the negative polarity mode were eluent A (5 mM ammonium acetate, pH 9.0) and eluent B (methanol). The solvent gradient was set as follows: 2% B, 1.5 min; 2%–85% B, 3 min; 85%–100% B, 10 min; 100%–2% B, 10.1 min; and 2% B, 12 min. The Q Exactive™ HF mass spectrometer was operated in the positive/negative polarity mode with a spray voltage of 3.5 kV, capillary temperature of 320°C, sheath gas flow rate of 35 psi, auxiliary gas flow rate of 10 L/min, S-lens RF level of 60, and auxiliary gas heater temperature of 350°C.

The raw data files generated by UHPLC–MS/MS were processed using the Compound Discoverer 3.1 software (CD3.1, Thermo Fisher Scientific) to perform peak alignment, peak picking, and quantitation for each metabolite. The peaks were matched with mzCloud (https://www.mzcloud.org/), mzVault, and MassList databases to obtain accurate qualitative and relative quantitative findings. The metabolites were annotated using the KEGG database (https://www.genome.jp/kegg/pathway.html), HMDB database (https://hmdb.ca/metabolites), and LIPID MAPS database (http://www.lipidmaps.org/). The metabolomics data processing software metaX (Wen et al., 2017) was used to convert the data in the multivariate statistical analysis section, and principal component analysis (PCA) and partial least squares discriminant analysis (PLS-DA) were performed to provide an overview of metabolic data, general clustering, trend, and outlier visualization and then obtain the contribution (VIP value) of each metabolite. The univariate analysis is based on the *t*-test to calculate the statistical significance (*p*-value) of each metabolite between the two groups and the fold change (FC) of the metabolite between the two groups, referred to as the FC value. VIP >1 and *p*-value <0.05 were the default criteria for differential metabolite screening. The volcano map was created using the R package ggplot2. Metabolites of interest may be selected by comprehending the three parameters of the metabolite: VIP value, $\log_2$ (fold change), and $-\log_{10}$ (*p*-value). The clustering heatmap was created using the R package Pheatmap, and the metabolite quantification data were standardized using the z-score. The statistically significant correlation between differential metabolites was calculated using cor. mtest () in R language, and a *p*-value <0.05 was considered statistically significant. The functions of these metabolites and metabolic pathways were studied using the KEGG database. The metabolic pathway enrichment of differential metabolites was performed. When the ratio was satisfied by x/n > y/N, the metabolic pathway was considered as enrichment, and when the *p*-value of the metabolic pathway was <0.05, the metabolic pathway was considered statistically significant enrichment.

3 Result

3.1 Damages to gill tissue during air exposure with or without SNP pretreatment

Gill filaments in normal clams exhibited a dense arrangement, interconnected at their free ends by densely concentrated cilia. The gill filaments' surface consisted of epithelial cells interspersed with goblets (Figure 1A). Following 6 h of SNP pretreatment, the fundamental tissue structure of the gill filaments remained unaltered. However, distinctive clusters of mucous glands appeared obviously at the base of the gill filaments (Figure 1B, marked by the black arrow). When the clams were exposed to air for 24 h, thinner gill filaments were observed, resulting in an increased inter-filament spacing and a notable proliferation of goblets within the epithelial cell layer (Figure 1C). After 72 h of air exposure, the gill tissue structure showed obvious damage (Figure 1G), with some epithelial cell detachment at the margin of gill filaments, thereby exposing the basal lamina (Figure 1E, indicated by the white arrow). When the clams were exposed to air for 24 h after a 6-h SNP pretreatment, the gill tissue structure remained intact and regular, as similar as those in control (Figure 1D). Even after 72 h of air exposure after SNP pretreatment, thinner gill filaments occurred and there was partial opening of inter-filament connections, resulting in increased inter-filament spacing. Nevertheless, the overall structural integrity remained, with minimal instances of epithelial cell detachment (Figures 1F, H).

3.2 Untargeted metabolome profiling

Untargeted metabolomics analysis was used in this research to explore potential adaptation mechanisms at the metabolomics level. In all, 436 metabolites were found in the positive ion mode and 245 in the negative ion mode. PCA analysis was used to examine the changes in metabolites in each group (C0, N6, NE, and CE) (Figure 2). The PCA score chart displayed no significant outliers,

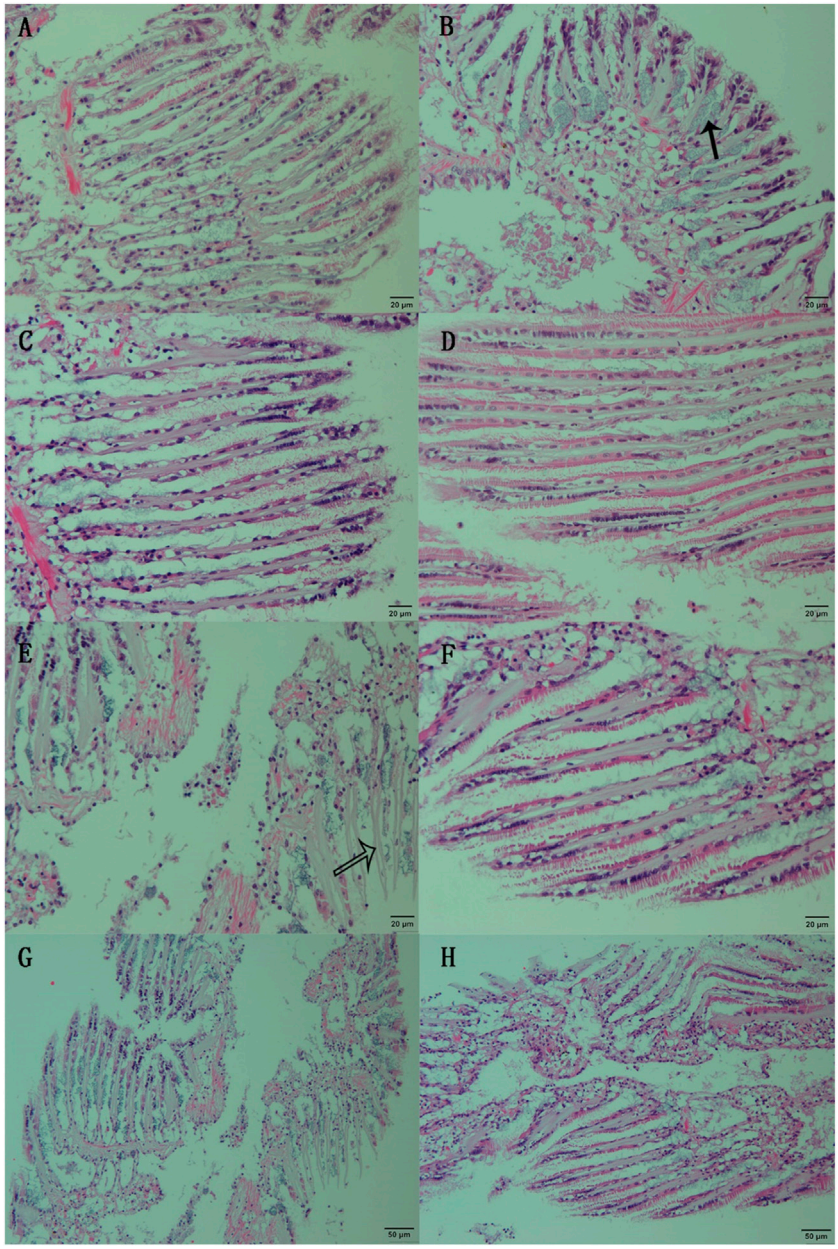

FIGURE 1
Histological observation of the gill of clam *Ruditapes philippinarum* undergoing air exposure and SNP pretreatment. **(A)** Gill in control (C0); **(B)** gill after 6 h of SNP treatment (N6); **(C)** gill after 24 h of air exposure (CE); **(D)** gill after 24 h of air exposure with SNP pretreatment (NE); **(E, G)** gill after 72 h of air exposure; and **(F, H)** gill after 72 h of air exposure with SNP pretreatment. Black arrow: clusters of mucous glands at the base of the gill filaments; white arrow: basal lamina after epithelial cell detachment.

showing that the four groups of metabolite aggregation are good. Furthermore, the overlap between the comparison groups is tiny, especially in the negative ion mode, demonstrating that the model has metabolite properties.

3.3 Analysis of differential metabolites

In this research, VIP ≥1, FC > 1.2 or FC < 0.833, and *p*-value <0.05 were used as screening thresholds to analyze metabolite differences in the positive and negative ion modes (Figure 3). The analysis of the N6 vs. C0 comparison group showed that six significantly different metabolites (SDMs) were upregulated and eight SDMs were downregulated in the positive ion mode; 18 SDMs were upregulated and 20 SDMs were downregulated in the negative ion mode. In the NE vs. C0 comparison group, 13 SDMs were upregulated and 60 SDMs were downregulated in the positive ion mode; 34 SDMs were upregulated and 33 SDMs were downregulated in the negative ion mode. There were 37 upregulated and 44 downregulated SDMs in the positive ion mode and 67 upregulated and 26 downregulated SDMs in the CE vs. C0 comparison

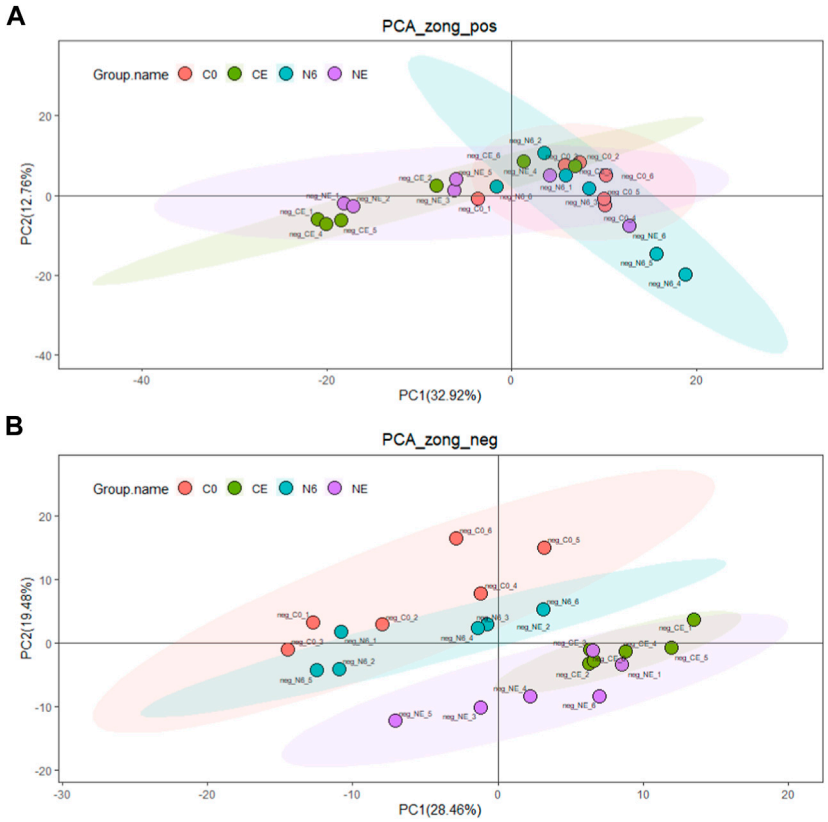

FIGURE 2
Principal component analysis of the clam *Ruditapes philippinarum* during air exposure with or without SNP pretreatment. **(A)** Positive ion (POS) and **(B)** negative ion (NEG). The red dots indicate the control group (C0), the green dots represent the air-exposed group (CE), the blue dots represent SNP exposure for 6 h (N6), and the purple dots represent the air-exposed clam after SNP pretreatment (NE).

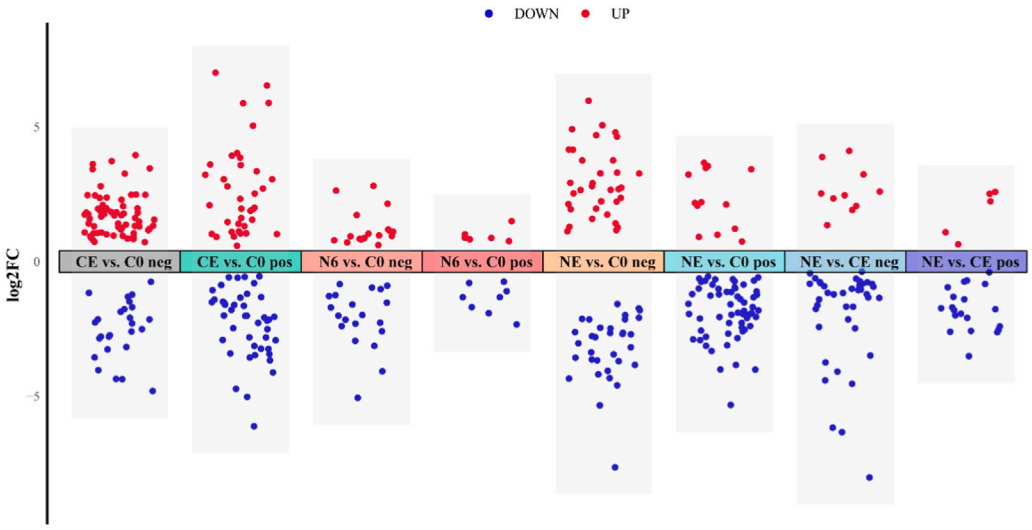

FIGURE 3
Metabolite visualization analysis of clam *Ruditapes philippinarum* exposed to SNP and air. Red dots represent upregulated metabolites, and blue dots represent downregulated metabolites.

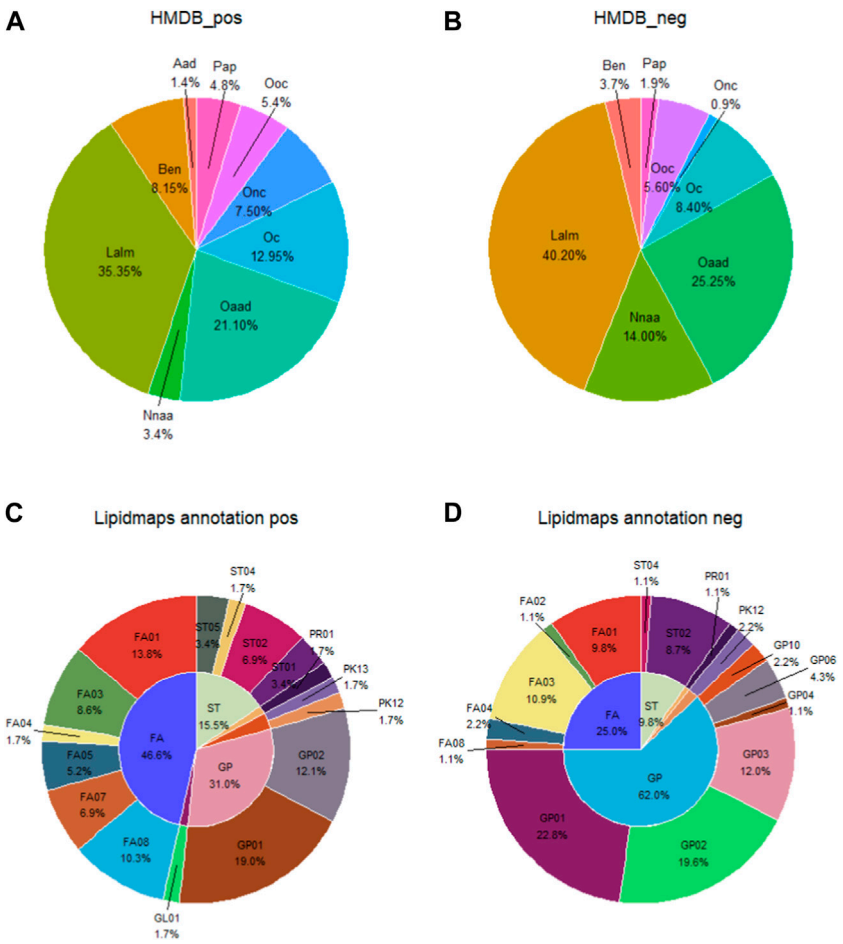

FIGURE 4
Account of metabolites annotated by the secondary classification (SuperClass) in HMDB **(A, B)** and the main level of classification (Main_Class) in LIPID MAPS **(C, D)**. Aad, alkaloids and derivatives; Ben, benzenoids; Lalm, lipids and lipid-like molecules; Nnaa, nucleosides nucleotides and analogs; Oaad, organic acids and derivatives; Oc, organoheterocyclic compounds; Onc, organic nitrogen compounds; Ooc, rganic oxygen compounds; Pap, phenylpropanoids and polyketides; FA, fatty acyls; ST, sterol lipids; GP, glycerophospholipids; FA01, fatty acids and conjugates; FA02, octadecanoids; FA03, eicosanoids; FA04, docosanoids; FA05, fatty alcohols; FA07, fatty esters; FA08, fatty amides; GL01, monoradylglycerols; GP01, glycerophosphocholines; GP02, glycerophosphoethanolamines; GP03, glycerophosphoserines; GP04, glycerophosphoglycerols; GP06, glycerophosphoinositols; GP10, glycerophosphates; PK12, flavonoids; PK13, aromatic polyketides; PR01, isoprenoids; ST01, sterols; ST02, steroids; ST04, bile acids and derivatives; and ST05, steroid conjugates.

group. Results from the NE vs. CE comparison group showed that five upregulated and 20 downregulated SDMs were in the positive ion mode; 10 and 39 were upregulated and downregulated, respectively, in the negative ion mode.

In the HDMB database secondary classification (SuperClass), the metabolites in the positive and negative ion patterns could be categorized into nine groups: alkaloids and derivatives; benzenoids; lipids and lipid-like molecules; nucleosides/nucleotides and analogs; organic acids and derivatives; organoheterocyclic compounds; organic nitrogen compounds; organic oxygen compounds; and phenylpropanoids and polyketides. The proportion of each category is shown in Figures 4A, B. In the positive ion mode, the top three metabolite classifications of HDMB classification annotation findings were lipids and lipid-like molecules, organic acids and derivatives, and organoheterocyclic compounds. In the negative ion mode, the top three were lipids and lipid-like molecules, organic acids and derivatives, and nucleosides/nucleotides and analogs.

In the Lipid Metabolites and Pathways Strategy (LIPID MAPS) database, the metabolites identified in the positive and negative ion modes could be classified into six categories: 1) fatty acids (FAs); 2) glycerolipids (GLs); 3) glycerophospholipids (GPs); 4) polyketides (PKs); 5) prenol lipids (PRs); and 6) sterol lipids (STs). The percentages of each category are shown in Figures 4A, B. Fatty acids and conjugates [FA01], glycerophosphocholines [GP01], and glycerophosphoethanolamines [GP02] are the top three metabolite species in the positive ion mode. Glycerophosphocholines [GP01], glycerophosphoethanolamines [GP02], and glycerophosphosrines [GP03] are the top three metabolites in the negative ion mode (Figures 4C, D).

The cluster heatmap indicated significant differences in metabolites between the groups, as shown in Figure 5. In the

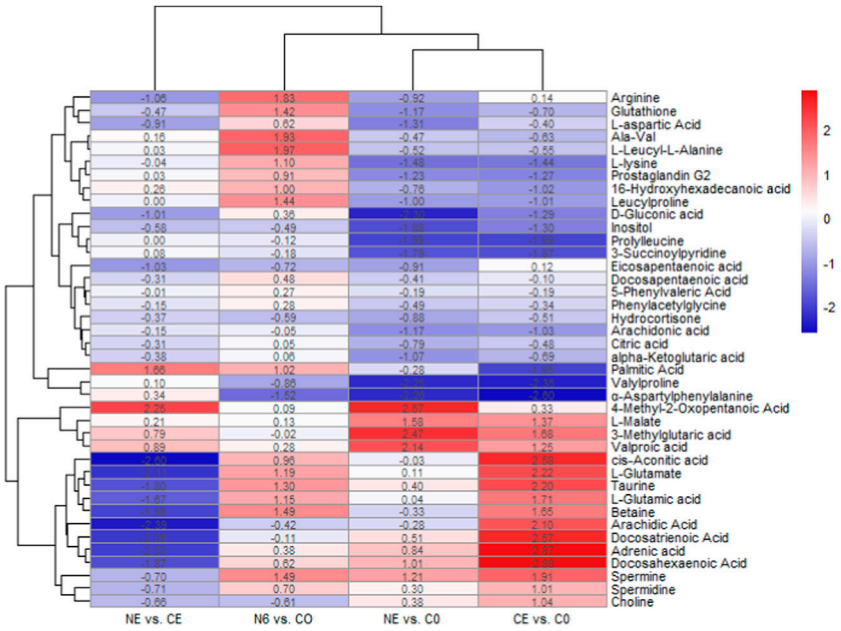

FIGURE 5
Clustering heatmap of metabolite expression after SNP pretreatment and air exposure in *Ruditapes philippinarum*. Metabolites in red are upregulated, and those in blue are downregulated.

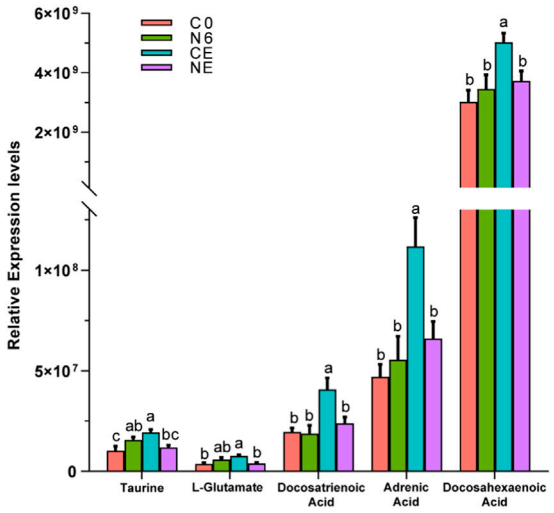

FIGURE 6
Comparative analysis of some metabolite expression levels in *Ruditapes philippinarum*. Different lowercase letters indicate significant differences in the levels of the same metabolite among distinct experimental groups.

comparison between CE and C0 groups, α-aspartylphenylalanine,valylproline, prolylleucine, palmitic acid, L-lysine, inositol, D-gluconic acid, glutathione, alpha-ketoglutaric acid, Ala-Val, citric acid, and L-aspartic acid were considerably downregulated, whereas cis-aconitic acid, taurine, spermine, L-glutamic acid, betaine, choline, and arginine were significantly upregulated. After 6 h of SNP exposure, arginine, spermine, and L-glutamic acid were all upregulated in the N6 group, indicating that the SNP exposure induced the production of NO in the body. It was also shown that the glutathione content was considerably higher in the N6 group. In the comparison between the NE and C0 groups, valylproline, α-aspartylphenylalanine, D-gluconic acid, prolylleucine, and glutathione were all downregulated. However, taurine showed no significant changes. It was found that there were more upregulated metabolites in the CE vs. C0 group compared to the NE vs. C0 group.

The relative levels of some metabolites, such as taurine, L-glutamate, and some aliphatic acids, are depicted in Figure 6. These metabolites showed the most significant changes in the air-exposed clam, all of which were higher than those in the control group ($p < 0.05$). However, there were no significant differences in these metabolites between the NE and C0 groups ($p > 0.05$).

3.4 Analysis of KEGG pathway enrichment

To better understand the functions of different metabolites, SDMs in the four comparison groups were annotated into the KEGG pathway for enrichment analysis. The results showed that the SDMs in the N6 vs. C0 group were enriched in beta-alanine metabolism, arginine and proline metabolism, and glutathione metabolism in the positive ion mode (pos) (Figure 7A) and glutathione metabolism, arginine biosynthesis, and aminoacyl-tRNA biosynthesis enrichment in the negative ion mode (neg) (Figure 8A). In the positive ion mode (pos) of the NE vs. C0 group, SDMs were enriched in the biosynthesis of unsaturated fatty acids, glutathione metabolism, and the pentose phosphate pathway (Figure 7B), whereas the negative ion mode was enriched in oxidative phosphorylation and pyruvate metabolism (Figure 8B). The CE vs. C0 group was enriched in taurine and

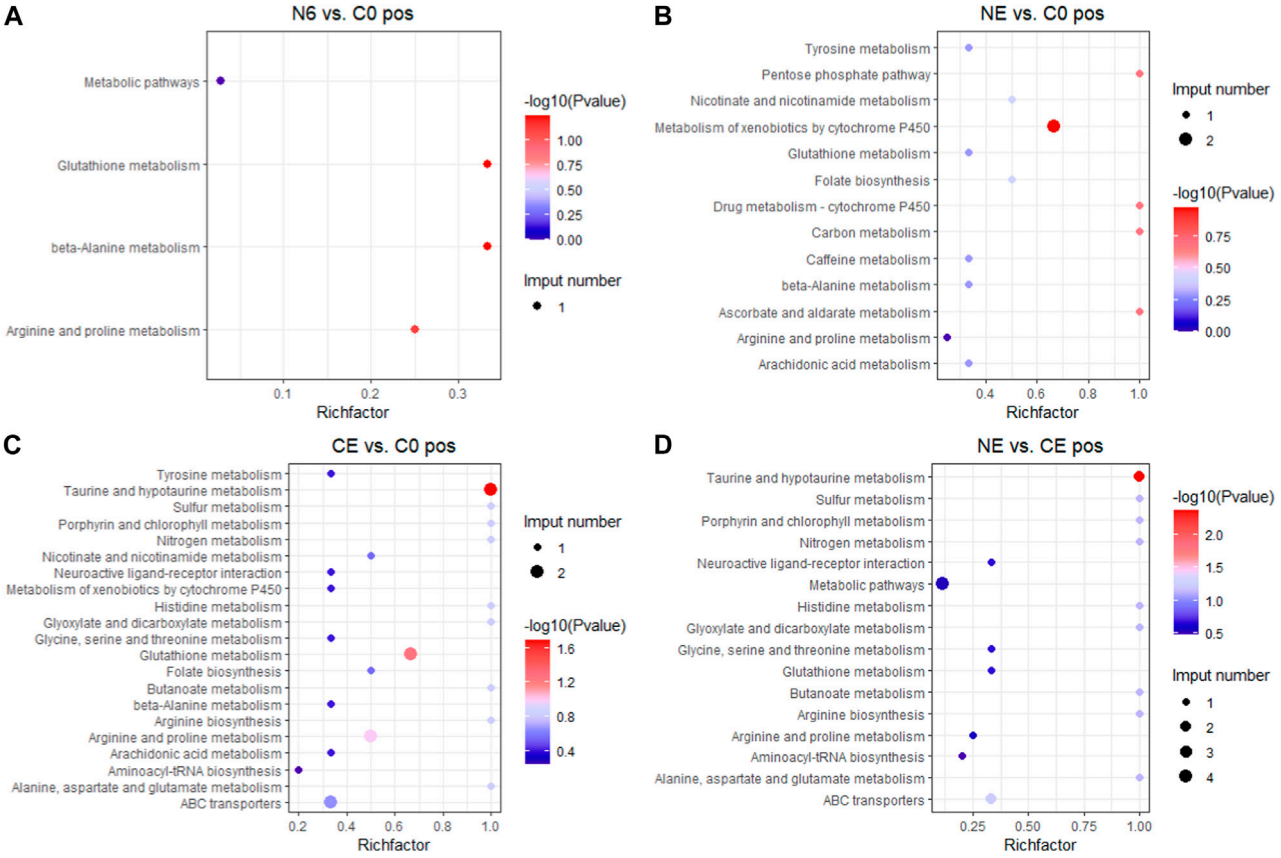

FIGURE 7
KEGG enrichment analysis in the positive ion mode across comparison groups. The larger the abscissa value, the greater the degree of enrichment of differential metabolites. The point's color shows the *p*-value of the hypergeometric test. The lower the value is, the more reliable the test is and the more statistically significant it is. The size of the dots represents the number of different metabolites in the pathway. **(A)** N6 vs. C0; **(B)** NE vs. C0; **(C)** CE vs. C0; and **(D)** NE vs. CE.

hypotaurine metabolism, glutathione metabolism, arginine and proline metabolism, and arginine biosynthesis in the positive ion mode (Figure 7C), and in the negative ion mode, biosynthesis of unsaturated fatty acids and oxidative phosphorylation were enriched (Figure 8C). The SDMs in the NE vs. CE group were enriched in taurine and hypotaurine metabolism, ABC transporters, and arginine biosynthesis in the positive ion mode (Figure 7D), and in the negative ion mode (neg), enrichment was observed in arginine biosynthesis, taurine and hypotaurine metabolism, and glutathione metabolism (Figure 8D).

4 Discussion

The LC–MS metabolomics technique was used for the first time in this research to determine the metabolic alterations of hemolymph after air exposure and SNP (NO donor) exposure in the Manila clam. The different metabolites in clams after air exposure and SNP treatment were mainly energy metabolism, osmoregulation, and the effects of oxidative stress. Air exposure was found to have an influence on important metabolic pathways such as amino acid metabolism, fatty acid metabolism, neurotransmitter transport, and osmoregulation (Liang et al., 2020). The cluster heatmap revealed that the amounts of various amino acids (prolylleucine, Ala-Val, leucylproline, L-aspartic acid, L-lysine, 5-phenylvaleric acid, citric acid, and alpha-ketoglutarate) dropped in clams exposed to air for 72 h. Amino acids have been shown to be a major source of energy metabolism in mollusks (Alfaro et al., 2021). A reduction in amino acids in bivalve mollusks suggests physiological changes in responses to several stresses. The contents of various amino acids decreased to different degrees under environmental stressors, such as high temperatures (Zhang et al., 2023), high temperatures and hypoxia (Hu et al., 2022), and air exposure (Nguyen et al., 2020). These results were consistent with our findings, which indicated that clams had substantial variations in metabolome profiles after air exposure. Long-term air exposure also causes oxygen deprivation in clams, which in turn affects several energy-related metabolites. The TCA cycle is an important pathway for the generation of energy in the animal body. TCA intermediate accumulation has been demonstrated to be caused by TCA cycle interruption in mollusks (Van Nguyen and Alfaro, 2019). When New Zealand surf clams (*Crassula aequilatera*) are exposed to air and high temperatures, they generate oxidative stress and an accumulation of TCA metabolic intermediates, with L-malate accumulating continuously (Alfaro et al., 2019). Similarly, the content of citric acid and alpha-ketoglutarate acid in clams exposed to air decreased continually in order to produce energy for the body, while

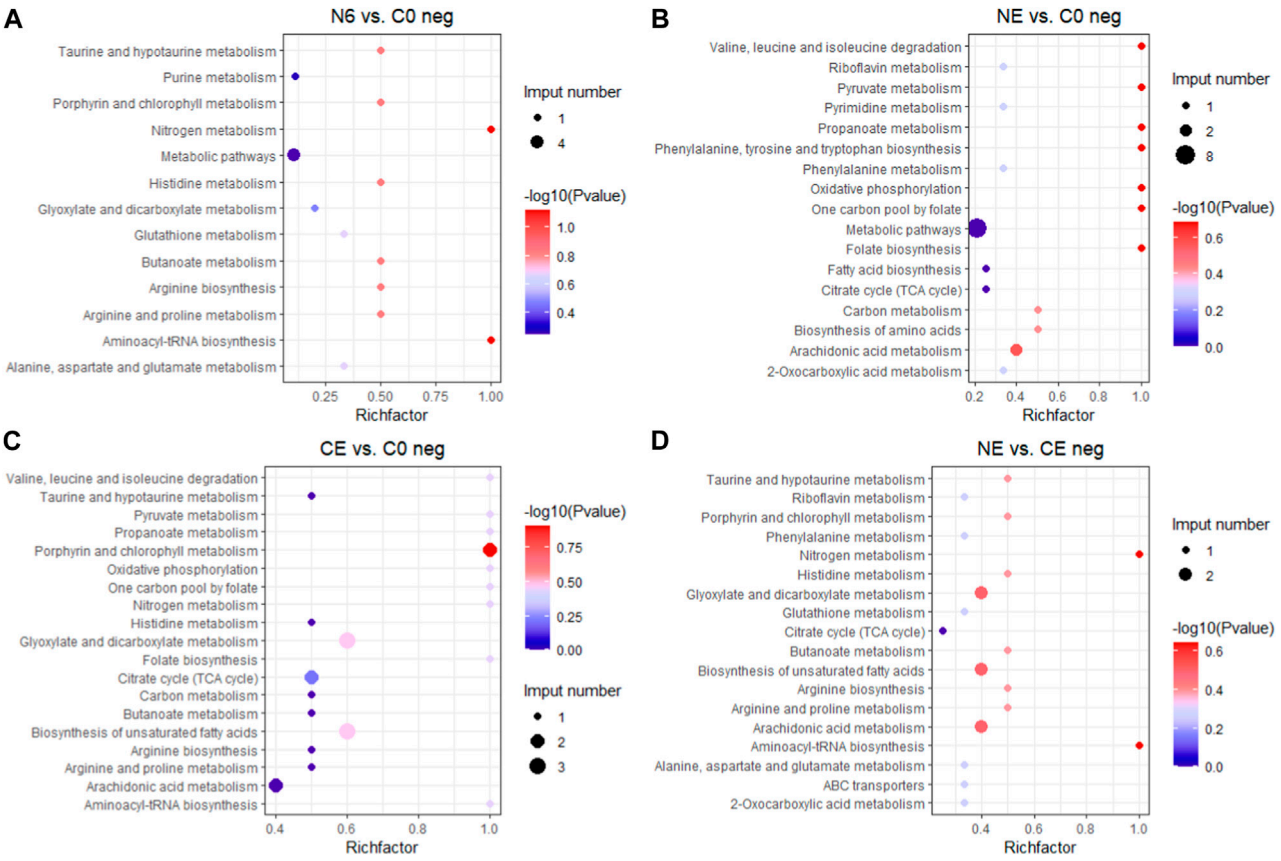

FIGURE 8
KEGG enrichment analysis in the negative ion mode across comparison groups. The larger the abscissa value, the greater the degree of enrichment of differential metabolites. The point's color shows the *p*-value of the hypergeometric test. The lower the value is, the more reliable the test is and the more statistically significant it is. The size of the dots represents the number of different metabolites in the pathway. **(A)** N6 vs. C0; **(B)** NE vs. C0; **(C)** CE vs. C0; and **(D)** NE vs. CE.

the content of L-malate and cis-aconitic acid increased, which confirmed that the TCA cycle was interrupted in clams during air exposure.

It should be noted that the contents of docosapentaenoic acid, docosahexaenoic acid, arachidic acid, L-glutamic acid, and taurine were significantly increased in clams during air exposure. Among them, taurine is considered an antioxidant and an osmotic agent in cellular metabolism and steady state (Schaffer and Kim, 2018). Its antioxidation includes binding peroxidation reaction products (Ahmed, 2023), inhibiting mitochondrial superoxide production (Jong et al., 2012) and preventing reactive oxygen species (ROS) through the destruction of antioxidant enzymes. Taurine in clam hemolymph stayed at a high level during air exposure in this research, which indicated that increased taurine expression might be a protective mechanism against oxidative damage in clams during air exposure. Similarly, Haider et al. (2020) also found in their research that the high survival rates of marine bivalves during hypoxic stress were correlated with high levels of taurine. In addition, taurine is related to the osmoregulatory regulation in marine mollusk during environmental changes (Hosoi et al., 2007). The taurine-related metabolism pathway has been proved to have a non-negligible role in mollusk osmoregulation under hypoxic stress (Sun et al., 2021). During air exposure, we obviously detected a significant increase in taurine and other osmolytes, including non-essential amino acids, which indicated that clams faced alterations in osmoregulation. It was concluded that taurine acted as an antioxidant and osmotic agent in the Manila clam during air exposure. It was reported that the blood ammonia would combine with L-glutamate to form the amide (Pequin and Serfaty, 1966). Therefore, the increase in L-glutamate in clams in the CE group in this study might indicate a higher blood ammonia level during the air exposure. In addition, it was found in this study that some polyunsaturated fatty acids (PUFAs), such as docosatrienoic acid, adrenic acid, docosahexaenoic acid, and arachidic acid, significantly increased in air-exposed clams. There is substantial evidence that these fatty acids are capable of partly inhibiting many aspects of inflammation, including leukocyte chemotaxis, adhesion molecule expression, and leukocyte–endothelial adhesive interactions (Calder, 2017). The increase in PUFAs in the results of this study indicated that clams might experience inflammatory reactions during the air exposure process.

NO can directly alleviate oxidative stress at low concentrations by impacting the membrane components of NADPH oxidase and reducing the production of ROS (Wink et al., 2001; Clancy et al., 1992). González et al. (2019) discovered that mussels in hypoxic circumstances produced NO to achieve vasodilation. Moreover, as oxygen contents decreased after shell closure, nitric oxide produced from the hemolymph induced physiological damage to the gills and lowered the metabolic rate of other tissues. This reveals a basal function

of NO in improving perfusion of hypoxic invertebrate tissues, which could be a key mechanism of tolerance toward environmental O_2 variations. NO was proved to protect cells by reducing intracellular $CytO_x$ and O_2 uptake during long-term hypoxia, and thus, arctic clams will not undergo ROS bursts or antioxidant upregulation during hypoxia and recovery (Strahl and Abele, 2020; Strahl et al., 2011). The glutathione content rose substantially after Manila clams were exposed to SNP for 6 h. Kuo et al. (1996) discovered that when faced with nitric oxide-mediated oxidative stress, GSH production was induced in order to maintain appropriate antioxidant levels. When the formation rate of the superoxide anion (O^{-2}) is constant, glutathione oxidation increases as NO increases. When the formation rate of NO is greater than that of these free radicals, GSH oxidation weakens and glutathione concentrations increase significantly (Wink et al., 2001). Both might account for the large increase in glutathione levels after SNP exposure. The results of this experimental research also revealed that the related antioxidant substances (such as taurine and glutathione) were significantly upregulated in SNP exposure experiments. These results indicated that NO can not only directly exert antioxidant effects but also induce the generation of antioxidant substances (such as taurine and glutathione), jointly achieving antioxidant function. When the clams were exposed to air after 6 h of SNP pretreatment (NE group), compared to the control group (C0), the taurine value was not significantly changed, while glutathione was at a reduced level. It was speculated that after SNP treatment, NO in the clam body can continue to exert antioxidant effects for some time, and the large amount of taurine and glutathione induced by NO can also resist the oxidative reaction during air exposure. Therefore, during the air exposure after SNP pretreatment (NE), most metabolites that significantly increased in the directly air-exposed group (CE), such as taurine, L-glutamate, and several PUFAs, showed no significant differences from those in the control group (C0).

Gill is an important organ for respiration and filtration, especially for bivalves (Zhan et al., 2021). In the present study, the structures of the gill of clams were remarkably destroyed after 72 h of air exposure. Large amounts of oxygen free radicals (ROS) would be produced in the gill due to the insufficient supply of oxygen molecules (Kim and Chung, 2007; Jing et al., 2023). The rupture of gill cells in clams during air exposure may be caused by excessive ROS production under respiratory obstruction and hypoxia. However, compared to the direct air exposure group, gill tissue was only slightly destroyed in clams exposed to air for 72 h after SNP pretreatment. Combined with the results of metabolomics, it was indicated that the stress response caused by air exposure in clams would be decreased after SNP (NO donor) pretreatment.

5 Conclusion

This research is the first to use untargeted metabolomics (LC–MS/MS) to analyze the adaptive mechanism of Manila clams during air exposure and the positive effect of SNP (NO donor) pretreatment before air exposure. A significant increase in taurine, L-glutamate, and several PUFAs in the Manila clam was detected, which indicated that clams may experience inflammatory reactions, oxidative stress, and an increase in the blood ammonia content during air exposure. NO induced by SNP could induce the production of taurine and glutathione in the clam. When the clams were exposed to air after 6 h of SNP pretreatment, NO could not only directly exert antioxidant effects but also induce the generation of antioxidant substances (such as taurine and glutathione), jointly achieving antioxidant function. Compared with the serious damages in the gills of clam directly exposed to air, gill tissue was only slightly destroyed in clams exposed to air for 72 h after SNP pretreatment. Therefore, it was indicated that a series of physiological responses during air exposure in *Ruditapes philippinarum* could be alleviated through SNP pretreatment.

Data availability statement

The original contributions presented in the study are included in the article/supplementary material; further inquiries can be directed to the corresponding author.

Ethics statement

The animal study was approved by the Experimental Animal Ethics Committee of Dalian Ocean University. The study was conducted in accordance with the local legislation and institutional requirements.

Author contributions

ZZ: data curation, formal analysis, investigation, methodology, project administration, software, validation, visualization, and writing–original draft. ZH: data curation, formal analysis, funding acquisition, resources, supervision, and writing–review and editing. KH: investigation, methodology, and writing–original draft. MJ: investigation and writing–original draft. XY: conceptualization, resources, and writing–review and editing. YL: data curation, formal analysis, and writing–original draft. YQ: data curation, formal analysis, funding acquisition, project administration, supervision, validation, visualization, and writing–review and editing.

Funding

The authors declare financial support was received for the research, authorship, and/or publication of this article. This work was sponsored by the National Key Research and Development Program of China (2018YFD0901400), the Outstanding Young Scientific and Technological Talents Foundation of Dalian (2021 RJ09), funds earmarked for Modern Agro-industry Technology Research System (CARS-49), and the Central Government Subsidy Project for Liaoning Fisheries (2023).

Conflict of interest

The authors declare that the research was conducted in the absence of any commercial or financial relationships that could be construed as a potential conflict of interest.

Publisher's note

References

Ahmed, A. O. H. (2023). A brief insight about taurine and its antioxidant effects. *Tob. Regul. Sci.*, 2929–2936. doi:10.18001/TRS.9.1.201

Alfaro, A. C., Nguyen, T. V., and Mellow, D. (2019). A metabolomics approach to assess the effect of storage conditions on metabolic processes of New Zealand surf clam (*Crassula aequilatera*). *Aquaculture* 498, 315–321. doi:10.1016/j.aquaculture.2018.08.065

Alfaro, A. C., Nguyen, T. V., Venter, L., Ericson, J. A., Sharma, S., Ragg, N. L., et al. (2021). The effects of live transport on metabolism and stress responses of abalone (*Haliotis Iris*). *Metabolites* 11 (11), 748. doi:10.3390/metabo11110748

Ali, F., and Nakamura, K. (1999). Effect of temperature and relative humidity on the tolerance of the Japanese clam, *Ruditapes philippinarum* (Adams and Reeve), to air exposure. *Aquacult. Res.* 30 (9), 629–636. doi:10.1046/j.1365-2109.1999.00303.x

Ali, F., and Nakamura, K. (2000). Metabolic characteristics of the Japanese clam *Ruditapes philippinarum* (Adams and Reeve) during aerial exposure. *Aquacult. Res.* 31 (2), 157–165. doi:10.1046/j.1365-2109.2000.00402.x

Byrne, R. A., McMahon, R. F., and Dietz, T. H. (1988). Temperature and relative humidity effects on aerial exposure tolerance in the freshwater bivalve *Corbicula fluminea*. *Biol. Bull.* 175 (2), 253–260. doi:10.2307/1541566

Calder, P. C. (2017). Omega-3 fatty acids and inflammatory processes: from molecules to man. *Biochem. Soc. Trans.* 45 (5), 1105–1115. doi:10.1042/BST20160474

Clancy, R. M., Leszczynska-Piziak, J., and Abramson, S. B. (1992). Nitric oxide, an endothelial cell relaxation factor, inhibits neutrophil superoxide anion production via a direct action on the NADPH oxidase. *J. Clin. Invest.* 90 (3), 1116–1121. doi:10.1172/JCI115929

Coleman, N. (1973). Water loss from aerially exposed mussels. *J. Exp. Mar. Biol. Ecol.* 12 (2), 145–155. doi:10.1016/0022-0981(73)90010-5

Förstermann, U., and Sessa, W. C. (2012). Nitric oxide synthases: regulation and function. *Eur. Heart J.* 33 (7), 829–837. doi:10.1093/eurheartj/ehr304

Gong, C., Liu, C., Li, H., Li, M., Liu, Z., Wang, W., et al. (2019). The transformation of energy metabolism and Endoplasmic Reticulum stress regulation in Pacific oyster *Crassostrea gigas* under air exposure. *Invertebr. Surviv. J.* 72–83. doi:10.25431/1824-307X/isj.v0i0.72-83

González, P. M., Rocchetta, I., Abele, D., and Rivera-Ingraham, G. A. (2019). Hypoxically induced nitric oxide: potential role as a vasodilator in *Mytilus edulis* gills. *Front. Physiol.* 9, 1709. doi:10.3389/fphys.2018.01709

Gu, Z., Wei, H., Cheng, F., Wang, A., and Liu, C. (2020). Effects of air exposure time and temperature on physiological energetics and oxidative stress of winged pearl oyster (*Pteria penguin*). *Aquacult. Rep.* 17, 100384. doi:10.1016/j.aqrep.2020.100384

Guijas, C., Montenegro-Burke, J. R., Warth, B., Spilker, M. E., and Siuzdak, G. (2018). Metabolomics activity screening for identifying metabolites that modulate phenotype. *Nat. Biotechnol.* 36 (4), 316–320. doi:10.1038/nbt.4101

Haider, F., Falfushynska, H. I., Timm, S., and Sokolova, I. M. (2020). Effects of hypoxia and reoxygenation on intermediary metabolite homeostasis of marine bivalves *Mytilus edulis* and *Crassostrea gigas*. *Comp. Biochem. Physiol.* A Mol. Integr. Physiol. 242, 110657. doi:10.1016/j.cbpa.2020.110657

Halliwell, B. (1999). Antioxidant defence mechanisms: from the beginning to the end (of the beginning). *Free Radic. Res.* 31 (4), 261–272. doi:10.1080/10715769900300841

Hosoi, M., Shinzato, C., Takagi, M., Hosoi-Tanabe, S., Sawada, H., Terasawa, E., et al. (2007). Taurine transporter from the giant Pacific oyster *Crassostrea gigas*: function and expression in response to hyper-and hypo-osmotic stress. *Fish. Sci.* 73, 385–394. doi:10.1111/j.1444-2906.2007.01346.x

Hu, Z., Feng, J., Song, H., Zhou, C., Yang, M. J., Shi, P., et al. (2022). Metabolic response of *Mercenaria mercenaria* under heat and hypoxia stress by widely targeted metabolomic approach. *Sci. Total Environ.* 809, 151172. doi:10.1016/j.scitotenv.2021.151172

Jia, R., Du, J., Cao, L., Li, Y., Johnson, O., Gu, Z., et al. (2019). Antioxidative, inflammatory and immune responses in hydrogen peroxide-induced liver injury of tilapia (GIFT, *Oreochromis niloticus*). *Fish. Shellfish Immunol.* 84, 894–905. doi:10.1016/j.fsi.2018.10.084

Jing, H., Liu, Z. H., Wu, B., Tu, K., Liu, Z. M., Sun, X. J., et al. (2023). Physiological and molecular responses to hypoxia stress in Manila clam *Ruditapes philippinarum*. *Aquat. Toxicol.* 257, 106428. doi:10.1016/j.aquatox.2023.106428

Jong, C. J., Azuma, J., and Schaffer, S. (2012). Mechanism underlying the antioxidant activity of taurine: prevention of mitochondrial oxidant production. *Amino acids* 42, 2223–2232. doi:10.1007/s00726-011-0962-7

Kawabe, S., and Yokoyama, Y. (2010). Molecular cloning of calnexin and calreticulin in the Pacific oyster *Crassostrea gigas* and its expression in response to air exposure. *Mar. Genomics* 3 (1), 19–27. doi:10.1016/j.margen.2010.01.002

Kim, B. M., and Chung, H. W. (2007). Hypoxia/reoxygenation induces apoptosis through a ROS-mediated caspase-8/Bid/Bax pathway in human lymphocytes. *Biochem. Biophys. Res. Commun.* 363 (3), 745–750. doi:10.1016/j.bbrc.2007.09.024

Kraft, A. D., and Harry, G. J. (2011). Features of microglia and neuroinflammation relevant to environmental exposure and neurotoxicity. *Int. J. Environ. Res. Public Health* 8 (7), 2980–3018. doi:10.3390/ijerph8072980

Kuo, P. C., Abe, K. Y., and Schroeder, R. A. (1996). Interleukin-1-induced nitric oxide production modulates glutathione synthesis in cultured rat hepatocytes. *Am. J. Physiol. Cell Physiol.* 271 (3), C851–C862. doi:10.1152/ajpcell.1996.271.3.C851

Li, Y., Lai, S., Wang, R., Zhao, Y., Qin, H., Jiang, L., et al. (2017). RNA-Seq analysis of the antioxidant status and immune response of *Portunus trituberculatus* following aerial exposure. *Mar. Biotechnol.* 19, 89–101. doi:10.1007/s10126-017-9731-2

Liang, R., Shao, X., Shi, Y., Jiang, L., and Han, G. (2020). Antioxidant defenses and metabolic responses of blue mussels (*Mytilus edulis*) exposed to various concentrations of erythromycin. *Sci. Total Environ.* 698, 134221. doi:10.1016/j.scitotenv.2019.134221

Nguyen, T. V., Ragg, N. L., Alfaro, A. C., and Zamora, L. N. (2020). Physiological stress associated with mechanical harvesting and transport of cultured mussels (*Perna canaliculus*): a metabolomics approach. *Aquaculture* 529, 735657. doi:10.1016/j.aquaculture.2020.735657

Nie, H., Dong, S., Li, D., Zheng, M., Jiang, L., Li, X., et al. (2018). RNA-Seq analysis of differentially expressed genes in the grand jackknife clam Solen grandis under aerial exposure. *Biochem. Physiol. D. Genomics Proteomics* 28, 54–62. doi:10.1016/j.cbd.2018.06.003

Nie, H., Jiang, K., Li, N., Li, D., and Yan, X. (2020). Transcriptomic analysis of *Ruditapes philippinarum* under aerial exposure and reimmersion reveals genes involved in stress response and recovery capacity of the Manila clam. *Aquaculture* 524, 735271. doi:10.1016/j.aquaculture.2020.735271

Nogueira, L., Mello, D. F., Trevisan, R., Garcia, D., da Silva Acosta, D., Dafre, A. L., et al. (2017). Hypoxia effects on oxidative stress and immunocompetence biomarkers in the mussel *Perna perna* (Mytilidae, Bivalvia). *Mar. Environ. Res.* 126, 109–115. doi:10.1016/j.marenvres.2017.02.009

Palumbo, A. (2005). Nitric oxide in marine invertebrates: a comparative perspective. *A Mol. Integr. Physiol.* 142 (2), 241–248. doi:10.1016/j.cbpb.2005.05.043

Pequin, L., and Serfaty, A. (1966). Acideglutamique et excrétionazotée chez la carpe commune, *Cyprinus carpio* L.Comp.Biochem. Physiol. 18 (1), 141–149. doi:10.1016/0010-406X(66)90338-0

Schaffer, S., and Kim, H. W. (2018). Effects and mechanisms of taurine as a therapeutic agent. *Biomol. Ther.* 26 (3), 225–241. doi:10.4062/biomolther.2017.251

Strahl, J., and Abele, D. (2020). Nitric oxide mediates metabolic functions in the bivalve *Arctica islandica* under hypoxia. *PLoS ONE* 15 (5), e0232360. doi:10.1371/journal.pone.0232360

Strahl, J., Dringen, R., Schmidt, M. M., Hardenberg, S., and Abele, D. (2011). Metabolic and physiological responses in tissues of the long-lived bivalve *Arctica islandica* to oxygen deficiency. *Comp. Biochem. Physiol. A Mol. Integr. Physiol.* 158 (4), 513–519. doi:10.1016/j.cbpa.2010.12.015

Sun, X., Tu, K., Li, L., Wu, B., Wu, L., Liu, Z., et al. (2021). Integrated transcriptome and metabolome analysis reveals molecular responses of the clams to acute hypoxia. *Mar. Environ. Res.* 168, 105317. doi:10.1016/j.marenvres.2021.105317

Van Nguyen, T., and Alfaro, A. C. (2019). Targeted metabolomics to investigate antimicrobial activity of itaconic acid in marine molluscs. *Metabolomics* 15, 97–12. doi:10.1007/s11306-019-1556-8

Want, E. J., Masson, P., Michopoulos, F., Wilson, I. D., Theodoridis, G., Plumb, R. S., et al. (2013). Global metabolic profiling of animal and human tissues via UPLC-MS. *Nat. Protoc.* 8 (1), 17–32. doi:10.1038/nprot.2012.135

Wei, W., Tang, B. J., Yin, F., Sun, P., Jiang, Y. Z., and Li, L. (2017). Effects of air exposure on filtration, respiration and excretion rates of *Meretrix meretrix*. *J. Guangdong Ocean. U.* 37, 37–42. doi:10.3969/j.issn.1673-9159.2017.06.007

Wen, B., Mei, Z., Zeng, C., and Liu, S. (2017). metaX: a flexible and comprehensive software for processing metabolomics data. *BMC Bioinform* 18, 183–214. doi:10.1186/s12859-017-1579-y

Wink, D. A., Miranda, K. M., Espey, M. G., Pluta, R. M., Hewett, S. J., Colton, C., et al. (2001). Mechanisms of the antioxidant effects of nitric oxide. *Antioxid. Redox Signal.* 3 (2), 203–213. doi:10.1089/152308601300185179

Xian, J. A., Guo, H., Li, B., Miao, Y. T., Ye, J. M., Zhang, S. P., et al. (2013). Measurement of intracellular nitric oxide (NO) production in shrimp haemocytes by flow cytometry. *Fish. Shellfish Immunol.* 35 (6), 2032–2039. doi:10.1016/j.fsi.2013.10.014

Xu, Z., Regenstein, J. M., Xie, D., Lu, W., Ren, X., Yuan, J., et al. (2018). The oxidative stress and antioxidant responses of *Litopenaeus vannamei* to low temperature and air exposure. *Fish. Shellfish Immunol.* 72, 564–571. doi:10.1016/j.fsi.2017.11.016

Yu, W., Wenwen, W., Shenhan, X., Meng, Y., Xiaoqian, D., Xiwu, Y., et al. (2021). The effects of air exposure and recovery on immune parameters of *Ruditapes philippinarum*. *J. Agric.* 11 (4), 38. doi:10.11923/j.issn.2095-4050.cjas2020-0157

Zhan, J., Wang, S., Li, F., Ji, C., and Wu, H. (2021). Dose-dependent responses of metabolism and tissue injuries in clam *Ruditapes philippinarum* after subchronic exposure to cadmium. *Sci. Total Environ.* 779, 146479. doi:10.1016/j.scitotenv.2021.146479

Zhang, X., Shi, J., Sun, Y., Habib, Y. J., Yang, H., Zhang, Z., et al. (2019). Integrative transcriptome analysis and discovery of genes involving in immune response of hypoxia/thermal challenges in the small abalone *Haliotis diversicolor*. *Fish. Shellfish Immunol.* 84, 609–626. doi:10.1016/j.fsi.2018.10.044

Zhang, Y., Nie, H., and Yan, X. (2023). Metabolomic analysis provides new insights into the heat-hardening response of Manila clam (*Ruditapes philippinarum*) to high temperature stress. *Sci. Total Environ.* 857, 159430. doi:10.1016/j.scitotenv.2022.159430

Zhang, Y., Sun, J., Mu, H., Li, J., Zhang, Y., Xu, F., et al. (2015). Proteomic basis of stress responses in the gills of the pacific oyster *Crassostrea gigas*. *J. Proteome Res.* 14 (1), 304–317. doi:10.1021/pr500940s

frontiers | Frontiers in Physiology

TYPE Original Research
PUBLISHED 11 January 2024
DOI 10.3389/fphys.2023.1332446

OPEN ACCESS

EDITED BY
Ranjeet Bhagooli,
University of Mauritius, Mauritius

REVIEWED BY
Amilcare Barca,
University of Salento, Italy
Jose-Luis Martinez-Guitarte,
National University of Distance Education (UNED), Spain

*CORRESPONDENCE
Michael B. Morgan,
mbmorgan@berry.edu

RECEIVED 02 November 2023
ACCEPTED 28 December 2023
PUBLISHED 11 January 2024

CITATION
Morgan MB, Williams J, Breeze B, English N, Higdon N, Onthank K and Qualley DF (2024), Synergistic and antagonistic interactions of oxybenzone and ocean acidification: new insight into vulnerable cellular processes in non-calcifying anthozoans.
Front. Physiol. 14:1332446.
doi: 10.3389/fphys.2023.1332446

Synergistic and antagonistic interactions of oxybenzone and ocean acidification: new insight into vulnerable cellular processes in non-calcifying anthozoans

Michael B. Morgan[1,2]*, Jacob Williams[1], Barrett Breeze[1,2], Nicholas English[1], Nathaniel Higdon[1], Kirt Onthank[3] and Dominic F. Qualley[2]

[1]Department of Biology, Berry College, Mount Berry, GA, United States, [2]Department of Chemistry and Biochemistry, Berry College, Mount Berry, GA, United States, [3]Department of Biology, Walla Walla University, College Place, WA, United States

Cnidarians face significant threats from ocean acidification (OA) and anthropogenic pollutants such as oxybenzone (BP-3). The convergence of threats from multiple stressors is an important area to investigate because of potential significant synergistic or antagonistic interactions. Real-time quantitative PCR was performed to characterize the expression profiles of twenty-two genes of interest (GOI) in sea anemones (*Exaiptasia diaphana)* exposed to one of four treatments: 1) 96 h of OA conditions followed by a 4 h exposure to 20 ppb BP-3; 2) Exposure to 4 h 20 ppb BP-3 without 96 h of OA; 3) Exposure to 96 h of OA alone; or 4) laboratory conditions with no exposure to BP-3 and/or OA. These 22 GOIs represent cellular processes associated with proton-dependent transport, sodium-dependent transport, metal cation binding/transport, extracellular matrix, amino acid metabolism/transport, immunity, and/or steroidogenesis. These 22 GOIs provide new insight into vulnerable cellular processes in non-calcifying anthozoans exposed to OA and BP-3. Expression profiles were categorized as synergistic, antagonistic, or additive of BP-3 in the presence of OA. Two GOIs were synergistic. Fifteen GOIs were antagonistic and the remaining five GOIs were additive in response to BP-3 in acidified seawater. A subset of these GOIs appear to be candidate biomarkers for future *in situ* investigations. In human health, proton-dependent monocarboxylate transporters (MCTs) are promising pharmacological targets and recognized as potential biomarkers. By comparison, these same MCTs appear to be targets of xenobiotic chemical pollutants in cnidarian physiology. In the presence of BP-3, a network of collagen synthesis genes are upregulated and antagonistic in their expression profiles. Cytochrome b561 is a critical protein required for collagen synthesis and *in silico* modeling demonstrates BP-3 binds in the pocket of cytochrome b561. Understanding the underlying molecular mechanisms of "drug-like" compounds such as BP-3 may lead to a more comprehensive interpretation of transcriptional expression profiles. The collective antagonistic responses of GOIs associated with collagen synthesis strongly suggests these GOIs should be considered candidate biomarkers of effect. GOIs with synergistic and additive responses represent candidate biomarkers of exposure. Results show the effects of OA and BP-3 are

interactive with respect to their impact on cnidarians. This investigation offers mechanistic data that supports the expression profiles and underpins higher order physiological responses.

KEYWORDS

ocean acidification, oxybenzone, gene expression profiles, biomarkers, multiple stressors, *in silico* modeling, synergistic response, antagonistic response

Introduction

Ocean acidification is a global concern characterized by the increase in the acidity of the world's oceans due to the uptake of anthropogenic carbon dioxide (CO_2) from the atmosphere. Atmospheric CO_2 concentrations have risen from pre-industrial levels of approximately 275 ppm (Macfarling Meure et al., 2006) to over 400 ppm (Dunn et al., 2020), with nearly a third of all annual production of anthropogenic production of CO_2 being absorbed by the world oceans (Doney et al., 2009). The resulting drop in pH of marine environments poses significant threats to a broad range of marine organisms (Fabry et al., 2008). Meta-analysis of extant taxa responding to OA reveals similar trends in the negative responses of diverse phyla including cnidarians, mollusks, echinoderms, crustaceans, and bony fish (Kroeker et al., 2013; Wittmann and Pörtner, 2013; Medeiros and Souza, 2023). For calcifying organisms, OA leads to the reduction in the saturation state of carbonate ions, which hinders the calcification process. For corals, OA critically impacts growth and survival (Hoegh-Guldberg et al., 2007). A majority of previous cnidarian investigations have focused on calcification, skeletal density, and/or early life stages (Moya et al., 2012; Putnam et al., 2013; Ramos-Silva et al., 2013; Traylor-Knowles and Connelly, 2017). Some phyla such as Cnidaria and Mollusca also have taxa which are not calcifiers, so investigations not directly linked to calcification are also needed for a broader understanding of OA impact. Sea anemones in the genus *Exaiptasia* are ideal representatives of non-calcifying anthozoans that are easily cultured in the laboratory and utilized for ecotoxicological studies. Representatives of the genus are found worldwide in tropical marine ecosystems, have the same body plan as scleractinian corals, and are capable of establishing/maintaining symbiotic relationships with zooxanthellae (Sunagawa et al., 2009; Main et al., 2010; Schlesinger et al., 2010; Howe et al., 2012; Siddiqui et al., 2015; Duckworth et al., 2017).

Tropical coastal marine ecosystems are particularly notable for a number of diverse features. Coastal upwellings are locations that increase the probability of OA conditions (Manzello, 2010; Murray et al., 2015). Concurrently, anthropogenic activity along coastlines displays a concentration gradient from highest to lowest (nearshore to offshore, respectively) and is routinely driven by seasonal climatic activity (Dachs et al., 1999; Gray et al., 2002; Yamashita and Tanoue, 2003; Fabry et al., 2008; Gavio et al., 2010; Linsmayer et al., 2020; Zhu et al., 2022). As a consequence, coastal marine ecosystems are exposed to a diversity of anthropogenic stressors and these environments are increasingly becoming "sinks" for complex mixtures of anthropogenic chemicals originating from diverse sources (Peters et al., 1997; Atkinson et al., 2003; Wurl and Obbard, 2004; Fent et al., 2006; Schiedek et al., 2007; Halpern et al., 2008; Jones, 2010; Burns and Brinkman, 2011; Dafforn et al., 2011; Vidal-Dorsch et al., 2012; French et al., 2015; Pie et al., 2015; Wear and Thurber, 2015; Downs et al., 2016; Archer et al., 2017; Law, 2017; Worm et al., 2017; Lebreton et al., 2018; Mitchelmore et al., 2019). As a consequence, marine organisms in coastal marine ecosystems face significant threats from diverse anthropogenic chemical pollutants.

Oxybenzone (BP-3), the active ingredient in sunscreen, is just one of many xenobiotics present in the marine environment (Vidal-Dorsch et al., 2012). It is estimated that 14,000 tons of sunscreens enter the oceans annually from beachgoers and domestic sewage effluent, and there is a growing body of evidence of BP-3 acts as an endocrine disruptor on cnidarians (Downs et al., 2016; Mitchelmore et al., 2019; Mitchelmore et al., 2021; Morgan et al., 2022).

The convergence of threats from OA and chemical pollution is an important area of investigation because of potential significant interactions between anthropogenic pollutants and OA conditions (Nikinmaa, 2013). The natural environment is a mixture of multiple stressors causing mixed effects and challenging organisms to acclimatize and/or adapt to physiologically demanding conditions (Evans and Hofmann, 2012; Stillman et al., 2015; Deidda et al., 2021). For example, heavy metal toxicity is known to be exacerbated in sea anemones experiencing OA (Siddiqui et al., 2015; Duckworth et al., 2017). Currently, there are knowledge gaps in cnidarian transcriptional responses to BP-3 within an environment of OA. This study seeks to characterize patterns of transcription in genes of interest (GOIs) in sea anemones responding to BP-3 and acidic seawater.

Materials and methods

CO_2-acidified conditions

Two 38 L glass aquaria were filled with raw seawater obtained from the Rosario Beach Marine Laboratory seawater system, which is in turn pumped from Rosario Bay, Fidalgo Island, Washington, US. Seawater was allowed to equilibrate to room temperature, approximately 21°C, before being added to the aquaria. Temperature and pH of each aquarium was monitored using an Open Acidification Tank Controller unit (Onthank et al., 2023). The pH of the treatment aquarium was adjusted lower by bubbling pure CO_2 into a bubble stone from a solenoid-equipped CO_2 regulator on a 2.3 kg high pressure CO_2 cylinder and controlled by the Open Acidification Tank Controller. A pH of 7.5 was the target pH for the treatment aquarium for two reasons: 1) the pH of 7.5 is approximately 0.3 units lower than present day pH of seawater found in Rosario Bay (Onthank et al., 2021), and 2) the pH of 7.5 is below BP-3's pKa of 7.6 (Fontanals et al., 2010). The pH of the control aquarium was not controlled. The temperature of the

aquaria was not controlled and allowed to match the room temperature. Independent measurements of pH were taken of each aquarium daily using the m-cresol purple spectrophotometric method (Dickson et al., 2007) as modified by Culler-Juarez and Onthank (2021). Total pH values were calculated from absorbance values in R using the "specpH" function found the in OTools package version 22.08.01 (https://github.com/KirtOnthank/Otools). Total alkalinity of each aquarium was measured on day 1 and day 4 using the open-cell titration method (Dickson et al., 2007) and alkalinity was calculated from titration data in R using the "at" function in the seacarb package version 3.2.14 (Gattuso et al., 2015). Salinity was measured daily using a Vernier salinity probe (SAL-BTA). Temperature was measured daily using a VWR precision liquid-in-glass thermometer. Partial pressure of carbon dioxide in each aquarium was calculated each day from daily pH, salinity, and temperature measurements, and from average of total alkalinity measurements for each aquarium in R using the "carb" function from in the "seacarb" function version 3.2.14 (Gattuso et al., 2015). All raw data and code to calculate derived values are available in a repository on Zenodo (https://doi.org/10.5281/zenodo.8011603).

Toxicant exposure

Sea anemones (*Exaiptasia diaphana)* were purchased from a supplier (Carolina Biological Supply, Burlington, NC, United States) and acclimated to laboratory conditions (recirculating natural seawater at 21°C, ambient laboratory lighting, and 29 ppt salinity) for 1 month prior to beginning the experiment. All BP-3 treatments were nominal concentrations for 4 h in 1L seawater under ambient laboratory lighting during the mid-summer season. The 20 ppb concentration was chosen to induce responses and does not necessarily reflect environmental conditions. Previous studies have demonstrated a toxicant concentration of 20 ppb will induce detectable differential gene expression after 4 h of exposure (Morgan et al., 2001; Morgan and Snell, 2002; Morgan and Snell, 2006; Morgan et al., 2012; Morgan et al., 2022). Variations in environmental conditions can influence the toxicity of xenobiotics (Xin et al., 2021). A 4 h exposure was arbitrarily chosen as an initial timeframe since environmental BP-3 is associated with anthropogenic beach activity. The 96 h timeframe of OA exposure was chosen since some coastal upwellings are known to have periodicities of fluctuation (Murray et al., 2015; Rodriguez-Ruano et al., 2023). Dynamic environments such as an acute 96 h exposure of OA followed by a 4 h pulse of BP-3 will challenge organisms to adapt to physiologically demanding conditions (Evans and Hofmann, 2012). BP-3 was solubilized in acetone at 100 µL/L prior to dilution in seawater. Anemones were divided into four treatments: 1) 96 h of OA conditions followed by a 4 h exposure to 20 ppb oxybenzone (BP-3); 2) Exposure to 4 h 20 ppb BP-3 without 96 h of OA; 3) Exposure to 96 h of OA alone; or 4) laboratory conditions without exposure to BP-3 and/or OA conditions. The 96 h timeframe was chosen because there is evidence of different patterns of responses between short- and long-term CO_2 exposures (Inbakandan, 2016; Medeiros and Souza, 2023).

Selecting candidate genes of interest

A plethora of studies have investigated OA effects on calcifying marine organisms. Meta-analysis of extant taxa responding to OA reveals similar trends in the negative responses of diverse phyla including cnidarias, mollusks, echinoderms, crustaceans, and bony fish (Kroeker et al., 2013; Wittmann and Pörtner, 2013). Some phyla (i.e., Cnidaria and Mollusca) also have taxa which are not calcifiers (i.e., anemones and octopus, respectively). Hence, there is value in investigating responses to OA in non-calcifying taxa within calcifying phyla. In this investigation, genes on a cnidarian stress EST library were compared to an *O. rubescens* transcriptome from octopus exposed to OA conditions (data unpublished). Previous studies on model eukaryotes have shown that only 5%–10% of their genes respond to stressed conditions (Adams et al., 2000; Gasch et al., 2000; Hill et al., 2000; Goldstone, 2008). Since both phyla contain calcifying and non-calcifying taxa, this comparison offers the opportunity to identify genes that are representative of stress responses of non-calcifying organisms responding to xenobiotic chemicals and OA conditions. Candidate genes of interest (GOIs) were identified from homologous proteins (BLASTX analysis: nr database, standard parameters) found in both the cnidarian stress EST library and the *O. rubescens* transcriptome data. Subsets of ESTs from the cnidarian stress library have previously been used to characterize other cnidarian stress responses (Morgan et al., 2012; Morgan et al. 2015; Morgan et al. 2022)

Reverse transcription reactions

Six to 10 anemones were pooled and homogenized for each treatment. Total RNA was isolated using Trizol (Invitrogen, United States). RNA concentration and quality were assessed using a NanoDrop ND-1000 spectrophotometer (Thermo Fisher Scientific, United States). Total RNA from pooled samples for each treatment was DNase I digested (New England BioLabs, United States), purified by chloroform/phenol extraction, and then reverse transcribed. First stand synthesis used SuperScript IV (Invitrogen, United States) along with random hexamers and oligo-dT primers to reverse transcribe 1 µg of total RNA. Reverse transcription conditions were 1 h at 37°C, followed by 1 min at each temperature between 42°C and 50°C.

Quantitative real-time PCR

A QuantStudio 7 Flex Real-Time PCR system (Applied Biosystems, United States) used a SYBR Green-based assay to perform qPCR. A 1/100 dilution of first-strand synthesis reactions were used as templates for all qPCR reactions. Primers for each GOI were created using Primer3 (https://primer3.org). Components for each 20 µL qPCR reaction included: 10 µL Luna® universal qPCR Mix (New England BioLabs, United States), 2.5 µL Forward primer (10 µM stock), 2.5 µL Reverse primer (10 µM stock), 2.5 µL dH_2O, 2.5 µL sample. Thermocycling conditions were 1 cycle at 95°C for 1 min; 40 cycles of 95°C for 15 s and then 60°C for 30 s; and concluding with 1 cycle of melt curve analysis. Three to four technical replicate

reactions were used for analyzing the relative expression of each GOI. Because of a consistent expression pattern, *RPL11* was used as the qPCR reference gene (Kenkel et al., 2011). Melt-curve analysis, primer efficiencies, and gel electrophoresis confirmed specificity of priming. Replicate Cq values were averaged to determine ΔCq and ΔΔCq for each treatment and GOI. All ΔCq and ΔΔCq values are based on the consistent expression of the endogenous reference control gene (*RPL11)* across all treatments. The ΔΔCq method was used to determine the differences between targeted GOIs and a single reference gene (Bustin et al., 2009). Two-way ANOVA was performed on Log 2 transformed relative quantity data to determine the significant of the main effects and interactions. All *p*-values were adjusted using the Benjamini–Hochberg FDR correction.

in silico molecular modelling

Human protein homologs have previously been used as substitutes for cnidarian proteins in molecular modelling (Khalturin et al., 2018). Some cnidarian proteins have such significant homology to human proteins that they are even capable of stimulating human responses (Dunn et al., 2006; Wood-Charlson and Weis, 2009; Duffy and Frank, 2011; Dani et al., 2014; Brennan et al., 2017; Mansfield et al., 2017). The most similar vertebrate structures were used for selecting the Protein Databank (PDB) files to be used for initial docking experiments. In the case of MCT1, cryo-EM structures of the homologous human protein in both inward-facing and outward-facing conformations are available in the PDB (PDB IDs 7cko and 7ckr, respectively). These structures were used for docking after removal of water and ligand molecules. The same treatment was applied to cytochrome b561, using 4o79 for the construct facing inward (cytosolic side) and 4o7g for the construct facing outward (non-cytosolic side). For MCTs 2 and 3, models were constructed using *H. sapiens* sequences corresponding to MCT2 (GenBank: AF049608.1) and MCT3 (GenBank: U81800.1) due to the lack of information on the cnidarian sequences. The cnidarian sequence was used to model MCT10 (GenBank: KXJ27932.1). All models of MCT2, 3, and 10 were constructed with the SWISS-MODEL web server (https://swissmodel.expasy.org) (Bertoni et al., 2017; Bienert et al., 2017; Waterhouse et al., 2018; Studer et al., 2020; Studer et al., 2021) using 7cko for inward-facing constructs and 7ckr for outward-facing constructs as templates. Ligands were created in Avogadro (Hanwell et al., 2012) and energy-minimized prior to docking. Docking was performed using AutoDock Vina (Trott and Olson, 2010); the search space was restricted to the known ligand binding site. Docking included protonated and deprotonated ligands. After docking, the results were analyzed in UCSF Chimera (Pettersen et al., 2004).

Statistical analysis

After assumptions were tested by Levene's test for homogeneity of variance across groups and Shapiro-Wilk Normality test, a two-way ANOVA was conducted for each gene to determine the significance of the main effects of OA and BP-3, as well as their potential interactions. The *p*-values obtained from these ANOVAs underwent an adjustment using the Benjamini–Hochberg False Discovery Rate (FDR) correction method to correct for multiple comparisons.

Genes were classified as "additive" where the interaction *p*-value exceeded 0.05, suggesting a non-significant interaction effect on gene expression between OA and BP-3. In this scenario, the combined effect of OA and BP-3 on the slope of gene expression can be interpreted as the summation of their independent effects. Genes were categorized as "synergistic" when both the slopes of interaction plots were either both positive or both negative with control OA being less steep than experimental OA exposure. In the context of this study, synergistic effects denote a scenario where the combined influence of OA and BP-3 on gene expression is greater than what would be anticipated from the sum of their individual effects. Lastly, "antagonistic" effects were identified for genes showing opposing slopes in the interaction plots, implying a counteracting influence between OA and BP-3 exposures on the anemone's gene expression. Data and code underlying these analyses is available at https://zenodo.org/doi/10.5281/zenodo.10056756.

Results

Acclimated anemones were separated into two groups (control and CO_2-acidified treatment). At the beginning of the 96 h of exposure to acidified seawater the starting pH was 8.25. At the end of 96 h of exposure to acidified seawater, pCO_2, pH, alkalinity, salinity, and temperature was recorded (see Table 1).

Genes of interest

This investigation quantified expression of 22 GOIs: 2-oxoglutarate and iron-dependent oxygenase domain-containing protein 2 (2OG-Fe (II)), 17β-hydroxysteroid dehydrogenase type 14 (17βHSD14), 17β-hydroxysteroid dehydrogenase type 12 (17βHSD12), Collagen alpha-2 (I) chain (COL1A2), Collagen alpha-1 (IV) chain (COL4A1), complement component C3 (C3), Cytochrome b561(CYB561), Glutamine synthetase (GLUL), Hephaestin (Heph), Integrin beta-PS (MYS), low affinity copper uptake protein 2 (SLC31A2-1), Monocarboxylate Transporter 2 (MCT2, SLC16A7), Monocarboxylate Transporter 3 (MCT3, SLC16A3), Monocarboxylate Transporter 10 (MCT10, SLC16A10), ornithine aminotransferase, mitochondrial-like (OAT), Serotransferrin-like (TF), Sodium/calcium exchanger 3 (SLC8A3), Soma ferritin-like (FTH1), Tauropine dehydrogenase (TaDH), Tenascin-R (TNR) has a FReD (containing a fibrinogen domain) and is also known as ryncolin-4), Transient receptor potential cation channel subfamily A member 1-like (TRPA1), Zinc transporter ZIP14 (SLC39A14). These GOIs are associated with proton-dependent transport, sodium-dependent transport, metal cation binding/transport, extracellular matrix, amino acid metabolism/transport, immunity, and/or steroidogenesis (see Table 2 for primers; Table 3 for accession numbers).

Transcriptional responses of GOIs

All 22 GOIs exhibited significant changes in transcription to OA conditions, and/or BP-3 exposure, and/or the interaction of OA and

TABLE 1 Experimental conditions at the end of exposure to 96hrs of acidified seawater.

Treatment	pCO_2 (μ atm)	pH	Alkalinity (μ mol kg^{-1})	Salinity (PSU)	Temperature (C)
Control	247 ± 47	8.348 ± 0.066	2048 ± 6	29.5 ± 0.1	21.3 ± 0.2
Elevated CO_2	2045 ± 45	7.499 ± 0.009	2040 ± 1	29.5 ± 0.1	21.4 ± 0.1

BP-3 (Figure 1: heatmap Table 4: *p*-values of significant responses). Twenty GOIs had significant responses to OA and two GOIs (TF, TNR) were not significantly responsive to OA. Fourteen GOIs were responsive to BP-3 exposure while the remaining eight GOIs were not responsive to BP-3 (2OG Fe(II), SLC39A14, MCT2, MCT3, SLC8A3, 17βHSD14, TRPA1, SLC31A2). Five GOIs did not have significant interactions between OA conditions and BP-3 exposure (MCT2, MCT10, GLUL, TF, TNR).

Docking simulations

In silico modeling was performed on MCT2, MCT3, MCT10, and CYB561. MCT2 and MCT3 docking simulations included binding affinities for lactate which is the recognized molecule of transport for proton-dependent transporters. MCT1 was modeled as a comparison since it is the most-well characterized proton-dependent transporter with known inhibitors (BAY8002 and 7ACC2). Docking simulations with MCT10 included amino acids with aromatic side chains which are the recognized molecules of transport (Table 5). Docking simulations of CYB561 reveal there are seven amino acid side chains that interact with BP-3 (Figure 2). By comparison, CYB561 has 4 amino acids interacting with ascorbate (see Figure 2). Table 5 provides a comparison of the binding affinities for BP-3 and ascorbate.

Categorizing synergistic, antagonistic, or additive effects

Figure 3 identifies which GOIs had synergistic, antagonistic, or additive effects. Table 4 identifies which GOIs had significant interactions. Two GOIs (TF and OAT) had significant synergistic transcriptional interactions on their respective gene networks (see Table 4 and Figure 3). Fifteen GOIs had significant transcriptional interactions with antagonistic effects (see Table 4 and Figure 3). Five GOIs (GLUL, MCT10, MCT2, TaDH, TNR) exhibit additive responses when BP-3 is present in acidified seawater (see Figure 3).

Discussion

pH in experimental setup

At the beginning of 1 month of acclimation, the pH was not measured. After 1 month of acclimation, the pH of 8.25 was recorded at the beginning of the experiment. The pH of the local seawater is typically between 7.8–8.0 (Murray et al., 2015; Onthank et al., 2021). Differences between the normative pH range of local waters and the pH measured at the beginning of the treatments is likely due to 1) anemone's algal symbionts favoring carbon fixation (removal of CO_2) under the laboratory conditions during the 1 month of acclimation; 2) bubbling of air into the control tank helped drive off excess pCO_2 from the local waters. Coral Reefs are known to experience fluctuations in pH of 0.5 units (Birkeland et al., 2008).

The pH range used in this investigation was important because it spanned the pKa of BP-3. Speciation of a compound is determined by pH and the compound's pKa. If a compound's pKa is the same as the pH, its ionized and unionized molecules are at equal concentrations (Xin et al., 2021). BP-3′s pKa is 7.6 (Fontanals et al., 2010). The laboratory-controlled acidic conditions of pH 7.5 favored a shift towards a protonated form of BP-3 but there was not a significant difference in the binding affinities of protonated *versus* deprotonated forms of BP-3 (see Table 5).

Functional significance of expression profiles

Monocarboxylate transporters and links to intracellular pH

While intracellular pH was not directly measured in this investigation, some expression profiles suggest intracellular pH was lowered by exposure to OA. MCT expression is known to be influenced by intracellular pH due to extracellular pH (Gopal et al., 2004). MCTs play a role in the maintenance of intracellular pH which is critical for physiological function (Casey et al., 2010; Halestrap, 2013). Monocarboxylate transporters function as sensors and regulators of pH (Casey et al., 2010; McBrian et al., 2013). MCT 1,2,3, and 4 are symporters of monocarboxylates and protons (1:1 ratio) and the direction of transport across plasma membrane is determined by the relative intra- and extracellular pH (Iwanaga and Kishimoto, 2015). Proton-dependent MCTs are stimulated by decreasing the pH from 8 to 6 and with lowered pH, the Km value (Michaelis constant) for MCTs decreases thereby improving efficiency for binding and transport (Halestrap and Meredith, 2004; Halestrap, 2013). MCT 1&2 pump compounds and protons in one direction while MCT 3&4 pump the same compounds and protons in the opposite direction (Yoshida, 2021). The process of different MCTs coordinating transport of the same compounds in opposite directions is commonly described as metabolic symbiosis (Payen et al., 2020). The expression profiles of MCT2 (SLC16A7) and MCT3 (SLC16A3) in the OA treatment is consistent with the concept of metabolic symbiosis as each would be pumping in opposite direction (see Figure 4A). Data herein is consistent previously published studies demonstrating downregulated transcription of proton-dependent MCTs under acidic conditions (Casey et al., 2010) (see Figure 4A). The gastrovascular pH is known to be more acidic than

10.3389/fphys.2023.1332446

TABLE 2 Genes of Interest and their corresponding primers used in qPCR reaction. Annealing temperature for all primers was 60°C.

Gene ID	Primers	Amplicon length in bases
2OG-Fe(II)	F: GGAGTTTTCAGGTGGTGAGC	196
	R: ATTGCGGACTTTTGATGACC	
17βHSD12	F: AGTCCAGATTTTCTTGCAACCA	226
	R: TAGACTTCAGTGGTGGGCAG	
17βHSD14	F: TGCACCCTTTGTTGTGACAT	209
	R: GATGGCATCCTCCAGAAAGA	
COL1A2	F: GATCCCAACAACGGCTGC	150
	R: TTCACTAAACCATTCTGCTCCG	
COL4A1	F: GCCAGGCAAGTGACTTCTTA	199
	R: GTTCCTCCCAAACAGCAAGT	
C3	F: TTATCATGGTCCTGGGTGCT	208
	R: GCGTCAAACTCGAACGTTTT	
CYB561	F: GGAGAAGCGCACTGGTCTA	157
	R: GCCTCCATTCTGCTGTCATG	
FTH1	F: GAGCTTGACTCGTCCTCCAC	197
	R: AGGAATCCATCAACCAGCAG	
GLUL	F: TCGTCTATCTTCAAGGTAGCCC	157
	R: CCCCAAGCAAGGACAAGACT	
Heph	F: ACAAGATGTTTGACGTGGGC	232
	R: CGTCTTTGTCAACTCGTGCA	
MCT2	F: TTGGTTACGGTGTAGGGGAG	217
	R: GCAAAGACTTCTAGCGAGCC	
MCT3	F: TGGTTGGTTTGTATCGCTGC	167
	R: AGCGGGCCAAATAGATACGA	
MCT10	F: ATCTCATGCCCGTATGTAGAC	151
	R: CCCATGTCGGCAACTCTAAT	
MYS	F: CGCAAAGACCTAGACAACCG	209
	R: AGGGATGTGTGACTGTGGAG	
OAT	F: CCTCGGTGGTATCTGTGGTT	120
	R: CCAAGCCGCTATAATCATATGGG	
SLC31A2	F: TGAAACAAAGGCTGAGAGAAGA	121
	R: TAGCCAACCTCGTGTATGCA	
SLC39A14	F: GATCAATGTCAAACACTGTCATCA	150
	R: CTTCATCAACACCTGCTCCA	
SLC8A3	F: CGGCGTGTTTGTTATTCTGC	241
	R: GTACGTGACCACATTCGAGC	
TaDH	F: CACGACCCCCATGATGTAGT	178
	R: GGTAGAACAAAGGCCGTTCA	

(Continued on following page)

TABLE 2 (*Continued*) Genes of Interest and their corresponding primers used in qPCR reaction. Annealing temperature for all primers was 60°C.

Gene ID	Primers	Amplicon length in bases
TF	F: TTTTACAATGAAAACGTCTCAAACTT	163
	R: GGCAAGTGCTATCCCAAGTC	
TNR	F: CTACCGTCTTCAATGCATCCC	225
	R: AGAATGAGTGGGCAATGCATC	
TRPA1	F: TGAAACCATGCATCGCTCAT	158
	R: TGAAAGACATGCAGACACAGC	

TABLE 3 Gene of interests (GOIs) and associated *Exaiptasia diaphana* accession numbers.

Putative gene	Gene abbreviation	Homolog accession #
2-oxoglutarate and iron-dependent oxygenase domain-containing protein 2	2OG-Fe (II)	XP_020905799
17-beta-hydroxysteroid dehydrogenase 12-like	17βHSD12	KXJ12187
17-beta-hydroxysteroid dehydrogenase 14-like	17βHSD14	KXJ20962
Collagen alpha-2 (I) chain	COL1A2	KXJ29536.1
Collagen alpha-1 (IV) chain	COL4A1	KXJ15297.1
Complement C3	C3	KXJ11955.1
Cytochrome b561	CYB561	KXJ17631.1
Glutamine synthetase	GLUL	AAR36878.1
Hephaestin-like	HEPH	XP_020906986.1
Integrin beta-PS	MYS	KXJ28340.1
low affinity copper uptake protein 2	SLC31A2, CTR2	XP_020892422.1
Monocarboxylate Transporter 2	SLC16A7, MCT2	XP_020903028
Monocarboxylate Transporter 3	SLC16A3, MCT3	XP_028513916
Monocarboxylate Transporter 10	SLC16A10, MCT10	KXJ27932.1
ornithine aminotransferase, mitochondrial-like	OAT	XP_020909112
Serotransferrin-like	TF	XP_020907010.1
Sodium/calcium exchanger 3	SLC8A3	XP_020912295
Soma ferritin-like	FTH1	XP_020908035.1
Tauropine dehydrogenase	TaDH	XP_020915529.1
Tenascin-R	TNR	KXJ05169.1
Transient receptor potential cation channel subfamily A member 1-like	TRPA1	KXJ26138.1
Zinc transporter ZIP14	SLC39A14, ZIP 14	KXJ16968.1

surrounding seawater (Cai et al., 2016; Bove et al., 2020). Since whole animal homogenate was used in this investigation, future studies should investigate *in situ* hybridization of MCT2 vs. MCT3 to determine which tissues are most likely to utilize which MCT. Calcium ATPase have previously been the focus of identifying potential proton exchangers that help regulate pH in stony corals (Zoccola et al., 2004; Tambutté et al., 2011). The responsiveness of the proton-dependent MCTs presented herein offers another potential regulator of intracellular pH to consider in future studies. Coupled with the responsiveness of SLC8A3 ($Na+/Ca^{2+}$ exchanger), these MCTs may provide an alternative mechanistic option for modulating Ca^{2+} and intracellular pH in stony corals.

Links to amino acid synthesis, reservoirs, and metabolism

The following amino acids are associated with expression profiles generated in the investigation: glutamine, glutamic acid,

10.3389/fphys.2023.1332446

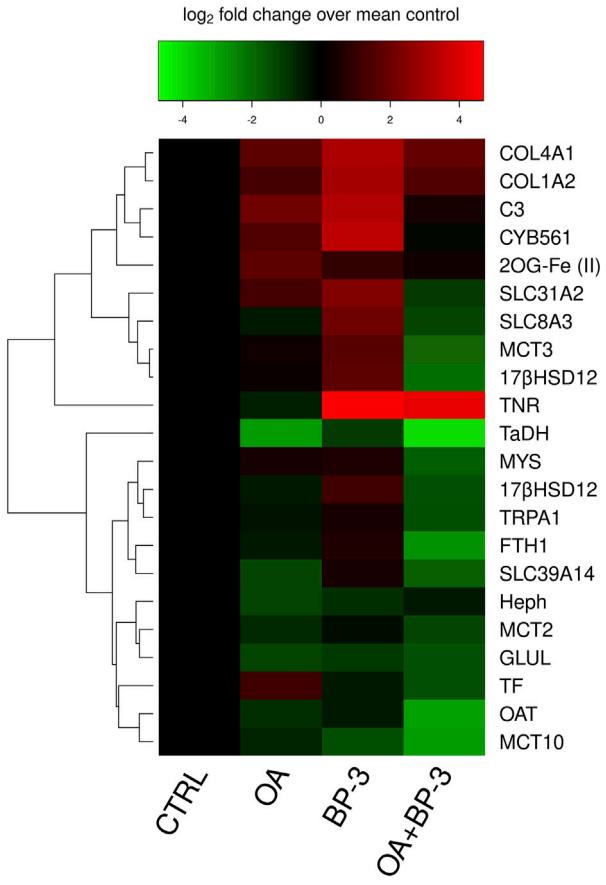

FIGURE 1
Heatmap of differential expression for all 22 genes of interest in each treatment.

TABLE 4 *p*-values for each GOI in the presence of OA, BP, or any significant interaction between OA and BP-3. Values in bold are significant.

Gene	OA	BP-3	Interaction
SLC39A14	**<0.001**	0.9341	**0.0213**
tadh	**<0.001**	**<0.001**	0.8246
TF	0.8556	**<0.001**	**<0.001**
FTH1	**<0.001**	**<0.001**	**<0.001**
2OG-Fe II	**0.0161**	0.3359	**<0.001**
TRPA1	**<0.001**	**0.0101**	**<0.001**
MYS	**<0.001**	**<0.001**	**<0.001**
TNR	0.3284	**<0.001**	0.9341
SLC8A3	**<0.001**	0.1243	**0.0037**
MCT10	**0.0043**	**<0.001**	0.1891
MCT3	**0.0021**	0.4997	**<0.001**
CYB561	**0.0093**	**0.0183**	**<0.001**
COL1A2-11	**0.0089**	**<0.001**	**<0.001**
COL4A1-11	**<0.001**	**<0.001**	**<0.001**
MCT2	**0.0227**	0.2464	0.6405
HSD14	**<0.001**	0.9436	**0.0046**
HSD12	**<0.001**	**0.024**	**<0.001**
C3	**0.0173**	**<0.001**	**<0.001**
GLUL	**<0.001**	**0.0057**	0.0843
OAT	**<0.001**	**<0.001**	**<0.001**
Heph	**0.0042**	**0.0042**	**<0.001**
SLC31A2-1	**<0.001**	0.9745	**<0.001**

proline, hydroxyproline, amino acids with aromatic side chains, and the non-proteinogenic amino acids taurine and tauropine.

Glutamine synthetase (GLUL) is required to convert glutamic acid into glutamine. Glutamine synthetase regulation is pH-sensitive (Frieg et al., 2021). The downregulated transcription of glutamine synthetase (Figure 4B) suggests lower cellular demand for glutamine allowing glutamate to be utilized/shifted towards other metabolic demands. Under intracellular acidic conditions, four biochemical reactions occur: 1) Glutamine is deamidated by direct hydrolysis (Li et al., 2010), 2) the interconversion of glutamate and α-ketogluarate by glutamate dehydrogenase (GDH) is driven in the direction of glutamate synthesis. 3) the interconversion between glutamate and glutamate-γ-semialdehyde (GSA) is driven towards GSA synthesis which is an intermediate precursor of proline. 4) the interconversion of ornithine and GSA relies on ornithine-δ-aminotransferase (OAT) and the reaction is driven in the direction of GSA (a proline precursor). Under acidic conditions, these four biochemical reactions all move in the direction of proline synthesis. Glutamate metabolism and proline synthesis are functional links between the TCA and urea cycles. Proline plays an important role in regulation of synthesis of ornithine, arginine, polyamines, glutamate and collagen (Karna et al., 2020). In this investigation, there is downregulated transcription of OAT because the cellular demand for converting ornithine into GSA is lessened because glutamate abundance is already elevated in the acidic environment (see Figure 4B). When OAT demand is upregulated, there is increased proline catabolism (Albaugh et al., 2017).

The upregulated transcription profiles of collagen chains I and IV (see Figure 4B) are consistent with an increased metabolic demand for proline synthesis since proline is a major component of collagen. Newly synthesized proline normally accumulates in cytoplasm where it helps buffer cytosolic pH (Meena et al., 2019). If cells are experiencing an intracellular acidic pH, then upregulated synthesis of proline won't offset intracellular acidic pH because newly synthesized proline is utilized in collagen synthesis. The upregulated transcription of collagen chains (COL1A2; COL4A1) (see Figure 4B) suggests increased cellular demand for synthesizing proline which must then be post-translationally modified to produce the hydroxyproline residues needed for collagen. Both proline and hydroxyproline have important metabolic and physiological roles (Li and Wu, 2018).

Tauropine dehydrogenase (TaDH) is responsible for the interconversion of two non-proteinogenic amino acids Tauropine and Taurine. The abundance of Tauropine typically correlates with the concentration of taurine (derivative of methionine or cysteine)

TABLE 5 *In silico* binding affinities (kcal/mol). BY8002 and 7ACC2 are recognized inhibitors of MCT1. Phe, Tyr, and Trp are the aromatic amino acids normally transported by MCT10. *actual structure used instead of homology model. Transporter orientation towards the cytosolic side of the plasma membrane are labeled "in". Transporter orientation towards the extracellular side of the plasma membrane are labeled "out". Values in bold are significant.

Receptor	Ligand					Template
	BP3 (protonated)	BP3 (deprotonated)	L-lactate	BAY8002	7ACC2	
MCT1-in	−8.202	−8.362	−3.852	−9.472	−10.555	7cko*
MCT1-out	−7.343	−8.088	−4.027	−10.679	−8.247	7ckr*
MCT2-in	−8.534	−8.733	−3.784			7cko
MCT2-out	−7.311	−7.356	−3.89			7ckr
MCT3-in	−7.681	−7.667	−3.811			7cko
MCT3-out	−6.531	−6.854	−3.591			7ckr
			Phe	**Tyr**	**Trp**	
MCT10-in	−6.829	−6.931	−6.166	−6.173	−6.659	7cko
MCT10-out	−7.458	−7.551	−6.201	−6.264	−7.279	7ckr
			ascorbate			
CYB561 (cytosolic)	−4.69	−4.705	−4.79			4o79*
CYB561 (noncytosolic)	−6.743	−6.938	−4.518			4o7g*

(Linsmayer et al., 2020). The expression profile of TaDH (see Figure 4B) reveals Tauropine and Taurine are relevant in the context of OA where the interconversion reaction is driven towards Taurine accumulation. Tauropine is produced under hypoxic (fermentation) conditions. There is growing recognition of the importance of fermentative metabolism for cnidarian biology (Linsmayer et al., 2020). Fermentation will increase demand for proton-dependent MCTs to pump lactate out of cells. Taurine levels increase in pathological conditions where its antioxidant capabilities help to downregulate of inflammatory mediators (Voskanyan et al., 2014). Taurine's buffering capacity reduces the negative impact of lactate by modulating intracellular free Ca^{2+} during fermentation conditions. Taurine lowers intracellular Ca^{2+} levels by inhibiting calcium influx from calcium channels including the reverse mode of Na+/Ca^{2+} exchanger (SLC8A3) (Li et al., 2005). Calcium influx can also occur through TRPA1 which is responsive to taurine (Redmond et al., 2014; Meents et al., 2019). Under acidic conditions, glutamate synthesis is elevated which elevates the intracellular Ca^{2+} concentration. Taurine reduces glutamate-induced elevated Ca^{2+} concentration (Ripps and Shen, 2012). Expression profiles for both SLC8A3 and TRPA1 are downregulated which reaffirms a reduced cellular demand for Ca^{2+} influx (see Figure 4B).

MCT10 transports amino acids with aromatic side chains (Imagawa et al., 2004; Yoshida, 2021). Cnidarians import essential amino acids (including phenylalanine and tyrosine) directly from symbiotic algae (Wang and Douglas, 1999) and tyrosine is known to be can be transferred to marine invertebrate larvae via the food chain (Heyland and Moroz, 2005). MCT10's recognized function offers a potential mechanistic explanation for how cnidarians import the amino acids referenced in these previous studies. It has also recently been discovered that another monocarboxylate transporter MCT7 will transport taurine, a non-proteinogenic amino acid (Higuchi et al., 2022).

Links to collagen synthesis and the extracellular matrix

The four major classes of proteins associated with the ECM are structural proteins, glycoproteins, glycosaminoglycans and proteoglycans, and matricellular proteins (Jones et al., 2015). Seven GOIs (COL1A2, COL4A1, CYB561, 2OG-Fe(II), GLUL, OAT, SLC31A2) are associated the collagen synthesis (Figure 4C). Collagen belongs to the structural class of the ECM proteins. The upregulated transcription of collagen chains I & 4 (COL1A2; COL4A1, respectively) suggests increased cellular demand for proline which must be post-translationally modified to produce hydroxyproline for collagen. Proline synthesis occurs through the glutamate cycle (requiring GOI: GLUL) and/or through modifications of ornithine (requiring GOI: OAT). Ascorbate is needed to hydroxylate proline residues in collagen processing which also requires 2-oxoglutarate oxygenase with Fe^{2+} as cofactor (GOI: 2OG-Fe(II)) and cytochrome b561 (GOI: CYB561) to bind ascorbate (Peterkofsky, 1991; Loenarz and Schofield, 2008; Berczi and Zimanyi, 2014). Cu^{2+} uptake is stimulated by ascorbate, which acts as a Cu^{2+} reductant (Schweigel-Röntgen, 2014). The upregulation of SLC31A2 (aka: CTR2) is consistent with expression profiles of genes associated the collagen synthesis and an increased metabolic demand for ascorbate (see Figure 4C).

Collagen is upregulated in wound healing (Albaugh et al., 2017). Under acidic conditions, collagen synthesis is upregulated and the proline incorporated into collagen removes it from the metabolic pool (Chalecka et al., 2021). Mechanical properties of collagen formed under alkaline conditions are better than collagen formed under acidic conditions (Zhang et al., 2022). Data herein cannot discern whether upregulated collagen

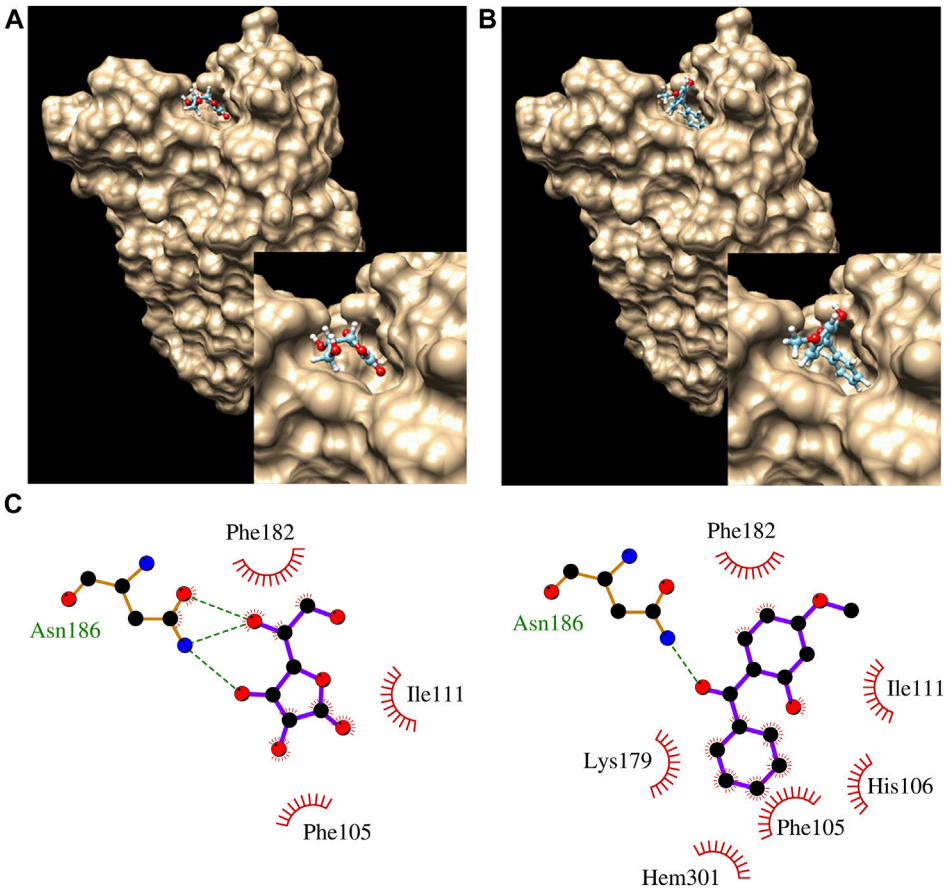

FIGURE 2
Docking results showing ascorbate **(A)** and BP3 **(B)** bound to CYB561. The inset pic at bottom right corner of A and B show closeup of ascorbate and BP3, respectively in binding pocket. **(C)** LigPlot analysis of ascorbate (left) and BP3 (right), showing interactions with nearby residues. Hem301 is a nearby heme group.

synthesis is due to demand for additional collagen or replacement of existing collagen.

Three GOIs (Mys, TNR, TF) have functional associations with the extracellular matrix (ECM) (Figure 4D). Integrins are transmembrane proteins that facilitate interactions between cells and ECM (Gotwals et al., 1994; White et al., 2004). Tenascin (TNR) (aka: ryncolin-4) has a FReD (fibrinogen domain), associated with wound healing, and known to be responsive to acidified seawater (Tran et al., 2004; Moya et al., 2012). TNR belongs to the matricellular class of ECM proteins. Serotransferrin (TF) is an iron-binding glycoprotein delivering iron to cells (Gkouvatsos et al., 2012). TF belongs to the glycoprotein class of ECM proteins. MCT 1-4 require and bind directly to basigin or embigin, single-pass transmembrane glycoproteins that are necessary for MCT activity (Halestrap, 2013; Muramatsu, 2016). Integrins strongly interact with glycoproteins (basigin or embigin) to facilitate integrin signaling inside of cell as well as the glycoprotein's activity (Muramatsu, 2016). During an acute phase of wound healing, a drop in pH can cause hypoxia and increased production of lactic acid (Jones et al., 2015). Expression profiles of the GOIs associated with collagen synthesis and the other ECM transcripts are consistent with previous cnidarian research demonstrating CO_2-driven acidification enhances synthesis of the extracellular matrix (Moya et al., 2012).

Links to ion transport

Seven GOIs (FTH1, Heph, SLC31A2, SLC39A14, SLC8A3, TF, TRPA1,) function in cation transport (Figure 4E). Two GOIs (SLC8A3, TRPA1) transport Ca^{2+}. The Na+/Ca^{2+} exchanger (SLC8A3) exchanges one Ca^{2+} for three Na+. The Na+/Ca^{2+} exchanger functions in both import and export of Ca^{2+} for maintenance of intracellular Ca^{2+} homeostasis, however the predominant mode is to export Ca^{2+} (Khananshvili, 2013; Barron et al., 2018). Transient receptor potential cation channel subfamily A member 1 (TRPA1) is a nonselective cation channel permeable to Ca^{2+}, Na+, and K+. The TRPA1 channel is strongly regulated by both extracellular and intracellular calcium (Meents et al., 2019). While SLC8A2 and TRPA1 are linked to calcium transport, they are not exclusively linked to calcification since anemones are not calcifiers.

Three GOIs (Heph, FTH1, TF) function in iron binding/transport. Hephaestin, a transmembrane ceruloplasmin homolog involved with iron efflux and considered an important link between copper and iron metabolism (Vulpe et al., 1999; Lang et al., 2012). Serotransferrin (TF) is an iron-binding glycoprotein involved with iron influx to cells (Gkouvatsos et al., 2012). Ceruloplasmin and TF are known to interact as positive and negative controls in an acute

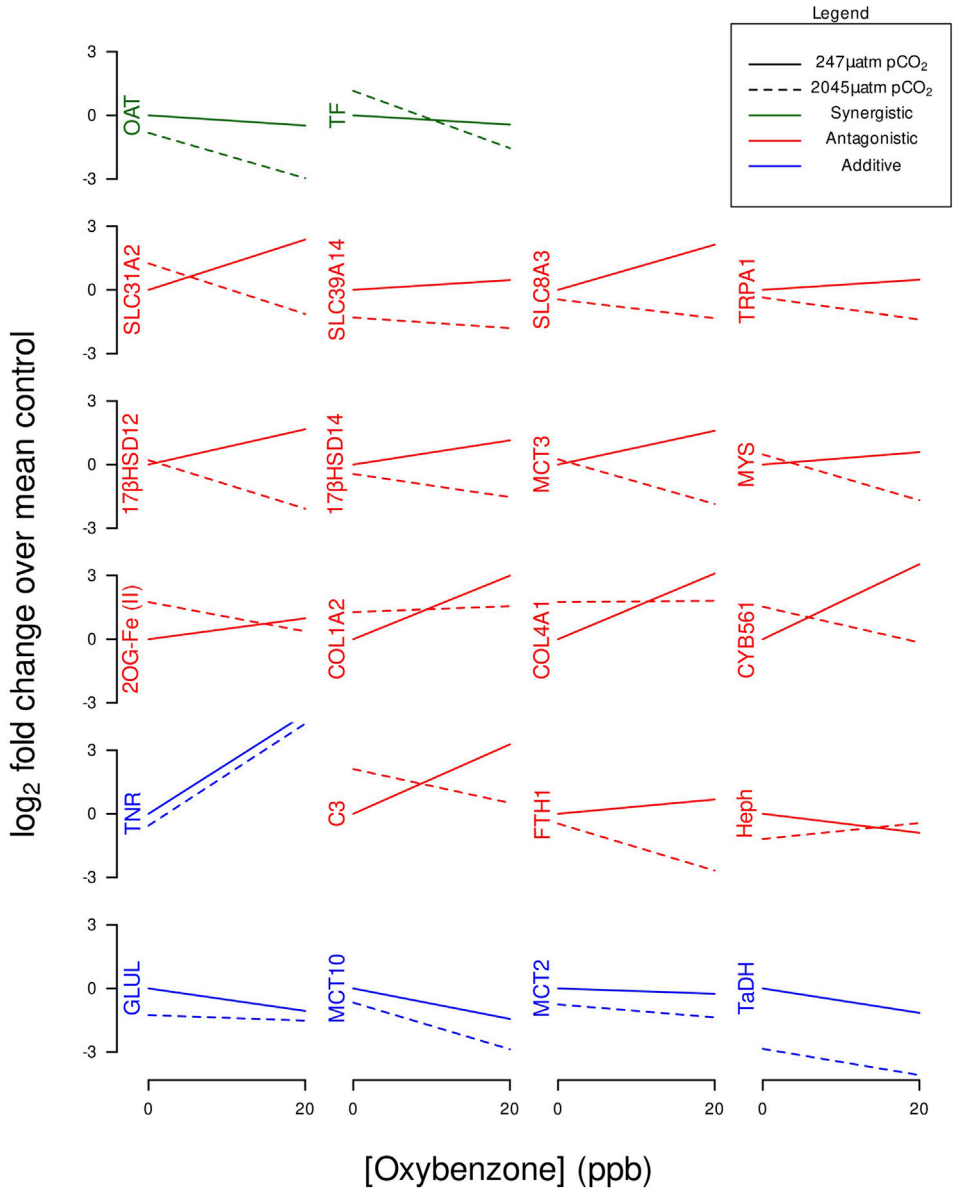

FIGURE 3
Interaction plots of GOI expression profiles categorized by synergistic, antagonistic, or additive effects.

phase response to perturbations of copper and iron metabolism (Golizeh et al., 2017). Hephaestin, a ceruloplasmin homolog has previously demonstrated acute responsiveness to exogenous copper (Morgan and Snell, 2006). Somaferratin (FTH1) functions in iron storage, detoxification, and innate immunity (Voolstra et al., 2009). Expression profiles for Heph, FTH1, and TF reveal the cellular demand for iron influx/eflux (TF expression) varied significantly with the presence/absence of BP-3 in OA conditions (see Figure 4E).

Intracellular concentrations of Cu^{2+} and Zn^{2+} are altered in response to OA. As a member of the SLC39 family, SLC39A14 is plasma membrane protein involved with Zn^{2+} influx and increasing the availability of cytosolic Zn^{2+} (Schweigel-Röntgen, 2014). Members of the SLC31 family act to regulate the intracellular Cu^{2+} concentration. SLC31A2 is mainly found in intracellular membranes of the late endosome and lysosome and is known to regulate intracellular Cu^{2+} concentration (Wee et al., 2013; Schweigel-Röntgen, 2014). Dysregulation of Zn^{2+} and Cu^{2+} are known to be associated with diseased conditions (Lynes et al., 2007; Schweigel-Röntgen, 2014).

Links to steroidal hormones

Twelve GOIs (2OG-Fe (II), 17βHSD14, 17βHSD12, COL1A2, COL4A1, CYB561, Heph, MCT2, MCT3, SLC31A2, SLC39A14, TF) have functional links to steroidal or tyrosine-based hormones (Figure 4F). BP-3 is recognized as an endocrine disruptor (Downs et al., 2016; LaPlante et al., 2018; Matouskova et al., 2020). *17βHSD14* and *17βHSD12* are associated with steroidogenesis. *17βHSD14* converts estradiol (E2) into estrone (E1); and testosterone (T) into androstenedione (A4), while *17βHSD12* performs the reverse reactions, E1 into E2, and

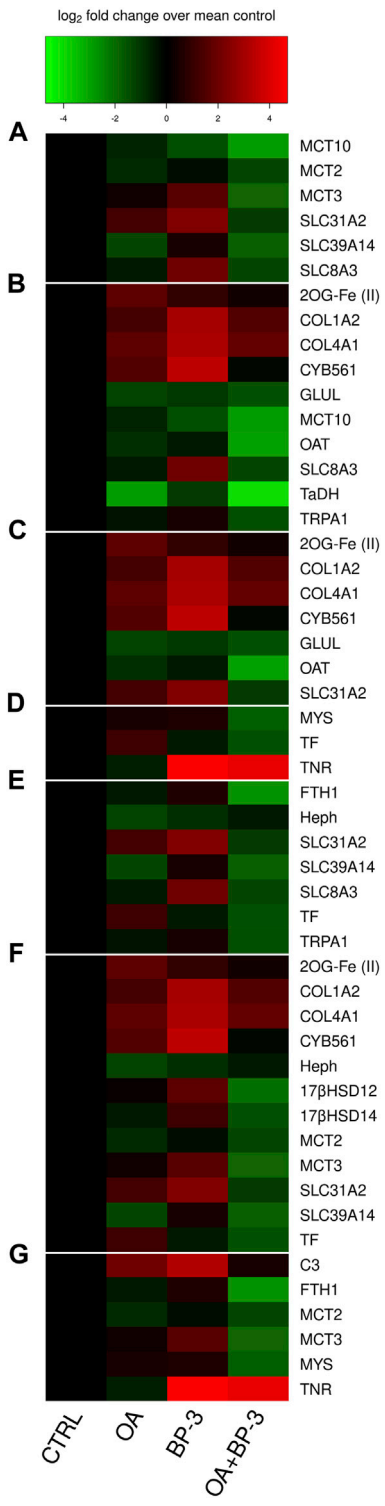

FIGURE 4
Categorized heatmaps of GOIs exhibiting significant differences in expression in response to OA and/or BP-3 exposure. Group **(A)** Soluble carrier proteins GOIs: SLC31A2, SLC39A14, SLC8A3, MCT3 (SLC16A3), MCT2 (SLC16A7), MCT10 (SLC16A10). Group **(B)** GOIs associated with amino acid synthesis, reservoirs, and metabolism. Group **(C)** GOIs associated with Collagen synthesis. Group **(D)** Extracellular matrix GOIs. Group **(E)** ion transport GOIs. Group **(F)** 12 GOIs with functional links to steroidal hormones. Group **(G)** Immune-related responses.

A4 into T (Tarrant et al., 2003; Luu-The et al., 2006; Shikina and Chang, 2016; Salah et al., 2019). Proton-dependent MCTs are regulated by sex hormones (Felmlee et al., 2020). Solute carrier transporters SLC39A and SLC31A families are known to be regulated by estrogen (Schweigel-Röntgen, 2014). Estrogen can transcriptionally regulate synthesis of TF and ceruloplasmin (Golizeh et al., 2017), therefore it is highly probable Hephaestin (a homolog of ceruloplasmin) will respond in a similar manner to estrogen. Biosynthesis of collagen is subject to steroidal hormone regulation (Karna et al., 2020).

The variability in expression of these 12 GOIs reveals how BP-3 exposure influences their expression profiles in the presence/absence of OA conditions. Expression profiles of 17βHSD14 and 17βHSD12 in the presence of BP-3 are consistent with a previous investigation where there was upregulated transcription of both 17βHSD14 and 17βHSD12 in the presence of BP-3 (Morgan et al., 2022). However, upregulated expression of 17βHSD14 in response to BP-3 in this investigation was not statistically significant (see Table 4) suggesting the cellular demand for converting E2 into E3 was not significantly different from the control condition. Future studies investigating the reproductive status of anemones at the time of BP-3 exposure can be important to ascertaining the sensitivity of the anemone's response to BP-3 alone *versus* in an environment of acidified seawater and BP-3. This will be particularly important in the abilities of these GOIs to detect endocrine disruption in a multi-stressor environment.

Links to immune responses

Six GOIs (FTH1, C3, MCT2, MCT3, MYS, TNR) have functional links to immune responses (Figure 4G). Cnidarian integrins are involved in multiple immunological cellular processes such as cell migration, differentiation, signal transduction, and wound repair (Miller et al., 2007; Knack et al., 2008; Shearer et al., 2012). Ferritins such as somaferritin (FTH1) are associated with innate immunity (Voolstra et al., 2009). C3 compliment is a recognized component of cnidarian innate immune system (Miller et al., 2007; Schwarz et al., 2008; Kvennefors et al., 2010; Palmer and Traylor-Knowles, 2012; Ocampo et al., 2015). Tenascin-R (TNR) is also known as ryncolin-4 is considered part of the innate immune system, involved with activating the Compliment pathway, and is upregulated in acidic conditions (OmPraba et al., 2010; Zúñiga-Soto et al., 2023). To be activated, proton-dependent MCTs need to bind immuno-globulin transmembrane glycoproteins (Muramatsu, 2016).

Functional links to *in silico* modeling

In silico modeling demonstrates BP-3 favorably binds to MCT2, MCT3 with affinities much closer to recognized inhibitors (see Table 5). MCT10′s binding affinity to BP-3 is most similar to tryptophan (see Table 5) which suggests a plausible mechanism for importing BP-3 into a cell. BP-3 binding into the pocket of CYB561 facing the extracellular side of the plasma membrane suggests exogenous BP-3 may act as competitive inhibitor of ascorbate (see Table 5 and Figure 2). This conclusion is

supported by the upregulated transcription of CYB561 (see Figures 1, 3). Structurally, Asn 186 functions by hydrogen bonding to the ligand; there are three putative hydrogen bonds to ascorbate and one hydrogen bond to BP-3. However, BP-3 has a greater surface area and is more hydrophobic compared to ascorbate, and the increase in van der Waals interactions between CYB561 and BP-3 explains the stronger binding affinity predicted by docking experiments. His 106, Lys 179, and the nearby heme group (Hem 301) are all involved in BP-3 binding, while these interactions are absent when ascorbate is bound. His 106 is highly conserved and known to participate in binding the two heme-b centers. In a previous study, a laboratory-induced F105W/H106E double mutation completely abolished the ascorbate-dependent redox activity of CYB561, and thus demonstrated His 106 is the single most critical residue for binding to the non-cytosolic side of the protein (Berczi and Zimanyi, 2014).

Final conclusion

Functional significance of synergistic, antagonistic, or additive interactions

Results herein reveal how synergistic, antagonistic, and/or additive responses potentially work in concert to produce cellular responses that might be described as homeostatic or adaptive.

While Serotransferrin (TF) had a significant synergistic interaction and Heph had a significant antagonistic interaction, both GOIs contribute to modulating the intracellular transcriptional demands for iron. TF is an iron-binding glycoprotein involved with iron influx (Castellano et al., 1994; Gkouvatsos et al., 2012). Hephaestin (Heph) is a transmembrane-bound homolog of ceruloplasmin involved with iron efflux and considered an important link between copper and iron metabolism (Vulpe et al., 1999; Lang et al., 2012). Ceruloplasmin and TF are known to interact as positive and negative controls in an acute phase response to perturbations of iron metabolism (Golizeh et al., 2017). These GOIs (TF and Heph) with significant but opposite interactions (see Figure 3) appear to represent the molecular underpinnings of iron homeostasis.

Under acidic conditions, the synergistic transcriptional response of OAT (reduce the biosynthesis of ornithine) coupled with the additive transcriptional response of GLUL (reduce the synthesis of glutamine) drive both pathways in the direction of proline synthesis. The biosynthesis of glutamate and proline can be linked to ornithine modifications (Majumdar et al., 2016).

Proline is a fundamental structural component of collagen. COL1A2, COL4A1, CYB561, and 2OG-Fe(II) are all involved with collagen synthesis and exhibit similar expression profiles under OA or BP-3 exposure (see Figures 1, 3). Multiple GOIs with similar significant interactions (i.e., antagonistic effects) involving the same process (i.e., collagen synthesis) appear to be in synchrony. Transcription of multiple GOIs needed for collagen synthesis represent the molecular underpinnings for the physiological response of adaptation to an acidic environment.

Antagonistic effects are representative of gene networks where the impacts of OA and BP-3 are working in opposition. Fifteen GOIs exhibit antagonistic effects when exposed to OA and BP-3 (see Figure 3). Twelve of these GOIs were downregulated when exposed to BP-3 in presence of acidified seawater reveals, whereas 14 GOIs were upregulated in the presence of BP-3 alone (see Figure 3). Under normal conditions, 17βHSD14 and 17βHSD12 perform functions that are opposite of each other. The expression profiles of these GOIs are consistent with a previous investigation where these GOIs exhibited transcriptional responses to an endocrine disruptive 20 ppb BP-3 exposure (Morgan et al., 2022). Future studies investigating longer exposures to BP-3 in an environment of OA will generate more comprehensive dose-response curves that will contribute to better characterization of the responsiveness of these GOIs and the other antagonistic responses.

GOIs as drug targets

Influx and efflux transporters can act with intracellular metabolizing enzymes to regulate drug effects (Giacomini and Sugiyama, 2006; Goldstone, 2008). There is growing evidence that MCTs and solute carrier transporters (SLC8A3, SLC31A2) are responsive to various drugs (Halestrap and Wilson, 2012; Njiaju et al., 2012; Halestrap, 2013; Khananshvili, 2013; Iwanaga and Kishimoto, 2015). MCT 1&2 are drug targets for compounds acting as selective inhibitors (Payen et al., 2020; Wang et al., 2021). Anthropogenic chemicals can upregulate expression MCTs (Genter et al., 2002). In human health, MCTs are promising pharmacological targets and in cnidarian physiology, MCTs interact with xenobiotic chemical pollutants (Goldstone, 2008). Structures that are similar to ascorbate can inhibit enzymes usually working on ascorbate (Majamaa et al., 1986). TRPA1 is a promiscuous chemical sensor capable of responding to an unusually wide variety of chemically diverse compounds including many natural products and irritants, environmental chemicals, and common pharmaceuticals (Bautista et al., 2006; Jagadeesan, 2016; Meents et al., 2019). Tauropine dehydrogenase (TaDH) belongs to the ornithine cyclodeaminase (OCD)/mu-crystallin family. Substrate utilization of opine dehydrogenases is notoriously promiscuous (Linsmayer et al., 2020). Understanding the underlying molecular mechanisms of "drug-like" compounds such as BP-3 may lead to a more comprehensive interpretation of the expression profiles herein.

Potential biomarkers of exposure to OA and BP-3

Developing transcriptional biomarkers in the laboratory will help to establish links between laboratory-based testing and adverse effects *in situ* (Depledge and Fossi, 1994). Development of biomarkers for cnidarian health are far behind biomarkers of human health. Using a reductionist approach, candidate biomarkers identified in this investigation can be valuable preliminary tools to future, more complex studies involving *in situ* monitoring. A first step biomarker development is to identify GOIs responsive to laboratory-controlled conditions on a single stressor (i.e., exposure to OA or BP-3). Eight GOIs representing collagen synthesis, zinc transport, transient receptor cation channel, and proteins containing a fibrinogen domain have previously demonstrated cnidarian responsiveness to OA (Moya et al., 2012;

Wu et al., 2022). Three GOIs (C3, 17βHSD14, 17βHSD12) previously demonstrated responsiveness to BP-3 (Morgan et al., 2022). The only GOIs with known responsiveness to other anthropogenic chemicals include TNR, Heph, and select members of the solute carrier protein family (Morgan and Snell, 2006; Goldstone, 2008; Morgan et al., 2012).

A second step in biomarker development is to use the same GOIs to investigate responses under conditions of two stressors such as OA and BP-3 exposure. MCT 1-4 are recognized as potential biomarkers of human diseases (Felmlee et al., 2020). This investigation offers evidence (expression of proton-dependent MCTs in an acidic environment and *in silico* modeling of BP-3 binding to proton-dependent MCTs) which may represent a mechanism not previously recognized for modulating changes in intracellular pH in cnidarians. Both MCT2 and MCT3 discern differences in OA vs. normal pCO_2 conditions which is consistent with MCT 2 and MCT 3 as pH regulators, but these MCTs cannot discern when BP-3 is present (see Table 4). MCT3 has a significant interaction between OA and BP-3 while MCT2 and MCT10 show no significant interactions between BP-3 and OA (see Table 4). MCT10 is downregulated in the presence of BP-3 (see Table 4) which could be environmentally relevant since increasing concentrations of free amino acids (including those with aromatic side chains) are known to occur in locations closer to anthropogenic sources (Yamashita and Tanoue, 2003). The value of CYB561 as a biomarker can be established by the OA/BP-3 and BP-3 expression profiles and confirmed by *in silico* docking of BP-3 which binds directly in the ascorbate binding pocket of CYB561 (see Figure 2).

A third step in the development of GOIs as biomarkers would be to investigate how they respond to multiple stressors such as OA, BP-3 exposure, and another stressor of global importance, thermal stress. GOIs associated with collagen synthesis and iron transport have previously demonstrated cnidarian responsiveness to elevated temperatures (Voolstra et al., 2009; DeSalvo et al., 2010; Kenkel et al., 2011). Critics cite multiple stressors causing mixed effects as being a vulnerable weakness for interpreting complex real-world conditions (Deidda et al., 2021). Anthropogenic activities represent complex mixtures of multiple stressors (Jones, 2010; Wear and Thurber, 2015; Mitchelmore et al., 2019; Mitchelmore et al., 2021). Cnidarian biomarkers for sensing changes in intracellular pH or pesticide exposure are emerging (Morgan and Snell, 2002; Barott et al., 2017). A biomarker developed in the lab subsequently demonstrated detectable responses in field sampling (Morgan and Snell, 2002). Characterizing the GOIs as synergistic, antagonistic, and additive responses provides a systematic process for interpreting the effects of multiple stressors. GOIs with synergistic and additive responses represent candidate biomarkers of exposure. The collective antagonistic responses of COL4A1, COL1A2, CYB561, and 2OG-Fe (II) strongly suggests these GOIs should be considered candidate biomarkers of effect. The observed changes in expression profiles of GOIs associated with collagen synthesis coupled with *in silico* binding of BP-3 to CYB561 offers a mechanistic explanation that underpins higher order physiological responses of organisms restructuring their extracellular matrix in response to an acidic environment.

Candidate biomarkers responsive to different stressed conditions can also be sensitive to different timeframes of stressor exposure. Results herein correlate well with previous transcriptional studies of cnidarian responses to short-term acidified seawater exposures or an acute exposure to 20ppb BP-3 (Moya et al., 2012; Morgan et al., 2022; Woo and Yum, 2022). The GOIs in this investigation represent responses not detected in study of >8000 genes in adult *A. millepora* after a 28-day exposure to acidic seawater (similar to pH in this investigation) that stimulated >600 differentially expressed transcripts (Kaniewska et al., 2012). Future studies establishing dose-response curves for these GOIs should be productive in elucidating differences in short-term vs. long-term responses to OA, exposure to BP-3, and/or the interaction between OA conditions and exposure to BP-3.

Transcriptional responses are the foundational framework for identifying candidate biomarkers. Gene expression profiling can be used to detect sub-lethal stress responses, differentiate the contribution of different anthropogenic stressors, and access an organism's condition in natural environments (Snell et al., 2003; Evans and Hofmann, 2012). Gene expression profiling provides a portal into responsive cellular processes that converge and culminate into altered physiology. Gene expression profiles reveal responses that precede translational activity. *In silico* modeling provides molecular details about the precise location of impact an exogenous chemical can have on a specific protein. Transcriptional responses coupled with *in silico* modeling offer new insight into how environmentally relevant exogenous anthropogenic chemicals impact specific proteins. Results herein are consistent with responses of SLCs known to be associated with transport of H+, Na+, Ca^{2+}, small chain aliphatic hydrocarbons, and amino acids (both proteinogenic and nonproteinogenic). The solute carrier family of proteins deserves further exploration in the context of xenobiotic chemical pollution in an environment of OA. Venn et al. (2013) stated "It is only with a better mechanistic perspective of the response of coral physiology to environmental change that forecasts of the future of coral reefs under ocean acidification and climate change can be improved". Results from this investigation offer seven distinctive elements: 1) The expression profiles of these 22 GOIs are representative of important cellular processes impacting non-calcifying cnidarians and 17 of the 22 GOIs have significant interactions between OA and BP-3. 2) Fifteen GOIs exhibit antagonistic interactions to the presence of BP-3 in an environment of acidified seawater. The compensatory actions to one stressor *versus* both stressors depend on the cellular process impacted. 3) Data herein provides a plausible mechanistic explanation for how BP-3 binds to CYB561 and stimulates upregulation of genes associated with collagen synthesis in an environment of OA; 4) Data herein offers a plausible mechanism for how cnidarians in an environment of OA can modulate intracellular pH through proton-dependent monocarboxylate transporters; 5) Identification of 5 GOIs that should be considered "drug targets" for binding exogenous BP-3; 6) Identifying 12 GOIs with recognized functional links to hormones that are also responding to BP-3 and OA represent new avenues to pursue in the context of endocrine disruption; 7) By characterizing the expression profiles of 22 GOIs in a laboratory-controlled multiple stressor environment, these GOIs are one step closer to being candidate biomarkers for *in situ* field testing. Servetto et al. (2021) succinctly articulated how an understanding the molecular mechanisms underpinning the physiological processes is critical to properly interpreting cnidarian responses to acidic pH and their ability cope in the Anthropocene. Interactive effects of global stressors (e.g., ocean warming and/or acidification) and local stressors (e.g., pollution) can be advanced with a better understanding of the

transcriptional responsiveness of these GOIs in the presence of multiple stressors. These 22 GOIs offer new directions for future studies on the interactions of ocean acidification and xenobiotic chemicals in cnidarians as well as other phyla containing calcifying and non-calcifying taxa.

Data availability statement

The datasets presented in this study can be found in online repositories. The names of the repository/repositories and accession number(s) can be found in the article/Supplementary material.

Ethics statement

The manuscript presents research on animals that do not require ethical approval for their study.

Author contributions

MM: Conceptualization, Project Administration, Resources, Writing–original draft, Writing–editing and review. JW: Formal analysis, Funding acquisition, Validation, Writing–original draft. BB: Data curation, Investigation, Validation. NE: Funding acquisition, Investigation, Validation. NH: Funding acquisition, Investigation, Validation, Writing–original draft. KO: Conceptualization, Data curation, Formal analysis, Investigation, Resources, Visualization, Writing–original draft, Writing–editing and review. DQ: Formal analysis, Investigation, Resources, Visualization, Writing–original draft.

Funding

The author(s) declare financial support was received for the research, authorship, and/or publication of this article. Financial support was provided by Berry College for one Richards Scholarship (JW), and two Richards Undergraduate Support Grants (NE; NH), Funding for publishing from the Berry College School of MNS Dean (MM; DQ). The funders had no role in the study design, data collection and analysis, decision to publish, or preparation of the manuscript.

Conflict of interest

The authors declare that the research was conducted in the absence of any commercial or financial relationships that could be construed as a potential conflict of interest.

Publisher's note

References

Adams, M., Celniker, S., Holt, R., Evans, C., Gocayne, J., Amanatides, P., et al. (2000). The genome sequence of *Drosophila melanogaster*. *Science* 287 (5461), 2185–2195. doi:10.1126/science.287.5461.2185

Albaugh, V. L., Mukherjee, K., and Barbul, A. (2017). Proline precursors and collagen synthesis: biochemical challenges of nutrient supplementation and wound healing. *J. Nutr.* 147 (11), 2011–2017. doi:10.3945/jn.117.256404

Archer, E., Petrie, B., Kasprzyk-Hordern, B., and Wolfaardt, G. M. (2017). The fate of pharmaceuticals and personal care products (PPCPs), endocrine disrupting contaminants (EDCs), metabolites and illicit drugs in a WWTW and environmental waters. *Chemosphere* 174, 437–446. doi:10.1016/j.chemosphere.2017.01.101

Atkinson, S., Atkinson, M. J., and Tarrant, A. M. (2003). Estrogens from sewage in coastal marine environments. *Environ. Health Perspec* 111 (4), 531–535. doi:10.1289/ehp.5233

Barott, K. L., Barron, M. E., and Tresguerres, M. (2017). Identification of a molecular pH sensor in coral. *Proc. R. Soc. B Biol. Sci.* 284 (1866), 20171769. doi:10.1098/rspb.2017.1769

Barron, M. E., Thies, A. B., Espinoza, J. A., Barott, K. L., Hamdoun, A., and Tresguerres, M. (2018). A vesicular Na+/Ca2+ exchanger in coral calcifying cells. *PLoS One* 13 (10), e0205367. doi:10.1371/journal.pone.0205367

Bautista, D. M., Jordt, S.-E., Nikai, T., Tsuruda, P. R., Read, A. J., Poblete, J., et al. (2006). TRPA1 mediates the inflammatory actions of environmental irritants and proalgesic agents. *Cell.* 124 (6), 1269–1282. doi:10.1016/j.cell.2006.02.023

Berczi, A., and Zimanyi, L. (2014). The trans-membrane cytochrome b561 proteins: structural information and biological function. *Curr. Protein Pept. S. C.* 15 (8), 745–760. doi:10.2174/1389203715666140828100351

Bertoni, M., Kiefer, F., Biasini, M., Bordoli, L., and Schwede, T. (2017). Modeling protein quaternary structure of homo-and hetero-oligomers beyond binary interactions by homology. *Sci. Rep.* 7 (1), 10480. doi:10.1038/s41598-017-09654-8

Bienert, S., Waterhouse, A., de Beer, T. A. P., Tauriello, G., Studer, G., Bordoli, L., et al. (2017). The SWISS-MODEL Repository—new features and functionality. *Nuc Acids Res.* 45 (D1), D313–D319. doi:10.1093/nar/gkw1132

Birkeland, C., Craig, P., Fenner, D., Smith, L., Kiene, W. E., and Riegl, B. M. (2008). Geologic setting and ecological functioning of coral reefs in American Samoa. *Coral Reefs U. S. A.*, 741–765. doi:10.1007/978-1-4020-6847-8_20

Bove, C. B., Whitehead, R. F., and Szmant, A. M. (2020). Responses of coral gastrovascular cavity pH during light and dark incubations to reduced seawater pH suggest species-specific responses to the effects of ocean acidification on calcification. *Coral Reefs* 39 (6), 1675–1691. doi:10.1007/s00338-020-01995-7

Brennan, J. J., Messerschmidt, J. L., Williams, L. M., Matthews, B. J., Reynoso, M., and Gilmore, T. D. (2017). Sea anemone model has a single Toll-like receptor that can function in pathogen detection, NF-κB signal transduction, and development. *P Natl. Acad. Sci.* 114 (47), E10122–E10131. doi:10.1073/pnas.1711530114

Burns, K., and Brinkman, D. (2011). Organic biomarkers to describe the major carbon inputs and cycling of organic matter in the central Great Barrier Reef region. *Estuar. Coast. Shelf Sci.* 93 (2), 132–141. doi:10.1016/j.ecss.2011.04.001

Bustin, S. A., Benes, V., Garson, J. A., Hellemans, J., Huggett, J., Kubista, M., et al. (2009). The MIQE guidelines: minimum information for publication of quantitative real-time PCR experiments. *Clin. Chem.* 55 (4), 611–622. doi:10.1373/clinchem.2008.112797

Cai, W.-J., Ma, Y., Hopkinson, B. M., Grottoli, A. G., Warner, M. E., Ding, Q., et al. (2016). Microelectrode characterization of coral daytime interior pH and carbonate chemistry. *Nat. Commun.* 7 (1), 11144. doi:10.1038/ncomms11144

Casey, J. R., Grinstein, S., and Orlowski, J. (2010). Sensors and regulators of intracellular pH. *Nat. Rev. Mol. Cell. Biol.* 11 (1), 50–61. doi:10.1038/nrm2820

Castellano, A. C., Barteri, M., Castagnola, M., Bianconi, A., Borghi, E., and Dellalonga, S. (1994). Structure-function relationship in the serotransferrin: the role of the pH on the conformational change and the metal ions release. *Biochem. Biophys. Res. Commun.* 198 (2), 646–652. doi:10.1006/bbrc.1994.1094

Chalecka, M., Kazberuk, A., Palka, J., and Surazynski, A. (2021). P5C as an interface of proline interconvertible amino acids and its role in regulation of cell survival and apoptosis. *Int. J. Mol. Sci.* 22 (21), 11763. doi:10.3390/ijms222111763

Culler-Juarez, M. E., and Onthank, K. L. (2021). Elevated immune response in Octopus rubescens under ocean acidification and warming conditions. *Mar. Biol.* 168 (9), 137. doi:10.1007/s00227-021-03913-z

Dachs, J., Bayona, J. M., Ittekkot, V., and Albaigés, J. (1999). Monsoon-driven vertical fluxes of organic pollutants in the western arabian sea. *Environ. Sci. Technol.* 33 (22), 3949–3956. doi:10.1021/es990200e

Dafforn, K. A., Lewis, J. A., and Johnston, E. L. (2011). Antifouling strategies: history and regulation, ecological impacts and mitigation. *Mar. Poll. Bull.* 62 (3), 453–465. doi:10.1016/j.marpolbul.2011.01.012

Dani, V., Ganot, P., Priouzeau, F., Furla, P., and Sabourault, C. (2014). Are Niemann-Pick type C proteins key players in cnidarian–dinoflagellate endosymbioses? *Mol. Ecol.* 23 (18), 4527–4540. doi:10.1111/mec.12876

Deidda, I., Russo, R., Bonaventura, R., Costa, C., Zito, F., and Lampiasi, N. (2021). Neurotoxicity in marine invertebrates: an update. *Biology* 10 (2), 161. doi:10.3390/biology10020161

Depledge, M. H., and Fossi, M. C. (1994). The role of biomarkers in environmental assessment (2). Invertebrates. *Ecotoxicology* 3 (3), 161–172. doi:10.1007/bf00117081

DeSalvo, M. K., Sunagawa, S., Voolstra, C. R., and Medina, M. (2010). Transcriptomic responses to heat stress and bleaching in the elkhorn coral *Acropora palmata*. *Mar. Ecol. Prog. Ser.* 402, 97–113. doi:10.3354/meps08372

Dickson, A. G., Sabine, C. L., and Christian, J. R. (2007). *Guide to best practices for ocean CO2 measurements*. New York: North Pacific Marine Science Organization.

Doney, S. C., Fabry, V. J., Feely, R. A., and Kleypas, J. A. (2009). Ocean acidification: the other CO2 problem. *Ann. Rev. Mar. Sci.* 1, 169–192. doi:10.1146/annurev.marine.010908.163834

Downs, C. A., Kramarsky-Winter, E., Segal, R., Fauth, J., Knutson, S., Bronstein, O., et al. (2016). Toxicopathological effects of the sunscreen UV filter, oxybenzone (Benzophenone-3), on coral planulae and cultured primary cells and its environmental contamination in Hawaii and the U.S. Virgin islands. *Arch. Environ. Contam. Tox* 70 (2), 265–288. doi:10.1007/s00244-015-0227-7

Duckworth, C. G., Picariello, C. R., Thomason, R. K., Patel, K. S., and Bielmyer-Fraser, G. K. (2017). Responses of the sea anemone, Exaiptasia pallida, to ocean acidification conditions and zinc or nickel exposure. *Aqua Tox* 182, 120–128. doi:10.1016/j.aquatox.2016.11.014

Duffy, D. J., and Frank, U. (2011). Modulation of COUP-TF expression in a Cnidarian by ectopic wnt signalling and allorecognition. *PLoS One* 6 (4), e19443. doi:10.1371/journal.pone.0019443

Dunn, R. J., Stanitski, D. M., Gobron, N., Willett, K. M., Ades, M., Adler, R., et al. (2020). "Global climate." *Bull. Am. Meteorological Soc.* 101(101 S9–S128. doi:10.1175/BAMS-D-20-0104.1

Dunn, S. R., Phillips, W. S., Spatafora, J. W., Green, D. R., and Weis, V. M. (2006). Highly conserved caspase and bcl-2 homologues from the sea anemone *Aiptasia pallida*: lower metazoans as models for the study of apoptosis evolution. *J. Mol. Evol.* 63 (1), 95–107. doi:10.1007/s00239-005-0236-7

Evans, T. G., and Hofmann, G. E. (2012). Defining the limits of physiological plasticity: how gene expression can assess and predict the consequences of ocean change. *Philos. Trans. R. Soc. Lond B Biol. Sci.* 367 (1596), 1733–1745. doi:10.1098/rstb.2012.0019

Fabry, V. J., Seibel, B. A., Feely, R. A., and Orr, J. C. (2008). Impacts of ocean acidification on marine fauna and ecosystem processes. *ICES J. Mar. Sci.* 65 (3), 414–432. doi:10.1093/icesjms/fsn048

Felmlee, M. A., Jones, R. S., Rodriguez-Cruz, V., Follman, K. E., and Morris, M. E. (2020). Monocarboxylate transporters (SLC16): function, regulation, and role in health and disease. *Pharmacol. Rev.* 72 (2), 466–485. doi:10.1124/pr.119.018762

Fent, K., Weston, A. A., and Caminada, D. (2006). Ecotoxicology of human pharmaceuticals. *Aqua Tox* 76 (2), 122–159. doi:10.1016/j.aquatox.2005.09.009

Fontanals, N., Cormack, P. A. G., Sherrington, D. C., Marcé, R. M., and Borrull, F. (2010). Weak anion-exchange hypercrosslinked sorbent in on-line solid-phase extraction–liquid chromatography coupling to achieve automated determination with an effective clean-up. *J. Chromatogr. A* 1217 (17), 2855–2861. doi:10.1016/j.chroma.2010.02.064

French, V. A., King, S. C., Kumar, A., Northcott, G., McGuinness, K., and Parry, D. (2015). Characterisation of microcontaminants in Darwin Harbour, a tropical estuary of northern Australia undergoing rapid development. *Sci. Total Environ.* 536, 639–647. doi:10.1016/j.scitotenv.2015.07.114

Frieg, B., Görg, B., Gohlke, H., and Häussinger, D. (2021). Glutamine synthetase as a central element in hepatic glutamine and ammonia metabolism: novel aspects. *Biol. Chem.* 402 (9), 1063–1072. doi:10.1515/hsz-2021-0166

Gasch, A. P., Spellman, P. T., Kao, C. M., Carmel-Harel, O., Eisen, M. B., Storz, G., et al. (2000). Genomic expression programs in the response of yeast cells to environmental changes. *Mol. Biol. Cell.* 11, 4241–4257. doi:10.1091/mbc.11.12.4241

Gattuso, J.-P., Epitalon, J.-M., Lavigne, H., Orr, J., Gentili, B., Hagens, M., et al. (2015). Package seacarb. Available at http://cran.r-project.org/package=seacarb.

Gavio, B., Palmer-Cantillo, S., and Mancera, E. J. (2010). Historical analysis (2000–2005) of the coastal water quality in san andrés Island, SeaFlower biosphere reserve, caribbean Colombia. *Mar. Poll. Bull.* 60 (7), 1018–1030. doi:10.1016/j.marpolbul.2010.01.025

Genter, M. B., Burman, D. M., Vijayakumar, S., Ebert, C. L., and Aronow, B. J. (2002). Genomic analysis of alachlor-induced oncogenesis in rat olfactory mucosa. *Physiol. Genomics* 12 (1), 35–45. doi:10.1152/physiolgenomics.00120.2002

Giacomini, K. M., and Sugiyama, Y. (2006). Membrane transporters and drug response. *Goodman Gilman's Pharmacol. basis Ther.* 11, 41–70.

Gkouvatsos, K., Papanikolaou, G., and Pantopoulos, K. (2012). Regulation of iron transport and the role of transferrin. *Biochim. Biophys. Acta (BBA) - Gen. Subj.* 1820 (3), 188–202. doi:10.1016/j.bbagen.2011.10.013

Goldstone, J. V. (2008). Environmental sensing and response genes in cnidaria: the chemical defensome in the sea anemone *Nematostella vectensis*. *Cell. Biol. Toxicol.* 24 (6), 483–502. doi:10.1007/s10565-008-9107-5

Golizeh, M., Lee, K., Ilchenko, S., Ösme, A., Bena, J., Sadygov, R. G., et al. (2017). Increased serotransferrin and ceruloplasmin turnover in diet-controlled patients with type 2 diabetes. *Free Radic. Biol. Med.* 113, 461–469. doi:10.1016/j.freeradbiomed.2017.10.373

Gopal, E., Fei, Y.-J., Sugawara, M., Miyauchi, S., Zhuang, L., Martin, P., et al. (2004). Expression of slc5a8 in kidney and its role in Na+-coupled transport of lactate. *J. Biol. Chem.* 279 (43), 44522–44532. doi:10.1074/jbc.M405365200

Gotwals, P. J., Fessler, L. I., Wehrli, M., and Hynes, R. O. (1994). Drosophila PS1 integrin is a laminin receptor and differs in ligand specificity from PS2. *P Natl. Acad. Sci.* 91 (24), 11447–11451. doi:10.1073/pnas.91.24.11447

Gray, J. S., Wu, R. S., and Or, Y. Y. (2002). Effects of hypoxia and organic enrichment on the coastal marine environment. *Mar. Ecol. Prog. Ser.* 238, 249–279. doi:10.3354/meps238249

Halestrap, A. P. (2013). Monocarboxylic acid transport. *Compr. Physiol.* 3 (4), 1611–1643. doi:10.1002/cphy.c130008

Halestrap, A. P., and Meredith, D. (2004). The SLC16 gene family—from monocarboxylate transporters (MCTs) to aromatic amino acid transporters and beyond. *Pflügers Arch.* 447, 619–628. doi:10.1007/s00424-003-1067-2

Halestrap, A. P., and Wilson, M. C. (2012). The monocarboxylate transporter family—role and regulation. *IUBMB Life* 64 (2), 109–119. doi:10.1002/iub.572

Halpern, B. S., Walbridge, S., Selkoe, K. A., Kappel, C. V., Micheli, F., D'Agrosa, C., et al. (2008). A global map of human impact on marine ecosystems. *Science* 319 (5865), 948–952. doi:10.1126/science.1149345

Hanwell, M. D., Curtis, D. E., Lonie, D. C., Vandermeersch, T., Zurek, E., and Hutchison, G. R. (2012). Avogadro: an advanced semantic chemical editor, visualization, and analysis platform. *J. Cheminformatics* 4 (1), 17. doi:10.1186/1758-2946-4-17

Heyland, A., and Moroz, L. L. (2005). Cross-kingdom hormonal signaling: an insight from thyroid hormone functions in marine larvae. *J. Exp. Biol.* 208 (23), 4355–4361. doi:10.1242/jeb.01877

Higuchi, K., Sugiyama, K., Tomabechi, R., Kishimoto, H., and Inoue, K. (2022). Mammalian monocarboxylate transporter 7 (MCT7/Slc16a6) is a novel facilitative taurine transporter. *J. Biol. Chem.* 298 (4), 101800. doi:10.1016/j.jbc.2022.101800

Hill, A. A., Hunter, C. P., Tsung, B. T., Tucker-Kellogg, G., and Brown, E. L. (2000). Genomic analysis of gene expression in *C. elegans*. *Science* 290, 809–812. doi:10.1126/science.290.5492.809

Hoegh-Guldberg, O., Mumby, P. J., Hooten, A. J., Steneck, R. S., Greenfield, P., Gomez, E., et al. (2007). Coral reefs under rapid climate change and ocean acidification. *Science* 318 (5857), 1737–1742. doi:10.1126/science.1152509

Howe, P. L., Reichelt-Brushett, A. J., and Clark, M. W. (2012). Aiptasia pulchella: a tropical cnidarian representative for laboratory ecotoxicological research. *Environ. Tox Chem.* 31 (11), 2653–2662. doi:10.1002/etc.1993

Imagawa, S., Nakano, Y., and Watanabe, T. (2004). Molecular analysis of a major soluble egg protein in the scleractinian coral Favites chinensis. *Comp. Biochem. Physiol. B* 137 (1), 11–19. doi:10.1016/j.cbpc.2003.09.011

Inbakandan, D. (2016). "Predicting the impacts of ocean acidifcation: approaches from an omics perspective," in *Marine omics* (USA: C. Press), 559–592.

Iwanaga, T., and Kishimoto, A. (2015). Cellular distributions of monocarboxylate transporters: a review. *Biomed. Res.* 36 (5), 279–301. doi:10.2220/biomedres.36.279

Jagadeesan, S. K. (2016). *Experimental approach for drug profiling of calcitriol in yeast*. China: Université d'Ottawa/University of Ottawa.

Jones, E. M., Cochrane, C. A., and Percival, S. L. (2015). The effect of pH on the extracellular matrix and biofilms. *Adv. Wound Care* 4 (7), 431–439. doi:10.1089/wound.2014.0538

Jones, R. (2010). Environmental contamination associated with a marine landfill ('seafill') beside a coral reef. *Mar. Poll. Bull.* 60 (11), 1993–2006. doi:10.1016/j.marpolbul.2010.07.028

Kaniewska, P., Campbell, P. R., Kline, D. I., Rodriguez-Lanetty, M., Miller, D. J., Dove, S., et al. (2012). Major cellular and physiological impacts of ocean acidification on a reef building coral. *PLoS One* 7 (4), e34659. doi:10.1371/journal.pone.0034659

Karna, E., Szoka, L., Huynh, T. Y. L., and Palka, J. A. (2020). Proline-dependent regulation of collagen metabolism. *Cell. Mol. Life Sci.* 77 (10), 1911–1918. doi:10.1007/s00018-019-03363-3

Kenkel, C. D., Aglyamova, G., Alamaru, A., Bhagooli, R., Capper, R., Cunning, R., et al. (2011). Development of gene expression markers of acute heat-light stress in reef-building corals of the genus *porites*. *PLoS One* 6 (10), e26914. doi:10.1371/journal.pone.0026914

Khalturin, K., Billas, I., Chebaro, Y., Reitzel, A. M., Tarrant, A. M., Laudet, V., et al. (2018). NR3E receptors in cnidarians: a new family of steroid receptor relatives extends the possible mechanisms for ligand binding. *J. Steroid Biochem. Mol. Biol.* 184, 11–19. doi:10.1016/j.jsbmb.2018.06.014

Khananshvili, D. (2013). The SLC8 gene family of sodium–calcium exchangers (NCX)–Structure, function, and regulation in health and disease. *Mol. aspects Med.* 34 (2-3), 220–235. doi:10.1016/j.mam.2012.07.003

Knack, B. A., Iguchi, A., Shinzato, C., Hayward, D. C., Ball, E. E., and Miller, D. J. (2008). Unexpected diversity of cnidarian integrins: expression during coral gastrulation. *BMC Evol. Biol.* 8, 136. doi:10.1186/1471-2148-8-136

Kroeker, K. J., Kordas, R. L., Crim, R., Hendriks, I. E., Ramajo, L., Singh, G. S., et al. (2013). Impacts of ocean acidification on marine organisms: quantifying sensitivities and interaction with warming. *Glob. Change Biol.* 19 (6), 1884–1896. doi:10.1111/gcb.12179

Kvennefors, E. C. E., Leggat, W., Kerr, C. C., Ainsworth, T. D., Hoegh-Guldberg, O., and Barnes, A. C. (2010). Analysis of evolutionarily conserved innate immune components in coral links immunity and symbiosis. *Dev. Comp. Immunol.* 34 (11), 1219–1229. doi:10.1016/j.dci.2010.06.016

Lang, M. L., Braun, C. L., Kanost, M. R., and Gorman, M. J. (2012). Multicopper oxidase-1 is a ferroxidase essential for iron homeostasis in *Drosophila melanogaster*. *Proc. Natl. Acad. Sci. U. S. A.* 109 (33), 13337–13342. doi:10.1073/pnas.1208703109

LaPlante, C. D., Bansal, R., Dunphy, K. A., Jerry, D. J., and Vandenberg, L. N. (2018). Oxybenzone alters mammary gland morphology in mice exposed during pregnancy and lactation. *J. Endocr. Soc.* 2 (8), 903–921. doi:10.1210/js.2018-00024

Law, K. (2017). Plastics in the marine environment. *Ann. Rev. Mar. Sci.* 9 (1), 205–229. doi:10.1146/annurev-marine-010816-060409

Lebreton, L., Slat, B., Ferrari, F., Sainte-Rose, B., Aitken, J., Marthouse, R., et al. (2018). Evidence that the great pacific garbage patch is rapidly accumulating plastic. *Sci. Rep.* 8 (1), 4666. doi:10.1038/s41598-018-22939-w

Li, F., Obrosova, I. G., Abatan, O., Tian, D., Larkin, D., Stuenkel, E. L., et al. (2005). Taurine replacement attenuates hyperalgesia and abnormal calcium signaling in sensory neurons of STZ-D rats. *Am. J. Physiol.-Endocrinol. Metab.* 288 (1), E29–E36. doi:10.1152/ajpendo.00168.2004

Li, P., and Wu, G. (2018). Roles of dietary glycine, proline, and hydroxyproline in collagen synthesis and animal growth. *Amino Acids* 50 (1), 29–38. doi:10.1007/s00726-017-2490-6

Li, X., Lin, C., and O'Connor, P. B. (2010). Glutamine deamidation: differentiation of glutamic acid and γ-glutamic acid in peptides by electron capture dissociation. *Anal. Chem.* 82 (9), 3606–3615. doi:10.1021/ac9028467

Linsmayer, L. B., Deheyn, D. D., Tomanek, L., and Tresguerres, M. (2020). Dynamic regulation of coral energy metabolism throughout the diel cycle. *Sci. Rep.* 10 (1), 19881. doi:10.1038/s41598-020-76828-2

Loenarz, C., and Schofield, C. J.(2008). Expanding chemical biology of 2-oxoglutarate oxygenases. *Nat. Chem. Biol.* 4, 152–156. doi:10.1038/nchembio0308-152

Luu-The, V., Tremblay, P., and Labrie, F. (2006). Characterization of type 12 17beta-hydroxysteroid dehydrogenase, an isoform of type 3 17beta-hydroxysteroid dehydrogenase responsible for estradiol formation in women. *Mol. Endocrinol.* 20 (2), 437–443. doi:10.1210/me.2005-0058

Lynes, M. A., Kang, J. Y., Sensi, S. L., Perdrizet, G. A., and Hightower, L. E. (2007). Heavy metal ions in normal physiology, toxic stress, and cytoprotection. *Ann. N. Y. Acad. Sci.* 1113 (1), 159–172. doi:10.1196/annals.1391.010

Macfarling Meure, C., Etheridge, D., Trudinger, C., Steele, P., Langenfelds, R., Van Ommen, T., et al. (2006). Law Dome CO2, CH4 and N2O ice core records extended to 2000 years BP. *Geophys. Res. Lett.* 33 (14). doi:10.1029/2006GL026152

Main, W. P. L., Ross, C., and Bielmyer, G. K. (2010). Copper accumulation and oxidative stress in the sea anemone, *Aiptasia pallida*, after waterborne copper exposure. *Comp. Biochem. Physiol. C Toxicol. Pharmacol.* 151 (2), 216–221. doi:10.1016/j.cbpc.2009.10.008

Majamaa, K., Günzler, V., Hanauske-Abel, H. M., Myllylä, R., and Kivirikko, K. I. (1986). Partial identity of the 2-oxoglutarate and ascorbate binding sites of prolyl 4-hydroxylase. *J. Biol. Chem.* 261 (17), 7819–7823. doi:10.1016/s0021-9258(19)57475-0

Majumdar, R., Barchi, B., Turlapati, S. A., Gagne, M., Minocha, R., Long, S., et al. (2016). Glutamate, ornithine, arginine, proline, and polyamine metabolic interactions: the pathway is regulated at the post-transcriptional level. *Front. Plant Sci.* 7, 78. doi:10.3389/fpls.2016.00078

Mansfield, K. M., Carter, N. M., Nguyen, L., Cleves, P. A., Alshanbayeva, A., Williams, L. M., et al. (2017). Transcription factor NF-κB is modulated by symbiotic status in a sea anemone model of cnidarian bleaching. *Sci. Rep.* 7 (1), 16025. doi:10.1038/s41598-017-16168-w

Manzello, D. P. (2010). Ocean acidification hotspots: spatiotemporal dynamics of the seawater CO2 system of eastern Pacific coral reefs. *Limnol. Ocean.* 55 (1), 239–248. doi:10.4319/lo.2010.55.1.0239

Matouskova, K., Jerry, D. J., and Vandenberg, L. N. (2020). Exposure to low doses of oxybenzone during perinatal development alters mammary gland morphology in male and female mice. *Reprod. Toxicol.* 92, 66–77. doi:10.1016/j.reprotox.2019.08.002

McBrian, M. A., Behbahan, S., Ferrari, R., Su, T., Huang, T.-W., Li, K., et al. (2013). Histone acetylation regulates intracellular pH. *Mol. Cell.* 49 (2), 310–321. doi:10.1016/j.molcel.2012.10.025

Medeiros, I. P. M., and Souza, M. M. (2023). Acid times in physiology: a systematic review of the effects of ocean acidification on calcifying invertebrates. *Environ. Res.* 231 (Pt 1), 116019. doi:10.1016/j.envres.2023.116019

Meena, M., Divyanshu, K., Kumar, S., Swapnil, P., Zehra, A., Shukla, V., et al. (2019). Regulation of L-proline biosynthesis, signal transduction, transport, accumulation and its vital role in plants during variable environmental conditions. *Heliyon* 5 (12), e02952. doi:10.1016/j.heliyon.2019.e02952

Meents, J. E., Ciotu, C. I., and Fischer, M. J. M. (2019). TRPA1: a molecular view. *J. Neurophysiol.* 121 (2), 427–443. doi:10.1152/jn.00524.2018

Miller, D. J., Hemmrich, G., Ball, E. E., Hayward, D. C., Khalturin, K., Funayama, N., et al. (2007). The innate immune repertoire in cnidaria--ancestral complexity and stochastic gene loss. *Genome Biol.* 8 (4), R59. doi:10.1186/gb-2007-8-4-r59

Mitchelmore, C. L., Burns, E. E., Conway, A., Heyes, A., and Davies, I. A. (2021). A critical review of organic ultraviolet filter exposure, hazard, and risk to corals. *Environ. Tox Chem.* 40, 967–988. doi:10.1002/etc.4948

Mitchelmore, C. L., He, K., Gonsior, M., Hain, E., Heyes, A., Clark, C., et al. (2019). Occurrence and distribution of UV-filters and other anthropogenic contaminants in coastal surface water, sediment, and coral tissue from Hawaii. *Sci. Total Environ.* 670, 398–410. doi:10.1016/j.scitotenv.2019.03.034

Morgan, M., Goodner, K., Ross, J., Poole, A. Z., Stepp, E., Stuart, C. H., et al. (2015). Development and application of molecular biomarkers for characterizing caribbean yellow band disease in *Orbicella faveolata*. *PeerJ* 3, e1371. doi:10.7717/peerj.1371

Morgan, M. B., Parker, C. C., Robinson, J. W., and Pierce, E. M. (2012). Using Representational Difference Analysis to detect changes in transcript expression of *Aiptasia* genes after laboratory exposure to lindane. *Aqua Tox* 110, 66–73. doi:10.1016/j.aquatox.2012.01.001

Morgan, M. B., Ross, J., Ellwanger, J., Phrommala, R. M., Youngblood, H., Qualley, D., et al. (2022). Sea anemones responding to sex hormones, oxybenzone, and benzyl butyl phthalate: transcriptional profiling and *in silico* modelling provide clues to decipher endocrine disruption in Cnidarians. *Front. Genet.* 12, 793306. doi:10.3389/fgene.2021.793306

Morgan, M. B., and Snell, T. W. (2002). Characterizing stress gene expression in reef-building corals exposed to the mosquitoside dibrom. *Mar. Poll. Bull.* 44 (11), 1206–1218. doi:10.1016/S0025-326X(02)00177-7

Morgan, M. B., and Snell, T. W. (2006). *Expression of a ceruloplasmin homolog in corals: an informative biomarker of stress*. Okinawa, Japan: The 10th International Coral Reef Symposium, 822–830. doi:10.13140/2.1.5077.3762

Morgan, M. B., Vogelien, D. L., and Snell, T. W. (2001). Assessing coral stress responses using molecular biomarkers of gene transcription. *Environ. Tox Chem.* 20 (3), 537–543. doi:10.1002/etc.5620200312

Moya, A., Huisman, L., Ball, E. E., Hayward, D. C., Grasso, L. C., Chua, C. M., et al. (2012). Whole transcriptome analysis of the coral Acropora millepora reveals complex responses to CO_2-driven acidification during the initiation of calcification. *Mol. Ecol.* 21 (10), 2440–2454. doi:10.1111/j.1365-294X.2012.05554.x

Muramatsu, T. (2016). Basigin (CD147), a multifunctional transmembrane glycoprotein with various binding partners. *J. Biochem.* 159 (5), 481–490. doi:10.1093/jb/mvv127

Murray, J. W., Roberts, E., Howard, E., O'Donnell, M., Bantam, C., Carrington, E., et al. (2015). An inland sea high nitrate-low chlorophyll (HNLC) region with naturally high pCO2. *Limnol. Ocean.* 60 (3), 957–966. doi:10.1002/lno.10062

Nikinmaa, M. (2013). Climate change and ocean acidification—interactions with aquatic toxicology. *Aqua Tox* 126, 365–372. doi:10.1016/j.aquatox.2012.09.006

Njiaju, U. O., Gamazon, E. R., Gorsic, L. K., Delaney, S. M., Wheeler, H. E., Im, H. K., et al. (2012). Whole-genome studies identify solute carrier transporters in cellular susceptibility to paclitaxel. *Pharmacogenet. Genom* 22 (7), 498–507. doi:10.1097/fpc.0b013e328352f436

Ocampo, I. D., Zárate-Potes, A., Pizarro, V., Rojas, C. A., Vera, N. E., and Cadavid, L. F. (2015). The immunotranscriptome of the Caribbean reef-building coral Pseudodiploria strigosa. *Immunogenetics* 67 (9), 515–530. doi:10.1007/s00251-015-0854-1

OmPraba, G., Chapeaurouge, A., Doley, R., Devi, K. R., Padmanaban, P., Venkatraman, C., et al. (2010). Identification of a novel family of snake venom proteins veficolins from cerberus rynchops using a venom gland transcriptomics and proteomics approach. *J. Proteome Res.* 9 (4), 1882–1893. doi:10.1021/pr901044x

Onthank, K. L., Foster, J., Carman, E. P., Jr, Foster, J. E., Culler-Juarez, M., Calvo, E., et al. (2023). The Open Acidification Tank Controller: an open-source device for the control of pH and temperature in ocean acidification experiments. *HardwareX* 14, e00435. doi:10.1016/j.ohx.2023.e00435

Onthank, K. L., Trueblood, L. A., Schrock-Duff, T., and Kore, L. G. (2021). Impact of short-and long-term exposure to elevated seawater Pco2 on metabolic rate and hypoxia tolerance in Octopus rubescens. *Physio Biochem. Zoo.* 94 (1), 1–11. doi:10.1086/712207

Palmer, C. V., and Traylor-Knowles, N. (2012). Towards an integrated network of coral immune mechanisms. *Proc. R. Soc. B-Biol. Sci.* 279 (1745), 4106–4114. doi:10.1098/rspb.2012.1477

Payen, V. L., Mina, E., Hée, V. F. V., Porporato, P. E., and Sonveaux, P. (2020). Monocarboxylate transporters in cancer. *Mol. Metab.* 33, 48–66. doi:10.1016/j.molmet.2019.07.006

Peterkofsky, B. (1991). Ascorbate requirement for hydroxylation and secretion of procollagen: relationship to inhibition of collagen synthesis in scurvy. *Am. J. Clin. Nutr.* 54 (6), 1135S–1140S. doi:10.1093/ajcn/54.6.1135s

Peters, E. C., Gassman, N. J., Firman, J. C., Richmond, R. H., and Power, E. A. (1997). Ecotoxicology of tropical marine ecosystems. *Environ. Tox Chem.* 16 (1), 12–40. doi:10.1002/etc.5620160103

Pettersen, E. F., Goddard, T. D., Huang, C. C., Couch, G. S., Greenblatt, D. M., Meng, E. C., et al. (2004). UCSF Chimera?A visualization system for exploratory research and analysis. *J. Comp. Chem.* 25 (13), 1605–1612. doi:10.1002/jcc.20084

Pie, H. V., Heyes, A., and Mitchelmore, C. L. (2015). Investigating the use of oil platform marine fouling invertebrates as monitors of oil exposure in the Northern Gulf of Mexico. *Sci. Total Environ.* 508, 553–565. doi:10.1016/j.scitotenv.2014.11.050

Putnam, H. M., Mayfield, A. B., Fan, T. Y., Chen, C. S., and Gates, R. D. (2013). The physiological and molecular responses of larvae from the reef-building coral Pocillopora damicornis exposed to near-future increases in temperature and pCO2. *Mar. Biol.* 160 (8), 2157–2173. doi:10.1007/s00227-012-2129-9

Ramos-Silva, P., Kaandorp, J., Huisman, L., Marie, B., Zanella-Cleon, I., Guichard, N., et al. (2013). The skeletal proteome of the coral *Acropora millepora*: the evolution of calcification by Co-option and domain shuffling. *Mol. Biol. Evol.* 30 (9), 2099–2112. doi:10.1093/molbev/mst109

Redmond, W. J., Gu, L., Camo, M., McIntyre, P., and Connor, M. (2014). Ligand determinants of fatty acid activation of the pronociceptive ion channel TRPA1. *PeerJ* 2, e248. doi:10.7717/peerj.248

Ripps, H., and Shen, W. (2012). Review: taurine: a "very essential" amino acid. *Mol. Vis.* 18, 2673–2686.

Rodriguez-Ruano, V., Toth, L. T., Enochs, I. C., Randall, C. J., and Aronson, R. B. (2023). Upwelling, climate change, and the shifting geography of coral reef development. *Sci. Rep.* 13 (1), 1770. doi:10.1038/s41598-023-28489-0

Salah, M., Abdelsamie, A. S., and Frotscher, M. (2019). Inhibitors of 17β-hydroxysteroid dehydrogenase type 1, 2 and 14: structures, biological activities and future challenges. *Mol. Cell. Endocrinol.* 489, 66–81. doi:10.1016/j.mce.2018.10.001

Schiedek, D., Sundelin, B., Readman, J. W., and Macdonald, R. W. (2007). Interactions between climate change and contaminants. *Mar. Poll. Bull.* 54 (12), 1845–1856. doi:10.1016/j.marpolbul.2007.09.020

Schlesinger, A., Kramarsky-Winter, E., Rosenfeld, H., Armoza-Zvoloni, R., and Loya, Y. (2010). Sexual plasticity and self-fertilization in the sea anemone aiptasia diaphana. *PLoS One* 5 (7), e11874. doi:10.1371/journal.pone.0011874

Schwarz, J. A., Brokstein, P. B., Voolstra, C., Terry, A. Y., Manohar, C. F., Miller, D. J., et al. (2008). Coral life history and symbiosis: functional genomic resources for two reef building Caribbean corals, *Acropora palmata* and *Montastraea faveolata*. *BMC Genom* 9, 97. doi:10.1186/1471-2164-9-97

Schweigel-Röntgen, M. (2014). The families of zinc (SLC30 and SLC39) and copper (SLC31) transporters. *Curr. Top. Membr.* 73, 321–355. doi:10.1016/b978-0-12-800223-0.00009-8

Servetto, N., Aranzamendi, M. C. d., Bettencourt, R., Held, C., Abele, D., Movilla, J., et al. (2021). Molecular mechanisms underlying responses of the Antarctic coral Malacobelemnon daytoni to ocean acidification. *Mar. Environ. Res.* 170, 105430. doi:10.1016/j.marenvres.2021.105430

Shearer, T. L., Rasher, D. B., Snell, T. W., and Hay, M. E. (2012). Gene expression patterns of the coral *Acropora millepora* in response to contact with macroalgae. *Coral Reefs* 31 (4), 1177–1192. doi:10.1007/s00338-012-0943-7

Shikina, S., and Chang, C.-F. (2016). "Sexual reproduction in stony corals and insight into the evolution of oogenesis in Cnidaria," in *The Cnidaria, past, present and future* (Germany: Springer), 249–268. doi:10.1007/978-3-319-31305-4_16

Siddiqui, S., Goddard, R. H., and Bielmyer-Fraser, G. K. (2015). Comparative effects of dissolved copper and copper oxide nanoparticle exposure to the sea anemone, Exaiptasia pallida. *Aqua Tox* 160, 205–213. doi:10.1016/j.aquatox.2015.01.007

Snell, T. W., Brogdon, S. E., and Morgan, M. B. (2003). Gene expression profiling in ecotoxicology. *Ecotoxicology* 12 (6), 475–483. doi:10.1023/B:ECTX.0000003033.09923.a8

Stillman, J. H., Paganini, A. W., Podrabsky, J. E., and Tomanek, L. (2015). Biochemical adaptation to ocean acidification. *J. Exp. Biol.* 218 (12), 1946–1955. doi:10.1242/jeb.115584

Studer, G., Rempfer, C., Waterhouse, A. M., Gumienny, R., Haas, J., and Schwede, T. (2020). QMEANDisCo—distance constraints applied on model quality estimation. *Bioinformatics* 36 (6), 2647–1771. doi:10.1093/bioinformatics/btaa058

Studer, G., Tauriello, G., Bienert, S., Biasini, M., Johner, N., and Schwede, T. (2021). ProMod3—a versatile homology modelling toolbox. *PLoS Comput. Biol.* 17 (1), e1008667. doi:10.1371/journal.pcbi.1008667

Sunagawa, S., Wilson, E. C., Thaler, M., Smith, M. L., Caruso, C., Pringle, J. R., et al. (2009). Generation and analysis of transcriptomic resources for a model system on the rise: the sea anemone *Aiptasia pallida* and its dinoflagellate endosymbiont. *BMC Genom* 10, 258. doi:10.1186/1471-2164-10-258

Tambutté, S., Holcomb, M., Ferrier-Pagès, C., Reynaud, S., Tambutté, É., Zoccola, D., et al. (2011). Coral biomineralization: from the gene to the environment. *J. Exp. Mar. Biol. Eco* 408 (1-2), 58–78. doi:10.1016/j.jembe.2011.07.026

Tarrant, A. M., Blomquist, C. H., Lima, P. H., Atkinson, M. J., and Atkinson, S. (2003). Metabolism of estrogens and androgens by scleractinian corals. *Comp. Biochem. Physiol. B* 136 (3), 473–485. doi:10.1016/s1096-4959(03)00253-7

Tran, K. T., Griffith, L., and Wells, A. (2004). Extracellular matrix signaling through growth factor receptors during wound healing. *Wound Repair Regen.* 12 (3), 262–268. doi:10.1111/j.1067-1927.2004.012302.x

Traylor-Knowles, N., and Connelly, M. T. (2017). What is currently known about the effects of climate change on the coral immune response. *Curr. Clim. Change Rep.* 3 (4), 252–260. doi:10.1007/s40641-017-0077-7

Trott, O., and Olson, A. J. (2010). AutoDock Vina: improving the speed and accuracy of docking with a new scoring function, efficient optimization, and multithreading. *J. Comp. Chem.* 31 (2), 455–461. doi:10.1002/jcc.21334

Venn, A. A., Tambutté, E., Holcomb, M., Laurent, J., Allemand, D., and Tambutté, S. (2013). Impact of seawater acidification on pH at the tissue–skeleton interface and calcification in reef corals. *P Natl. Acad. Sci.* 110 (5), 1634–1639. doi:10.1073/pnas.1216153110

Vidal-Dorsch, D. E., Bay, S. M., Maruya, K., Snyder, S. A., Trenholm, R. A., and Vanderford, B. J. (2012). Contaminants of emerging concern in municipal wastewater effluents and marine receiving water. *Environ. Tox Chem.* 31 (12), 2674–2682. doi:10.1002/etc.2004

Voolstra, C. R., Schnetzer, J., Peshkin, L., Randall, C. J., Szmant, A. M., and Medina, M. (2009). Effects of temperature on gene expression in embryos of the coral Montastraea faveolata. *BMC Genom* 10 (1), 627. doi:10.1186/1471-2164-10-627

Voskanyan, A., Vardapetyan, H., Hovhannisyan, M., Antonyan, M., and Darbinyan, A. (2014). THE ANTINOCICEPTIVE EFFECT OF TAURINE AGAINST LEVANTINE VIPER (*Macrovipera lebetina* obtusa) VENOM. *J. Exp. Biol.* 2, 6.

Vulpe, C. D., Kuo, Y. M., Murphy, T. L., Cowley, L., Askwith, C., Libina, N., et al. (1999). Hephaestin, a ceruloplasmin homologue implicated in intestinal iron transport, is defective in the *sla* mouse. *Nat. Genet.* 21, 195–199. doi:10.1038/5979

Wang, J. T., and Douglas, A. E. (1999). Essential amino acid synthesis and nitrogen recycling in an alga–invertebrate symbiosis. *Mar. Biol.* 135 (2), 219–222. doi:10.1007/s002270050619

Wang, N., Jiang, X., Zhang, S., Zhu, A., Yuan, Y., Xu, H., et al. (2021). Structural basis of human monocarboxylate transporter 1 inhibition by anti-cancer drug candidates. *Cell.* 184 (2), 370–383.e13. doi:10.1016/j.cell.2020.11.043

Waterhouse, A., Bertoni, M., Bienert, S., Studer, G., Tauriello, G., Gumienny, R., et al. (2018). SWISS-MODEL: homology modelling of protein structures and complexes. *Nuc Acids Res.* 46, W296. Web Server issue). doi:10.1093/nar/gky427

Wear, S. L., and Thurber, R. (2015). Sewage pollution: mitigation is key for coral reef stewardship. *Ann. N. Y. Acad. Sci.* 1355 (1), 15–30. doi:10.1111/nyas.12785

Wee, N. K. Y., Weinstein, D. C., Fraser, S. T., and Assinder, S. J. (2013). The mammalian copper transporters CTR1 and CTR2 and their roles in development and disease. *Int. J. Biochem. Cell. Biol.* 45 (5), 960–963. doi:10.1016/j.biocel.2013.01.018

White, D. J., Puranen, S., Johnson, M. S., and Heino, J. (2004). The collagen receptor subfamily of the integrins. *Int. J. Biochem. Cell. Biol.* 36 (8), 1405–1410. doi:10.1016/j.biocel.2003.08.016

Wittmann, A. C., and Pörtner, H.-O. (2013). Sensitivities of extant animal taxa to ocean acidification. *Nat. Clim. Chang.* 3 (11), 995–1001. doi:10.1038/nclimate1982

Woo, S., and Yum, S. (2022). Transcriptional response of the azooxanthellate octocoral Scleronephthya gracillimum to seawater acidification and thermal stress. *Comp. Biochem. Physiology Part D Genomics Proteomics* 42, 100978. doi:10.1016/j.cbd.2022.100978

Wood-Charlson, E. M., and Weis, V. M. (2009). The diversity of C-type lectins in the genome of a basal metazoan, *Nematostella vectensis*. *Dev. Comp. Immunol.* 33 (8), 881–889. doi:10.1016/j.dci.2009.01.008

Worm, B., Lotze, H. K., Jubinville, I., Wilcox, C., and Jeambeck, J. (2017). Plastic as a persistent marine pollutant. *Ann. Rev. Environ. Resour.* 42, 1–26. doi:10.1146/annurev-environ-102016-060700

Wu, H., Li, J., Chai, G., Xiao, Y., Song, Q., and Li, Z. (2022). Synergistic effects of ocean acidification and warming on coral host, Symbiodinium and nutrients exchange-based symbioses indicated by metatranscriptome. *Authorea*. doi:10.22541/au.164864741.18158605/v1

Wurl, O., and Obbard, J. (2004). A review of pollutants in the sea-surface microlayer (SML): a unique habitat for marine organisms. *Mar. Poll. Bull.* 48 (11-12), 1016–1030. doi:10.1016/j.marpolbul.2004.03.016

Xin, X., Huang, G., and Zhang, B. (2021). Review of aquatic toxicity of pharmaceuticals and personal care products to algae. *J. Hazard Mater* 410, 124619. doi:10.1016/j.jhazmat.2020.124619

Yamashita, Y., and Tanoue, E. (2003). Distribution and alteration of amino acids in bulk DOM along a transect from bay to oceanic waters. *Mar. Chem.* 82 (3-4), 145–160. doi:10.1016/s0304-4203(03)00049-5

Yoshida, G. J. (2021). The harmonious interplay of amino acid and monocarboxylate transporters induces the robustness of cancer cells. *Metabolites* 11 (1), 27. doi:10.3390/metabo11010027

Zhang, T., Yu, Z., Ma, Y., Chiou, B.-S., Liu, F., and Zhong, F. (2022). Modulating physicochemical properties of collagen films by cross-linking with glutaraldehyde at varied pH values. *Food Hydrocoll.* 124, 107270. doi:10.1016/j.foodhyd.2021.107270

Zhu, W., Ren, Y., Liu, X., Huang, D., Xia, J., Zhu, M., et al. (2022). The impact of coastal upwelling on coral reef ecosystem under anthropogenic influence: coral reef community and its response to environmental factors. *Front. Mar. Sci.* 9, 888888. doi:10.3389/fmars.2022.888888

Zoccola, D., Tambutté, E., Kulhanek, E., Puverel, S., Scimeca, J.-C., Allemand, D., et al. (2004). Molecular cloning and localization of a PMCA P-type calcium ATPase from the coral Stylophora pistillata. *Biochim. Biophys. Acta (BBA) - Biomembr.* 1663 (1-2), 117–126. doi:10.1016/j.bbamem.2004.02.010

Zúñiga-Soto, N., Pinto-Borguero, I., Quevedo, C., and Aguilera, F. (2023). Secretory and transcriptomic responses of mantle cells to low pH in the Pacific oyster (*Crassostrea gigas*). *Front. Mar. Sci.* 10, 1156831. doi:10.3389/fmars.2023.1156831

frontiers | Frontiers in Marine Science

TYPE Original Research
PUBLISHED 15 February 2024
DOI 10.3389/fmars.2024.1321865

OPEN ACCESS

EDITED BY
Aldo Cróquer,
The Nature Conservancy,
Dominican Republic

REVIEWED BY
Guoxin Cui,
King Abdullah University of Science and Technology, Saudi Arabia
Lei Jiang,
Chinese Academy of Sciences (CAS), China

*CORRESPONDENCE
Kefu Yu
kefuyu@scsio.ac.cn

RECEIVED 15 October 2023
ACCEPTED 23 January 2024
PUBLISHED 15 February 2024

CITATION
Wei X, Yu K, Qin Z, Chen S, Pan N and Lan M (2024) The acute and chronic low-temperature stress responses in *Porites lutea* from a relatively high-latitude coral reef of the South China Sea.
Front. Mar. Sci. 11:1321865.
doi: 10.3389/fmars.2024.1321865

The acute and chronic low-temperature stress responses in *Porites lutea* from a relatively high-latitude coral reef of the South China Sea

Xuelu Wei[1], Kefu Yu[1,2]*, Zhenjun Qin[1], Shuchang Chen[1], Nengbin Pan[1] and Mengling Lan[1]

[1]Coral Reef Research Center of China, Guangxi Laboratory on the Study of Coral Reefs in the South China Sea, School of Marine Sciences, Guangxi University, Nanning, China, [2]Southern Marine Science and Engineering Guangdong Laboratory (Guangzhou), Guangzhou, China

Relatively high-latitude coral reefs could be potential "refuges" for corals under climate change. One of the most important aspects limiting their availability as refuges is low-temperature stress. However, the mechanisms underlying the response of coral holobionts to low-temperature stress is unclear. In this study, we aimed to explore the underlying mechanisms by recording the maximum quantum yields of photosystem II (*Fv/Fm*) and transcriptome responses of *Porites lutea* under acute (1–2 weeks) and chronic (6–12 weeks) low-temperature stress at 20°C and 14°C. The *P. lutea* samples were collected from a relatively high-latitude coral reef in the South China Sea (109°00′–109°15′E and 21°00′–21°10′N). The study suggested that: (1) Under acute low-temperature stress, the *Fv/Fm* of Symbiodiniaceae dropped by 64%, which was significantly higher than the 49% observed under chronic stress. Low-temperature stress inhibited photosystem II (PSII) functioning, with greater inhibition under acute stress. (2) Downregulation of sugar metabolism-related genes under low-temperature stress implied that the decrease in energy was due to obstruction of PSII. (3) Under low-temperature stress, calcification-related genes were downregulated in coral hosts, possibly because of energy deprivation caused by inhibited photosynthesis, Symbiodiniaceae expulsion, and oxidative phosphorylation uncoupling in mitochondria. (4) Acute low-temperature stress induced the upregulation of genes related to the TNF signaling pathway and endoplasmic reticulum stress, promoting apoptosis and coral bleaching. However, these phenomena were not observed during chronic stress, suggesting acclimation to chronic low-temperature stress and a greater survival pressure of acute low-temperature stress on coral holobionts. In conclusion, low-temperature stress inhibits Symbiodiniaceae PSII functioning, reducing energy production and affecting calcification in coral holobionts. Acute low-temperature stress is more threatening to coral holobionts than chronic stress.

KEYWORDS

relatively high-latitude coral reef, low-temperature stress, coral holobionts, *Fv/Fm*, apoptosis

1 Introduction

Coral reef ecosystems rank among the most important global ecosystems, with high levels of biodiversity and primary productivity (Moberg and Folke, 1999). In recent years, climate change and anthropogenic stressors have precipitated degradation of coral reefs. Many coral species are on the verge of extinction (Carpenter et al., 2008; Heron et al., 2016; Hughes et al., 2017). Anomalies in sea surface temperature (SST) have led to extensive coral bleaching events, and elevated SST is the main cause of coral bleaching (McGowan and Theobald, 2017; Karnauskas, 2020). High-latitude reefs are postulated to serve as thermal refuges for corals (Greenstein and Pandolfi, 2008; Beger et al., 2014; Camp et al., 2018). However, modern ecological surveys and geological evidence suggest that low-temperature stress is an important factor limiting the survival of corals in high-latitude coral reefs (Yu et al., 2004; Sommer et al., 2018; Tuckett and Wernberg, 2018).

In high-latitude reefs, coral bleaching may be induced by low winter temperatures and acute SST declines due to upwelling, tidal activities, and tropical cyclones (Carrigan and Puotinen, 2014; Rayson et al., 2015; Schlegel et al., 2017; Rayson et al., 2018; Green et al., 2019; Riegl et al., 2019). For example, a severe cold spell in January 1981 caused coral bleaching in Florida (Schlegel et al., 2021). Under low-temperature stress, the photosystem II (PSII) of Symbiodiniaceae is damaged, resulting in the accumulation of reactive oxygen species (ROS) in tissues (Tracey et al., 2003; Marangoni et al., 2021). Excess ROS causes tissue damage and the expulsion of Symbiodiniaceae from corals, ultimately leading to the bleaching and death of coral holobionts (Jones et al., 1998; Tracey et al., 2003; Thornhill et al., 2008; Marangoni et al., 2021). RNA-seq analyses revealed that coral hosts modulate immunity, apoptosis, and autophagy while suppressing metabolic activity under low-temperature stress (Wuitchik et al., 2021; Huang et al., 2022). However, the responses of coral holobionts to temp perturbations seem to vary with changes in the stress intensity, rate, and duration (Evensen et al., 2021). The density and photosynthetic rate of Symbiodiniaceae show a lesser decrease under acute low-temperature stress (5 h) than under chronic stress (2 weeks) (Marangoni et al., 2021). Furthermore, previous research demonstrated inhibition of photosynthesis at the onset of low-temperature stress, and coral holobionts gradually adapted to the conditions, with chlorophyll a content and Symbiodiniaceae density gradually restored within 2–3 weeks (Roth et al., 2012).

It's imperative to study the response of coral holobionts to low temperatures, though the underlying mechanisms are still unclear. We aimed to explore these mechanisms by investigating the changes in maximum quantum yields in photosystem II (*Fv/Fm*) and transcriptional responses under acute and chronic low-temperature stress in *Porites lutea*. Weizhou Island (WI) located at 109°00′–109° 15′E and 21°00′–21°10′ N, is considered a potential refuge for corals in the South China Sea during global warming. The annual mean SST on WI is 24.6°C; the lowest monthly mean SST in winter is 17.3°C, varying from 14.7°C to 20°C, and the highest monthly mean SST in summer is 30.4°C, varying from 29.5°C to 31.1°C (Yu and Jiang, 2004; Chen et al., 2013). WI was subjected to extreme low-temperature events in 1984, 1985, 1989 and 2008,with lowest monthly mean SST as low as 14.7°C, 16°C, 15.5°C and 14.4°C, respectively (Chen et al., 2009; Chen et al., 2013). The corals of WI might be threatened by low temperatures (Southward et al., 1995; Yu et al., 2019). *P. lutea* is a dominant coral species around WI, and its principal symbiotic Symbiodiniaceae species is *Cladocopium C15* (Chen et al., 2019; Yu et al., 2019). Exploring the response mechanisms of *P. lutea* to acute and chronic low temperatures will further our understanding of the cold tolerance mechanisms of coral holobionts around WI.

2 Materials and methods

2.1 Coral sampling and experimental design

Three colonies of *P. lutea* were collected from the WI reef in September 2021 at a 3–5 m water depth. Three colonies were randomly assigned to each treatment. The samples were cultured in an indoor aquarium for 30 days prior to acute and chronic temperature stress experiments. Experiments utilized temperature gradients of 26°C, 20°C, and 14°C, with an initial temperature of 26°C. The lowest temperatures are in reference to the extreme low temperatures in WI(Chen et al., 2009; Chen et al., 2013). The sample were taken in the beginning of temperature decrease as the control treatment. In acute stress treatment, the temperature decreased by one gradient weekly, while in the chronic stress treatment, the temperature reduced by 1°C weekly (Figure 1). Three biological replicates were performed for each temperature gradient.

2.2 Symbiodiniaceae *Fv/Fm* determination

The *Fv/Fm* of Symbiodiniaceae was determined in the acute and chronic stress groups with different temperature gradients. The *Fv/Fm* of the Symbiodiniaceae was measured using a portable pulse amplitude modulation fluorometer (Diving-PAM)

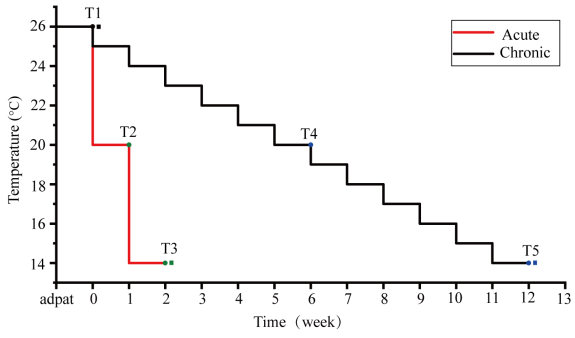

FIGURE 1
Temperature settings for acute and chronic stress groups. The red line represents the temperature change in the acute stress group, and the black line represents the temperature change in the chronic stress group. T1 is the control group, T2 and T3 are timepoints of the acute stress group, and T4 and T5 are timepoints the chronic stress group. Circles are the maximum quantum yields of photosystem II (*Fv/Fm*) measurement points and squares are transcriptome sampling points.

(Ralphet al., 1999). The coral holobionts were dark-adapted for 30 min before the *Fv/Fm* measurements. The fibreoptic cable was maintained approximately 1 mm from the coral surface. Kruskal–Wallis analysis was performed on the *Fv/Fm* data based on different temperature gradients for different stress groups.

We computed the hypothermic critical threshold *Fv/Fm* measurements (Evensen et al., 2021), which were fitted to log-logistic dose–response curves using the "drc" package in R (Ritz et al., 2016), with model selection based on Akaike's Information Criterion and individual curves fit for each experiment. From these, an ED_{50} parameter (effective dose 50) was obtained for each experiment, representing the x-value at the inflection point of the curve (in this case the temperature) where *Fv/Fm* values in the model fit were 50% lower than the starting values of the model. This provided a quantitative thermal threshold, designated as the *Fv/Fm*ED_{50}, for *P. lutea* in each experiment (Evensen et al., 2021). All code used in the statistical analyses is available in the Supplementary Material.

2.3 RNA-seq analyses

Transcriptomic analyses were performed on control samples (maintained at 26°C) and those exposed to extreme low-temperature stress (14°C). Coral samples were washed with sterile water, and approximately 50 mg of each was excised using forceps, placed into lyophilization tubes, and promptly snap-frozen in liquid nitrogen. Library construction was performed using the Illumina TruSeq RNA Sample Prep Kit.Total RNA was extracted from the coral samples using TRIzol® Reagent. Then RNA quality was determined by 5300 Bioanalyser (Agilent) and quantified using the ND-2000 (NanoDrop Technologies). mRNA was isolated from the total RNA using magnetic bead-labeled oligonucleotides (dT) and was used as a template to synthesize cDNA strands via reverse transcription using reverse transcriptase. cDNA was blunt-ended by adding End Repair Mix, followed by the addition of an "A" base at the 3′ end to prepare the RNA sequencing library. All mRNAs transcribed from the samples were sequenced using an Illumina NovaSeq 6000 sequencing platform. The raw sequences were deposited in the NCBI Sequence Read Archive (SRA) database (accession number: PRJNA1026091).

The base distribution and quality fluctuations of sequenced sequences were counted using fastp to meet the criteria of Q30 > 80% for base quality values and a sequencing error rate of < 0.1% (Chen et al., 2018). After quality control, The remaining high-quality clean reads were mapped to the reference transcriptomes using HISAT2(Kim et al., 2015). Coral hosts and Symbiodiniaceae's reference transcriptomes derived from http://plut.reefgenomics.org/. The Symbiodiniaceae were referred to as *Cladocopium C15*, and the coral hosts were referred to as *P. lutea*. The mapped reads of each sample were assembled by StringTi in a reference-based approach (Pertea et al., 2015).

To identify DEGs (differential expression genes) between two different treatment, the expression level of each transcript was calculated according to the transcripts per million reads (TPM) method. RSEM was used to quantify gene abundances(Li and Dewey, 2011). Essentially, differential expression analysis was performed using the DESeq2(Love et al., 2014). DEGs with $|\log2FC| \geq 1$ and FDR≤ 0.05 were considered to be significantly different expressed genes. Two pairwise comparisons were designated in the DEG analyses:CK26 versus A14, CK26versus C14.

KEGG functional-enrichment analysis were performed to identify which DEGs were significantly enriched in pathways at Bonferroni-corrected P-value ≤0.05 compared with the whole-transcriptome background. KEGG pathway analysis were carried out by KOBAS (Xie et al., 2011). In addition, the expression of genes in the samples was subjected to principal component analysis (PCA) to explore the relationship between the samples and the magnitude of variation.

3 Results

3.1 The *Fv/Fm* variation of *P. lutea*-symbiotic Symbiodiniaceae under acute and chronic low-temperature stress

Acute and chronic low-temperature stress altered the appearance of corals. At 20°C, the color became lighter without reaching bleaching. At 14°C, the color was lighter than at 20°C, and in the acute stress group, there was localized pre-bleaching (Figure 2A). The *Fv/Fm* values decreased under acute and chronic low-temperature stress. At 26°C (CK), the *Fv/Fm* was 0.61 ± 0.03 (mean ± SD) and 0.60 ± 0.05 (mean ± SD) in the acute and chronic stress groups, respectively (Figure 2B; Supplementary Table S1). At 20°C, a decline in *Fv/Fm* was observed, but it was not significant (Kruskal–Wallis test, chronic: P = 0.077 acute: P = 0.085). At 14°C, both the acute and chronic stress groups exhibited significant Fv/Fm reduction compared to control (Kruskal–Wallis test, chronic: P < 0.001, acute: P< 0.001), registering values of 0.22 ± 0.03 (mean ± SD) and 0.31 ± 0.05 (mean ± SD), equating to 36% and 51% of the control values, respectively (Figure 2B; Supplementary Table S1). At 14°C, the Fv/Fm of the acute stress group was significantly lower (Kruskal–Wallis test, P = 0.001) than that of the chronic stress group (Figure 2B).

The *Fv/Fm*ED_{50} represents the temperature at which 50% of the photosynthetic efficiency is lost relative to the baseline temperature. From *Fv/Fm*ED_{50}, we found that the cold threshold was 14.99°C for acute stress and 13.86°C for chronic stress (Figure 2C). This indicates that PSII functioning in Symbiodiniaceae was inhibited by low-temperature stress at 14°C, whereby the acute stress group exhibited greater inhibition than the chronic stress group.

3.2 Transcriptional changes in *P. lutea*-symbiotic Symbiodiniaceae under acute and chronic low-temperature stress

Transcriptome analysis was performed on samples from the 26°C (CK), acute 14°C (A14), and chronic 14°C (C14) groups. The percentage of Q30 bases in clean data is above 93.2%. (Supplementary Table S2). The expression of Symbiodiniaceae genes was quantitatively analyzed using RSEM to obtain a quantitative index in terms of transcripts per million (TPM) (Supplementary Table S3). PCA showed that PC1 and PC2 accounted for 31.00% and 19.29% of

10.3389/fmars.2024.1321865

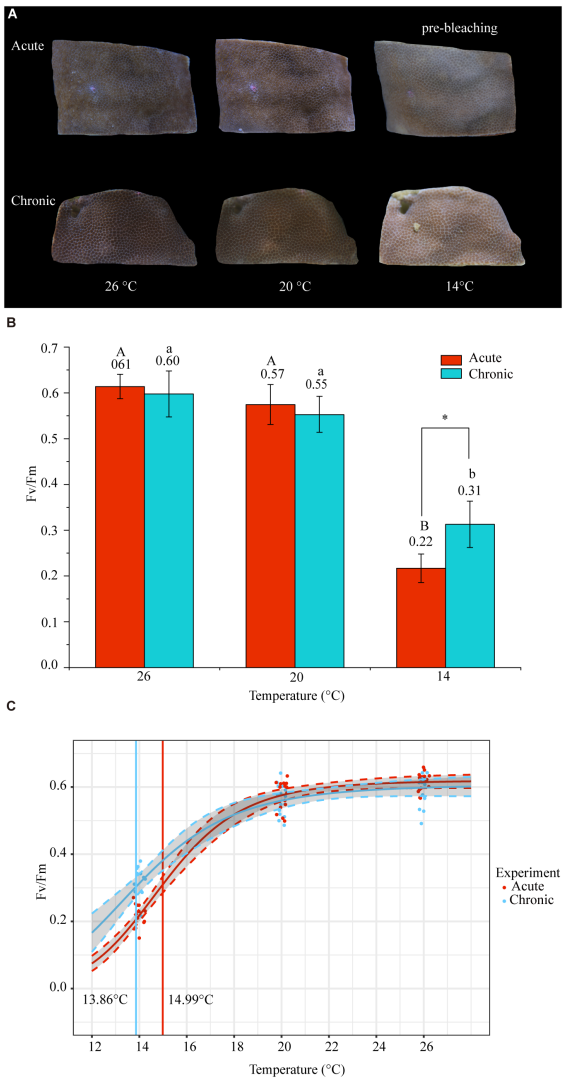

FIGURE 2
Changes in physiological indicators under acute and chronic low-temperature stress. **(A)** Appearance of corals during low-temperature stress. At 26°C, normal color was observed with extended tentacles; at 20°C, the color became lighter without reaching bleaching; at 14°C, the color became lighter than at 20°C, and in the acute stress group, there was localized pre-bleaching. **(B)** Maximum quantum yields of photosystem II (*Fv/Fm*) of *P. lutea* under different temperature conditions and during acute and chronic stress. 'A' and 'a' represent the differences between temperatures in the acute and chronic stress groups, respectively (Kruskal–Wallis test, $P < 0.05$). * represents significant differences (Kruskal–Wallis test, $P < 0.05$) between acute and chronic stresses at the same temperature. **(C)** *Fv/Fm* fit to log-logistic, dose-response curves (dashed lines indicate 95% confidence intervals). Curve fitting was used to determine *Fv/Fm*ED_{50} (effective dose 50).

the total variance, respectively (Figure 3A). Differential expression analysis between groups was performed using DESeq2. Compared with expression levels of the control group, the acute 14°C group had 487 DEGs, among which 200 genes were upregulated and 287 were downregulated; meanwhile, the chronic 14°C group had 2,566 DEGs, among which 1,041 were upregulated 1,525 were downregulated (Figures 3C, D; Supplementary Table S4). Of these, 299 DEGs were common to both groups, 188 were specific to the acute 14°C group, and 2,267 were specific to the chronic 14°C group (Figure 3B; Supplementary Table S4).

In the 14°C chronic stress group, ribosomes, pyrimidine metabolism, alanine, aspartate and glutamate metabolism, starch and sucrose metabolism, pyruvate metabolism, and carbon fixation in photosynthetic organisms comprised pathways that were enriched among downregulated genes (Figures 4A, B; Supplementary Table S5). The main DEGs were the ribosomal constitutive protein-related genes, glutamate dehydrogenase (*GDH2*), phosphoglycerate kinase (*PGK*), glucoamylase (*SGA1*), and beta-glucosidase (*bglX*), among others. Although the glutathione metabolic pathway was not enriched among the upregulated genes, glutathione S-transferase (*GST*) expression was significantly upregulated (Figure 4C; Supplementary Table S5).

Based on Padjust < 0.05, there were no enriched pathways in the acute 14°C stress group. However, the *PGK*, *SGA1*, and *bglX* were significantly downregulated. Meanwhile, the ribosomal constitutive protein-related genes, *GDH2* and *GST* were upregulated (Figure 4C; Supplementary Table S5).

3.3 Transcriptional changes in coral hosts under acute and chronic low-temperature stress

The expression of coral host genes was quantitatively analyzed using RSEM to obtain a quantitative index in terms of TPM (Supplementary Table S6). The results of PCA showed that PC1 and PC2 accounted for 43.5% and 23.78% of the total variance, respectively (Figure 5A). Compared with the control group (CK), the acute 14°C group (A14) had 5,703 DEGs, among which 1,943 were upregulated and 3,760 were downregulated (Figure 5C). Meanwhile, the chronic 14°C group (C14) had 4,637 DEGs, of which 1,565 were upregulated and 3,072 were downregulated (Figure 5D; Supplementary Table S7). Among these DEGs 1,885 were common to both groups, 3,818 were specific to the acute 14°C group and 2, 752 were common to the chronic 14°C group (Figure 5B; Supplementary Table S7).

Based on a threshold of Padjust < 0.05, apoptosis-multiple species, protein processing in endoplasmic reticulum (ER), TNF signaling pathway, and oxidative phosphorylation pathway were significantly enriched among the upregulated genes in the acute 14°C group (Figure 6A; Supplementary Table S7). The major DEGs were caspase 3 (*Casp3*), caspase 8 (*Casp8*), caspase 9 (*Casp9*), apoptosis regulator Bcl-X ($bcl\text{-}x_L$), heat shock 70kDa protein 1 (*HSPA1*), ER chaperone BiP (*BIP*), molecular chaperone HtpG (*HSP90A*), ubiquitin-conjugating enzyme E2G1 (*UBE2G1*), TNF receptor-associated factor 2 (*TNFR2*), the gene related to NADH dehydrogenase, succinate dehydrogenase, cytochrome c reductase, and cytochrome c oxidase. In addition, the mitochondrial uncoupling protein (*UCP2_3*) was significantly upregulated (Figure 6E; Supplementary Table S7).

The Wnt signaling pathway, Notch signaling pathway, nitrogen metabolism, and other pathways were enriched among the downregulated genes (Figure 6B; Supplementary Table S7). The main DEGs were the wingless-type MMTV integration site family (*WNTs*), frizzled 9/10 (*FZD9_10*), and low density lipoprotein

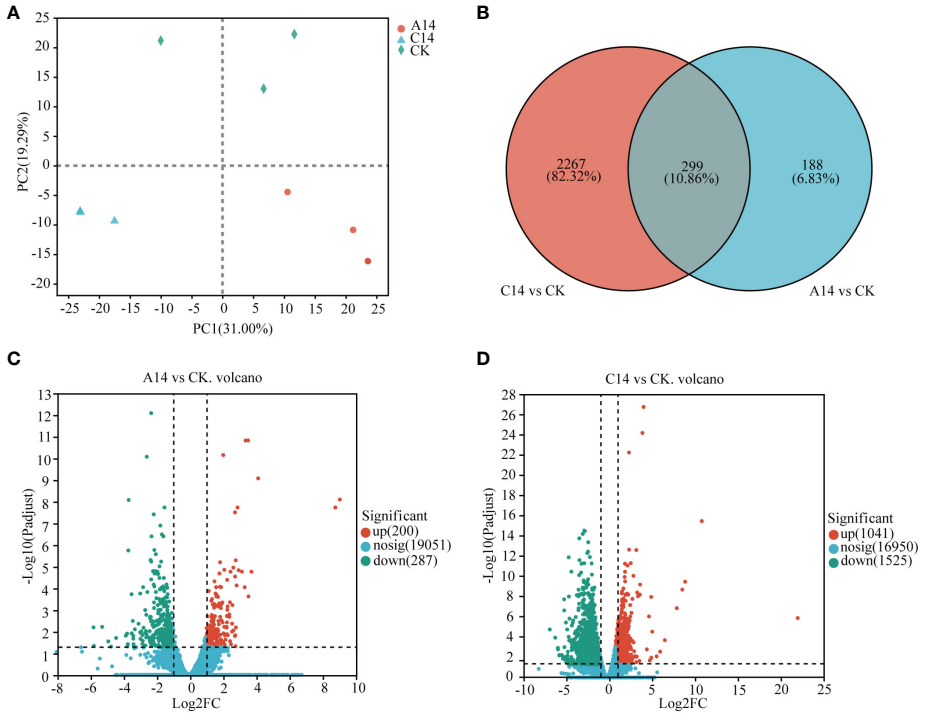

FIGURE 3
Differential expression of genes(DEGs) in Symbiodiniaceae under acute and chronic stress. **(A)** PCA between samples. **(B)** Venn analysis of Symbiodiniaceae DEGs, where red circles represent the number of DEGs in the chronic 14 °C group, and blue circles represent the number of differentially expressed genes in the acute 14 °C group. **(C)** Volcano plot of Symbiodiniaceae DEGs in the acute 14°C group. **(D)** Volcano plot of DEGs in the chronic 14°C group, where red dots indicate significantly upregulated genes, green dots indicate significantly downregulated genes, and blue dots represent non-significant differentially expressed genes. A, acute stress; C, chronic stress;
CK, control; 14, 14°C.

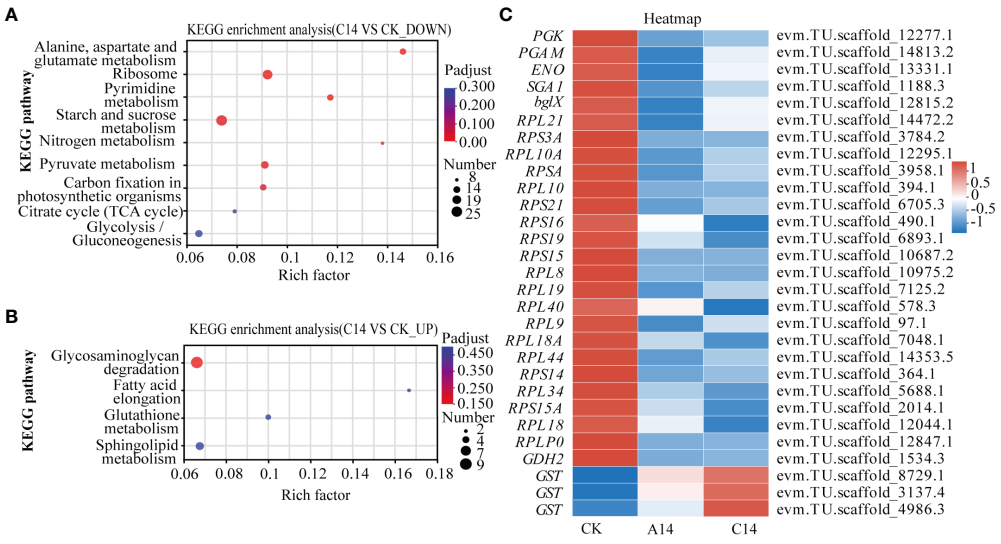

FIGURE 4
KEGG enrichment and heatmap of DEGs in Symbiodiniaceae under acute and chronic low-temperature stress. **(A)** KEGG enrichment results of significantly downregulated genes under chronic 14°C stress. **(B)** KEGG enrichment results of significantly upregulated genes under chronic 14°C stress, where the size of the dots indicates how many genes are in the pathway, and the color of the dots corresponds to different Padjust ranges. **(C)** Heatmap of key DEGs in Symbiodiniaceae under acute and chronic low-temperature stress. The color in the graph indicates the expression value of the gene after normalization treatment. A, acute stress; C, chronic stress; CK, control; 14, 14°C.

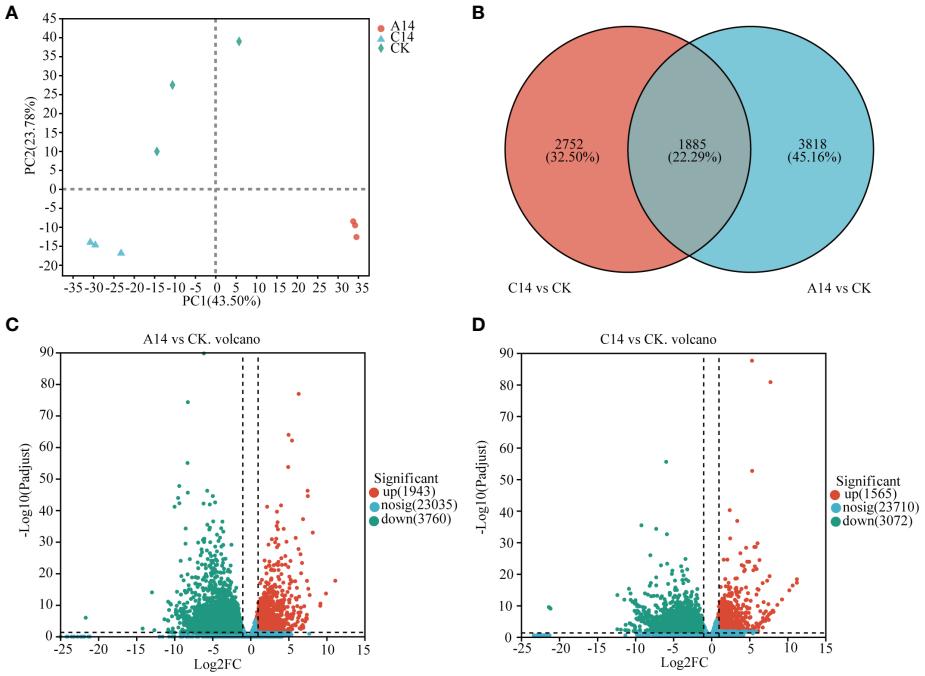

FIGURE 5
DEGs of coral host under acute and chronic low-temperature stress. **(A)** PCA between samples. **(B)** Venn analysis of host DEGs, where red circles represent the number of DEGs in the chronic 14°C group, and blue circles represent the number of differentially expressed genes in the acute 14°C group. **(C)** Volcano plot of host DEGs in the acute 14°C group. **(D)** Volcano plot of host DEGs in the chronic 14°C group, where red dots indicate upregulated genes, green dots indicate downregulated genes, and blue dots represent non-significant differentially expressed genes. A, acute stress; C, chronic stress; CK, control; 14, 14°C.

receptor-related protein 5/6 (*LRP5_6*). In addition, carbonic anhydrase (*CA*) and bone morphogenetic protein (*BMP*), associated with calcification and oxidative stress-associated superoxide dismutase (*SOD1*), respectively, were significantly downregulated (Figure 6E; Supplementary Table S7).

In the chronic 14°C group, retinol metabolism, lysosomes, oxidative phosphorylation, and other pathways were enriched among upregulated genes (Figure 6C; Supplementary Table S7). The major DEGs were those related to NADH dehydrogenase, succinate dehydrogenase, cytochrome c reductase, and cytochrome c oxidase. Additionally, mitochondrial uncoupling protein (*UCP4*) was significantly upregulated (Figure 6E; Supplementary Table S7).

NF-kappa B, Wnt, and TNF signaling pathways, among others, were enriched among the downregulated genes (Figure 6D). The major DEGs were *WNTs*, *LRP5_6*, and *TNFR2*. In addition, the apoptosis-related genes *Casp8*, calcification-related *CAs*, and *BMPs* were significantly downregulated (Figure 6E; Table S7).

4 Discussion

4.1 Acute stress inhibits PSII functioning in *P. lutea*-symbiotic Symbiodiniaceae more than chronic low-temperature stress

The *Fv/Fm* of Symbiodiniaceae was significantly reduced under acute and chronic stress at 14°C, measuring 0.22 ± 0.03 and 0.31 ± 0.05, respectively. The cold threshold was 14.99°C for acute stress and 13.86°C for chronic stress based on the *Fv/Fm*ED_{50} parameter. When photosynthesis is working at peak efficiency, *Fv/Fm* values for Symbiodiniaceae typically range between 0.50 and 0.70 (Tunala et al., 2019). Under 14°C, the *Fv/Fm* values of *P. lutea*-symbiotic Symbiodiniaceae were always < 0.5, indicating that photosystem II functioning was inhibited. In a previous study, *Fv/Fm*ED_{50} was used to determine the temperature threshold for bleaching (Evensen et al., 2021). At 14°C, the acute stress group reached the bleaching threshold and coral holobionts were in a pre-bleaching state, but the chronic stress group did not reach the bleaching threshold. This indicates that acute low-temperature stress has a higher propensity to induce coral bleaching compared to chronic stress. Following an 8-day temperature decrease from 22°C to 12°C, the *Fv/Fm* values of coral holobionts remained stable (Büchel and Wilhelm, 1993; Keshavmurthy et al., 2021). However, coral holobionts exposed acutely to 10°C showed a significant decrease in *Fv/Fm* and died within 48 h of stress (Keshavmurthy et al., 2021). The *Fv/Fm* of *Montipora digitata* decreased after 3, 6, and 12 h of 20°C stress, but not significantly after 18 h, and recovered within 72 h of stress (Tracey et al., 2003). These phenomena could be attributed to the effects of stress rate or duration on the photophysiological response of Symbiodiniaceae.

Our results show that low-temperature stress has an inhibitory effect on photosynthesis in *P. lutea*-symbiotic Symbiodiniaceae. Notably, acute low-temperature stress inhibits photosystem II functioning of Symbiodiniaceae to a much greater extent than chronic stress.

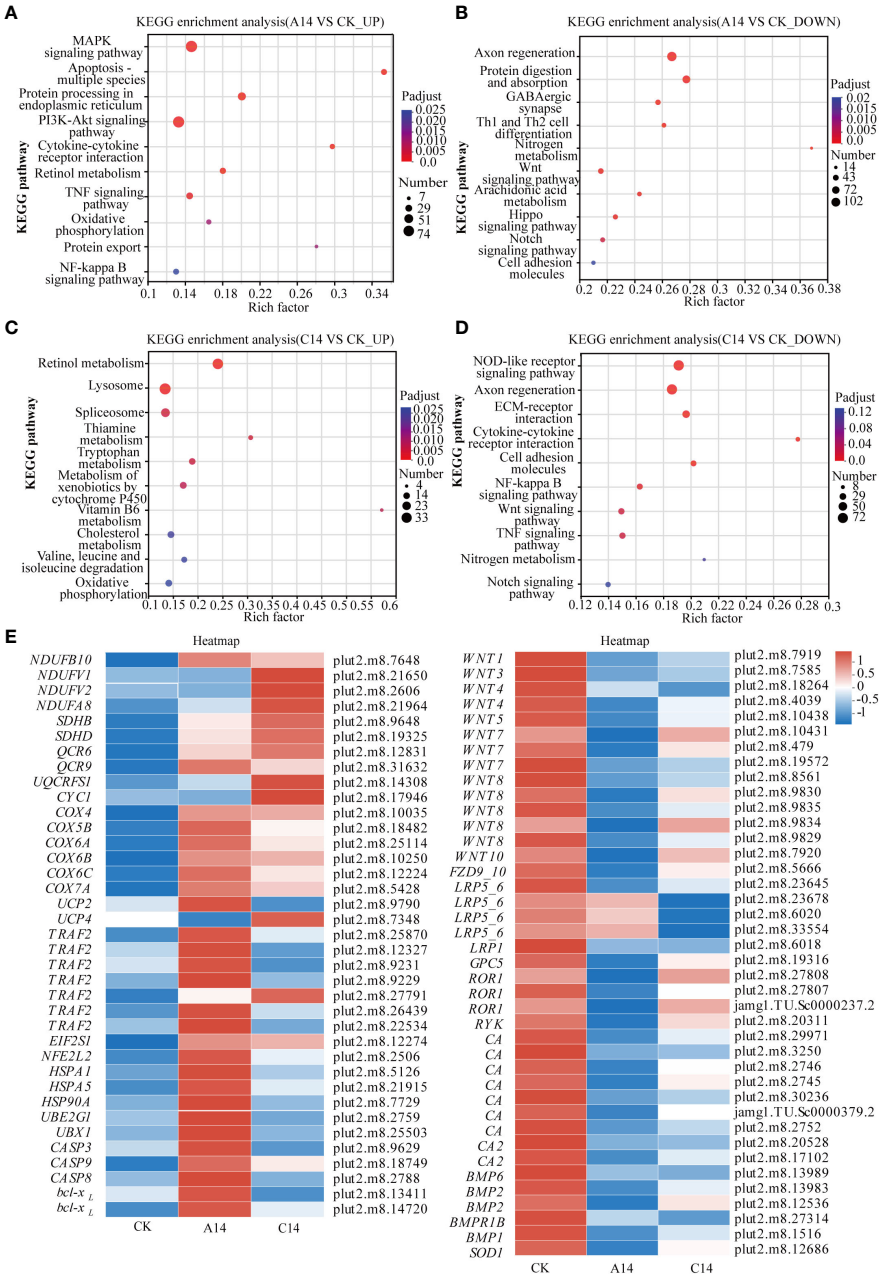

FIGURE 6
KEGG enrichment and heatmap of DEGs in *P. lutea* under acute and chronic low-temperature stress. **(A)** KEGG enrichment results for significantly upregulated genes in the acute 14 °C group. **(B)** KEGG enrichment results for significantly downregulated genes in the acute 14 °C group. **(C)** KEGG Enrichment results for significantly upregulated genes in the chronic 14 °C group. **(D)** KEGG enrichment results for significantly downregulated genes in the chronic 14 °C group, where the size of the dots indicates the number of genes in the pathway, and the color of the dots corresponds to different P adjust ranges. **(E)** Heatmap of key DEGs in *P. lutea* under acute and chronic low-temperature stress. The color indicates the expression value of the gene after normalization treatment. A, acute stress; C, chronic stress; CK, control; 14 = 14 °C.

4.2 Low-temperature stress leads to energy deprivation in *P. lutea*-symbiotic Symbiodiniaceae

Under acute and chronic low-temperature stress, *PGK*, *SGA1*, *bglX*, *GDH2*, and ribosomal protein-related genes were significantly downregulated, while *GST* was significantly upregulated. The glycolysis and hydrolysis of cellulose and starch to glucose are interconnected with the energy productivity of organisms. In glycolysis, PGK catalyzes the acyl phosphate transfer from 1,3-bisphosphoglycerate to the high-energy phosphate group of ADP, resulting in the production of ATP (Joshi et al., 2016). Low expression of PGK could lead to reduced production of pyruvate and ATP, causing energy deprivation in Symbiodiniaceae (Rosa-Téllez et al., 2017). Additionally, a correlation was observed between the reduction in *Fv/Fm* and the diminished activity of PGK. Low

PGK activity impedes the regeneration of essential electron acceptors for the photosynthetic electron transport chain, thereby affecting photosynthesis (Rosa-Téllez et al., 2017). The *SGA1* gene related to β-glucosidase and the *bglX* gene related to glucoamylase are involved in the hydrolysis of cellulose and starch to glucose, respectively. The downregulation of *SGA1* and *bglX* during acute and chronic low-temperature stress further implies energy deprivation in Symbiodiniaceae.

Energy is important for maintaining physiological functions. Low-temperature stress inhibited PSII functioning in *P. lutea*-symbiotic Symbiodiniaceae, culminating in a decline in glucose production and, consequently, an energy shortage. Energy deprivation triggers a series of reactions that threaten the survival of organisms (Mia et al., 2006). Symbiodiniaceae coordinates the relationship between resistance to low-temperature stress and basal metabolism to maintain long-term survival. For example, in *P. lutea*-symbiotic Symbiodiniaceae, *GST*, related to glutathione metabolism.Glutathione S-transferases (GSTs) have glutathione peroxidase activity, through which they perform an oxygen-detoxifying function(Mannervik, 1985). GSTs play a significant role in decreasing ROS to protecting against oxidative stress (Liu et al., 2016). *GST* is upregulated in response to ROS overproduction stimulated by acute and chronic low-temperature stress (Ravelo et al., 2022). The downregulation of ribosomal protein-related genes and *GDH2* involved in ammonia assimilation in Symbiodiniaceae. Photosynthates are important for the tricarboxylic acid (TCA) cycle, a process that provides energy and substrates for nitrogen metabolism (Zhang and Fernie, 2018). Protein synthesis and ammonia assimilation are important processes in nitrogen metabolism (Zhang and Fernie, 2018). Ribosomes are the main site of protein synthesis (Cassaignau et al., 2020). Glutamate dehydrogenase 2 (GDH2) operating at the interface of carbon and nitrogen metabolism has the potential capacity to assimilate inorganic N by combining ammonium with 2-Oxoglutarate to form glutamate (Dubois et al., 2003).It has been observed that reduction in photosynthetic rate was accompanied by the decrease in the activities of GDH (Singh et al., 2016).The downregulation of ribosomal protein-related genes and GDH2 could potentially be ascribed to substrate scarcity and energy deprivation. In summary, *P. lutea*-symbiotic Symbiodiniaceae PSII functioning is inhibited under low-temperature stress, which affects energy production by Symbiodiniaceae and leads to an energy shortage.

4.3 Low-temperature stress limits the calcification of *P. lutea*

In this study, the genes related to CA, BMP, and the Wnt signaling pathway were downregulated in coral hosts under acute and chronic low-temperature stress. The genes related to uncoupling proteins (UCPs), oxidative phosphorylation-related NADH dehydrogenase, succinate dehydrogenase, and cytochrome c oxidase were upregulated. Moreover, the gene related to superoxide dismutase (SOD) was significantly downregulated under acute stress and downregulated under chronic stress, but the differences were not significant ($P > 0.05$).

CA is associated with calcification in coral holobionts and facilitates the reversible hydration of CO_2 to bicarbonate, thereby sustaining the CO_2/HCO_3^- equilibrium (Furla et al., 2000; Zoccola et al., 2009; Bertucci et al., 2013; Hemond et al., 2014; Hopkinson et al., 2015). Extracellular CA plays a role in the uptake of CO_2. Intracellular CA can convert ingested and respired CO_2 into HCO_3^- (Bertucci et al., 2013; Hopkinson et al., 2015). CA is pivotal in both supplying carbon for calcification and facilitating carbon-concentrating mechanisms during Symbiodiniaceae photosynthesis (Hopkinson et al., 2015).Where PSII functioning is impaired, and the ATP and NADPH required for carbon assimilation may be reduced (Burlacot and Peltier, 2023). Thus, the reduction of inorganic carbon that can be fixed(Burlacot and Peltier, 2023). This reduction could lead to a downregulation of *CA*.The downregulation of *CAs* could potentially hinder the assimilation of inorganic carbon from seawater by coral holobionts, thereby constraining calcification (Tambutté et al., 2007). Additionally, BMP participate in the formation of cartilage and bone in animals and constitute an essential component of the skeletal organic matrix in corals (Mass et al., 2016). The downregulation of *BMPs* also indicates that coral calcification was affected. The Wnt signaling pathway has been demonstrated to promote osteogenesis in animals and potentially affect coral calcification (Broun et al., 2005; Guder et al., 2006; Plickert et al., 2006; Duffy et al., 2010; Hemond et al., 2014). The downregulation of the genes associated with Wnt signaling pathway, *CAs*, and *BMPs* revealed potential constraints of coral calcification under low-temperature stress.

Calcification is related to the energy supply. The photosynthesis of Symbiodiniaceae provides the energy for calcification, thereby serving as a crucial role for coral calcification (Hatcher, 1988). Under energy loss, coral hosts regulate various metabolic activities to maintain the stability of coral holobionts (Rinkevich, 1996; Sokolova, 2013; Tang et al., 2020; Leinbach et al., 2021). In this study, photosystem II functioning was inhibited in Symbiodiniaceae under acute and chronic low-temperature stress, culminating in a reduction in energy acquisition by the coral host. Furthermore, previous studies have indicated that low-temperature stress impairs Symbiodiniaceae's PSII, elevating ROS levels in tissues (Jones et al., 1998; Tracey et al., 2003; Thornhill et al., 2008; Marangoni et al., 2021). Utilizing antioxidant enzymes to scavenge excess ROS is vital for coral redox homeostasis (Zhang et al., 2022). However, in this study, the genes related to the antioxidant enzyme SOD in *P. lutea* were not upregulated under low-temperature stress. It is possible that *P. lutea* scavenges excess ROS by expelling Symbiodiniaceae with impaired photosynthesis. Therefore, the host would have a reduced demand for the antioxidant enzyme. Previous studies have demonstrated that damaged Symbiodiniaceae expulsion diminishes coral host ROS levels under low-temperature stress (Higuchi et al., 2015; Marangoni et al., 2021). This also resulted in a reduction in the energy supply derived from Symbiodiniaceae to the host.

Upregulation of genes related to UCPs may induce energy loss in the coral host. UCP-mediated oxidative phosphorylation decoupling in mitochondria potentially reduces mitochondrial ROS and contributes to antioxidative effects (Mailloux and Harper, 2011; Slocińska et al., 2016). However, UCP decoupling decreases oxidative phosphorylation efficiency, limiting the energy

harnessed from the electron transport chain for ATP synthesis (Slocinska et al., 2016). Under acute and chronic low-temperature stress, the genes related to NADH dehydrogenase, succinate dehydrogenase, cytochrome c reductase, and cytochrome c oxidase related to oxidative phosphorylation were upregulated in *P. lutea*, but the expression of genes related to ATP synthesis did not change significantly. This also implies oxidative phosphorylation uncoupling in *P. lutea*. Under acute and chronic low-temperature stress, *P. lutea* may facilitate phosphorylation uncoupling through UCP-related genes upregulation, partially leading to energy loss.

Low-temperature stress inhibited Symbiodiniaceae PSII functioning, prompted expulsion from the coral host, and uncoupled oxidative phosphorylation, leading to energy deprivation. Under an energy shortage, *P. lutea* limits calcification by downregulating *CAs* and *BMPs*.

4.4 Under low temperature, acute stress induces *P. lutea* apoptosis, whereas chronic stress facilitates acclimation

Our results showed upregulation of genes associated with apoptotic processes in coral hosts under acute low-temperature stress, including *Casp3*, *Casp8*, *Casp9*, *bcl-x$_L$*, and TNF signaling pathway-related gene *TRAF2*, and ER stress-related genes *EIF2S1*, *NRF2*, *HSPA1*, *HSPA5*, *HSP90*, *UBE2G1*, and *UBX1*, among others. However, under chronic low-temperature stress, key genes associated with apoptotic processes, such as *TNFR2*, *HSP90*, and *Casp3*, among others, either remained unchanged or were downregulated.

Apoptosis is pivotal in development, morphogenesis, and immunity (Shao et al., 2016). However, excessive apoptosis leads to coral bleaching (Desalvo et al., 2008; DeSalvo et al., 2012; Yu et al., 2017). Apoptosis is a form of programmed cell death that occurs in multicellular organisms and is triggered by the proteolytic caspase cascade (Shao et al., 2016). Caspase 8 and caspase 9 are promoters that regulate apoptosis (Tummers and Green, 2021). Caspase 3 is central to apoptosis regulation (Yu et al., 2017). Its activation usually indicates that the cell has undergone apoptosis (Yu et al., 2017). The apoptotic genes *Casp3*, *Casp8*, and *Casp9* was upregulated, thereby substantiating the induction of apoptosis in *P. lutea*. Anti-apoptotic *bcl-x$_L$* was upregulated in our study. This indicates a counterbalance stage between apoptosis and anti-apoptosis in coral. Previous studies have shown that apoptotic and anti-apoptotic processes coexist within cells (Kvitt et al., 2016; Majerova et al., 2021). The balance between anti-apoptotic and pro-apoptotic genes within the cell dictates the ultimate apoptotic rate(Kvitt et al., 2016; Majerova et al., 2021; Jiang et al., 2023). This also suggests that *P. lutea* under acute stress at 14°C was in a pre-bleaching stage. If low-temperature stress continues, then *P. lutea* might become bleached and die owing to apoptosis. However, if conditions are restored to a suitable temperature, *P. lutea* might recover from the pre-bleaching state.

TRAF2, related to the TNF signaling pathway, was upregulated in response to acute low-temperature stress. The TNF signaling pathway is pivotal in modulating immunity, inflammation, apoptosis, and cell proliferation and differentiation (Cho et al., 2003). Previous studies have shown that activation of the TNF signaling pathway mediated by TNF-α can trigger apoptosis and bleaching in corals (Cho et al., 2003). The TNF receptor ligand family (TNFRSF/TNFSF) is a central mediator of apoptosis (Quistad et al., 2014). Upon external stimulation, TNF binds to TNF receptors, initiating downstream signaling cascades that culminate in apoptosis (Quistad et al., 2014). This study indicates that under acute low-temperature stress, *P. lutea* induces apoptosis through the TNF signaling pathway. This could be an important mechanism of cold bleaching.

Excessive ER stress can precipitate apoptosis (Haas, 1994; Springer et al., 1999). Peptides undergo assembly, folding, and posttranslational modifications in the ER (Haas, 1994; Springer et al., 1999). Only properly folded proteins enter the Golgi apparatus from the ER via transport vesicles. ER stress, induced by the accumulation of misfolded proteins, triggering the unfolded protein response (Haas, 1994; Springer et al., 1999). Under acute low-temperature stress, increased *EIF2S1* and *NRF2* expression potentially signals unfolded protein response transmission to the nucleus. The final misfolded proteins are retro-translocated to the cytoplasm and undergo ubiquitin-mediated proteasomal degradation via the ER-associated degradation process (Maor-Landaw et al., 2014). Heat shock proteins and ubiquitin-coupling enzyme E2 play important roles in this process (Maor-Landaw et al., 2014). The genes involved in ER-associated degradation and ubiquitin-mediated hydrolysis are upregulated. This suggests that *P. lutea* experiences ER stress and uses these mechanisms to process the aggregated misfolded proteins in response to acute low-temperature stress. However, if these stressors are not relieved, then apoptosis is triggered.

Under chronic low-temperature stress, *TNFR2*, *HSP90*, *Casp3*, and other genes remained unchanged or downregulated, indicating that the cells did not enter the apoptosis stage. Therefore, acute low-temperature stress presents a heightened threat to coral holobionts compared to chronic low-temperature stress.

5 Conclusion

Low-temperature stress impedes the potential of relatively high-latitude coral reefs to function as refuges for coral. In this study, the response mechanisms of coral holobionts to low-temperature stress was explored. Our study indicates that *P. lutea* from high-latitude coral reefs in the South China Sea manifests photophysiological and gene expression responses to both acute and chronic low-temperature stress. Low-temperature stress resulted in a significant decrease in the *Fv/Fm* of Symbiodiniaceae, indicating the inhibition of PSII functioning, which might have contributed to energy deprivation in both Symbiodiniaceae and coral hosts. During low-temperature stress, calcifications-related genes were downregulated, possibly because of the reduced investment of energy-scarce coral hosts in calcification. Additionally, the acute stress group displayed a markedly diminished *Fv/Fm* relative to the chronic stress group, potentially catalyzing coral bleaching and mortality through induced cell apoptosis, thereby constituting a more severe threat to coral holobionts.

Data availability statement

The original contributions presented in the study are publicly available. This data can be found here: https://www.ncbi.nlm.nih.gov, BioProject: PRJNA1026091.

Ethics statement

Ethical approval was not required for the study involving animals in accordance with the local legislation and institutional requirements because no subjects requiring ethical clearance were involved.

Author contributions

XW: Data curation, Formal analysis, Validation, Visualization, Writing – original draft. KY: Conceptualization, Funding acquisition, Methodology, Writing – review & editing. ZQ: Conceptualization, Investigation, Methodology, Supervision, Writing – review & editing. SC: Software, Validation, Visualization, Writing – review & editing. NP: Software, Validation, Visualization, Writing – review & editing. ML: Software, Validation, Visualization, Writing – review & editing.

Funding

The author(s) declare financial support was received for the research, authorship, and/or publication of this article. This research was supported by the National Natural Science Foundation of China (42090041, 42030502, 42206157), the Natural Science Foundation of Guangxi Province (2022GXNSFBA035449), and the Guangxi Scientific Projects (nos. AD17129063 and AA17204074).

Conflict of interest

The authors declare that the research was conducted in the absence of any commercial or financial relationships that could be construed as a potential conflict of interest.

Publisher's note

All claims expressed in this article are solely those of the authors and do not necessarily represent those of their affiliated organizations, or those of the publisher, the editors and the reviewers. Any product that may be evaluated in this article, or claim that may be made by its manufacturer, is not guaranteed or endorsed by the publisher.

Supplementary material

The Supplementary Material for this article can be found online at: https://www.frontiersin.org/articles/10.3389/fmars.2024.1321865/full#supplementary-material

References

Beger, M., Sommer, B., Harrison, P. L., Smith, S. A. D., and Pandolfi, J. M. (2014). Conserving potential coral reef refuges at high latitudes. *Diversity Distributions* 20, 245–257. doi: 10.1111/ddi.12140

Bertucci, A., Moya, A., Tambutté, S., Allemand, D., Supuran, C. T., and Zoccola, D. (2013). Carbonic anhydrases in anthozoan corals—A review. *Bioorganic Medicinal Chem.* 21, 1437–1450. doi: 10.1016/j.bmc.2012.10.024

Broun, M., Gee, L., Reinhardt, B., and Bode, H. R. (2005). Formation of the head organizer in hydra involves the canonical Wnt pathway. *Development* 132, 2907–2916. doi: 10.1242/dev.01848

Burlacot, A., and Peltier, G. (2023). Energy crosstalk between photosynthesis and the algal CO2-concentrating mechanisms. *Trends Plant Sci.* 28 (7), 795–807. doi: 10.1016/j.tplants.2023.03.018

Büchel, C., and Wilhelm, C. (1993). *In vivo* analysis of slow chlorophyll fluorescence induction kinetics in algae: progress, problems and perspextives. *Photochem. Photobiol.* 58, 137–148. doi: 10.1111/j.1751-1097.1993.tb04915.x

Camp, E. F., Schoepf, V., Mumby, P. J., Hardtke, L. A., Rodolfo-Metalpa, R., Smith, D. J., et al. (2018). The future of coral reefs subject to rapid climate change: lessons from natural extreme environments. *Front. Mar. Sci.* 5. doi: 10.3389/fmars.2018.00004

Carpenter, K. E., Abrar, M., Aeby, G., Aronson, R. B., Banks, S., Bruckner, A., et al. (2008). One-third of reef-building corals face elevated extinction risk from climate change and local impacts. *Science* 321, 560–563. doi: 10.1126/science.1159196

Carrigan, A. D., and Puotinen, M. (2014). Tropical cyclone cooling combats region-wide coral bleaching. *Global Change Biol.* 20, 1604–1613. doi: 10.1111/gcb.12541

Cassaignau, A. M. E., Cabrita, L. D., and Christodoulou, J. (2020). How does the ribosome fold the proteome? *Annu. Rev. Biochem.* 89 (1), 389–415. doi: 10.1146/annurev-biochem-062917-012226

Chen, B., Yu, K., Liang, J., Huang, W., Wang, G., Su, H., et al. (2019). Latitudinal variation in the molecular diversity and community composition of Symbiodiniaceae in coral from the South China Sea. *Front. Microbiol.* 10. doi: 10.3389/fmicb.2019.01278

Chen, T., Li, S., Yu, K., Zheng, Z., Wang, L., and Chen, T. (2013). Increasing temperature anomalies reduce coral growth in the Weizhou Island, northern South China Sea. *Estuarine Coast. Shelf Sci.* 130, 121–126. doi: 10.1016/j.ecss.2013.05.009

Chen, T., Yu, K., Shi, Q., Li, S., Price, G. J., Wang, R., et al. (2009). Twenty-five years of change in scleractinian coral communities of Daya Bay (northern South China Sea) and its response to the 2008 AD extreme cold climate event. *Chin. Sci. Bulletin.* 54, 2107–2117. doi: 10.1007/s11434-009-0007-8

Chen, S., Zhou, Y., Chen, Y., and Gu, J. (2018). fastp : an ultra-fast all-in-one FASTQ preprocessor. *Bioinformatics* 34 (17), i884–i890. doi: 10.1093/bioinformatics/bty560

Cho, K.-H., Shin, S.-Y., Lee, H.-W., and Wolkenhauer, O. (2003). Investigations into the analysis and modeling of the TNFα-mediated NF-κB-signaling pathway. *Genome Res.* 13, 2413–2422. doi: 10.1101/gr.1195703

DeSalvo, M. K., Estrada, A., Sunagawa, S., and Medina, S. M. (2012). Transcriptomic responses to darkness stress point to common coral bleaching mechanisms. *Coral Reefs* 31, 215–228. doi: 10.1007/s00338-011-0833-4

Desalvo, M. K., Voolstra, C. R., Sunagawa, S., Schwarz, J. A., Stillman, J. H., Coffroth, M. A., et al. (2008). Differential gene expression during thermal stress and bleaching in the Caribbean coral Montastraea faveolata. *Mol. Ecol.* 17, 3952–3971. doi: 10.1111/j.1365-294X.2008.03879.x

Dubois, F., Tercé-Laforgue, T., Gonzalez-Moro, M.-B., Estavillo, J.-M., Sangwan, R., Gallais, A., et al. (2003). Glutamate dehydrogenase in plants: is there a new story for an old enzyme? *Plant Physiol. Biochem.* 41 (6), 565–576. doi: 10.1016/S0981-9428(03)00075-5

Duffy, D. J., Plickert, G., Kuenzel, T., Tilmann, W., and Frank, U. (2010). Wnt signaling promotes oral but suppresses aboral structures in Hydractinia metamorphosis and regeneration. *Development* 137, 3057–3066. doi: 10.1242/dev.046631

Evensen, N. R., Fine, M., Perna, G., Voolstra, C. R., and Barshis, D. J. (2021). Remarkably high and consistent tolerance of a Red Sea coral to acute and chronic thermal stress exposures. *Limnol. Oceanogr.* 66, 1718–1729. doi: 10.1002/lno.11715

Furla, P., Allemand, D., and Orsenigo, M.-N. (2000). Involvement of H+-ATPase and carbonic anhydrase in inorganic carbon uptake for endosymbiont photosynthesis. *Am. J. Physiology-Regulatory Integr. Comp. Physiol.* 278, R870–R881. doi: 10.1152/ajpregu.2000.278.4.R870

Green, R. H., Lowe, R. J., Buckley, M. L., Foster, T., and Gilmour, J. P. (2019). Physical mechanisms influencing localized patterns of temperature variability and coral bleaching within a system of reef atolls. *Coral Reefs* 38, 759–771. doi: 10.1007/s00338-019-01771-2

Greenstein, B. J., and Pandolfi, J. M. (2008). Escaping the heat: range shifts of reef coral taxa in coastal Western Australia. *Global Change Biol.* 14, 513–528. doi: 10.1111/j.1365-2486.2007.01506.x

Guder, C., Pinho, S., Nacak, T. G., Schmidt, H. A., Hobmayer, B., Niehrs, C., et al. (2006). An ancient Wnt-Dickkopf antagonism in Hydra. *Development* 133, 901–911. doi: 10.1242/dev.02265

Haas, I. G. (1994). BiP (GRP78), an essential hsp70 resident protein in the endoplasmic reticulum. *Experientia* 50, 1012–1020. doi: 10.1007/BF01923455

Hatcher, B. G. (1988). Coral reef primary productivity: A beggar's banquet. *Trends Ecol. Evolution* 3, 106–111. doi: 10.1016/0169-5347(88)90117-6

Hemond, E. M., Kaluziak, S. T., and Vollmer, S. V. (2014). The genetics of colony form and function in Caribbean Acropora corals. *BMC Genomics* 15, 1133. doi: 10.1186/1471-2164-15-1133

Heron, S. F., Maynard, J. A., van Hooidonk, R., and Eakin, C. M. (2016). Warming trends and bleaching stress of the world's coral reefs 1985–2012. *Sci. Rep.* 6, 38402. doi: 10.1038/srep38402

Higuchi, T., Agostini, S., Casareto, B. E., Suzuki, Y., and Yuyama, I. (2015). The northern limit of corals of the genus Acropora in temperate zones is determined by their resilience to cold bleaching. *Sci. Rep.* 5, 18467. doi: 10.1038/srep18467

Hopkinson, B. M., Tansik, A. L., and Fitt, W. K. (2015). Internal carbonic anhydrase activity in the tissue of scleractinian corals is sufficient to support proposed roles in photosynthesis and calcification. *J. Exp. Biol.* 218, 2039–2048. doi: 10.1242/jeb.118182

Huang, W., Yang, E., Yu, K., Meng, L., Wang, Y., Liang, J., et al. (2022). Lower cold tolerance of tropical Porites lutea is possibly detrimental to its migration to relatively high latitude refuges in the South China Sea. *Mol. Ecol.* 31, 5339–5355. doi: 10.1111/mec.16662

Hughes, T. P., Kerry, J. T., Álvarez-Noriega, M., Álvarez-Romero, J. G., Anderson, K. D., Baird, A. H., et al. (2017). Global warming and recurrent mass bleaching of corals. *Nature* 543, 373–377. doi: 10.1038/nature21707

Jiang, L., Liu, C.-Y., Cui, G., Huang, L.-T., Yu, X.-L., Sun, Y.-F., et al. (2023). Rapid shifts in thermal reaction norms and tolerance of brooded coral larvae following parental heat acclimation. *Mol. Ecol.* 32 (5), 1098–1116. doi: 10.1111/mec.16826

Jones, R. J., Hoegh-Guldberg, O., Larkum, A. W. D., and Schreiber, U. (1998). Temperature-induced bleaching of corals begins with impairment of the CO_2 fixation mechanism in zooxanthellae. *Plant Cell Environment* 21, 1219–1230. doi: 10.1046/j.1365-3040.1998.00345.x

Joshi, R., Karan, R., Singla-Pareek, S. L., and Pareek, A. (2016). Ectopic expression of Pokkali phosphoglycerate kinase-2 (OsPGK2-P) improves yield in tobacco plants under salinity stress. *Plant Cell Rep.* 35, 27–41. doi: 10.1007/s00299-015-1864-z

Karnauskas, K. B. (2020). Physical diagnosis of the 2016 great barrier reef bleaching event. *Geophysical Res. Letters* 47, e2019GL086177. doi: 10.1029/2019GL086177

Keshavmurthy, S., Beals, M., Hsieh, H. J., Choi, K. S., and Chen, C. A. (2021). Physiological plasticity of corals to temperature stress in marginal coral communities. *Sci. Total Environment* 758, 143628. doi: 10.1016/j.scitotenv.2020.143628

Kim, D., Langmead, B., and Salzberg, S. L. (2015). HISAT: a fast spliced aligner with low memory requirements. *Nat. Methods* 12 (4), 357–360. doi: 10.1038/nmeth.3317

Kvitt, H., Rosenfeld, H., and Tchernov, D. (2016). The regulation of thermal stress induced apoptosis in corals reveals high similarities in gene expression and function to higher animals. *Sci. Rep.* 6, 30359. doi: 10.1038/srep30359

Leinbach, S. E., Speare, K. E., Rossin, A. M., Holstein, D. M., and Strader, M. E. (2021). Energetic and reproductive costs of coral recovery in divergent bleaching responses. *Sci. Rep.* 11, 23546. doi: 10.1038/s41598-021-02807-w

Li, B., and Dewey, C. N. (2011). RSEM: accurate transcript quantification from RNA-Seq data with or without a reference genome. *BMC Bioinf.* 12 (1), 323. doi: 10.1186/1471-2105-12-323

Liu, S., Liu, F., Jia, H., Yan, Y., Wang, H., Guo, X., et al. (2016). A glutathione S-transferase gene associated with antioxidant properties isolated from Apis cerana cerana. *Sci. Nature* 103 (5), 43. doi: 10.1007/s00114-016-1362-3

Love, M. I., Huber, W., and Anders, S. (2014). Moderated estimation of fold change and dispersion for RNA-seq data with DESeq2. *Genome Biol.* 15 (12), 550. doi: 10.1186/s13059-014-0550-8

Mailloux, R. J., and Harper, M.-E. (2011). Uncoupling proteins and the control of mitochondrial reactive oxygen species production. *Free Radical Biol. Med.* 51, 1106–1115. doi: 10.1016/j.freeradbiomed.2011.06.022

Majerova, E., Carey, F. C., Drury, C., and Gates, R. D. (2021). Preconditioning improves bleaching tolerance in the reef-building coral Pocillopora acuta through modulations in the programmed cell death pathways. *Mol. Ecol.* 30, 3560–3574. doi: 10.1111/mec.15988

Mannervik, B. (1985). Glutathione peroxidase. *Methods Enzymol. Acad. Press* 113, 490–495. doi: 10.1016/S0076-6879(85)13063-6

Maor-Landaw, K., Karako-Lampert, S., Ben-Asher, H. W., Goffredo, S., Falini, G., Dubinsky, Z., et al. (2014). Gene expression profiles during short-term heat stress in the red sea coral Stylophora pistillata. *Global Change Biol.* 20, 3026–3035. doi: 10.1111/gcb.12592

Marangoni, L., Rottier, C., and Ferrier-Pagès, C. (2021). Symbiont regulation in Stylophora pistillata during cold stress: an acclimation mechanism against oxidative stress and severe bleaching. *J. Exp. Biol.* 224, jeb235275. doi: 10.1242/jeb.235275

Mass, T., Putnam, H. M., Drake, J. L., Drake, J. L., Zelzion, E., Gates, R. D., et al. (2016). Temporal and spatial expression patterns of biomineralization proteins during early development in the stony coral Pocillopora damicornis. *Proc. R. Soc. B: Biol. Sci.* 283, 20160322. doi: 10.1098/rspb.2016.0322

McGowan, H., and Theobald, A. (2017). ENSO weather and coral bleaching on the great barrier reef, Australia. *Geophysical Res. Lett.* 44, 10,601–610,607. doi: 10.1002/2017GL074877

Mia, O. H., Kenneth, R. N. A., and Sean, R. C. (2006). Energetic cost of photoinhibition in corals. *Mar. Ecol. Prog. Series* 313, 1–12. doi: 10.3354/meps313001

Moberg, F., and Folke, C. (1999). Ecological goods and services of coral reef ecosystems. *Ecol. Economics* 29, 215–233. doi: 10.1016/S0921-8009(99)00009-9

Pertea, M., Pertea, G. M., Antonescu, C. M., Chang, T.-C., Mendell, J. T., and Salzberg, S. L. (2015). StringTie enables improved reconstruction of a transcriptome from RNA-seq reads. *Nat. Biotechnol.* 33 (3), 290–295. doi: 10.1038/nbt.3122

Plickert, G., Jacoby, V., Frank, U., Müller, W. A., and Mokady, O. (2006). Wnt signaling in hydroid development: Formation of the primary body axis in embryogenesis and its subsequent patterning. *Dev. Biol.* 298, 368–378. doi: 10.1016/j.ydbio.2006.06.043

Quistad, S. D., Stotland, A., Barott, K. L., Smurthwaite, C. A., Hilton, B. J., Grasis, J. A., et al. (2014). Evolution of TNF-induced apoptosis reveals 550 My of functional conservation. *Proc. Natl. Acad. Sci.* 111, 9567–9572. doi: 10.1073/pnas.1405912111

Ralph, P. J., Gademann, R., Larkum, A. W. D., and Schreiber, U. (1999). *In situ* underwater measurements of photosynthetic activity of coral zooxanthellae and other reef-dwelling dinoflagellate endosymbionts. *Mar. Ecol. Prog. Series* 180, 139–147. doi: 10.3354/meps180139

Ravelo, S. F., Posadas, N., and Conaco, C. (2022). Transcriptome analysis reveals the expressed gene complement and acute thermal stress response of acropora digitifera endosymbionts. *Front. Mar. Sci.* 9. doi: 10.3389/fmars.2022.758579

Rayson, M. D., Ivey, G. N., Jones, N. L., and Fringer, O. B. (2018). Resolving high-frequency internal waves generated at an isolated coral atoll using an unstructured grid ocean model. *Ocean Modelling* 122, 67–84. doi: 10.1016/j.ocemod.2017.12.007

Rayson, M. D., Ivey, G. N., Jones, N. L., Lowe, R. J., Wake, G. W., and McConochie, J. D. (2015). Near-inertial ocean response to tropical cyclone forcing on the Australian North-West Shelf. *J. Geophysical Res.: Oceans* 120, 7722–7751. doi: 10.1002/2015JC010868

Riegl, B., Glynn, P. W., Banks, S., Keith, I., Rivera, F., and Vera-Zambrano, M. (2019). Heat attenuation and nutrient delivery by localized upwelling avoided coral bleaching mortality in northern Galapagos during 2015/2016 ENSO. *Coral Reefs* 38, 773–785. doi: 10.1007/s00338-019-01787-8

Rinkevich, B. (1996). Do reproduction and regeneration in damaged corals compete for energy allocation? *Mar. Ecol. Prog. Series* 143, 297–302. doi: 10.3354/meps143297

Ritz, C., Baty, F., Streibig, J. C., and Gerhard, D. (2016). Dose-response analysis using R. *PloS One* 10, e0146021. doi: 10.1371/journal.pone.0146021

Rosa-Téllez, S., Anoman, A. D., Flores-Tornero, M., Toujani, W., Alseek, S., Fernie, A. R., et al. (2017). Phosphoglycerate kinases are co-regulated to adjust metabolism and to optimize growth. *Plant Physiol.* 176, 1182–1198. doi: 10.1104/pp.17.01227

Roth, M. S., Goericke, R., and Deheyn, D. D. (2012). Cold induces acute stress but heat is ultimately more deleterious for the reef-building coral Acropora yongei. *Sci. Rep.* 2, 240. doi: 10.1038/srep00240

Schlegel, R. W., Darmaraki, S., Benthuysen, J. A., Filbee-Dexter, K., and Oliver, E. C. J. (2021). Marine cold-spells. *Prog. Oceanogr.* 198, 102684. doi: 10.1016/j.pocean.2021.102684

Schlegel, R. W., Oliver, E. C. J., Wernberg, T., and Smit, A. J. (2017). Nearshore and offshore co-occurrence of marine heatwaves and cold-spells. *Prog. Oceanogr.* 151, 189–205. doi: 10.1016/j.pocean.2017.01.004

Shao, Y., Li, C., Zhang, W., Duan, X., Li, Y., Jin, C., et al. (2016). Molecular cloning and characterization of four caspases members in Apostichopus japonicus. *Fish Shellfish Immunol.* 55, 203–211. doi: 10.1016/j.fsi.2016.05.039

Singh, M., Singh, V. P., and Prasad, S. M. (2016). Responses of photosynthesis, nitrogen and proline metabolism to salinity stress in Solanum lycopersicum under different levels of nitrogen supplementation. *Plant Physiol. Biochem.* 109, 72–83. doi: 10.1016/j.plaphy.2016.08.021

Slocinska, M., Barylski, J., and Jarmuszkiewicz, W. (2016). Uncoupling proteins of invertebrates: A review. *IUBMB Life.* 68, 691–699. doi: 10.1016/j.fsi.2016.05.039

Slocińska, M., Rosinski, G., and Jarmuszkiewicz, W. (2016). Activation of mitochondrial uncoupling protein 4 and ATP-sensitive potassium channel cumulatively decreases superoxide production in insect mitochondria. *Protein Pept. Letters* 23, 63–68. doi: 10.1002/iub.1535

Sokolova, I. M. (2013). Energy-limited tolerance to stress as a conceptual framework to integrate the effects of multiple stressors. *Integr. Comp. Biol.* 53, 597–608. doi: 10.1093/icb/ict028

Sommer, B., Beger, M., Harrison, P. L., Babcock, R. C., and Pandolfi, J. M. (2018). Differential response to abiotic stress controls species distributions at biogeographic transition zones. *Ecography* 41, 478–490. doi: 10.1111/ecog.02986

Southward, A. J., Hawkins, S. J., and Burrows, M. T. (1995). Seventy years' observations of changes in distribution and abundance of zooplankton and intertidal organisms in the western English Channel in relation to rising sea temperature. *J. Thermal Biol.* 20, 127–155. doi: 10.1016/0306-4565(94)00043-I

Springer, S., Spang, A., and Schekman, R. (1999). A primer on vesicle budding. *Cell* 97, 145–148. doi: 10.1016/S0092-8674(00)80722-9

Tambutté, S., Tambutté, E., Zoccola, D., Caminiti, N., Lotto, S., Moya, A., et al. (2007). Characterization and role of carbonic anhydrase in the calcification process of the azooxanthellate coral Tubastrea aurea. *Mar. Biol.* 151, 71–83. doi: 10.1007/s00227-006-0452-8

Tang, J., Ni, X., Wen, J., Wang, L., Luo, J., and Zhou, Z. (2020). Increased Ammonium Assimilation Activity in the Scleractinian Coral Pocillopora damicornis but Not Its Symbiont After Acute Heat Stress. *Front. Mar. Sci.* 7. doi: 10.3389/fmars.2020.565068

Thornhill, D. J., Kemp, D. W., Bruns, B. U., Fitt, W. K., and Schmidt, G. W. (2008). Correspondence between cold tolerance and temperate biogeography in a western atlantic symbiodinium(dinophyta) lineagei. *J. Phycol.* 44, 1126–1135. doi: 10.1111/j.1529-8817.2008.00567.x

Tracey, S., William, C. D., and Ove, H.-G. (2003). Photosynthetic responses of the coral Montipora digitata to cold temperature stress. *Mar. Ecol. Prog. Series* 248, 85–97. doi: 10.3354/meps248085

Tuckett, C. A., and Wernberg, T. (2018). High latitude corals tolerate severe cold spell. *Front. Mar. Sci.* 5. doi: 10.3389/fmars.2018.00014

Tummers, B., and Green, D. R. (2021). The evolution of regulated cell death pathways in animals and their evasion by pathogens. *Physiol. Rev.* 102, 411–454. doi: 10.1152/physrev.00002.2021

Tunala, L. P., Tâmega, F. T. S., Duarte, H. M., and Coutinho, R. (2019). Stress factors in the photobiology of the reef coral Siderastrea stellata. *J. Exp. Mar. Biol. Ecol.* 519, 151188. doi: 10.1016/j.jembe.2019.151188

Wuitchik, D. M., Almanzar, A., Benson, B. E., Brennan, S., Chavez, J. D., Liesegang, M. B., et al. (2021). Characterizing environmental stress responses of aposymbiotic Astrangia poculata to divergent thermal challenges. *Mol. Ecol.* 30 (20), 5064–5079. doi: 10.1111/mec.16108

Xie, C., Mao, X., Huang, J., Ding, Y., Wu, J., Dong, S., et al. (2011). KOBAS 2.0: a web server for annotation and identification of enriched pathways and diseases. *Nucleic Acids Res.* 39 (suppl_2), W316–W322. doi: 10.1093/nar/gkr483

Yu, X., Huang, B., Zhou, Z., Tang, J., and Yu, Y. (2017). Involvement of caspase3 in the acute stress response to high temperature and elevated ammonium in stony coral Pocillopora damicornis. *Gene* 637, 108–114. doi: 10.1016/j.gene.2017.09.040

Yu, K., and Jiang, M. (2004). Latest forty two years' sea surface temperature change of Weizhou Island and its influence on coral reef ecosystem. *Chin. J. Appl. Ecol.* 2004 (03), 506–510. doi: 10.13287/j.1001−9332.2004.0110

Yu, W., Wang, W., Yu, K., Wang, Y., Huang, X., Huang, R., et al. (2019). Rapid decline of a relatively high latitude coral assemblage at Weizhou Island, northern South China Sea. *Biodiversity Conserv.* 28, 3925–3949. doi: 10.1007/s10531-019-01858-w

Yu, K.-F., Zhao, J.-X., Liu, T.-S., Wei, G.-J., Wang, P.-X., and Collerson, K. D. (2004). High-frequency winter cooling and reef coral mortality during the Holocene climatic optimum. *Earth Planetary Sci. Letters* 224, 143–155. doi: 10.1016/j.epsl.2004.04.036

Zhang, Y., Chen, R.-W., Liu, X., Zhu, M., Li, Z., Wang, A., et al. (2022). Oxidative stress, apoptosis, and transcriptional responses in Acropora microphthalma under simulated diving activities. *Mar. pollut. Bulletin.* 183, 114084. doi: 10.1016/j.marpolbul.2022.114084

Zhang, Y., and Fernie, A. R. (2018). On the role of the tricarboxylic acid cycle in plant productivity. *J. Integr. Plant Biol.* 60 (12), 1199–1216. doi: 10.1111/jipb.12690

Zoccola, D., Moya, A., Béranger, G. E., Tambutté, E., Allemand, D., Carle, G. F., et al. (2009). Specific expression of BMP2/4 ortholog in biomineralizing tissues of corals and action on mouse BMP receptor. *Mar. Biotechnol.* 11, 260–269. doi: 10.1007/s10126-008-9141-6

frontiers | Frontiers in Physiology

TYPE Original Research
PUBLISHED 21 February 2024
DOI 10.3389/fphys.2024.1346045

OPEN ACCESS

EDITED BY
Shengming Sun,
Shanghai Ocean University, China

REVIEWED BY
Adán Guillermo Jordán-Garza,
Universidad Veracruzana, Mexico
Liliana Rojo,
Centro de Investigación Biológica del Noroeste (CIBNOR), Mexico

*CORRESPONDENCE
Kaho H. Tisthammer,
kahot@hawaii.edu

RECEIVED 28 November 2023
ACCEPTED 05 February 2024
PUBLISHED 21 February 2024

CITATION
Tisthammer KH, Martinez JA, Downs CA and Richmond RH (2024), Differential molecular biomarker expression in corals over a gradient of water quality stressors in Maunalua Bay, Hawaii.
Front. Physiol. 15:1346045.
doi: 10.3389/fphys.2024.1346045

Differential molecular biomarker expression in corals over a gradient of water quality stressors in Maunalua Bay, Hawaii

Kaho H. Tisthammer[1]*, Jonathan A. Martinez[2], Craig A. Downs[3] and Robert H. Richmond[1]

[1]Kewalo Marine Laboratory, University of Hawaii at Manoa, Honolulu, HI, United States, [2]U.S. Fish and Wildlife Service, Albuquerque, NM, United States, [3]Haereticus Environmental Laboratory, Clifford, VA, United States

Coral reefs globally face unprecedented challenges from anthropogenic stressors, necessitating innovative approaches for effective assessment and management. Molecular biomarkers, particularly those related to protein expressions, provide a promising avenue for diagnosing coral health at the cellular level. This study employed enzyme-linked immunosorbent assays to evaluate stress responses in the coral *Porites lobata* along an environmental gradient in Maunalua Bay, Hawaii. The results revealed distinct protein expression patterns correlating with anthropogenic stressor levels across the bay. Some proteins, such as ubiquitin and Hsp70, emerged as sensitive biomarkers, displaying a linear decrease in response along the environmental gradient, emphasizing their potential as indicators of stress. Our findings highlighted the feasibility of using protein biomarkers for real-time assessment of coral health and the identification of stressors. The identified biomarkers can aid in establishing stress thresholds and evaluating the efficacy of management interventions. Additionally, we assessed sediment and water quality from the inshore areas in the bay and identified organic contaminants, including polycyclic aromatic hydrocarbons and pesticides, in bay sediments and waters.

KEYWORDS

corals, coral reefs, biomarkers, protein expression, stress responses, environmental gradients, water quality

1 Introduction

Coral reefs worldwide have been severely impacted by anthropogenic activities, ranging from global level stressors of climate change to various local stressors, including land-based sources of pollution resulting in reduced water quality, overfishing, and disease outbreaks (Wilkinson, 2004; Richmond and Wolanski, 2011; Hoegh-Guldberg, 2014; Birkeland, 2015). For coral reefs in Hawaii, reduced water quality is one of the most important local threats. As the health of coral reefs continues to deteriorate, we are facing the pressing need for effective and informative assessment tools for both diagnosing the effects of specific stressors and applying such knowledge to improve coral health.

Ecological approaches to environmental assessment have traditionally focused on mortality as a metric to assess coral health, such as coral cover reductions, percentage of colony bleaching and/or mortality, and loss of individuals or species. Mortality is not an adequate metric of health or stress level, as it leaves little room for management or

mitigation interventions. Additionally, ecological parameters can only provide correlation between putative stressors and effects, rather than actual causation. The application of molecular tools to assess sublethal stress levels in corals has increasingly gained attention and is being more broadly applied to identify the "smoking guns" in multi-stressor situations and provide metrics for evaluating the effectiveness of management interventions over periods of weeks to months, *versus* years to decades (Parkinson et al., 2020).

Molecular biomarkers, such as changes in protein expressions, enzymatic activity levels, gene expressions, and DNA damage, have been successfully developed and applied to capture sub-lethal stress levels in corals (e.g., Downs et al., 2005; Seneca et al., 2009; Kenkel et al., 2011; Richmond, 2011; Rougée, 2011; Edge et al., 2013; Seveso et al., 2013; Seneca and Palumbi, 2015; Murphy and Richmond, 2016). Since proteins directly affect organismal physiology and hence, represent functional adaptations (Feder and Walser, 2005; Tomanek, 2011), protein biomarkers are especially effective tools for assessing the sub-lethal stress responses in organisms. For example, following the ship grounding in Yap, Downs et al. (2006) conducted a field study to assess damage in corals using protein expressions in areas not visibly oiled and showed that elevated physiological stress, such as oxidative stress response and xenobiotic response, along with the presence of Benzo(a)pyrene-7,8-dihydrodiol-9,10-epoxide (BPDE) adducted proteins, provided the evidence for oil exposure, relative to corals from a reference site.

Working with corals, which are non-model organisms, is challenging and the field of coral molecular biomarker analysis (ecotoxicology) is still at a relatively early stage. No coral-specific antibodies are available commercially to analyze their protein expressions. However, previous studies suggest many key biomarker proteins may be highly conserved across metazoans (e.g., Barshis et al., 2010; Seveso et al., 2016), and therefore, in search of usable antibodies, commercially available antibodies (mostly made from vertebrates) were explored for application in corals by aligning protein sequences translated from the available coral transcriptomes, with the antibody sequences, selecting potentially compatible antibodies, and testing with extracted coral proteins. The initial protein studies, including the one presented here, were performed using enzyme-linked immunosorbent assays (ELISA) and Western blotting (e.g., Downs et al., 2006; 2012), targeting single protein per assay based on the existing knowledge. As technology became more available and affordable, the omics approach opened the door to investigating cellular responses without *a priori* hypotheses, which has been especially beneficial for non-model organisms for which we have limited knowledge about cellular and molecular responses/pathways (Parkinson et al., 2020). The more traditional protein assays, such as ELISA and Western blotting, are still useful in screening initial response time, and in identifying response patterns and dosages, since little information is often available to accurately predict organismal response direction and timing when working with non-model organisms like corals.

Maunalua Bay in Oahu, Hawaii is an important area for marine recreation and ocean activities, which receives discharges from nine sub-watersheds. The historical changes both on land and in the coastal ocean have been documented (Wolanski et al., 2009): Notably, poor land-use practices have resulted in the bay receiving large quantities of terrigenous sediment and a variety of pollutants. The channelization and concrete lining of streams, and other human activities within the adjacent watersheds have caused extensive habitat degradation and loss, which has resulted in the loss of coastal resources, including fishes and corals (Wolanski et al., 2009; Storlazzi et al., 2010; Presto et al., 2012). A range of stakeholders including local businesses, fishers, homeowners, canoe paddlers, divers, and resource managers joined together to address coral reef health declines and requested support from the research community in determining options for mitigation and recovery, which motivated us and others to assess the state of coral health along with water quality in Maunalua Bay. The urbanization and coastal development in the bay have created steep environmental gradients of anthropogenic stressors from the nearshore towards offshore in the bay, which ironically provided an opportunity for examining the impacts of urbanization on coral reefs.

In this study of corals in Maunalua Bay, we assessed protein expressions of stress response-related proteins in the lobe coral, *Porites lobata*, collected along the existing environmental gradient (e.g., Presto et al., 2012) from the mouth of the bay towards offshore. Our study aimed to 1) determine differences in sub-lethal cellular stress levels that corals experienced across different environments, 2) reveal the potential causes underlying such molecular stress responses, and 3) identify molecular markers that can be used for management purposes. We also tested sediment and water quality from the inshore areas from the bay for the presence of organic toxicants using gas chromatography-mass spectrometry (GC-MS). Our results revealed key stressors of concern and candidate coral biomarkers for anthropogenic stress levels using the widely distributed, pan-Pacific coral species, *P. lobata*.

2 Materials and methods

2.1 Coral biomarker analysis

2.1.1 Coral collection

Porites lobata samples were collected from five locations along the existing environmental gradients in Maunalua Bay (Figure 1). We also selected a site away from coastal development and anthropogenic stressors as a reference site and sampled *P. lobata* from La Perouse Bay in Maui. At each site, 5–7 colonies of similar sizes with no apparent mortality or lesions were randomly selected, and small plugs (1 cm^2) were obtained using a metal coral punch and a hammer, and flash frozen immediately by placing them in liquid nitrogen. All locations were relatively shallow (2–6 m), and environmental conditions were well characterized from previous studies, with inshore sites experiencing higher turbidity and fluctuations of temperature and salinity (Wolanski et al., 2009; Storlazzi et al., 2010; Presto et al., 2012; Tisthammer et al., 2021). All frozen corals were transported to the Kewalo Marine Laboratory and kept in a—80°C freezer until processed.

2.1.2 Coral sample processing and ELISA

Samples were assayed following the methods from Downs (2005) and Downs et al. (2012). Briefly, the *P. lobata* nubbins were ground while frozen to a fine powder using liquid nitrogen, placed in microcentrifuge tubes along with 1,400 mL of a denaturing

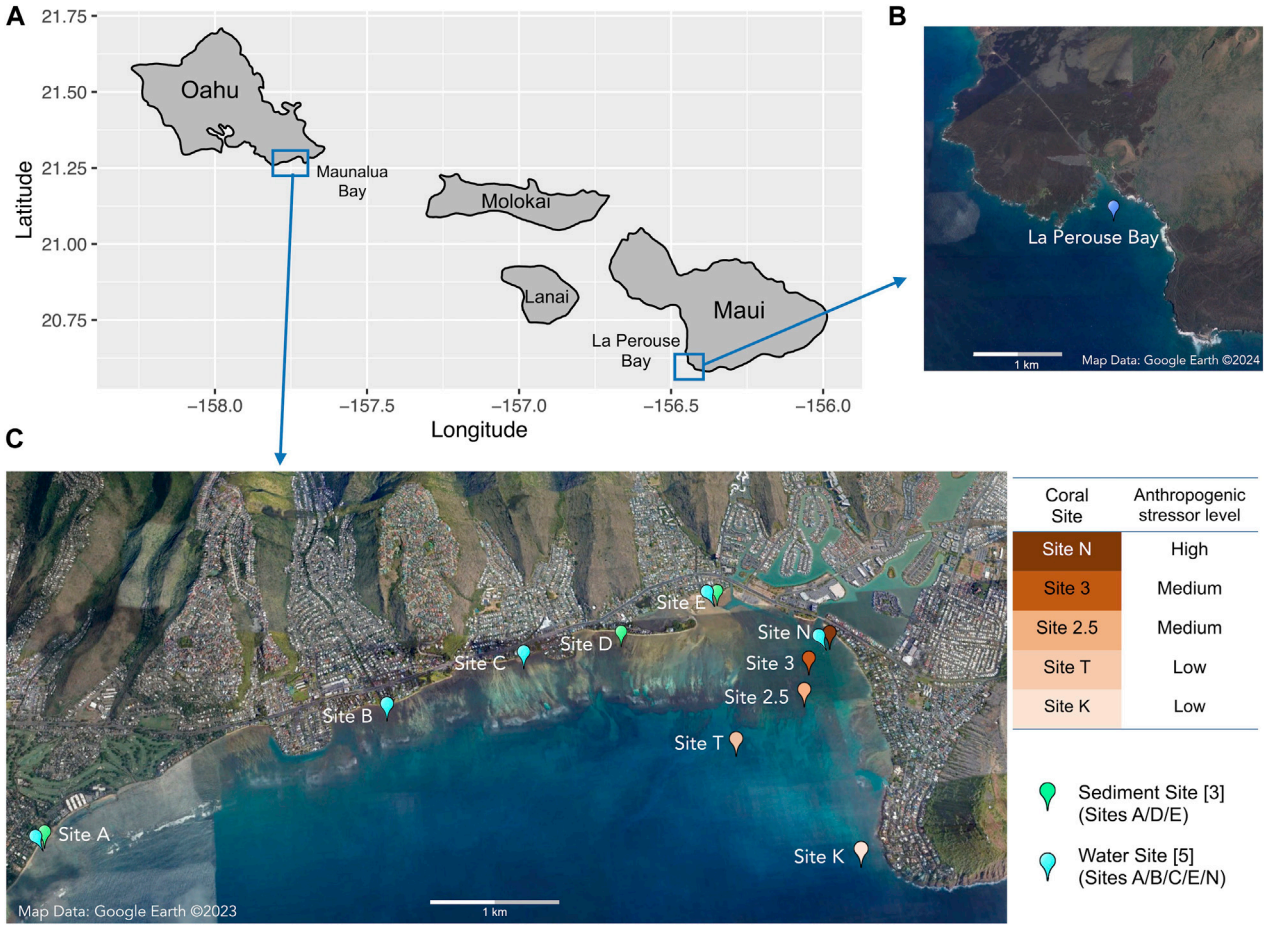

FIGURE 1
Map of **(A)** the Hawaiian Islands with sampling locations, **(B)** the reference site of Le Perouse Bay, Maui, and **(C)** the study site of Maunalua Bay, Oahu with sampling locations. Coral sampling sites are colored based on the anthropogenic stressor levels (water quality).

buffer (2% SDS, 50 mM Tris–HCl (pH 7.8), 15 mM dithiothreitol, 10 mM EDTA, 3% polyvinylpolypyrrolidone (wt/vol), 0.005 mM salicylic acid, 0.001% (v/v) dimethyl sulfoxide, 0.01 mM 4-(2-aminoethyl) benzenesulfonyl fluoride hydrochloride (AEBSF), 0.04 mM bestatin, 0.001 E–64, 2 mM phenylmethylsulfonyl fluoride, 2 mM benzamide, 5 mM a-amino-caproic acid, and 1 µg/100 mL pepstatin A). Samples were vortexed, heated at 93°C for 6 min, incubated at 25°C for 10 min, and centrifuged (13,500 g for 10 min). The middlephase supernatant was placed into a new tube, and protein concentrations were determined using the method of Ghosh et al. (1988).

We used the following 10 EnVirtue Biotechnologies, Inc. antibodies (generated in rabbits) that were specific to only the cnidarian animal targets, and not the coral's dinoflagellate symbiont: 1) anti-ubiquitin (AB-U100), 2) anti-cnidarian heat-shock protein 70 (Hsp70) (AB-H101-CDN), 3) anti-cnidarian heat-shock protein 60 (Hsp60) (AB-H100-IN), 4) anti-cnidarian glutathione-S-transferase (GST) (AB-G100-MU), 5) anti-cnidarian copper/zinc superoxide dismutase (SOD) (cytosolic isoform, lot 1517), 6) anti-cnidarian glutathione peroxidase (GPx) (AB-GPX-IN), 7) anti-MutY (lot 3217), 8) anti-multi-xenobiotic resistance protein (MXR) (ABC family of proteins; P-glycoprotein 140 and 160; AB-MDR160), 9) anti-cnidarian protoporphyrinogen oxidase IX (lot 1945), and 10) anti-cnidarian heme oxygenase I (lot 3114). All antibodies were mono-specific polyclonal antibodies made against a synthetic 8–12 amino-acid residue polypeptide that reflects a specific and unique region of the target protein, which included sequences of cnidarian (*Nematostella vectenesis*, *Orbicella annularis*, *Acropora millepora*, and *Porites astreoides*). One-dimensional SDS-PAGE and Western blotting were performed to optimize the separation of target proteins and validate the use of specific antibodies for *P. lobata* protein extracts following the methods of Downs (2005) and Downs et al. (2012). The sequences of the antibodies and the images of blotting of these antibodies used on coral samples are available in Downs and Downs (2007), Figures 1–4) and Downs et al. (2012), Figure 2 and Electronic Supplementary Material). Antibodies and samples were optimized and the level of precision for each ELISA was determined using an 8 9 6 9 4 factorial design (Crowther, 2000). A Beckman-Coulter Biomek 2000 Laboratory Automation Workstation using 384-well microplates was used to conduct the ELISA assays. All samples were assayed in triplicate, and an eight-point calibrant curve using a calibrant relevant to each antibody was plated in triplicate for each plate.

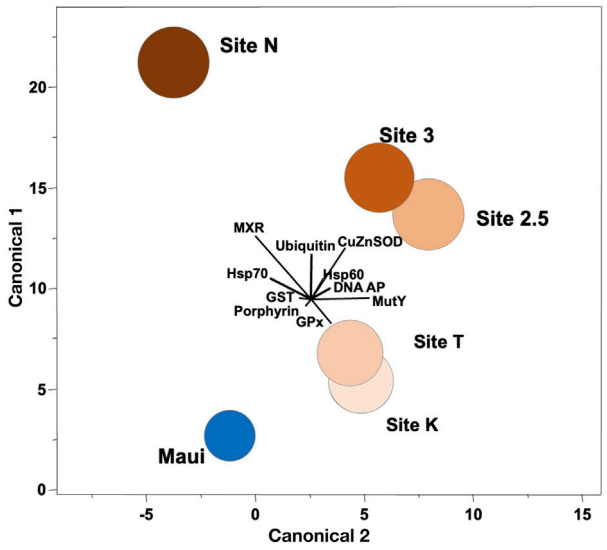

FIGURE 2
Canonical correlation of ten biomarkers in corals collected along the environmental gradient in Maunalua Bay. Colors of the sites correspond to those of Figure 1. Spheroids show the 95% confidence intervals around the distribution centroid of each site, and biplots show directions of original biomarker responses in canonical space.

2.1.3 DNA damage analysis

DNA abasic or apurinic/apyrimidinic lesions (DNA AP sites) were used as an indicator of genetic damage. DNA was isolated from coral tissues according to the manufacturer's instructions using the Dojindo pureDNA kit-Cell, Tissue (GK03-20; Dojindo Molecular Technologies) with one slight modification to address Maillard chemistry artifact. Coral tissues were added to the kit's lysis buffer containing 100 mg of polyvinylpolypyrrolidone (PVPP, Sigma-Aldrich Corporation, St. Louis, Missouri, United States). DNA purity was determined spectrophotometrically using the 260/280 nm method (Sambrook and Russel, 2001). The DNA concentration was measured using an Invitrogen/Molecular Probes Quant-iT™ DNA Assay Kit, Broad Range (catalog # Q33130; Life Technologies Corporation) using a Bio-Tek FL800 fluorescent microplate reader (BioTeck Industries, Incorporated, Winooski, Vermont, United States). DNA AP (abasic site) sites were quantified using the Dojindo DNA Damage Quantification Kit-AP Site Counting (catalog # DK-02-10; Dojindo Molecular Technologies, Inc.) and conducted according to the manufacturer's instructions.

2.1.4 Data analysis

The results from ELISA and DNA AP sites were tested for normality using the Kolmogorov–Smirnov test (with Lilliefors' correction) and for equal variance using the Levene Median test. When the data were normally distributed and homogeneous, a one-way analysis of variance (ANOVA) was employed. When data did not meet the homogeneity of variances requirement for one-way ANOVA, a Kruskal-Wallis One-Way Analysis of Variance on Ranks (Kruskal-Wallis H test) was used. When significant differences were found among treatment means, we used Tukey–Kramer Honestly Significant Difference (Tukey-HSD) test for the markers that met the parametric test assumptions and Dunn's *post hoc* test for the rest, and applied the Holm-Sidak method as an exact alpha-level test to determine differences between pairwise populations (Holm, 1979; Sokal and Rohlf, 1995). Statistical significance was defined as p-value < 0.05. Correlation analysis was conducted using the distance from the mouth of the bay (21°16.878′, −157°42.688′) and protein expression levels using Pearson's or Spearman's correlation test. We used canonical correlation analysis (CCA) as a heuristic tool to illustrate how biomarkers could be used to discriminate among populations/sites. CCA reveals the basic relationships between two matrices, in our case those of the six sites (Sites N, 3, 2.5, K, T and Maui as a categorical location variable) and the biomarker data (total of 10 biomarkers, excluding heme oxygenase as no data for the reference site were collected). The CCA provided an objective statistical tool for determining if corals from the studied sites were significantly different from one another using sets of cellular biomarkers that are indicative of a cellular process and if so, which biomarkers contributed to those differences. This analysis required combining data from all six populations into one matrix, which we did by expressing biomarker responses in a given population as a proportion of their mean levels.

2.2 Sediment chemistry analysis (3 sites)

2.2.1 Sample collection

Sediments were sampled at three locations, a) Waialae Beach Park (Site A), b) Paiko coastline (Site D), and c) Kuliouou Beach Park (Site E) in Maunalua Bay, in triplicate, except for Site E, which had four samples (Figure 1). At Site A, all samples were taken about 50 yards perpendicular from the shore between the two discharge points. At Site D, all three samples were taken about 4.5~6 m from the shore at the passage located between residential houses to the beach. At Site E, three samples were taken just off the bottom substrate line at the low tide, and one sample was taken about 1.5 m offshore.

2.2.2 Reagents

Dichloromethane and acetone were pesticide grade solvents (Fisher Scientific). Analytical standards were purchased from Ultra Scientific, RI, United States. Two stock standards were prepared. The first was SVOC stock which included: semi-volatile mixture (SVM-525) and organochlorine pesticide mixture (PPM-525E) (see table for list of analytes). The second was NP stock which included: nitrogen/phosphorous pesticide mixture 1 (NPM-525C) and nitrogen/phosphorous pesticide mixture 2 (NPM-525B). The internal standard solution (ISM- 510) was used for GC-MS quantitation. Sodium sulfate (Fisher Scientific) was baked at 200°C overnight and then pre-rinsed with hexane before use.

2.2.3 Sample preparation

Marine sediment samples were placed in 125 mL pre-cleaned amber glass jars with Teflon-lined lids (I-Chem 300 series, VWR). Samples were collected, transported, and stored in the walk-in refrigerator until extraction. Sediment samples were extracted using an ASE 200 (Dionex Corporation, Sunnyvale, CA, United States). Approximately 5 g wet weight marine sediment was placed in a hexane rinsed aluminum dish and diatomaceous earth (Dionex Corporation, Sunnyvale, CA, United States) was added and ground until dry. This mixture was added to a 22 mL

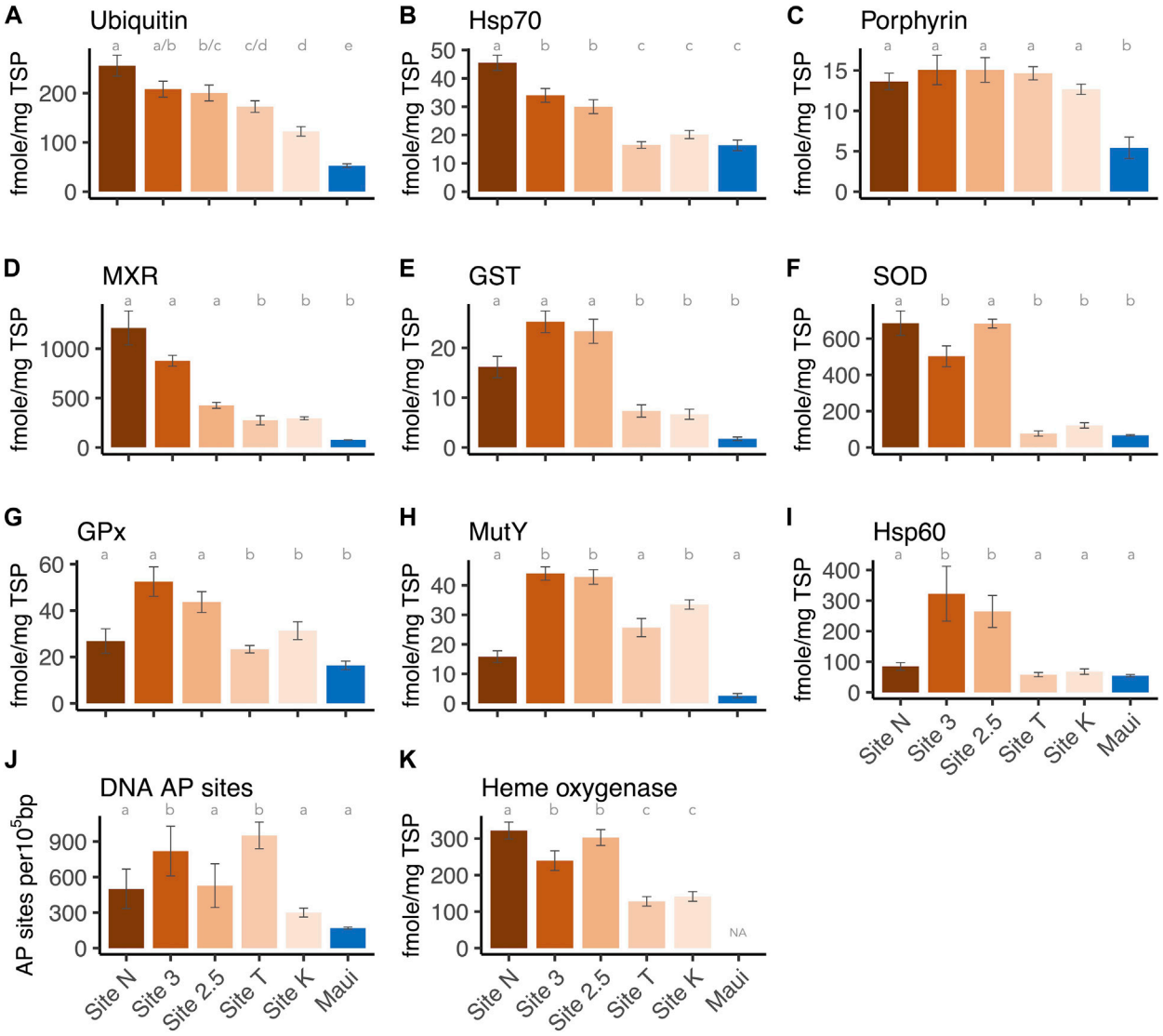

FIGURE 3
Expression levels of each biomarker per site: **(A)** Ubiquitin, **(B)** Hsp70, **(C)** Protoporphyrinogen oxidase IX, **(D)** MXR, **(E)** GST, **(F)** Cu/Zn SOD, **(G)** GPx, **(H)** Hsp60, **(J)** DNA AP sites, and **(K)** Heme oxygenase I. The letters above the bars indicate the statistically significant difference (Tukey-HSD or Dunn's test with adjusted p-value < 0.05).

ASE extraction cell. Blank and spike (5 g/L = 5 ppm) samples were prepared in Ottawa Sand (mesh 200–300, Fisher Scientific) and diatomaceous earth. ASE extraction solvent was dichloromethane: acetone (1:1) run at 1,500 psi, 100°C for 5 min with flush of 50% ASE cell volume and nitrogen purge for 80 s. The ASE extract was passed through sodium sulfate, dried, and quantitatively transferred to a GC vial. Internal standards were added (acenaphthene-d10, phenanthrene-d10, and chrysene-d12) and the extract was analyzed by GC-MS.

2.2.4 Instrument analysis

Two separate GC-MS methods were developed which included a semi-volatile/organochlorine (SVOC) method and a nitrogen/phosphorous (NP) method. These methods were the same except for the analyte list. Samples were run on a Varian 3800 GC/Saturn 2200 ion trap mass spectrometer (Varian Inc. Walnut Creek, CA, United States). The gas chromatograph was equipped with a 30 m VF-5ms column (0.25 mm i.d., 0.25 mm film) run at 1.1 mL/min helium with a pressure pulse of 45 psi for 0.8 min. The oven temperature started at 70°C with a 1-min hold, then was raised to 300°C at 4°C/min and held at 300°C for 2 min. A 1 uL sample was injected split/splitless at 250°C using a Varian CP-8400 autosampler. The transfer line temperature was 270°C, trap at 200°C, and manifold at 80°C. The mass spectrometer was run in full scan mode. Data was analyzed using Saturn GC-MS Workstation version 6.42.

2.2.5 Quality control

A five-point standard curve was run for all compounds (0.01–10 ug/mL) which had a correlation coefficient greater than 0.99 with less than 15% standard deviation. Samples, blanks, and spikes were all run in duplicate reporting results as an average.

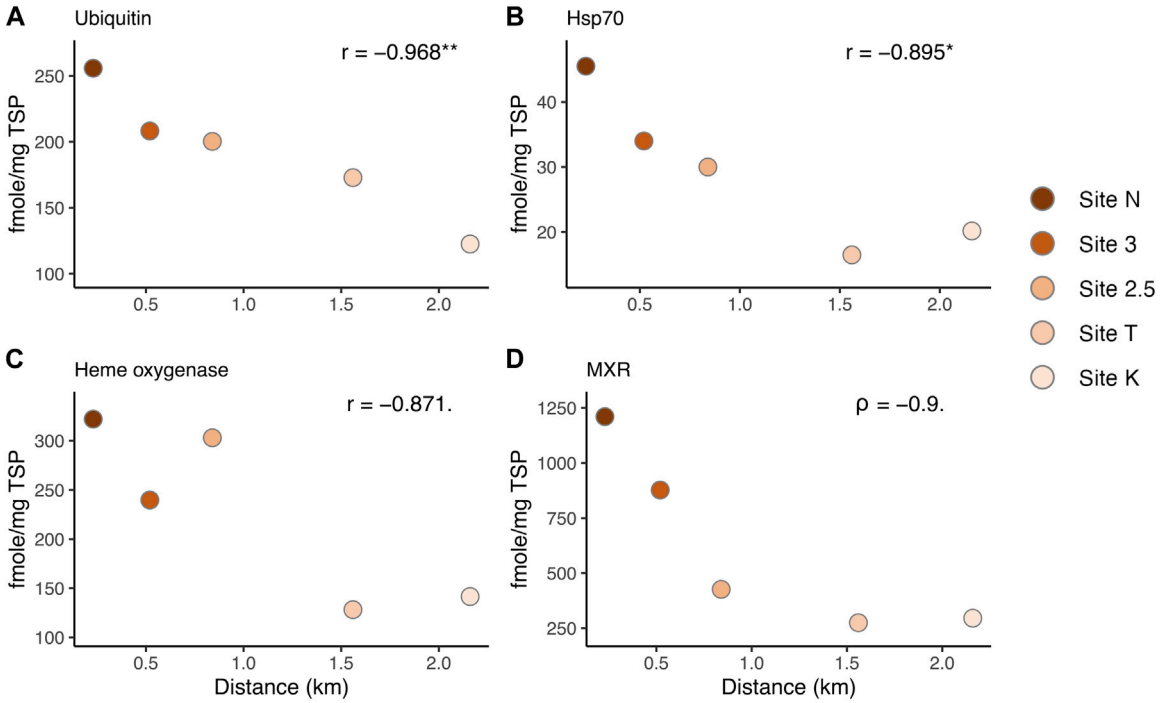

FIGURE 4
Correlation between protein biomarker expression levels and the distance from the mouth of the bay, representing the environmental (anthropogenic stressor) gradient: **(A)** Ubiquitin, **(B)** Hsp70, **(C)** Heme oxygenase I, and **(D)** MXR. *r*: Pearson's correlation coefficient. Asterisks denote statistical significance (* = $p < 0.05$, ** = $p < 0.01$). Dots denote a marginally significant *p*-value (< 0.1).

2.3 Water quality analysis (5 sites)

2.3.1 Sample collection

Water samples were collected from five inshore sites in Maunalua Bay (Figure 1, Sites A/B/C/E/N). The samples were brought back to the Kewalo Marine Laboratory, and processed or used immediately for solid-phase extraction (3.2).

2.3.2 Instrument analysis

Collected samples in solid phase cartridges were sent to Jupiter Environmental Laboratories (Jupiter, FL) for select organic compound analysis by GC-MS and LC-MS. Briefly, the cartridges were eluted with 2.5 mL of methanol twice to a final volume of 5 mL. The samples were allowed to settle and spun at 5 K for 4 min. The top layer was drawn off to avoid any salts that settled out of the cartridge. An open scan GC-MS analysis was performed and all peaks were checked against the NIST library. The open scan runs displayed few peaks, and when the Library search yielded nothing, high-performance liquid chromatography-tandem mass spectrometry (HPLC-MS/MS) was performed as an orthogonal discovery technology with much greater sensitivity. The samples were run against Multiple Reaction Monitoring transitions for triazine herbicides, chlorophenoxy herbicides, organophosphate pesticides, and pharmaceuticals and personal care products (PPCPs). Samples were listed as qualitatively positive if they were found to be above our LOQ, had a matching secondary ion and matching retention time when run by HPLC-MS/MS.

3 Results

3.1 Coral stress responses segregate over distance from the discharge

We conducted ordination analysis to assess if the aggregate expression patterns of biomarkers in *P. lobata* differed between sites. The analysis results showed clear segregation of the responses over distance from the mouth of the bay (Site N to Site K/T) along the canonical axis 1 (Figure 2). The inshore site (Site N) was characterized by signs of toxicant exposure, reflected in MXR, GST, and ubiquitin, and the mid-station sites (Site 3/2.5) had notable signs of oxidative damage reflected in SOD. The outer sites (Site K/T) with the lowest anthropogenic stressor level, also displayed some toxicant exposure signatures but were different from the rest of the sites. The reference site (Maui) was distinctly segregated from all sites, and was closest to the outer sites, suggesting the ordination results reflected well the water quality of the habitats where corals were sampled. Interestingly, toxicant exposure signatures of corals from the outer sites included signs of DNA damage reflected in DNA AP sites and MutY biomarkers, which may be due to pesticide exposure (from terrestrial runoff) or from chlorine or bromine exposure from swimming pool water discharges into that site from the nearby residential area (Portlock, east of Site K) (Richardson et al., 2010). When these pools are drained, the water is often discharged into the storm drains which empty into the ocean at the affected site.

Each biomarker was also analyzed separately to determine how expression levels differed between sites. All markers showed overall differences among sites (one-way ANOVA or Kruskal-Wallis H test, p-values < 0.001, Supplementary Material S1). Post-hoc pairwise analysis revealed that Hsp 70 and ubiquitin showed the most variable expression levels between sites: Ubiquitin concentrations from all five sites in the bay were significantly higher than those from the Maui reference site (Tukey-HSD, adjusted p-values < 0.05), as well as the inshore site (Site N) having a significantly higher level than the outer and middle sites (Site K/T, 2.5) (Tukey-HSD, adjusted p-values < 0.05) (Figure 3A). The two middle sites (Site 3/2.5) also had significantly higher ubiquitin levels than the outer Site K (Tukey-HSD, adjusted p-values < 0.05), indicating ubiquitin as a sensitive biomarker of anthropogenic stressors/toxicant exposure. For Hsp70, on the other hand, the corals at the inshore and middle sites (Site N, 3/2.5) had significantly higher concentrations than those from Maui and the outer sites (Site K/T) (Tukey-HSD, adjusted p-value < 0.05), but the concentrations of the proteins from the corals at the outer sites did not differ from those of Maui (Figure 3B). This suggests that ubiquitin and Hsp70 are potentially useful biomarkers of anthropogenic stressors, but ubiquitin is more sensitive than Hsp70. Porphyrin concentrations in corals from all five sites in the bay were significantly higher than in those from Maui (Tukey-HSD adjusted p-value < 0.05), but within the bay, there were no differences (Figure 3C), suggesting ubiquitous organochlorine exposure and heightened antioxidant activity in corals within the bay. For MXR and GST, corals from the inshore and middle sites (Site N, 3/2.5) had significantly higher expression levels than those from Maui (Dunn's test, adjusted p-value < 0.05), but not the offshore corals (Site K/T) ((Figures 3D, E), as seen in Hsp70. SOD showed a similar pattern, with the inner and middle site corals having significantly higher levels than Maui corals (Dunn's test, adjusted p-value < 0.05), but corals from Site 3 did not differ from those in Maui (Figure 3F). GPx and MutY showed significantly higher levels only in the middle and offshore sites (Site 3/2.5, K) compared to Maui (Tukey-HSD/Dunn's test, adjusted p-value < 0.05) (Figures 3G, H). Hsp60 was only higher in the middle site corals (Site 3/2.5) compared to those from Maui (Dunn's test, adjusted p-value < 0.05) (Figure 3I), and DNA AP sites were significantly higher in Site 3 and Site T compared to Maui (Tukey-HSD, adjusted p-value < 0.05) (Figure 3A). Heme oxygenase, which was only tested among corals from the bay (no Maui), showed the inner and middle site corals (Site N, 3/2.5) with significantly higher expression levels than the outer site corals (Site K/T) (Tukey-HSD, adjusted p-value < 0.05), again reflecting the higher stress levels experienced by the inner and middles site corals.

3.2 Some biomarkers showed the dose-response relationship along the environmental gradient

Several of the biomarkers showed decreased responses in a linear fashion from inshore to offshore along the environmental gradient (Figure 4). Hsp70 and ubiquitin showed a significant correlation between the distances from the mouth of the bay (i.e., anthropogenic stressor levels) and the expression levels (Pearson test, ubiquitin: p-value = 0.007, Hsp70: p-value = 0.04, Figures 4A, B). MXR and heme oxygenase showed a marginally significant relationship (heme oxygenase: Pearson test, p-value = 0.055, MXR: Spearman test, p-value = 0.08). These results help direct the choice of biomarkers for future work depending on the stressors of interest. However, there was no breakpoint along the gradient in Maunalua Bay, where protein biomarker levels were as low as those found in corals from the reference site (Maui) (Figures 3, 4), suggesting the corals of this Bay are all under the influence of land-based sources of stress and pollution. Nonlinear responses were also observed in several biomarkers, including SOD and MutY. Studies have found that nonlinear responses do occur in corals (e.g., Gil, 2013; Bove et al., 2019), with some proteins and associated metabolic pathways responding differently based on exposure concentrations and timing.

TABLE 1 Contaminants detected from sediment samples collected from inshore three sites in Maunalua Bay. We considered "Hit" (◎) as above 80% match with the NIST library, "Presence" (○) as below 80% match with NIST library, and • represents suspected presence. Those with no symbols represent "not detected".

Type	Contaminant	Site A	Site D	Site E
PAHs	benzo [a]pyrene	◎		○
PAHs	benzo [b]fluoranthene	◎		○
PAHs	benzo [k]fluoranthene	◎		○
PAHs	pyrene			◎
PAHs	benzo [a]anthracene	◎		
PAHs	phenanthrene	◎		
PAHs	anthracene	◎		
Pesticide	alpha-Chlordane	◎		
Pesticide	trans-Nonachlor	◎		
PAHs	benzo [ghi]perylene	○		
PAHs	ideno [1,2,3cd]pyrene	○		
PAHs	chrysene	•		
Pesticide	DDD/DDE	•		

3.3 Organic contaminants were present in inshore sediments and water

Various organic contaminants were found through our analysis of marine sediments collected from three discharge sites across Maunalua Bay (Table 1). At both Sites A and E, benzo [a]pyrene, benzo [b]fluoranthene, and benzo [k]fluoranthene were detected, indicating relatively ubiquitous presence of polycyclic aromatic hydrocarbons (PAHs) in inshore areas of the bay. At Site A, additional eight contaminants were found along with the suspected presence of chrysene and DDD/DDE. At Site E, one additional PAH (pyrene) was identified, while none were detected at Site D. Variations in detected contaminants among sites likely represent the sediment flushing/retention rates at particular sites and/or limitations or difficulties of detecting trace compounds from a single sampling method.

TABLE 2 Contaminants detected from water samples collected from five inshore sites in Maunalua Bay. Here, "Hit" (◎) is a compound concentration detected at a trace level (<5 µg/L), and "Presence" (○) is at an ultra-trace level (<0.05 µg/L). The symbol ◉ indicates a high Hit (96.5 µg/L). Those with no symbols represent "not detected".

	Site A	Site B	Site C	Site E	Site N
BPA	◎	◎	◎	◎	◎
oxybenzone	◎	◎	◎	◎	◎
atrazene			○		○
simazine			○		○
dicamba					◉

Water chemistry was also analyzed from samples collected from five inshore sites across Maunalua Bay, which showed trace levels (<5 µg/L) of Bisphenol A (BPA) and oxybenzone in all samples (Table 2). Ultra trace levels of atrazine and simazine (<0.05 µg/L) were also found at Sites C and N. Relatively high concentration of herbicide dicamba (96.5 µg/L) was detected at Site N. Triazine herbicides were negative for all samples. Again, we do not know if the differences among sites for the ultra-trace level contaminants are due to the detection limit, rather than due to true water quality differences. However, the ubiquitous presence of BPA and oxybenzone in the nearshore waters is indisputable.

4 Discussion

The documented declines in coral reef health are the result of multiple stressors acting in concert. Two specific requests from coral reef resource managers and stakeholders were 1) for techniques that could identify cause-and-effect relationships between putative stressors and coral health at the sublethal level, when interventions had the greatest potential for leading to positive outcomes and 2) for tools and associated metrics that would allow for determining the efficacy of management actions in real time, meaning over weeks to months rather than years to decades. The biomarker approach described here, which was modeled after those used for diagnosing and treating human health issues and maladies, met both needs. The elevated expression levels of stress induced proteins in corals from Maunalua Bay, especially those from inshore areas near discharge sites, relative to those from the reference site in Maui demonstrated that the sublethal stress in corals due to anthropogenic stressors (water quality) can be reliably detected. We also showed that some proteins, such as ubiquitin, Hsp70, and MXR, can be used to create a dose-response curve, which will help create the "thresholds' for assessing the effects of individual environmental stressors, and those acting in concert. Proteomics/transcriptomics can show the stress response or adaptive mechanisms of corals to environmental stressors (e.g., Thomas et al., 2019; Tisthammer et al., 2021). However, to establish the stress threshold efficiently and cost-effectively, here we showed that a dozen of (or fewer) proteins can be used as diagnostic biomarkers.

The fact that the same proteins used to diagnose human ailments worked in corals is not surprising, as such responses occur at the cellular level, regardless of the "host" organism. In this study, antibodies raised against Cnidarians were used, but we have found many commercially available antibodies raised against vertebrates, such as catalase, cytochrome P450 A1, and Hsp90, to be effective in assessing protein expression levels in corals (unpublished data). This further affirms that practical biomarkers for diagnosing coral health can be available without extensive further studies. Indeed, deployable diagnosing tools in corals are gaining attention in recent years and are in development. For example, Meng et al. (2022) tested human urinalysis strips on corals and found that ketone and leukocytes were reliably detected by the strips.

Some of the proteins that were upregulated in corals exposed to reduced water quality, particularly toxicants, such as pesticides and polycyclic aromatic hydrocarbons (PAHs) ubiquitously detected in this study, are steroidal clearance/detoxification and regeneration enzymes that also play a role in reproduction (Rougée et al., 2006; Rougée et al., 2015; Rougée et al., 2021). Just as coral colony energetic allocation to maintenance and repair can compromise reproductive success including gamete quality and fecundity, so too can the allocation of key proteins to detoxification reduce the availability for reproduction and hence, population replenishment. As many coral reefs have suffered notable losses in coral colony density to levels below 10% (Eddy et al., 2021), populations are no longer capable of replenishment from local sources due to the Allee effect (Courchamp et al., 2008), where gamete dilution during spawning events prevents egg-sperm interactions, and hence, successful fertilization. Active coral reef restoration programs are viewed as essential for many reefs, particularly in the Atlantic/Caribbean, but will be unsustainable if transplanted corals are non-reproductive. Water quality is an essential parameter in the selection of sites for coral reef restoration, and the protein-based tools presented here can be used to assess the appropriateness of sites based on key biological responses, particularly on fecundity, gamete quality, and availability of essential steroidal proteins that can be allocated to reproduction on top of detoxification.

Since protein expression can be analyzed both qualitatively for identifying key stressors and quantitatively for determining threshold levels, protein expressions are a valuable tool for use by coral reef managers in efforts to protect and restore coral reefs. As the financial, institutional and human resources available for such tasks are limited, it is essential to use science-based approaches to develop management plans and to assess the efficacy of efforts to ensure positive outcomes. Our data demonstrate how the emerging tools and technologies can be applied. Future efforts to improve cellular diagnostics and advance the technologies for *in situ* analyses and monitoring will enhance the functionality and broader application of these tools.

Data availability statement

The datasets presented in this study can be found in online repositories. The names of the repository/repositories and accession number(s) can be found below: https://github.com/kahot/maunaluabay.

Ethics statement

Ethical approval was not required for the study involving animals in accordance with the local legislation and institutional requirements because it was not required for studies using corals.

Author contributions

KT: Data curation, Formal Analysis, Validation, Visualization, Writing–original draft, Writing–review and editing. JM: Investigation, Methodology, Writing–review and editing. DC: Data curation, Investigation, Methodology, Project administration, Resources, Software, Supervision, Visualization, Writing–review and editing. RR: Conceptualization, Funding acquisition, Investigation, Project administration, Resources, Supervision, Writing–original draft, Writing–review and editing.

Funding

The author(s) declare financial support was received for the research, authorship, and/or publication of this article. The majority of this work was funded by Hawaii Coral Reef Initiative (Grant Number NA09NOS4260242). Additional support came from the National Oceanic and Atmospheric Administration (Grant number NA17NMF4520144) and the National Fish and Wildlife Foundation (Project number 0302.17.056606/56606).

Acknowledgments

We thank all funders, including Hawaii Coral Reef Initiative, the National Oceanic and Atmospheric Administration and the National Fish and Wildlife Foundation. We also thank the Kewalo Marine Laboratory for supporting the project.

Conflict of interest

The authors declare that the research was conducted in the absence of any commercial or financial relationships that could be construed as a potential conflict of interest.

Publisher's note

Supplementary material

The Supplementary Material for this article can be found online at: https://www.frontiersin.org/articles/10.3389/fphys.2024.1346045/full#supplementary-material

References

Barshis, D. J., Stillman, J. H., Gates, R. D., Toonen, R. J., Smith, L. W., and Birkeland, C. (2010). Protein expression and genetic structure of the coral Porites lobata in an environmentally extreme Samoan back reef: does host genotype limit phenotypic plasticity? *Mol. Ecol.* 19, 1705–1720. doi:10.1111/j.1365-294X.2010.04574.x

Birkeland, C. (2015). in *Coral reefs in the anthropocene*. Editor C. Birkeland (Dordrecht, Netherlands: Springer Netherlands). doi:10.1007/978-94-017-7249-5

Bove, C. B., Ries, J. B., Davies, S. W., Westfield, I. T., Umbanhowar, J., and Castillo, K. D. (2019). Common Caribbean corals exhibit highly variable responses to future acidification and warming. *Proc. R. Soc. B* 286, 2840. doi:10.1098/rspb.2018.2840

Courchamp, F., Berec, L., and Gascoigne, J. (2008). *Allee effects in ecology and conservation*. Oxford, UK: OUP Oxford.

Crowther, J. R. (2001). *The ELISA guidebook*. Totowa, NJ, USA: Humana Press.

Downs, C. A. (2005). "Cellular diagnostics and its application to aquatic and marine toxicology," in *Techniques in aquatic toxicology*. Editor G. K. Ostrander (Boca Raton, FL, USA: CRC Press), 2, 181–208.

Downs, C. A., Fauth, J. E., Robinson, C. E., Curry, R., Lanzendorf, B., Halas, J. C., et al. (2005). Cellular diagnostics and coral health: declining coral health in the Florida Keys. *Mar. Pollut. Bull.* 51, 558–569. doi:10.1016/j.marpolbul.2005.04.017

Downs, C. A., Ostrander, G. K., Rougee, L. R. A., Rongo, T., Knutson, S., Williams, D. E., et al. (2012). The use of cellular diagnostics for identifying sub-lethal stress in reef corals. *Ecotoxicology* 21, 768–782. doi:10.1007/s10646-011-0837-4

Downs, C. A., Richmond, R. H., Mendiola, W. J., Rougee, L. R. A., and Ostrander, G. K. (2006). Cellular physiological effects of the MV Kyowa violet fuel-oil spill on the hard coral, Porites lobata. *Environ. Toxicol. Chem.* 25, 3171–3180. doi:10.1897/05-509r1.1

Eddy, T. D., Lam, V. W. Y., Reygondeau, G., Cisneros-Montemayor, A. M., Greer, K., Palomares, M. L. D., et al. (2021). Global decline in capacity of coral reefs to provide ecosystem services. *One Earth* 4, 1278–1285. doi:10.1016/j.oneear.2021.08.016

Edge, S. E., Shearer, T. L., Morgan, M. B., and Snell, T. W. (2013). Sub-lethal coral stress: detecting molecular responses of coral populations to environmental conditions over space and time. *Aquat. Toxicol.* 128 (129), 135–146. doi:10.1016/j.aquatox.2012.11.014

Feder, M. E., and Walser, J. C. (2005). The biological limitations of transcriptomics in elucidating stress and stress responses. *J. Evol. Biol.* 18, 901–910. doi:10.1111/j.1420-9101.2005.00921.x

Ghosh, S., Gepstein, S., Heikkila, J. J., and Dumbroff, E. B. (1988). Use of a scanning densitometer or an ELISA plate reader for measurement of nanogram amounts of protein in crude extracts from biological tissues. *Anal. Biochem.* 169, 227–233. doi:10.1016/0003-2697(88)90278-3

Gil, M. A. (2013). Unity through nonlinearity: a unimodal coral-nutrient interaction. *Ecology* 94, 1871–1877. doi:10.1890/12-1697.1

Hoegh-Guldberg, O. (2014). Coral reef sustainability through adaptation: glimmer of hope or persistent mirage? *Curr. Opin. Environ. Sustain.* 7, 127–133. doi:10.1016/j.cosust.2014.01.005

Holm, S. (1979). A simple sequentially ejective multiple test procedure. *Scand. J. Stat.* 6, 65–79.

Kenkel, C. D., Aglyamova, G., Alamaru, A., Bhagooli, R., Capper, R., Cunning, R., et al. (2011). Development of gene expression markers of acute heat-light stress in reef-building corals of the genus Porites. *PLoS ONE* 6, e26914. doi:10.1371/journal.pone.0026914

Meng, Z., Williams, A., Liau, P., Stephens, T. G., Drury, C., Chiles, E. N., et al. (2022). Development of a portable toolkit to diagnose coral thermal stress. *Sci. Rep.* 12, 14398. doi:10.1038/s41598-022-18653-3

Murphy, J. W. A., and Richmond, R. H. (2016). Changes to coral health and metabolic activity under oxygen deprivation. *PeerJ* 4, e1956. doi:10.7717/peerj.1956

Parkinson, J. E., Baker, A. C., Baums, I. B., Davies, S. W., Grottoli, A. G., Kitchen, S. A., et al. (2020). Molecular tools for coral reef restoration: beyond biomarker discovery. *Conserv. Lett.* 13, e12687. doi:10.1111/conl.12687

Presto, K. M., Storlazzi, C. D., Logan, J. B., Reiss, T. E., and Rosenberger, K. J. (2012). "Coastal circulation and potential coral-larval dispersal in Maunalua bay, Oahu, Hawaii -measurements of waves, currents, temperature, and salinity june-september 2010," in *U.S. Geological survey open-file report 2012-1040* (Virginia, VA, USA: USGS). Available at: http://pubs.usgs.gov/of/2012/1040/.

Richardson, S. D., DeMarini, D. M., Kogevinas, M., Fernandez, P., Marco, E., Lourencetti, C., et al. (2010). What's in the pool? A comprehensive identification of disinfection by-products and assessment of mutagenicity of chlorinated and brominated swimming pool water. *Environ. Health Perspect.* 118, 1523–1530. doi:10.1289/ehp.1001965

Richmond, R. H. (2011). HCRI annual progress report: watersheds impacts on coral reefs in Maunalua bay, Oahu, Hawaii. *Hawaii Coral Reef. Initiat.* Available at: http://www.hcri.ssri.hawaii.edu/research/richmond2008.html.

Richmond, R. H., and Wolanski, E. (2011). "Coral research: past efforts and future horizons," in *Corals reefs: an ecosystem in transition*. Editors Z. Dubinsky and N. Stambler (Berlin, Germany: Springer), 3–12. Available at: http://link.springer.com/chapter/10.1007/978-94-007-0114-4_1.

Rougée, L., Downs, C. A., Richmond, R. H., and Ostrander, G. K. (2006). Alteration of normal cellular profiles in the scleractinian coral (Pocillopora damicornis) following laboratory exposure to fuel oil. *Environ. Toxicol. Chem.* 25, 3181–3187. Available at: http://onlinelibrary.wiley.com/doi/10.1897/05-510R2.1/full. doi:10.1897/05-510r2.1

Rougée, L. R. A. (2011). Expression and activity of xenobiotic metabolizing enzymes in the reef coral *Pocillopora damicornis*. *A Dessertation* 121.

Rougée, L. R. A., Collier, A. C., and Richmond, R. H. (2021). Chronic exposure to 4-nonylphenol alters UDP-glycosyltransferase and sulfotransferase clearance of steroids in the hard coral, pocillopora damicornis. *Front. Physiology* 12, 608056. doi:10.3389/fphys.2021.608056

Rougée, L. R. A., Richmond, R. H., and Collier, A. C. (2015). Molecular reproductive characteristics of the reef coral Pocillopora damicornis. *Comp. Biochem. Physiology, Part A* 189, 38–44. doi:10.1016/j.cbpa.2015.07.012

Seneca, F. O., Forêt, S., Ball, E. E., Smith-Keune, C., Miller, D. J., and Oppen, M. J. H. (2009). Patterns of gene expression in a scleractinian coral undergoing natural bleaching. *Mar. Biotechnol.* 12, 594–604. doi:10.1007/s10126-009-9247-5

Seneca, F. O., and Palumbi, S. R. (2015). The role of transcriptome resilience in resistance of corals to bleaching. *Mol. Ecol.* 24, 1467–1484. doi:10.1111/mec.13125

Seveso, D., Montano, S., Strona, G., Orlandi, I., Galli, P., and Vai, M. (2013). Exploring the effect of salinity changes on the levels of Hsp60 in the tropical coral Seriatopora caliendrum. *Mar. Environ. Res.* 90, 96–103. doi:10.1016/j.marenvres.2013.06.002

Seveso, D., Montano, S., Strona, G., Orlandi, I., Galli, P., and Vai, M. (2016). Hsp60 expression profiles in the reef-building coral Seriatopora caliendrum subjected to heat and cold shock regimes. *Mar. Environ. Res.* 119, 1–11. doi:10.1016/j.marenvres.2016.05.007

Sokal, R. R., and Rohlf, F. J. (1995). *Biometry: the principles and practice of statistics in biological research*. 3rd. New York, NYm USA: W. H. Freeman.

Storlazzi, C. D., Presto, K. M., Logan, J. B., and Field, M. E. (2010). Coastal circulation and sediment dynamics in Maunalua Bay, Oahu, Hawaii; *Measurements Of Waves, Currents, Temperature, Salinity, And Turbidity; November 2008-February 2009*. USGS, Virginia, VA, USA, Available at: http://pubs.usgs.gov/of/2010/1217/.

Thomas, L., López, E. H., Morikawa, M. K., and Palumbi, S. R. (2019). Transcriptomic resilience, symbiont shuffling, and vulnerability to recurrent bleaching in reef-building corals. *Mol. Ecol.* 232, 3371–3382. doi:10.1111/mec.15143

Tisthammer, K. H., Timmins-Schiffman, E., Seneca, F. O., Nunn, B. L., and Richmond, R. H. (2021). Physiological and molecular responses of lobe coral indicate nearshore adaptations to anthropogenic stressors. *Sci. Rep.* 11, 3423. doi:10.1038/s41598-021-82569-7

Tomanek, L. (2011). Environmental proteomics: changes in the proteome of marine organisms in response to environmental stress, pollutants, infection, symbiosis, and development. *Annu. Rev. Mar. Sci.* 3, 373–399. doi:10.1146/annurev-marine-120709-142729

Wilkinson, C. (2004). *Status of coral reefs of the World: 2004*, 1. Australia, Australian Institute of Marine Science. Available at: http://www.vliz.be/imisdocs/publications/213234.pdf.

Wolanski, E., Martinez, J. A., and Richmond, R. H. (2009). Quantifying the impact of watershed urbanization on a coral reef: Maunalua Bay, Hawaii. *Estuar. Coast. Shelf Sci.* 84, 259–268. doi:10.1016/j.ecss.2009.06.029

frontiers | Frontiers in Marine Science

TYPE Original Research
PUBLISHED 07 March 2024
DOI 10.3389/fmars.2024.1330894

OPEN ACCESS

EDITED BY
Ranjeet Bhagooli,
University of Mauritius, Mauritius

REVIEWED BY
Adán Guillermo Jordán-Garza,
Universidad Veracruzana, Mexico
Inês Martins,
University of the Azores, Portugal

*CORRESPONDENCE
Stefania Gorbi
s.gorbi@univpm.it
Carlos Jimenez
c.jimenez@enaliaphysis.org.cy

RECEIVED 31 October 2023
ACCEPTED 25 January 2024
PUBLISHED 07 March 2024

CITATION
Nardi A, Resaikos V, Papatheodoulou M, Di Carlo M, Vedhanarayanan H, Regoli F, Gorbi S and Jimenez C (2024) Cellular adaptations of the scleractinian coral *Madracis pharensis* to chronic oil pollution in a Mediterranean shipwreck. *Front. Mar. Sci.* 11:1330894. doi: 10.3389/fmars.2024.1330894

Cellular adaptations of the scleractinian coral *Madracis pharensis* to chronic oil pollution in a Mediterranean shipwreck

Alessandro Nardi[1,2], Vasilis Resaikos[3], Magdalene Papatheodoulou[3], Marta Di Carlo[1,2], Harini Vedhanarayanan[4], Francesco Regoli[1,2], Stefania Gorbi[1,2]* and Carlos Jimenez[2,5]*

[1]Department of Life and Environmental Sciences, Università Politecnica delle Marche, Ancona, Italy, [2]National Biodiversity Future Center (NBFC), Palermo, Italy, [3]Enalia Physis Environmental Research Centre, Nicosia, Cyprus, [4]Ghent University, Ghent, Belgium, [5]Energy, Environmental and Water Research Center, The Cyprus Institute, Nicosia, Cyprus

Chemical pollution in marine ecosystems is a factor of stress interacting in multiple and complex ways with other major causes of deterioration, such as warming seas due to climate change. Here we surveyed epibenthic communities from a shipwreck in the Levantine Basin for temporal and spatial changes in the community in relation to chronic oil pollution, comparing results collected from an area of the wreck characterized by chronic oil leakage with another area not affected by oil. Polycyclic aromatic hydrocarbons (PAHs) bioaccumulation analyses were integrated with characterization of the efficiency of xenobiotics biotransformation processes and antioxidant network of the scleractinian coral *Madracis pharensis*, chosen as bioindicator species. Results highlighted the two areas hosting different epibenthic communities over a period of 11 years. Significant changes in the percentage cover of *M. pharensis* could be the result of recent mass mortality associated to Marine Heat Waves. Biological investigation conducted in *M. pharensis* tissues revealed an increased content of PAHs in specimens collected from the oil-impacted area, coupled with an increased capability of oxyradicals scavenging capacity and a lower functionality of phase II biotransformation mechanisms associated to glutathione S-transferase. Overall, the results suggest that *M. pharensis* has the capability to develop cellular and physiological adaptations to chemical-mediated stress, with yet unknown possible energy trade-offs to sustain stress response.

KEYWORDS

pollution, PAHs, epibenthic biodiversity, detoxification, oxidative stress, Levantine Sea

Introduction

Epibenthic communities from shipwrecks are studied intensively due to the characteristics that make the wreck an artificial reef. Knowledge about the ecological processes operating on these assemblages (e.g., recruitment, competition, predation) assist in the elaboration of management options for the restoration of degraded habitats, population dynamics of invasive species, to concentrate human activities in specific areas, and more often than not, for the enhancement or creation of habitat (Brockinton et al., 2022; Hughes et al., 2023). Behind the apparent benefits of shipwrecks to the general biodiversity of an area, that is, by providing free substrate for epibenthic species that are fast and successful colonizers (Hoeksema et al., 2023) and refuge for mobile species increasing thus the biodiversity (Monchanin et al., 2021), wrecks might also contribute to local pollution by leaking chemicals (*e.g.*, van der Schyff et al., 2020). Such is the case with Zenobia shipwreck in Cyprus, where rich epibenthic communities of corals and sponges live closely related to chronic leakage of oil, noticeable in various sections of the wreck's structure (Jimenez et al., 2017a).

In general, scleractinian corals are good indicators of chemical pollution (Guzmán and Jiménez, 1992), and corals from shipwrecks have been reported to show higher concentrations of pollutants, *e.g.* heavy metals, compared to corals from other substrates sampled in areas away from the wrecks (van der Schyff et al., 2020). Coral species' capability to accumulate PAHs from surrounding environments with diverse degree of contamination has been extensively reported, and studies on PAHs effects in Scleractinia under laboratory conditions highlighted a plethora of alterations ranging from the lower levels of biological organization, *i.e.* changes in gene expression, genotoxicity, to the higher ones, *i.e.* physiological and morphological alterations, mortality (Menezes et al., 2023 and references therein; Turner and Renegar, 2017 and references therein). On the other hand, studies on the sub-lethal alterations at cellular level, mechanisms of stress-response and adaptations in coral species under real environmental scenarios of chronic oil pollution are yet globally underrepresented (Turner and Renegar, 2017).

Once within organisms, chemical pollutants may exert disturbance at various levels of biological organization, and pathways of chemicals toxicity strictly depend on their typology, which determines initiating events at cellular level (Allen et al., 2016). It is now well recognized that PAHs toxicity arise from the metabolic processes aimed to breakdown these chemicals and allow for their elimination. Indeed, PAHs, as polychlorobiphenyls (PCBs) and dioxins, bind the cytosolic aryl hydrocarbon receptor (AhR), and form a ligand-receptor complex that once transported to the nucleus binds to xenobiotic metabolism specific regions of the DNA, known as dioxin responsive element (DRE), through the interaction with ARNT, AhR nuclear translocator (Regoli and Giuliani, 2014; Wang et al., 2020). This molecular initiating event activates the transcription of several genes involved in the biotransformation and metabolism of xenobiotics, as CYP1 and CYP1B. Such biotransformation reactions of xenobiotics are aimed to decrease their lipophilicity, but these may not be sufficient and organic xenobiotics metabolism may proceed toward phase II conjugation reactions, catalysed by glutathione S-transferase, UDP- glucuronosyl transferases (UGTs) and sulfotransferases (SULTs) which use endogenous cofactors as reduced glutathione (GSH), glucuronic acid and sulfate, respectively, and are as well modulated through the Ah-gene battery.

PAHs toxicity partly derives from their bioactivation through these reactions, which can produce metabolites that show higher toxicity compared to parent compounds and damage cellular macromolecules, *e.g.* forming DNA adducts (as 7,8-dihydrodiol-9,10-oxide, the DNA-adduct forming metabolite of benzo(a)pyrene responsible for its carcinogenicity, Regoli and Giuliani, 2014). At the same time, PAHs metabolism is also recognized as one of the main processes causing the release of reactive oxygen species (ROS), consequential to electron transport uncoupling occurring during the slow oxidation of substrates and to "redox cycling" of metabolites (Schlezinger et al., 2006; Shakunthala, 2010; Regoli and Giuliani, 2014).

Cells are able to neutralize the negative effects of oxyradicals through a complex network of low molecular weight scavengers and enzymes, collectively recognized as antioxidant system, universally developed to counteract the naturally occurring production of ROS from several cellular pathways of aerobic metabolism, as mitochondrial electron transport chain and active phagocytosis (Benedetti et al., 2015, 2022; Lushchak, 2011; Regoli and Giuliani, 2014). Reduced glutathione, ascorbic and uric acid scavenge ROS by directly acting as reducing agents on oxyradicals, but are also fundamental co-factors for the functioning of other antioxidants, enzymes that catalyze highly specific reactions, as superoxide dismutase (SOD), catalase (CAT), glutathione reductase (GR), glutathione peroxidases (GPx) and glutathione S-transferases (GST), the main involved (Lushchak, 2011). In this respect, the efficiency of antioxidant defenses is especially fundamental in symbiotic organisms, as sclearactinians and sponges, which show physiological adaptations to counteract the toxicity of photosynthetically produced oxygen, which can easily undergo univalent reduction to form $O_2^{\cdot-}$, H_2O_2 and HO• (Regoli et al., 2004a; Regoli et al., 2004b; Lesser, 2006).

Due to the sensitivity of the antioxidant defenses, their functionality has been extensively studied in marine species under chemical exposure and more in general abiotic stress, especially when aiming to understand mechanisms behind the onset of oxidative stress and cellular damages. Activities of SOD, CAT, GR, GST, GPx, as well as cellular homeostasis of glutathione have been demonstrated to be either increased or decreased by exogenous cellular stressors as chemical pollutants, namely trace metals, PAHs, dioxins, microplastics and active pharmaceutical ingredients (Lushchak, 2011; Benedetti et al., 2022). On the other hand, specific methodologies have been developed to quantify and characterize the overall capability and functionality of cellular antioxidant network, as the total oxyradical scavenging capacity assay (TOSCA, Regoli and Winston, 1998; Gorbi and Regoli, 2003). This methodology, compared to the evaluation of single antioxidant defenses, provide a more comprehensive picture of cellular redox status, and therefore health. Such approach has been successfully applied in several field and laboratory investigations, to characterize marine species antioxidant defenses, their capability to neutralize

oxyradicals and prevent oxidative damage when subjected to exogenous stressors as chemical pollutants, algal toxins, thermal stress and hypercapnia (Regoli et al., 2004a; Regoli et al., 2004b; Gorbi et al., 2012; Gorbi et al. 2014; Nardi et al., 2017; Nardi et al., 2018; Iannello et al., 2021).

In this study we aimed to characterize the composition of epibenthic communities, as well as PAHs bioaccumulation, antioxidant network and xenobiotics biotransformation efficiency of a selected scleractinian coral species, *Madracis pharensis*, at two sites of the Zenobia wreck, one under the influence of oil leakages and one considered free from this environmental stressor. Obtained results were intended to further elucidate aspects of Scelractinians' biology and their mechanisms of tolerance and responsiveness to chemical stress, as well as and deepen our understanding on the capability of coral species to adapt to chronic subtle pollution.

Materials and methods

Study site

The large ferry MS Zenobia (10,000ton, 172m length) loaded with vehicles, lorries and cargo capsized in 1980 in Larnaka Bay, Cyprus (34° 55.128'N, 33° 39.354'E; Figure 1A). Since then, Zenobia has been resting horizontally on its portside (Figure 1B) in about 43m depth. The sea bottom of Larnaka Bay is characterized by scattered, small-sized rocky outcrops and extensive sandy and muddy areas. Given the large dimension of Zenobia, the low deterioration of its hull, complexity and heterogeneity of the metal structure, it is not surprising to find a rich biodiversity associated with the shipwreck. For example, the high abundance and diversity of fish and colorful epibenthic communities are well known among the international diving community that ranks Zenobia among the most popular recreational dives sites of the world (Scuba, 2022). A more detailed description of the shipwreck and the biotic and environmental factors that operate in the Larnaka Bay area can be found in Jimenez et al. (2017a). For this study, two contrasting environments of the wreck were selected: the Car Deck and the Smokestacker areas, both at 25m depth (Figure 1B). In the Car Deck area, constant leakage of oil from the wreck accumulates in "ponds" between spaces on the bulwark of the starboard side, which corresponds to the "upper" shaded surface. Organisms in this area live in close contact with those stagnant "oil ponds", corals in particular (Figure 1C). On the contrary, the epibenthic communities in the Smokestacker area are not affected by oil leakages (Figure 1D). In both sites, epibenthic biodiversity was assessed, and an in-depth focus on pollutants bioaccumulation and cellular alterations was conducted on the scleractinian *M. pharensis*, as described below.

Epibenthic biodiversity assessment

The diverse epibenthic communities of Zenobia thrive at the shaded undersides of the wreck's external structures and inside the hull, where the high heterogeneity of surfaces, relatively open areas (e.g., cabins, corridors), and multitude crannies offer shelter from direct exposure to the sunlight. The benthic cover (>25% on average) is mainly composed by sponges, corals, bryozoans, and other organisms (Jimenez et al., 2017a).

To assess the status of the epibenthic communities, the percentage of benthic cover was measured from photo-quadrats following the protocol of Jimenez et al. (2017a). Succinctly, 15 photos from each area were taken consecutively, avoiding overlap,

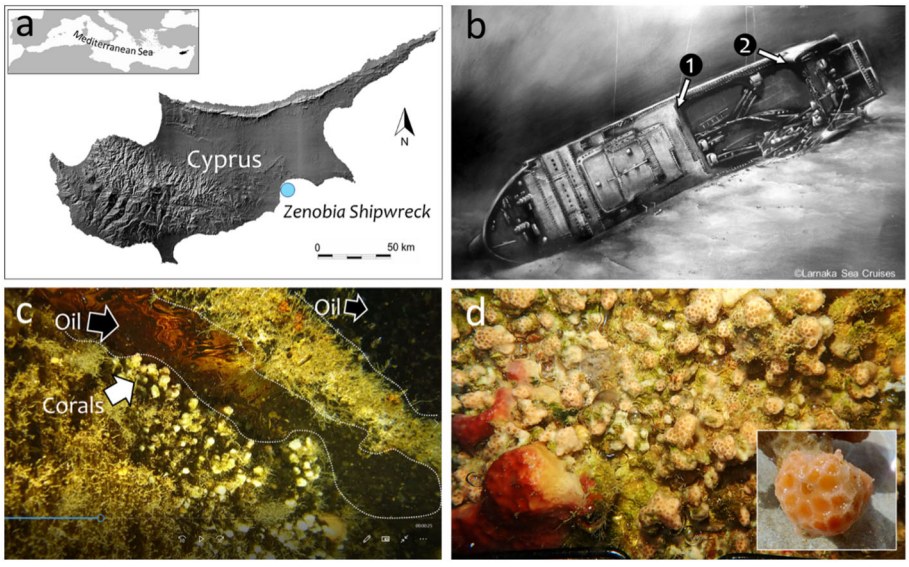

FIGURE 1
Location of the Zenobia shipwreck in Cyprus **(A)**. Sampling stations along the starboard side of the shipwreck (25-27m depth): 1=inside the "Car Deck" (oil); 2=below the "Smokestack" (no oil) **(B)**. Madracis pharensis coral colonies from station 1 in contact with oil "ponds"; snapshot from a video **(C)**. Community of M. pharensis and sponges from station 2; insert=detail of a coral sample **(D)**.

with a frame (13cm x 19cm) at a fixed distance from the digital camera (Olympus Tough equipped with strobes). Analysis of the photos was made using Coral Point Count program (Kohler and Gill, 2006) with a systematic lay-out of 225 points. The pre-existing code files were modified with the following seven categories: live coral, dead coral, macro algae, calcareous algae, porifera, other (e.g., serpulid polychaetes, bivalves, bryozoans, cyanobacteria), and substrate (not occupied by organisms). The selection of this categories was based on other similar studies in Cyprus (Jimenez et al., 2017a, Jimenez et al., 2017b; Jimenez et al., 2022). The percentage of cover from multiple image frames was grouped together for single site evaluation and to allow comparisons between the two sites (see below).

Madracis pharensis sampling and tissue collection

Samples of the scleractinian coral *M. pharensis* (Heller 1868) were collected at the Car Deck and Smokestacker sites for the analysis of PAHs bioaccumulation, total oxyradical scavenging capacity assay and biotransformation processes. This species is a facultative zooxanthellate coral that is abundant in Cyprus and can be found up to a depth of 100m. In general, colonies of *M. pharensis* can exhibit encrusting or knobby morphologies. This species was chosen due to its abundance on the shipwreck and simplicity of collection. Four small knobby-shaped colonies were collected from each site by gently removing the coral from the substrate with a thin metal chisel and small hammer and transported to the support vessel in seawater-filled plastic containers. Onboard, the seawater was decanted from the containers and the coral samples were placed in dry ice and transported to the laboratory, where they were stored into a -80° C freezer.

PAHs bioaccumulation, detoxification mechanisms and total oxyradical scavenging capacity in *Madracis pharensis*

For the analysis of polycyclic aromatic hydrocarbons (PAHs), about 3 g (wet weight) of coral samples (soft tissue and skeleton) were extracted in 5 mL 0.5 M potassium hydroxide in methanol using a microwave system at 55°C for 20 min (800 Watt) (Mars6, CEM Corporation, Matthews NC). After centrifugation at 3,000 × g for 10 min, the supernatants (methanolic solution) were concentrated using a rotational vacuum concentrator (RVC 2-18 Cdplus, CHRIST) and purified with solid-phase extraction (Octadecyl C18, 500 mg × 6 mL, Merck). A final volume of 1 mL was recovered with pure, analytical HPLC gradient grade acetonitrile, and HPLC analyses were carried out in a water and acetonitrile gradient by fluorimetric and diode array detection. The PAHs were identified according to the retention times of an appropriate pure standards solution (EPA 610 Polynuclear Aromatic Hydrocarbons Mix), and classified as low molecular weight (LMW: naphthalene, acenaphthylene, 1-methyl naphthalene, 2-methyl naphthalene, acenaphthene, fluorene, phenanthrene, anthracene) or high molecular weight (HMW: fluoranthene, pyrene, benzo(a)anthracene, chrysene, 7,12-dimethyl benzo(a)anthracene, benzo(b)fluoranthene, benzo(k)fluoranthene, benzo(a)pyrene, dibenzo(a,h)anthracene, benzo(g,h,i)perylene, indeno(1,2,3,c,d)pyrene). Quality assurance and quality control were done by processing blank and reference samples (freeze-dried mussel tissues SRM 2974a, NIST), and concentrations obtained for the SRM were always within the 95% confidence interval of certified value. The water content in tissues was determined in all the samples and concentrations of PAHs expressed as ng/g dw (Iannello et al., 2021).

Coral samples for biological analyses were gently washed with PBS buffer, ground powdered in liquid nitrogen and then homogenized with a homogenization ratio 1:5 (w:v) in a 100 mM K-phosphate buffer pH 7.5, with 2.5% NaCl, 0.1 mM phenyl-methyl sulphonyl fluoride (PMSF), 0.008 trypsin inhibitor unit (TIU) mL −1 aprotinin, 1 ng mL−1 leupeptin, 0.5 ng mL−1 pepstatin, and 0.1 mg mL−1 bacitracin. Sample homogenates were centrifuged at 12,000 x g for 70 min at 4° C, and the zooxanthellae-free supernatant collected, divided into aliquots and stored at −80° C until analysis (Yakovleva et al., 2004; Tang et al., 2018).

Protein content in each sample was measured through a modification of the Lowry's method (Lowry et al., 1951), and used to normalize the results of biological investigations described after. Briefly, samples aliquots were diluted 100 times, and 500 µL of these were incubated in tubes with 2.5 mL of reaction medium (0.01% $CuSO_4$, 0.02% $Na_3C_6H_5O_7$, 2% Na_2CO_3, and 0.4% NaOH in water). After 25 minutes, 250 µL of a solution made of Folin-Ciocalteau:water (1:1) was added to each sample, and these were left in incubation for 50 minutes. Protein standards prepared with albumin from bovine serum (BSA) at different concentrations (0, 20, 50, 100, 200, 400 µg/mL) were treated with the same procedure. At the end of the second incubation, the absorbance of standards and samples was acquired with triplicate readings at the spectrophotometer (ƛ=750 nm). The absorbance values of standards were plotted for creating the standard curve used to fit the absorbance of samples and calculate the proteins' concentration of each sample.

Glutathione S-transferases activity was spectrophotometrically determined at 340 nm using 1-chloro-2,4-dinitrobenzene as substrate (CDNB). The assay consists in measuring the increment of the product of conjugation of 1.5 mM CDNB with 1 mM GSH in 100 mM K-phosphate buffer pH 6.5, GS-DNB. Enzymatic activity is expressed as µmol GS-DNB/min/mg protein, with ε = 9.6 mM−1 cm−1 (Habig and Jakoby, 1981).

The overall capability of cellular antioxidants to neutralize peroxyl (ROO•) and hydroxyl (HO•) radicals was measured through the total oxyradical scavenging capacity (TOSC) assay, by evaluating the inhibition of 0.2 mM α-keto-γ-methiolbutyric acid (KMBA) oxidation to ethylene gas (Regoli and Winston, 1998). Thermal homolysis in 100 mM phosphate buffer pH 7.4 of 20 mM 2-2-azo-bis-(2-methylpropionamide)-dihydrochloride (ABAP), and Fenton reaction of 1.8 µM iron-3.6 µM EDTA plus 180 µM ascorbate were used to generate peroxyl (ROO•) and hydroxyl (HO•) radicals, respectively. For each sample, ethylene formation was evaluated with GC-method at 10 min intervals in sample and blank reaction and used to calculate the total oxyradical scavenging capacity (TOSC) value with the equation: TOSC = 100−(∫SA/∫BA ×

100), where ∫SA and ∫BA are the integral areas calculated from the ethylene kinetic curve measured during the reaction, for sample and blank reactions, respectively. The obtained specific TOSC value was normalized on the relative protein concentration measured with the Lowry method, and results expressed as U TOSC/µg protein.

Statistical analyses

The 2022 epibenthic community composition from Car Deck and Smokestacker stations was statistically analyzed after the inclusion of data from a previous survey conducted in 2011 (Jimenez et al., 2017a). The analysis tested for any temporal (2011 vs. 2022) or spatial (between stations) similarities between the two communities. To visualize the dissimilarity in the community compositions of the two stations, metaMDS and ordination plots, with Bray Curtis dissimilarity measure, were plotted in R (Version Ri386 3.4.4) and statistically compared with ANOSIMs (Analysis Of SIMlarities; permutations = 9999, distance = Bray) and SIMPER analysis (Similarity Percentage; permutation = 999). Furthermore, for the metaMDS, an envfit analysis, which indicates which species may be driving the distribution patterns observed, was also run. Since corals were the main focus, further analysis of the data was concentrated on this category (*e.g.*, live and dead coral percentages), and more specifically with the species *M. pharensis*, which was also selected for the investigation of cellular effects. Linearized models (LMs; Supplementary Table S1) were run in R to investigate the changes in (i) the percentage of coral species' cover, and (ii) percentage of mortality, across the two stations and the two time periods. Significance was determined using the p-values (significance level= 0.05) from the ANOVA and t-tests. Linearized models were applied to investigate differences among corals sampled at the two stations in terms of PAHs bioaccumulation, detoxification mechanisms and total oxyradical scavenging capacity.

Results

Epibenthic biodiversity assessment

The community composition between the two stations (Car Deck and Smokestaker; Supplementary Figure S1) was different in 2011 (ANOSIM; R2 = 0.44, p < 0.001) and in 2022 (ANOSIM; R2 = 0.15, p < 0.001). The dissimilarity in the two stations in 2011 was due to the organism groups 'Other organisms' (p = 0.02), 'Substrate' (p = 0.001), and 'Calcareous organisms' (p = 0.001), while the dissimilarity in the 2022 data where due to the organism groups 'Substrate' (p = 0.001) and 'Porifera' (p = 0.03) (SIMPER; Supplementary Materials, Supplementary Table S5).

Similarly, the composition was statistically different when pooling stations (Figure 2; ANOSIM, R2 = 0.15, $p < 0.001$) and years (Figure 2; ANOSIM, R2 = 0.33, $p < 0.001$) into a single analysis. The NMDS (dark grey clusters), shows that the community composition between two stations, 'Car Deck' and 'Smokestacker' are not completely dissimilar, but have differences. The organism groups responsible for the dissimilarity between the two stations were 'Substrate' ($p = 0.001$) and 'Porifera' ($p = 0.041$) (SIMPER; Supplementary Materials, Supplementary Table S5). As with the stations, year in the NMDS (light grey clusters) illustrates that there are differences in the community composition across the year 2011 and 2022. For year the dissimilarities were due to a bigger range of groups including 'Corals' ($p = 0.001$), 'Substrate' ($p = 0.001$), 'Other organisms' ($p = 0.001$), 'Calcareous algae' ($p = 0.02$), and 'Algae' ($p = 0.004$) (SIMPER; Supplementary Materials, Supplementary Table S5). Moreover, the envfit (Supplementary Materials, Supplementary Table S6), which tells us which species may be driving the distribution patterns observed in the NMDS, imply that all organism groups are responsible (Corals, Porifera, Other organism, and substrate have a $p = 0.001$; Algae $p = 0.006$, and Calcareous algae $p = 0.004$).

The percentage cover of three coral species (*Caryophyllia inornata*, *Phyllangia mouchezii* and *Polycyathus muellerae*) found in the two stations did not show significant changes across years and locations, with the exception of *M. pharensis* (Figure 3; Supplementary Table S1). This species experienced an increment in the percentage of cover from the year 2011 to 2022, range 9.6% to 12.3% and 24.4% to 26.7%, respectively (T-test, t=2.298, p=0.022; Figure 3A, Supplementary Table S2), but the increase was proportional across the two stations (Figure 3B, Supplementary Table S2). Overall, the percentage of cover of dead and living corals (all species polled, Supplementary Table S3) was similar in both stations (range 4.4% to 7.1% and 10.1% and 30.4%, respectively) but there were more living corals in the 2022 survey compared to 2011 (Figure 4; T-test, t=2.041, p=0.04; Supplementary Table S4).

PAHs bioaccumulation in *Madracis pharensis*

Analyses of PAHs in corals samples confirmed the exposure of *M. pharensis* to PAHs, with significantly higher levels of total PAHs (Figure 5A) bioaccumulated in organisms collected at the Car Deck site (273.2 ± 166.9 ng/g d.w.) compared to those collected at Smokestacker site (34.9 ± 21.8 ng/g d.w.). Overall, both low molecular and high molecular weight PAHs significantly contributed to the observed differences (Figures 5B, C): low molecular PAHs were 33.6 ± 22.2 and 70.9 ± 2.19 ng/g d.w. at Smokestacker and Car Deck sites, respectively, while high molecular PAHs were 1.32 ± 0.45 and 202.3 ± 169.1 ng/g d.w. at Smokestacker and Car Deck sites, respectively. On the other hand, high molecular weight PAHs accounted for roughly 75% of the total PAHs in organisms sampled at Car Deck site, while these represented almost only 10% of total PAHs in tissues of organisms sampled at Smokestacker site.

Among the contributors to these differences, 1-methylnaphthylene was the main low molecular weight PAH congener presenting different levels in organisms sampled in the two sites, while pyrene, chrysene, 7,12-dimethylbenz(a)anthracene, benzo(b)fluoranthene and benzo(k) fluoranthene were the main high molecular weight PAH congeners supporting the differences in PAHs bioaccumulation in *M. pharensis*

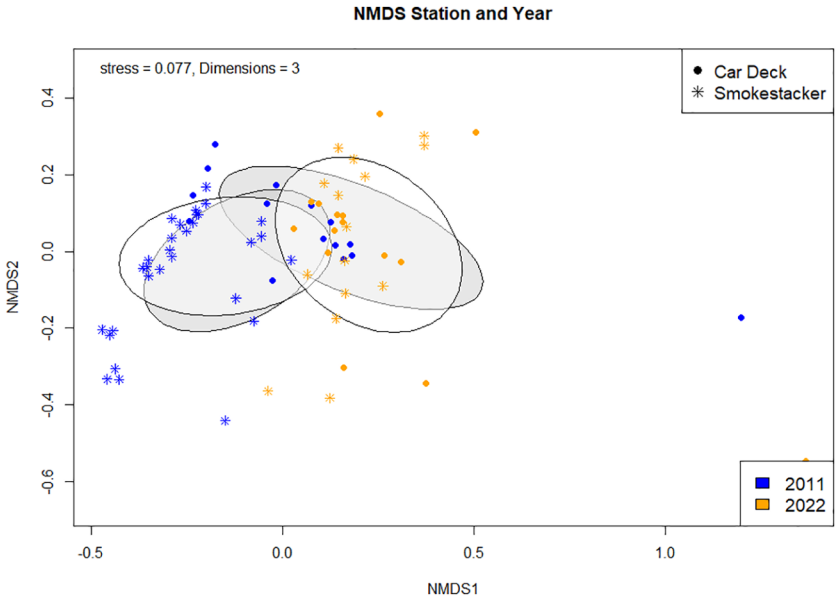

FIGURE 2
metaMDS ordination with Bray Curtis Dissimilarity distance calculation comparing community composition between stations and years.

sampled the two sites (Supplementary Materials, Supplementary Table S7).

Detoxification mechanisms and total oxyradical scavenging capacity in *Madracis pharensis*

A statistically significant decrease of glutathione S-transferases activity (Figure 6A) was measured in tissues of *M. pharensis* organisms sampled at the Car Deck site (8.25 ± 0.57 nmol/min/mg protein) compared to those collected at Smokestacker site (13.21 ± 2.27 nmol/min/mg protein).

On the other hand, significant differences of total oxyradical scavenging capacity towards both peroxyl (TOSC ROO•) and hydroxyl radicals (TOSC HO•) were measured in *M. pharensis*, with lower values in organisms collected from Car Deck site compared to specimens collected from Smokestacker site (Figures 6B, C). Values were 1.44 ± 0.24 and 2.01 ± 0.20 U TOSC ROO•/μg protein for *M. pharensis* sampled at Smokestacker and Car Deck sites, respectively, while 1.41 ± 0.27 and 2.74 ± 0.06 U TOSC HO•/μg protein for *M. pharensis* sampled at Smokestacker and Car Deck sites, respectively.

Discussions

The communities' composition of the studied areas of the Zenobia shipwreck were distinct between sites and changed over time, from the first survey in 2011 to the recent study in 2022. These

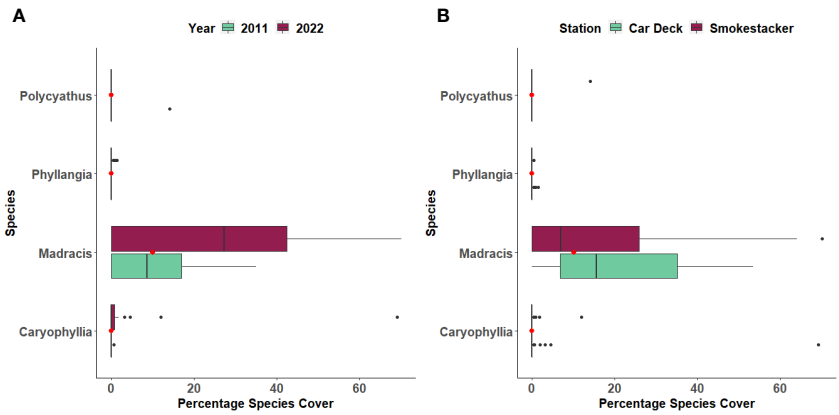

FIGURE 3
Percentage cover of four coral species across **(A)** Years and **(B)** Stations. The boxplots indicate the median (horizontal line), interquartile range (boxes), minimum/maximum values (whiskers), outliers (black points), as well as the combined median of both groups (red point).

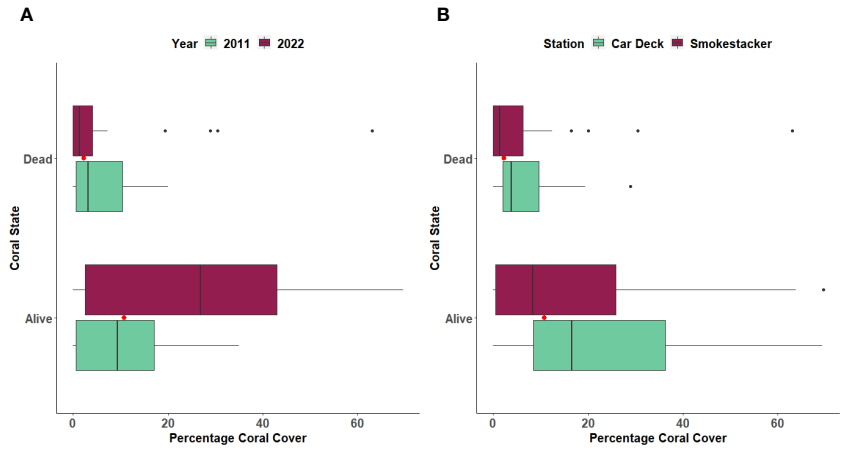

FIGURE 4
Percentage of cover of Dead and Living corals between **(A)** Years and **(B)** Stations. The boxplots indicate the median (horizontal line), interquartile range (boxes), minimum/maximum values (whiskers), outliers (black points), as well as the combined median of both groups (red point).

findings are not unexpected given the particularities of each area and the major ecological changes that have occurred in Cyprus during those 11 years: population collapse of key species, such as habitat forming corals, bryozoans, seagrasses, and echinoid grazers (Garrabou et al., 2022; see below). Considering the spatial component, the communities of the Car Deck are under limiting conditions in contrast to the Smokestacker. Hydrodynamism, availability of light, substrate and structural features (i.e., heterogeneity) are among the main abiotic factors affecting epibenthic communities and ecological processes on shipwrecks (González-Duarte et al., 2018; Hill et al., 2021; Achilleos et al., 2023; Jimenez et al., 2023). To the best of our knowledge, there is only one source of information regarding oceanographic conditions at the shipwreck (i.e., Jimenez et al., 2017a). However, we can complement that limited amount of data with unpublished observations stemming from our regular (seasonal) visits to the shipwreck since 2010. In the Car Deck area, the penetration of light and the water circulation decrease just a few meters from the gateway. The sector where the sampling was made can be considered a semi-dark zone of confined hydrological conditions. The restricted water circulation allows the accumulation of positively buoyant debris from the wreck itself (e.g., plastic containers from the cargo, shreds of carpeting material), including the oil leaking from the piping system. These almost still-conditions also affect the arrival of nutrients, exchange of gases, dispersion of larvae, etc. that are highly dependent on water circulation. The epibenthic communities at the Smokestacker are under radically different conditions. Even though the sampling site is under the large structure, it is a well-lit environment of high hydrodynamism (days with very strong currents are common, making diving there difficult). In consequence, the differences in composition between the communities from both sampling locations are product of the species' adaptation to site-related characteristics.

Regarding the ecological changes experienced in Cyprus during the last decade, five mass mortalities of epibenthic organisms occurred around the island since the first survey in 2011 of the Zenobia wreck (Jiménez et al., 2016; Garrabou et al., 2022, Jimenez unpublished data). These mortality events are strongly related to the

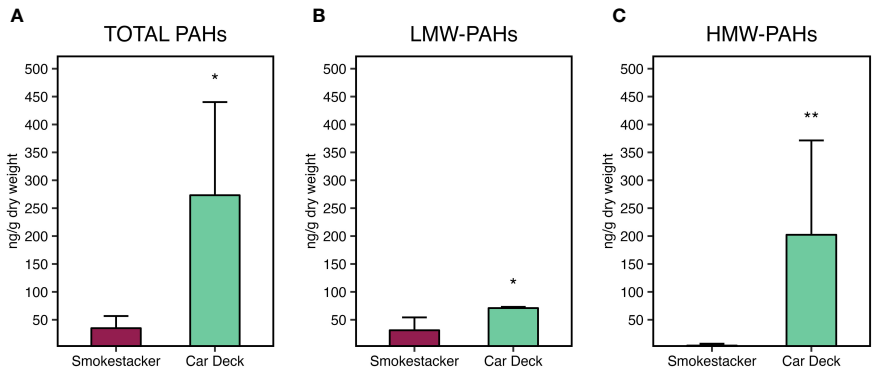

FIGURE 5
Bioaccumulation of **(A)** total PAHs, **(B)** low molecular weight PAHs, and **(C)** high molecular weight PAHs, in *M. pharensis* samples collected from Smokestacker and Car Deck sites, respectively. Results are given as mean ± standard deviation (n=4), asterisks denote significant differences between the two sites (*: $p < 0.05$; **: $p < 0.01$; ***: $p < 0.001$).

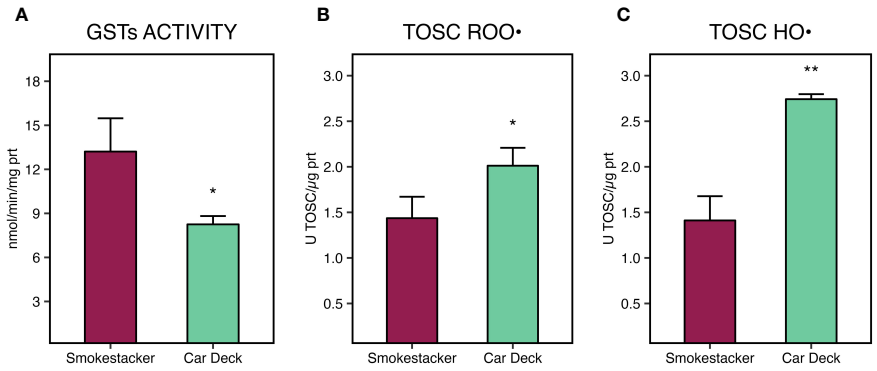

FIGURE 6
Glutathione S-transferases (GSTs) activity **(A)**, total oxyradical scavenging capacity (TOSC) towards peroxyl **(B)** and hydroxyl radicals **(C)**, in *M. pharensis* samples collected from Smokestacker and Car Deck sites, respectively. Results are given as mean ± standard deviation (n=4), asterisks denote significant differences between the two sites (*: $p < 0.05$; **: $p < 0.01$; ***: $p < 0.001$).

increase in frequency and intensity of Marine Heat Waves (MHWs) affecting Cyprus and the Mediterranean in general (Garrabou et al., 2022; Stipcich et al., 2023). But it is during the period 2018-2021 that the Zenobia wreck showed prolonged (ca. 18 months) and wide-spread (almost in all sections of the wreck, from 18m to 44m depth) mortalities during the MHWs (Jimenez unpublished data). Massive sponges were among the most affected epibenthic species; independently from the location, entire necrotic colonies (from 2-3cm to 80cm in diameter) decayed for weeks until only spongin fibers remained. Other sponges in various stages of necrosis fell on the sandy bottom from the vertical walls or "ceiling" surface of the starboard side of the wreck's structure. The net result of the disappearance of massive sponges was the increase in available substrate (open space) for colonization, expansion of "creeping" species that first grow expanding branches along the surface, such as *Madracis*, and certainly the reduction of competition for resources in the epibenthic communities. Competition for space between corals and sponges is a classic example of a biological factor affecting species' assemblages in natural and artificial substrates, in the Mediterranean and elsewhere (Chadwick and Morrow, 2011; Kayal and Adjeroud, 2022). Several life-traits allow sponges to thrive and outcompete other species in limiting environments such as those found in shipwrecks; for example, sciaphilic species and physical and chemical defenses against other benthic organisms (Wulff, 2006, González-Murcia et al., 2023). We believe that less competition with sponges is probably the main reason behind the increase in *Madracis'* percentage of cover at both sampling sites in the 2022 survey. During the 2010-2012 MHWs, this coral species was observed to be less affected than others, such as *Cladocora caespitosa*, *P. mouchezii*, and *P. muellerae* (Jiménez et al., 2016), also in the 2022 survey, "creeping branches" of *Madracis* were observed extending in an almost rivulet-like fashion. It is also possible that the disappearance of massive sponges facilitates the visual counting in the photo quadrats; but we support the competition-release explanation in view of the low mortality experienced by *Madracis*.

Despite *M. pharensis* coverage increased in both investigated stations from 2011 to 2022, corals living closely to "oil ponds" at Car Deck site showed to be threatened by chemical stress, causing the onset of cellular stress responses. Indeed, despite the origin and chemical composition of these "oil ponds" has not been addressed in this study, the investigation revealed a consistent accumulation of PAHs in organisms' sampled at Car Deck site, with levels significantly higher than the ones sampled at Smokestacker, namely high molecular weight PAHs (HMW-PAHs). We hypothesize that HMW-PAHs accumulation may be the result of the exposure to petroleum fuels and lubricants, composed by noticeable amounts of such congeners, which have low biodegradation rates, high lipophilicity, and long persistence (Head et al., 2006; Beolchini et al., 2010; Goto et al., 2021). This has also been suggested in a mesocosm study of Yamada et al., 2003, in which a simulated dispersion of the water-available fraction of heavy residual oil highlighted HMW PAHs to persist longer than low molecular weight compounds. PAHs levels comparable to those measured in this study have been observed in tissues of corals sampled from reefs of South China Sea (Han et al., 2020), and in massive corals of the Sanya coral reef regions (Xiang et al., 2018), both being coastal areas impacted by anthropogenic activities.

Noticeably, HMW-PAHs such as chrysene, 7,12-dimethylbenz (a)anthracene, benzo(b)fluoranthene and benzo(k)fluoranthene, found to be present at high concentrations in organisms from Car Deck site, have been addressed as potentially carcinogenic for vertebrates (Baird et al., 2005; Honda and Suzuki, 2020). Indeed, biotransformation and detoxification processes of PAHs generate reactive metabolites which can bind DNA, triggering the formation of adducts and the onset of genotoxic effects (Benedetti et al., 2015). Benzo(b)fluoranthene and benzo(k)fluoranthene are also listed in the priority group of substances to be monitored in EU water bodies with the Water Framework Directive 2000/60/EC (European Commission, 2000).

While organic xenobiotics metabolism is well characterized in vertebrates, and known to be inducible through AhR by different typologies of planar organic chemicals as PAHs, PCB, and dioxins (Regoli and Giuliani, 2014; Benedetti et al., 2015), the specificity of AhR binding has been proposed to be restricted to chordates

(Reitzel et al., 2014) and other xenobiotic biotranformation and detoxification pathways can be induced in marine invertebrates, as carboxylesterases and glutathione S-transferases (Regoli and Giuliani, 2014; Solé et al., 2021). Interestingly, in this study GSTs activity was significantly lower in corals sampled at Car Deck site compared to those sampled at Smokestack, and thus negatively correlated with PAHs in corals tissue; this result is of particular interest when compared to other findings on corals under organic xenobiotic stress: indeed, early induction of GSTs activity has been described in the coral *Montastraea faveolata* under acute short-term exposure to 0.1 ppm benzo[a]pyrene for 72h (Ramos and García, 2007), and similarly GST-pi gene induction was observed in *Pocillopora damicornis* after 24h under different concentrations of water available fraction of oil (Rougée et al., 2006). To date, a negative effect on GSTs activity was described in the reef-building coral *Orbicella flaveolata* affected by the Carribean yellow band disease under anthracene exposure (Montilla et al., 2016), and in the scleractinian *P. damicornis* exposed to polystyrene microplastics (Tang et al., 2018). The observed inverse relationship between GSTs activity and PAHs in corals tissues allows to hypothesize different possible mechanisms causing the lower activity of this detoxification process. The activity of GST might be directly disrupted by the PAHs accumulated in the cellular milieu, as previously observed in the mussels *Dreissena polymorpha* and *Mytilus galloprovincialis* exposed to PAHs- and PCB-contaminated sediments and benzo(a)pyrene, respectively (Akcha et al., 2000; Osman et al., 2007); on the other hand, a lower activity of the enzyme could be the consequence of a decreased availability of its main co-factor, reduced glutathione (GSH), either consumed by other enzymes of the antioxidants' network (*e.g.* glutathione peroxidases, glyoxalase) or directly involved in oxyradicals scavenging, and not promptly replenished (Karami et al., 2011; Regoli and Giuliani, 2014; Benedetti et al., 2015; Vašková et al., 2023). Nonetheless, the accumulation of other chemicals, not assessed in this study, might have contributed to the GST activity decrease, as previously described for graphene oxide, flame retardants, insecticides, and pesticides (Özaslan et al., 2018; Josende et al., 2020; Bellas et al., 2022).

During xenobiotic metabolism, certain chemicals and their metabolites may undergo redox cycling (Cohen and D'Arcy Doherty, 1987; Regoli and Giuliani, 2014; Benedetti et al., 2015) resulting in the production of reactive oxygen species (ROS) and in redox homeostasis unbalance (Regoli and Giuliani, 2014; Benedetti et al., 2015). This oxidative pathway of chemicals toxicity often leads to the activation of the antioxidant system through the up-regulation of genes controlled by the antioxidant responsive element (ARE), coding for enzymes as catalase, superoxide dismutase, glutathione peroxidases, glutathione S-transferases, among others (Regoli and Giuliani, 2014).

In this study, we characterized for the first time the efficiency of the antioxidant system of *M. pharensis* through the evaluation of the total oxyradical scavenging capacity towards peroxyl and hydroxyl radicals: our results suggest that *M. pharensis* possess an efficient cellular antioxidant defense network, as shown to other marine symbiotic species (Dykens and Shick, 1982; Dykens et al., 1992; Regoli et al., 2004b; Liñán-Cabello et al., 2010; Liñán-Cabello et al., 2011). Indeed, symbiotic species have been indicated to possess a relevant antioxidant machinery to balance the significant pro-oxidant challenge generated by the photosintetically-mediated cellular hyperoxic conditions (Lesser, 2006). Specimens of *M. pharensis* sampled at the "Smokestack" site, not impacted by pollution, showed TOSC levels consistent with those measured in other symbiotic cnidarian species, such as the sea anemone *Bunodosoma cavernatum* and the sponges *Petrosia ficiformis* and *Haliclona dancoi*, when in concomitant with increased temperature, symbiont density and photosynthetically-mediated boost of pro-oxidative pressure (Regoli and Winston, 1998; Regoli et al., 2004a, b). Moreover, *M. pharensis* presented, in average, 2 to 5 times higher TOSC levels that other marine species, as the bivalves *M. galloprovincialis*, *Flexopecten glaber*, *Ruditapes philippinarum*, polychaetes *Platynereis dumerilii*, *Polyophthalmus pictus, Syllis prolifera* (Nardi et al., 2017; Iannello et al., 2021, 2018; Ricevuto et al., 2015).

Regarding organisms sampled at the Car Deck site, these exhibited an increased oxyradicals scavenging capacity towards ROO• and HO•, allowing to suggest an increased ROS production at cellular level mediated by the high levels of bioaccumulated PAHs, which results in a sustained activation of the response toward oxidative stress. A similar response has been previously described in the cnidarian *Nematostella vectensis* following short-term exposure to crude oil (Tarrant et al., 2014), in the scleractinians *P. damicornis* following an acute laboratory exposure to fuel oil (Rougée et al., 2006) and in *Porites lobata* sampled 3 months after an oil spill in the Federated States of Micronesia (Downs et al., 2006); nonetheless, a generalized increase of the total antioxidant capacity was observed in the coral *Mussismilia harttii* and in the hydrocoral *Millepora alcicornis* sampled in Abrolhos Reef Banks (Brazil) 2 and 4 months after the rupture of a mine dam (Dal Pizzol et al., 2022). Noteworthy, Rougée et al. (2006) and Downs et al. (2006) described a significant increase of GST-pi protein content in corals subjected to chemical pollution. As previously discussed, in this study GST enzymatic activity was significantly reduced in corals with higher PAHs content, which reinforces the discussed hypothesis that the lower enzymatic activity may result from chemicals-mediated effects on the functionality of this detoxification mechanism under chronic pollution conditions rather than from a lower expression at transcriptional level.

These overall findings suggest that despite our study revealed a sustained presence and growth of *M. pharensis* in both investigated sites, those living in close contact with oil ponds may be subjected to increased environmental stress, with possible implications on long-term species distribution at local scale. Indeed, sustaining the antioxidant defenses network under chronic stress conditions is an energetic cost adaptation, that could lead to energy trades-off, reducing the amount of energy available to be allocated to physiological processes other than stress-response and thus leading to suboptimal growth and reduced reproductive rates (Sokolova, 2013; Lachs et al., 2023). These aspects, along to a more in-depth characterization of *Madracis pharensis* stress

response dynamics at transcriptional, physiological, and ecological levels, deserve further studies to fully elucidate the mechanisms underlying the capability of this species to survive under a chronic chemical stress.

Data availability statement

The raw data supporting the conclusions of this article will be made available by the authors, without undue reservation.

Author contributions

AN: Conceptualization, Data curation, Formal analysis, Writing – original draft, Writing – review & editing. VR: Data curation, Investigation, Writing – review & editing. MP: Visualization, Writing – original draft, Writing – review & editing, Formal analysis. MDC: Investigation, Writing – original draft, Data curation. HV: Formal analysis, Investigation, Writing – original draft. FR: Writing – review & editing, Supervision. SG: Conceptualization, Writing – original draft, Writing – review & editing, Project administration. CJ: Conceptualization, Funding acquisition, Investigation, Writing – original draft, Writing – review & editing, Project administration.

Funding

The author(s) declare that no financial support was received for the research, authorship, and/or publication of this article.

Acknowledgments

Author would like to thank Marios Papageorgiou (ENALIA) for his advice during the study but also for his administrative and logistical support, Constantina Stylianou (ENALIA) and Valentina Fossati (ENALIA) for assisting with administrative and analytical tools, respectively. The International Master of Science in Marine Biological Resources provided support to HV.

Conflict of interest

The authors declare that the research was conducted in the absence of any commercial or financial relationships that could be construed as a potential conflict of interest.

Publisher's note

Supplementary material

The Supplementary Material for this article can be found online at: https://www.frontiersin.org/articles/10.3389/fmars.2024.1330894/full#supplementary-material

References

Achilleos, K., Jimenez, C., and Petrou, A. (2023). "Wreck site formation process: the use of bryozoans," in *The Kyrenia Ship Final Excavation Report, Volume I: History of the Excavation, Amphoras, Ceramics, Coins and Evidence for Dating*. Eds. S. Womer Katzev and H. Wylde Swiny (Oxford: Oxbow Books), 166–171.

Akcha, F., Izuel, C., Venier, P., Budzinski, H., Burgeot, T., and Narbonne, J.-F. (2000). Enzymatic biomarker measurement and study of DNA adduct formation in benzo[a]pyrene-contaminated mussels, *Mytilus galloprovincialis*. *Aquat. Toxicol.* 49, 269–287. doi: 10.1016/S0166-445X(99)00082-X

Allen, T. E. H., Goodman, J. M., Gutsell, S., and Russell, P. J. (2016). A history of the molecular initiating event. *Chem. Res. Toxicol.* 29, 2060–2070. doi: 10.1021/acs.chemrestox.6b00341

Baird, W. M., Hooven, L. A., and Mahadevan, B. (2005). Carcinogenic polycyclic aromatic hydrocarbon-DNA adducts and mechanism of action. *Environ. Mol. Mutagenesis* 45, 106–114. doi: 10.1002/em.20095

Bellas, J., Rial, D., Valdés, J., Vidal-Liñán, L., Bertucci, J. I., Muniategui, S., et al. (2022). Linking biochemical and individual-level effects of chlorpyrifos, triphenyl phosphate, and bisphenol A on sea urchin (*Paracentrotus lividus*) larvae. *Environ. Sci. pollut. Res.* 29, 46174–46187. doi: 10.1007/s11356-022-19099-w

Benedetti, M., Giuliani, M. E., Mezzelani, M., Nardi, A., Pittura, L., Gorbi, S., et al. (2022). Emerging environmental stressors and oxidative pathways in marine organisms: Current knowledge on regulation mechanisms and functional effects. *Biocell* 46, 37–49. doi: 10.32604/biocell.2022.017507

Benedetti, M., Giuliani, M. E., and Regoli, F. (2015). Oxidative metabolism of chemical pollutants in marine organisms: Molecular and biochemical biomarkers in environmental toxicology. *Ann. New York Acad. Sci.* 1340, 8–19. doi: 10.1111/nyas.12698

Beolchini, F., Rocchetti, L., Regoli, F., and Dell'Anno, A. (2010). Bioremediation of marine sediments contaminated by hydrocarbons: Experimental analysis and kinetic modeling. *J. Hazard. Maters* 182, 403–407. doi: 10.1016/j.jhazmat.2010.06.047

Brockinton, E. E., Peterson, M. R., Wang, H.-H., and Grant, W. E. (2022). Importance of anthropogenic determinants of *tubastraea coccinea* invasion in the northern gulf of Mexico. *Water* 14, 1365. doi: 10.3390/w14091365

Chadwick, N. E., and Morrow, K. M. (2011). "Competition Among Sessile Organisms on Coral Reefs," in *Coral Reefs: An Ecosystem in Transition*. Eds. Z. Dubinsky and N. Stambler (Springer, Dordrecht). doi: 10.1007/978-94-007-0114-4_20

Cohen, G. M., and D'Arcy Doherty, M. (1987). Free radical mediated cell toxicity by redox cycling chemicals. *Br. J. Cancer* 55, 46–52.

Dal Pizzol, J. L., Marques, J. A., da Silva Fonseca, J., Costa, P. G., and Bianchini, A. (2022). Metal accumulation induces oxidative stress and alters carbonic anhydrase activity in corals and symbionts from the largest reef complex in the South Atlantic ocean. *Chemosphere* 290, 133216. doi: 10.1016/j.chemosphere.2021.133216

Dykens, J. A., and Shick, J. M. (1982). Oxygen production by endosymbiotic algae controls superoxide dismutase activity in their animal host. *Nature* 297, 579–580. doi: 10.1038/297579a0

Dykens, J. A., Shick, J. M., Benoit, C., Buettner, G. R., and Winston, G. W. (1992). Oxygen radical production in the sea anemone *anthopleura elegantissima* and its endosymbiotic algae. *J. Exp. Biol.* 168, 219–241. doi: 10.1242/jeb.168.1.219

Downs, C. A., Richmond, R. H., Mendiola, W. J., Rougée, L., and Ostrander, G. K. (2006). Cellular physiological effects of the MV Kyowa Violet fuel-oil spill on the hard coral, Porites lobata. *Environ. Toxicol. Chem.* 25 (12), 3171–3180. doi: 10.1897/05-509R1.1

European Commission (2000). Directive 2000/60/EC of the European Parliament and of the Council of 23 October 2000 establishing a framework for Community action in the field of water policy. *Offic. J. Eur. Commun. L* 327, 1.

Garrabou, J., Gómez-Gras, D., Medrano, A., Cerrano, C., Ponti, M., Schlegel, R., et al. (2022). Marine heatwaves drive recurrent mass mortalities in the Mediterranean Sea. *Global Change Biol.* 28 (19), 5708–5725. doi: 10.1111/gcb.16301

González-Duarte, M. M., Fernández-Montblanc, T., Bethencourt, M., and Izquierdo, A. (2018). Effects of substrata and environmental conditions on ecological succession on historic shipwrecks. *Estuarine Coast. Shelf Sci.* 200, 301–310. doi: 10.1016/j.ecss.2017.11.014

González-Murcia, S., Ekins, M., Bridge, T. C. L., Battershill, C. N., and Jones, G. P. (2023). Substratum selection in coral reef sponges and their interactions with other benthic organisms. *Coral Reefs* 42, 427–442. doi: 10.1007/s00338-023-02350-2

Gorbi, S., Bocchetti, R., Binelli, A., Bacchiocchi, S., Orletti, R., Nanetti, L., et al. (2012). Biological effects of palytoxin-like compounds from Ostreopsis cf. ovata: A multibiomarkers approach with mussels Mytilus galloprovincialis. *Chemosphere* 89, 623–632. doi: 10.1016/j.chemosphere.2012.05.064

Gorbi, S., Giuliani, M. E., Pittura, L., d'Errico, G., Terlizzi, A., Felline, S., et al. (2014). Could molecular effects of Caulerpa racemosa metabolites modulate the impact on fish populations of Diplodus sargus? *Mar. Environ. Res.* 96, 2–11. doi: 10.1016/j.marenvres.2014.01.010

Gorbi, S., and Regoli, F. (2003). Total oxyradical scavenging capacity as an index of susceptibility to oxidative stress in marine organisms. *Comments Toxicol.* 9, 303–322. doi: 10.1080/08865140390450395

Goto, Y., Nakamuta, K., and Nakata, H. (2021). Parent and alkylated PAHs profiles in 11 petroleum fuels and lubricants: Application for oil spill accidents in the environment. *Ecotoxicol. Environ. Saf.* 224, 112644. doi: 10.1016/j.ecoenv.2021.112644

Guzmán, H. M., and Jiménez, C. E. (1992). Contamination of coral reefs by heavy metals along the Caribbean coast of Central America (Costa Rica and Panama). *Mar. pollut. Bull.* 24, 554–561. doi: 10.1016/0025-326X(92)90708-E

Habig, W. H., and Jakoby, W. B. (1981). Assays for differentiation of glutathione-S-transferase. *Methods Enzymol.* 77, 398–405. doi: 10.1016/s0076-6879(81)77053-8

Han, M., Zhang, R., Yu, K., Li, A., Wang, Y., and Huang, X. (2020). Polycyclic aromatic hydrocarbons (PAHs) in corals of the South China Sea: Occurrence, distribution, bioaccumulation, and considerable role of coral mucus. *J. Hazard. Maters* 384, 121299. doi: 10.1016/j.jhazmat.2019.121299

Head, I. M., Jones, D. M., and Röling, W. F. (2006). Marine microorganisms make a meal of oil. *Nat. Rev. Microbiol.* 4, 173–182. doi: 10.1038/nrmicro1348

Hill, C. E. L., Lymperaki, M. M., and Hoeksema, B. W. (2021). A centuries-old manmade reef in the Caribbean does not substitute natural reefs in terms of species assemblages and interspecific competition. *Mar. Pollut. Bull.* 169, 112576. doi: 10.1016/j.marpolbul.2021.112576

Hoeksema, B. W., zu Schlochtern, M. P. M., Samimi-Namin, K., and McFadden, C. S. (2023). In the aftermath of Hurricane Irma: Colonization of a 4-year-old shipwreck by native and non-native corals, including a new cryptogenic species for the Caribbean. *Mar. pollut. Bull.* 188, 114649. doi: 10.1016/j.marpolbul.2023.114649

Honda, M., and Suzuki, N. (2020). Toxicities of polycyclic aromatic hydrocarbons for aquatic animals. *Int. J. Environ. Res. Public Health* 17, 1363. doi: 10.3390/ijerph17041363

Hughes, T. P., Baird, A. H., Morrison, T. H., and Torda, G. (2023). Principles for coral reef restoration in the anthropocene. *One Earth* 6, 656–665. doi: 10.1016/j.oneear.2023.04.008

Iannello, M., Mezzelani, M., Dalla Rovere, G., Smits, M., Patarnello, T., Ciofi, C., et al. (2021). Long-lasting effects of chronic exposure to chemical pollution on the hologenome of the Manila clam. *Evolution. Appl.* 14, 2864–2880. doi: 10.1111/eva.13319

Jimenez, C., Achilleos, K., Petrou, A., and Hadjioannou, L. (2023). "Tales from taphonomic amphoras: marine biofouling as interpretive ecological tool on wreck-site formation," in *The Kyrenia Ship Final Excavation Report, Volume I: History of the Excavation, Amphoras, Ceramics, Coins and Evidence for Dating*. Eds. S. Womer Katzev and H. Wylde Swiny (Oxford: Oxbow Books), 156–165.

Jimenez, C., Andreou, V., Evriviadou, M., Munkes, B., Hadjioannou, L., Petrou, A., et al. (2017a). Epibenthic communities associated with unintentional artificial reefs (modern shipwrecks) under contrasting regimes of nutrients in the Levantine Sea (Cyprus and Lebanon). *PloS One* 12, e0182486. doi: 10.1371/journal.pone.0182486

Jimenez, C., Hadjioannou, L., Petrou, A., Andreou, V., and Georgiou, A. (2017b). Fouling communities of two accidental artificial reefs (Modern shipwrecks) in Cyprus (Levantine sea). *Water* 9, 1–11. doi: 10.3390/w9010011

Jiménez, C., Hadjioanou, L., Petrou, A., Nikolaides, A., Evriviadou, M., and Lange, M. A. (2016). Mortality of the scleractinian coral *Cladocora caespitosa* during a warming event in the Levantine Sea (Cyprus). *Region. Environ. Change* 16, 1963. doi: 10.1007/s10113-014-0729-2

Jimenez, C., Petrou, A., Papatheodoulou, M., and Resaikos, V. (2022). "No one is safe: destruction of coralligenous concretions and other benthic sciaphilic communities in the MPA Cape Greco (Cyprus)," in *4th Mediterranean Symposium on the conservation of Coralligenous & other Calcareous Bio-Concretions*, Genoa, Italy, 20-21 September 2022. 74–79.

Josende, M. E., Nunes, S. M., de Oliveira Lobato, R., González-Durruthy, M., Kist, L. W., Bogo, M. R., et al. (2020). Graphene oxide and GST-omega enzyme: An interaction that affects arsenic metabolism in the shrimp *Litopenaeus vannamei*. *Sci. Total Environ.* 716, 136893. doi: 10.1016/j.scitotenv.2020.136893

Karami, A., Christianus, A., Ishak, Z., Syed, M. A., and Courtenay, S. C. (2011). The effects of intramuscular and intraperitoneal injections of benzo[a]pyrene on selected biomarkers in Clarias gariepinus. *Ecotoxicol. Environ. Saf.* 74, 1558–1566. doi: 10.1016/j.ecoenv.2011.05.012

Kayal, M., and Adjeroud, M. (2022). The war of corals: patterns, drivers and implications of changing coral competitive performances across reef environments. *R. Soc. Open Sci.* 9, 220003. doi: 10.1098/rsos.220003

Kohler, K. E., and Gill, S. M. (2006). Coral Point Count with Excel extensions (CPCe): A Visual Basic program for the determination of coral and substrate coverage using random point count methodology. *Comput. Geosci.* 32, 1259–1269. doi: 10.1016/j.cageo.2005.11.009

Lachs, L., Humanes, A., Pygas, D. R., Bythell, J. C., Mumby, P. J., Ferrari, R., et al. (2023). No apparent trade-offs associated with heat tolerance in a reef-building coral. *Commun. Biol.* 6 (1), art. no. 400. doi: 10.1038/s42003-023-04758-6

Lesser, M. P. (2006). Oxidative stress in marine environments: Biochemistry and physiological ecology. *Annu. Rev. Physiol.* 68, 253–278. doi: 10.1146/annurev.physiol.68.040104.110001

Liñán-Cabello, M. A., Flores-Ramírez, L. A., Zenteno-Savin, T., Olguín-Monroy, N. O., Sosa-Avalos, R., Patiño-Barragan, M., et al. (2010). Seasonal changes of antioxidant and oxidative parameters in the coral *Pocillopora capitata* on the Pacific coast of Mexico. *Mar. Ecol.* 31, 407–417. doi: 10.1111/j.1439-0485.2009.00349.x

Liñán-Cabello, M. A., Lesser, M. P., Flores-Ramírez, L. A., Zenteno-Savín, T., and Reyes-Bonilla, H. (2011). Oxidative stress in coral-photobiont communities. *Oxid. Stress Aquat. Ecosyst.* 127–137. doi: 10.1002/9781444345988.ch9

Lowry, O. H., Rosebrough, N. J., Farr, A. L., and Randall, R. J. (1951). Protein measurement with the Folin phenol reagent. *J. Biol. Chem.* 193, 265–275. doi: 10.1016/S0021-9258(19)52451-6

Lushchak, V. I. (2011). Environmentally induced oxidative stress in aquatic animals. *Aquat. Toxicol.* 101, 13–30. doi: 10.1016/j.aquatox.2010.10.006

Menezes, N., Cruz, I., da Rocha, G. O., de Andrade, J. B., and Leão, Z. M. A. N. (2023). Polycyclic aromatic hydrocarbons in coral reefs with a focus on Scleractinian corals: A systematic overview. *Sci. Total Environ.* 877, 162868. doi: 10.1016/j.scitotenv.2023.162868

Monchanin, C., Mehrotra, R., Haskin, E., Scott, C. M., Plaza, P. U., Allchurch, A., et al. (2021). Contrasting coral community structures between natural and artificial substrates at Koh Tao, Gulf of Thailand. *Mar. Environ. Res.* 172, 105505. doi: 10.1016/j.marenvres.2021.105505

Montilla, L. M., Ramos, R., García, E., and Cróquer, A. (2016). Caribbean yellow band disease compromises the activity of catalase and glutathione S-transferase in the reef-building coral *Orbicella faveolata* exposed to anthracene. *Dis. Aquat. Organ.* 119, 153–161. doi: 10.3354/dao02980

Nardi, A., Benedetti, M., Fattorini, D., and Regoli, F. (2018). Oxidative and interactive challenge of cadmium and ocean acidification on the smooth scallop *Flexopecten glaber*. *Aquat. Toxicol.* 196, 53–60. doi: 10.1016/j.aquatox.2018.01.008

Nardi, A., Mincarelli, L. F., Benedetti, M., Fattorini, D., d'Errico, G., and Regoli, F. (2017). Indirect effects of climate changes on cadmium bioavailability and biological effects in the Mediterranean mussel *Mytilus galloprovincialis*. *Chemosphere* 169, 493–502. doi: 10.1016/j.chemosphere.2016.11.093

Osman, A. M., Van Den Heuvel, H., and Van Noort, P. C. M. (2007). Differential responses of biomarkers in tissues of a freshwater mussel, *Dreissena polymorpha*, to the exposure of sediment extracts with different levels of contamination. *J. Appl. Toxicol.* 27, 51–59. doi: 10.1002/jat.1183

Özaslan, M. S., Demir, Y., Aksoy, M., Küfrevioğlu, Ö.I., and Beydemir, Ş. (2018). Inhibition effects of pesticides on glutathione-S-transferase enzyme activity of Van Lake fish liver. *J. Biochem. Mol. Toxicol.* 32, e22196. doi: 10.1002/jbt.22196

Ramos, R., and García, E. (2007). Induction of mixed-function oxygenase system and antioxidant enzymes in the coral Montastraea faveolata on acute exposure to benzo(a) pyrene. *Comp. Biochem. Physiol. - C Toxicol. Pharmacol.* 144, 348–355. doi: 10.1016/j.cbpc.2006.11.006

Regoli, F., Cerrano, C., Chierici, E., Chiantore, M. C., and Bavestrello, G. (2004a). Seasonal variability of prooxidant pressure and antioxidant adaptation to symbiosis in the Mediterranean demosponge *Petrosia ficiformis*. *Mar. Ecol. Prog. Ser.* 275, 129–137. doi: 10.3354/meps275129

Regoli, F., and Giuliani, M. E. (2014). Oxidative pathways of chemical toxicity and oxidative stress biomarkers in marine organisms. *Mar. Environ. Res.* 93, 106–117. doi: 10.1016/j.marenvres.2013.07.006

Regoli, F., Nigro, M., Chierici, E., Cerrano, C., Schiapparelli, S., Totti, C., et al. (2004b). Variations of antioxidant efficiency and presence of endosymbiotic diatoms in the Antarctic porifera *Haliclona dancoi*. *Mar. Environ. Res.* 58, 637–640. doi: 10.1016/j.marenvres.2004.03.055

Regoli, F., and Winston, G. W. (1998). Applications of a new method for measuring the total oxyradical scavenging capacity in marine invertebrates. *Mar. Environ. Res.* 46, 439–442. doi: 10.1016/S0141-1136(97)00119-0

Reitzel, A. M., Passamaneck, Y. J., Karchner, S. I., Franks, D. G., Martindale, M. Q., Tarrant, A. M., et al. (2014). Aryl hydrocarbon receptor (AHR) in the cnidarian

Nematostella vectensis: Comparative expression, protein interactions, and ligand binding. *Dev. Genes Evol.* 224, 13–24. doi: 10.1007/s00427-013-0458-4

Ricevuto, E., Benedetti, M., Regoli, F., Spicer, J. I., and Gambi, M. C. (2015). Antioxidant capacity of polychaetes occurring at a natural CO2 vent system: Results of an in *situ* reciprocal transplant experiment. *Mar. Environ. Res.* 112, 44–51. doi: 10.1016/j.marenvres.2015.09.005

Rougée, L., Downs, C. A., Richmond, R. H., and Ostrander, G. K. (2006). Alteration of normal cellular profiles in the scleractinian coral (*Pocillopora damicornis*) following laboratory exposure to fuel oil. *Environ. Toxicol. Chem.* 25, 3181–3187. doi: 10.1897/05-510R2.1

Schlezinger, J. J., Struntz, W. D. J., Goldstone, J. V., and Stegeman, J. J. (2006). Uncoupling of cytochrome P450 1A and stimulation of reactive oxygen species production by co-planar polychlorinated biphenyl congeners. *Aquat. Toxicol.* 77, 422–432. doi: 10.1016/j.aquatox.2006.01.012

Scuba (2022) *The Best Shipwreck Dive Sites in the World*. Available online at: https://www.scuba.com/blog/best-shipwreck-dive-sites/ (Accessed 20 September, 2023).

Shakunthala, N. (2010). New cytochrome P450 mechanisms: Implications for understanding molecular basis for drug toxicity at the level of the cytochrome. *Expert Opin. Drug Metab. Toxicol.* 6, 1–15. doi: 10.1517/17425250903329095

Solé, M., Freitas, R., and Rivera-Ingraham, G. (2021). The use of an in *vitro* approach to assess marine invertebrate carboxylesterase responses to chemicals of environmental concern. *Environ. Toxicol. Pharmacol.* 82, 103561. doi: 10.1016/j.etap.2020.103561

Stipcich, P., Beca-Carretero, P., Álvarez-Salgado, X. A., Apostolaki, E. T., Chartosia, N., Efthymiadis, P. T., et al. (2023). Effects of high temperature and marine heat waves on seagrasses: Is warming affecting the nutritional value of *Posidonia oceanica*? *Mar. Environ. Res.* 184, 105854. doi: 10.1016/j.marenvres.2022.105854

Sokolova, I. M. (2013). Energy-limited tolerance to stress as a conceptual framework to integrate the effects of multiple stressors. *Integr. Comp. Biol.* 53 (4), 597–608. doi: 10.1093/icb/ict028

Tang, J., Ni, X., Zhou, Z., Wang, L., and Lin, S. (2018). Acute microplastic exposure raises stress response and suppresses detoxification and immune capacities in the scleractinian coral Pocillopora damicornis. *Environ. Pollut.* 243, 66–74. doi: 10.1016/j.envpol.2018.08.045

Tarrant, A. M., Reitzel, A. M., Kwok, C. K., and Jenny, M. J. (2014). Activation of the cnidarian oxidative stress response by ultraviolet radiation, polycyclic aromatic hydrocarbons and crude oil. *J. Exp. Biol.* 217, 1444–1453. doi: 10.1242/jeb.093690

Turner, N. R., and Renegar, D. A. (2017). Petroleum hydrocarbon toxicity to corals: A review. *Mar. pollut. Bull.* 119, 1–16. doi: 10.1016/j.marpolbul.2017.04.050

van der Schyff, V., du Preez, M., Blom, K., Kylin, H., Choong, N. S., Yive, K., et al. (2020). Impacts of a shallow shipwreck on a coral reef: a case study from st. Brandon's Atoll, Mauritius, Indian Ocean. *Mar. Environ. Res.* 156, 104916. doi: 10.1016/j.marenvres.2020.104916

Vašková, J., Kočan, L., Vaško, L., and Perjési, P. (2023). Glutathione-related enzymes and proteins: A review. *Molecules* 28, 1447. doi: 10.3390/molecules28031447

Wang, H., Pan, L., Zhang, X., Ji, R., Si, L., and Cao, Y. (2020). The molecular mechanism of AhR-ARNT-XREs signaling pathway in the detoxification response induced by polycyclic aromatic hydrocarbons (PAHs) in clam Ruditapes philippinarum. *Environ. Res.* 183, 109165. doi: 10.1016/j.envres.2020.109165

Wulff, J. L. (2006). Ecological interactions of marine sponges. *Can. J. Zool.* 84, 146–166. doi: 10.1139/z06-019

Xiang, N., Jiang, C., Yang, T., Li, P., Wang, H., Xie, Y., et al. (2018). Occurrence and distribution of Polycyclic aromatic hydrocarbons (PAHs) in seawater, sediments and corals from Hainan Island, China. *Ecotoxicol. Environ. Saf.* 152, 8–15. doi: 10.1016/j.ecoenv.2018.01.006

Yakovleva, I., Bhagooli, R., Takemura, A., and Hidaka, M. (2004). Differential susceptibility to oxidative stress of two scleractinian corals: Antioxidant functioning of mycosporine-glycine. *Comp. Biochem. Physiol. - B Biochem. Mol. Biol.* 139, 721–730. doi: 10.1016/j.cbpc.2004.08.016

Yamada, M., Takada, H., Toyoda, K., Yoshida, A., Shibata, A., Nomura, H., et al. (2003). Study on the fate of petroleum-derived polycyclic aromatic hydrocarbons (PAHs) and the effect of chemical dispersant using an enclosed ecosystem, mesocosm. *Mar. Pollut. Bull.* 47, 105–113. doi: 10.1016/S0025-326X(03)00102-4

frontiers | Frontiers in Physiology

TYPE Original Research
PUBLISHED 11 June 2024
DOI 10.3389/fphys.2024.1303681

OPEN ACCESS

EDITED BY
Ranjeet Bhagooli,
University of Mauritius, Mauritius

REVIEWED BY
Michael Morgan,
Berry College, United States
Israel Aníbal Vega,
CONICET Dr. Mario H. Burgos Institute of Histology and Embryology (IHEM), Argentina

*CORRESPONDENCE
Colin Lock,
clockdive@gmail.com

‡PRESENT ADDRESS
Colin Lock,
Climate Change Cluster, University of Technology Sydney, Ultimo, New South Wales, Australia

RECEIVED 28 September 2023
ACCEPTED 10 May 2024
PUBLISHED 11 June 2024

CITATION
Lock C, Gabriel MM and Bentlage B (2024), Transcriptomic signatures across a critical sedimentation threshold in a major reef-building coral.
Front. Physiol. 15:1303681.
doi: 10.3389/fphys.2024.1303681

Transcriptomic signatures across a critical sedimentation threshold in a major reef-building coral

Colin Lock *‡, Melissa M. Gabriel and Bastian Bentlage

Marine Laboratory, University of Guam, Mangilao, GU, United States

Sedimentation is a major cause of global near-shore coral reef decline. Although the negative impacts of sedimentation on coral reef community composition have been well-documented, the effects of sedimentation on coral metabolism *in situ* have received comparatively little attention. Using transcriptomics, we identified gene expression patterns changing across a previously defined sedimentation threshold that was deemed critical due to changes in coral cover and community composition. We identified genes, pathways, and molecular processes associated with this transition that may allow corals, such as *Porites lobata*, to tolerate chronic, severe sedimentation and persist in turbid environments. Alternative energy generation pathways may help *P. lobata* maintain a persistent stress response to survive when the availability of light and oxygen is diminished. We found evidence for the expression of genes linked to increased environmental sensing and cellular communication that likely allow *P. lobata* to efficiently respond to sedimentation stress and associated pathogen challenges. Cell damage increases under stress; consequently, we found apoptosis pathways over-represented under severe sedimentation, a likely consequence of damaged cell removal to maintain colony integrity. The results presented here provide a framework for the response of *P. lobata* to sedimentation stress under field conditions. Testing this framework and its related hypotheses using multi-omics approaches can deepen our understanding of the metabolic plasticity and acclimation potential of corals to sedimentation and their resilience in turbid reef systems.

KEYWORDS

apoptosis, cell adhesion, immune response, metabolism, gene expression, stress, Symbiodiniaceae, Porites

Introduction

Coral reefs play important cultural, ecological, and economic roles in Guam and throughout the Northern Mariana Islands (Burdick et al., 2008). Reefs recycle nutrients, provide a habitat for marine organisms, and prevent coastline erosion from strong storms and wave action (Hughes et al., 2003). Stony corals (Scleractinia) are complex holobionts, with approximately half of the more than 1,600 described species hosting an endosymbiotic assemblage of dinoflagellate algae (Symbiodiniaceae) that are central to metabolic homeostasis through nutritional mutualism (Gault et al., 2021). However, climate change and other anthropogenic stressors threaten this mutualistic relationship and, in turn, coral reefs (National Academies of Sciences, Engineering, and Medicine, 2019). Upland erosion caused by human activities such as wild-land arson, deforestation,

construction and development, and recreational off-roading has increased turbidity and sedimentation in Guam's watersheds, exerting significant stress on near-shore coral reef ecosystems (Reynolds et al., 2014; Minton et al., 2022). The destruction of wetlands and streams by coastal development has further increased sedimentation impacts on near-shore reefs in Guam (Scheman et al., 2002; Wolanski et al., 2003; Minton et al., 2022). The increasing erosion of soils and the resulting near-shore sedimentation are widespread global problems, leading to a decline in diversity and ecosystem services provided by coral reefs (Rogers and Ramos-Scharrón, 2022).

Suspended sediment particles increase turbidity and form aggregations that are deposited on corals through sedimentation, negatively impacting coral metabolism (Weber et al., 2012; Sheridan et al., 2014; Bollati et al., 2021; Tuttle and Donahue, 2022). Fine sediments and decaying organic matter deposited in near-shore reef systems deplete the available oxygen, which decreases pH and increases the oxygen demand of corals, resulting in oxidative stress (Erftemeijer et al., 2012; Flores et al., 2012; Tuttle and Donahue, 2022). To survive under such conditions, corals employ mitigation processes, such as increased mucus production and ciliary movement to shed the deposited sediment (Weber et al., 2012; Bessell-Browne et al., 2017), exerting high energetic costs that can lead to a decrease or cessation of other metabolic functions (Riegl and Branch, 1995; Anthony and Larcombe, 2000; Tuttle and Donahue, 2022). Sedimentation triggers coral immune responses that further deplete energy stores (Sheridan et al., 2014) and increase disease susceptibility (Sheppard et al., 2009). Increased turbidity caused by suspended sediments results in a decrease in the photosynthetic activity of coral-associated Symbiodiniaceae (Fabricius, 2005; Jones et al., 2020; Philipp and Fabricius, 2003). Bacteria (Franco et al., 2020) and anthropogenic chemicals (Ishibashi and Takeuchi, 2023) associated with runoff and sedimentation present further challenges beyond the physical removal of particulates from coral polyps. Critical thresholds for sedimentation at which coral mortality drastically increases range from as low as 10 mg cm^{-2} day^{-1} to as high as 300 mg cm^{-2} day^{-1}, depending on the coral species impacted, reef location, types of sediments deposited, and length of exposure to sedimentation (Erftemeijer et al., 2012; Jones et al., 2020; Tuttle and Donahue, 2022). Massive *Porites* spp., such as *Porites lobata*, are one of the few coral species groups known for their persistence under moderate-to-severe sedimentation (Rogers, 1990; Golbuu et al., 2011). Many *Porites* species have been observed to produce thick mucus envelopes that effectively help with the removal of sediment from tissue, and mucus thickness appears to be correlated with increasing sediment load (Bessell-Browne et al., 2017). Documented responses of *P. lobata* to sedimentation range from mortality caused by sedimentation rates as low as 30 mg cm^{-2} day^{-1} (Hodgson, 1990) to bleaching but no apparent mortality under severe sedimentation of 200 mg cm^{-2} day^{-1} for 6–8 days (Stafford-Smith, 1993). Large discrepancies in the reported sedimentation tolerances of *P. lobata* may suggest physiological plasticity within this species or represent uncertainties in the identification of massive *Porites* spp. and species-specific differences in acclimation potential. Regardless, the persistence of massive *Porites* spp. in environments affected by moderate-to-severe sedimentation represents unique opportunities for identifying the mechanisms of acclimation to sedimentation.

Transcriptome-level characterization of gene expression in corals provides insights into complex metabolic processes, which deepens our understanding of how corals respond to stressors, such as sedimentation, and, ultimately, their future survival (Barshis et al., 2013; Barshis et al., 2014). This approach has been used successfully to lay the foundation for identifying the molecular mechanisms that allow certain coral species to survive or thrive in marginal habitats (Barshis et al., 2014). Understanding the thresholds of sedimentation tolerance in corals may inform decision-making processes for coral reef conservation and restoration (Burdick et al., 2008; Barshis et al., 2014; Hughes et al., 2017; Tuttle and Donahue, 2022). Recent experimental work investigated coral gene expression in response to acute sedimentation under laboratory conditions and identified genes associated with energy metabolism and immune responses (Bollati et al., 2021). Under laboratory conditions, coral responses to sedimentation are generally tested by smothering corals under sediments for short periods of time (Bollati et al., 2021; Tuttle and Donahue, 2022). Considering that sedimentation stress under ecologically relevant conditions in the field may be more complex than laboratory experiments simulate, we used transcriptome data from field-collected corals to test whether the genes and pathways identified by Bollati et al. (2021) are differentially expressed under field conditions in a reef system impacted by sedimentation. Specifically, we employed transcriptomics to examine the gene expression profiles of *P. lobata* colonies tagged *in situ* for repeat sampling (Figure 1A, B) to understand the metabolic response of *P. lobata* and its endosymbiotic Symbiodiniaceae community living in a habitat characterized by moderate-to-severe sedimentation. Our analyses identified significant changes in gene expression profiles across a previously identified critical threshold of sedimentation across which coral mortality increases and community composition changes significantly in Fouha Bay, southern Guam (Minton et al., 2022). The genes identified by our analyses are consistent with the coral response mechanisms to sedimentation identified previously under laboratory conditions and provide insights into coral acclimation mechanisms in turbid, sedimentation-impacted reef ecosystems that act on an ecologically relevant scale.

Materials and methods

Study site and environment

The Humåtak watershed in southern Guam (13°28′ N, 144°45′ E) is characterized by basaltic rock, steep slopes, and lateritic soils that readily erode during heavy rainfalls (Foster and Ballendorf, 2023). The La Sa Fu'a River and its 5 km^2 catchment area belong to the Humåtak watershed that drains into Fouha Bay (Scheman et al., 2002), providing mean monthly freshwater discharges ranging from 0.3 m^3 s^{-1} (March–May) to 2.9 m^3 s^{-1} (August–October) (United States Geological Survey monitoring site 16809600 data averaged from 1953 to 2018; USGS, 2023), corresponding to dry- and wet-season rainfall patterns. Heavy rain events that occur primarily during the wet season and last, on average, 1–2 h transport sediment from eroding soils downstream into Fouha Bay, creating pulses of thick plumes that frequently exceed a suspended solid concentration (SSC) of 1,000 mg L^{-1} (Wolanski

10.3389/fphys.2024.1303681

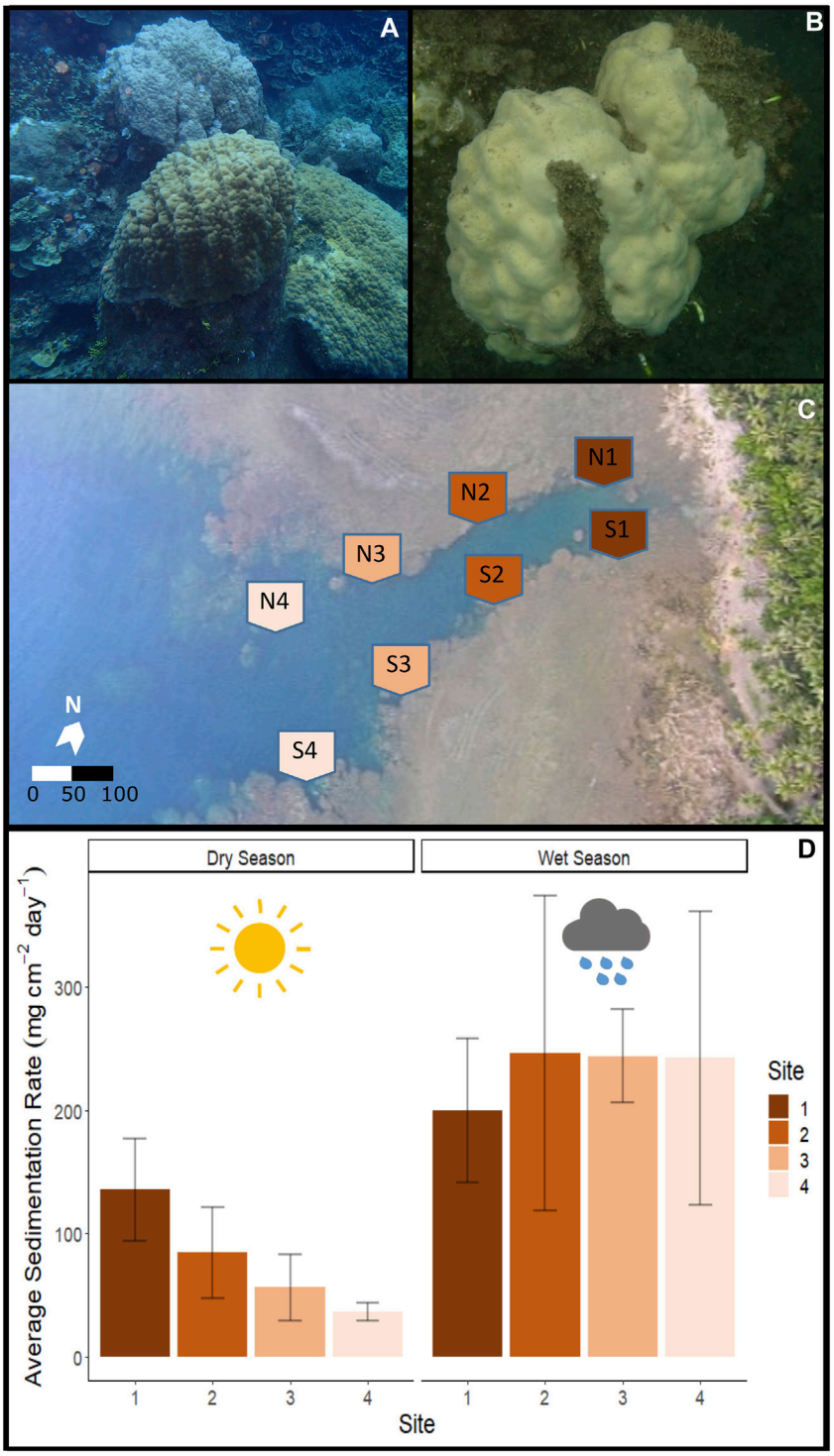

FIGURE 1
Fouha Bay (Guam) sampling locations and sedimentation rates. **(A)** *Porites lobata* colony sampled from the outer zone (N4) that shows minimal sediment accumulation (images taken during the dry season). **(B)** *P. lobata* colony sampled from the inner location (S1) that shows heavy sediment accumulation. **(C)** Aerial view of Fouha Bay and sampling sites. **(D)** Average sedimentation rate across sampling sites (N/S 1–4) during the dry and wet seasons.

et al., 2003). Suspended solids flocculate and slowly precipitate as marine snow when reaching the bay, dissipating the plume over a time span of approximately 5 days (Wolanski et al., 2003). Large sedimentation events occur, on average, 10 times annually in Fouha Bay, with approximately 75% of sediments staying within the bay for an estimated residence time of 4.5 years (Wolanski et al., 2003).

Massive *Porites* of the *P. lobata/lutea* species complex (Figures 1A, B) represent one of the few coral species groups that persist in

Fouha Bay along a gradient of sedimentation ranging from severe (sedimentation rate >50 mg cm^{-2} day^{-1}) to moderate (sedimentation rate ~10–~50 mg cm^{-2} day^{-1}) to light (sedimentation rate <10 mg cm^{-2} day^{-1}) as distance from the river mouth increases (Minton et al., 2022). Sites close to the river mouth are further characterized by decreased light available for coral photosynthesis due to high turbidity and decreased salinity due to freshwater discharge (Fifer et al., 2022).

To evaluate previously established sedimentation dynamics across Fouha Bay (Rongo, 2004; Minton et al., 2022), sedimentation rates during the period of this study were estimated using a sediment trap deployed at eight sites established within the bay following the procedure used by Rongo (2004) (Figure 1C). We deployed U24 HOBO (Onset, Bourne, MA) data loggers to record water conductivity and temperature at each sampling site. Conductivity was converted to salinity using the Practical Salinity Scale 1978 (PSS-78), as implemented in HOBOware Pro of Onset. Sediment was collected over a time period of 31 days during the dry (2 May 2018 to 1 June 2018) and wet (21 September 2018 to 22 October 2018) seasons using vertical PVC traps (diameter of 5 cm and height of 50 cm), following the recommendations of Storlazzi et al. (2011). The collected sediments were processed following the protocol proposed by Ensminger (2016). Wet-strengthened 120-micron filters (Whatman, Little Chalfont, United Kingdom) were first rinsed with deionized water and dried for 24 h at 100°C; the weight of each dried filter was recorded. The collected sediment samples were rinsed with deionized water to remove salt and allowed to settle again for 24 h; the organisms contained in the sediment samples were removed. The cleaned samples were then filtered using the previously dried 120-micron filters using a vacuum pump, followed by the drying of sediments collected on filter paper at 100°C.

The drying filters and sediments were weighed repeatedly over a period of 2 days until the weights remained constant, indicating that the samples had dried completely, allowing for the calculation of the accumulated sediment. The total accumulated sediment for each sample was normalized to mg cm^{-2} day^{-1} by dividing it by the diameter of the PVC sediment trap and the number of days that trap had been deployed. A Shapiro–Wilk test was used to test normality in the sedimentation dataset, and then ANOVA was used to compare sedimentation rates between sites, seasons, and sides (using the AOV function in base R, version 4.2.3). Similarly, ANOVA was used to test for differences in the daily average temperature and salinity between all sites and seasons and the interaction of sites and seasons on the days of transcriptomic sampling (16 May 2018 and 3 October 2018 for dry and wet seasons, respectively).

Coral tagging and identification

To identify the response of *P. lobata* and its Symbiodiniaceae endosymbionts (the experimental unit) in Fouha Bay, individual corals representing independent biological replicates (the unit of observation) were tagged at eight sites in Fouha Bay. At each of the eight sites in Fouha Bay (Figure 1C), at least three corals were tentatively identified in the field as *P. lobata* based on gross morphology and tagged for repeated sampling with cow tags that were zip-tied to adjacent reef pavements. Sediments and corals were sampled from the north and south sides of the channel into which the La Sa Fu'a River drains to capture the variation in sediment deposition and transcriptomic response, respectively. Coral colonies ranged in diameter from approximately 15 cm to 2 m, with colonies closer to the river mouth being smaller than more distant ones. Replicate colonies were chosen so that all colonies tagged were representative of the size classes observed at each site. Species were identified using a combination of corallite morphology and, given the difficulty of species-level identification of massive *Porites* species, DNA barcoding. Approximately 4 cm^2 fragments from all 24 tagged colonies were collected from the center of the colony using a hammer/chisel and preserved in ethanol for DNA extraction.

DNA was extracted from each tagged colony using the GenCatch Genomic DNA Extraction Kit (Epoch Life Science, Sugar Land, TX) following the manufacturer's protocol for tissue samples. Mitochondrial regions COX3-COX2 and ND5-tRNA-Trp-ATP8-COX1 were amplified with primer sets mt-16 and mt-20, respectively (Paz-García et al., 2016), in 25 µL reactions using 0.3 µM primers, 0.3 mM dNTP, 1× HiFi Fidelity Buffer, and 2.5 units of Taq (KAPA HiFi 1U). The thermocycler profile included an initial denaturation at 94°C for 120 s, followed by 30 cycles of 94°C for 30 s, 54°C for 30 s, and 72°C for 60 s, followed by a final extension at 72°C for 300 s. PCR products were sequenced using Sanger sequencing, and the resulting sequences were assembled using the overlap–layout–consensus algorithm implemented in Geneious Prime (Biomatters, Auckland, New Zealand). Following assembly, consensus sequences for each specimen were aligned to publicly available *Porites* spp. mitochondrial genomes using MAFFT v7.453. The maximum likelihood phylogeny was inferred from the concatenated, aligned regions using RAxML v8.2.12 (Stamatakis, 2014) under the GTRCAT model to allow for the efficient modeling of site heterogeneity across alignment regions that spanned multiple genes. The resulting phylogeny was rooted using *Porites fontanesii* following recent phylogenomic analyses (Terraneo et al., 2021); the robustness of the phylogeny was assessed using 1,000 non-parametric bootstrap replicates. Specimens grouped with *Porites lutea* were excluded from RNA sequencing, while specimens grouped with *P. lobata* were included in the set of specimens selected for gene expression analysis.

RNA extraction, sequencing, and transcriptome assembly

Tagged colonies were sampled on 16 May 2018 during the dry season and on 3 October 2018 during the wet season, following the passing of two tropical depressions that led to significant rainfalls. A single fragment of each coral colony was sampled using a hammer/chisel and immediately preserved in RNAlater (Sigma-Aldrich, St. Louis, MO, United States), followed by storage at −80°C until RNA extraction. RNA from specimens identified as *P. lobata* (see section above) was extracted using the E.Z.N.A. Mollusc RNA Kit (Omega Bio-Tek, Norcross, GA, United States), following the manufacturer's protocol. The extracted RNA was quantified using a Qubit Fluorometer (Life Technologies, Carlsbad, CA), and its integrity

was verified using a bioanalyzer (Agilent Technologies, Santa Clara, CA), leading to the selection of 32 samples from different colonies for RNA sequencing. Sequencing libraries were constructed using NEBNext library kits (New England Biolabs, Ipswich, MA, United States) and sequenced on a NextSeq 550 Sequencer (Illumina, San Diego, CA, United States), generating 150-bp paired-end data. Adapter sequences and bases with a Phred-scaled quality score of less than 30 were removed using Trim Galore (Martin, 2011). The sequence data were deposited in GenBank of the NCBI (accession numbers are provided in Supplementary Table S1).

We employed *de novo* transcriptome assembly, following the best practices outlined by Grabherr et al. (2013). After the exclusion of two samples that yielded few sequencing reads (Supplementary Table S2), the sequencing data were combined and normalized using the Trinity v2.10.0 (Grabherr et al., 2013) *in silico* normalization function with maximum coverage set to 50 to reduce the computational requirements of the transcriptome assembly that used the default parameters of Trinity. After transcriptome assembly, TransDecoder v5.5.0 (Haas et al., 2013) was used to predict open reading frames (ORFs), followed by the removal of non-coding transcripts. Non-target contaminant sequences were identified and removed from the transcriptome assembly using the Perl script Alien Index (Ryan, 2014) with the approach outlined by Lock et al. (2022). Representative proteomes inferred from translated coding sequences (391,427 sequences) for each major bacterial clade (Schulz et al., 2017), fungi, *Stramenopiles*, poriferans, arthropods, molluscs, and annelids were obtained from GenBank of the NCBI and indexed in a non-target (alien) BLAST (Altschul et al., 1990) database; 57,401 coral and 72,664 Symbiodiniaceae proteome sequences were included as target sequences (file S1). Protein BLAST searches (e-value < $1e^{-3}$) using the ORFs predicted from our transcriptome assembly by TransDecoder as queries were run against the combined non-target (alien) and target (Cnidaria plus Symbiodiniaceae) protein databases to identify and remove likely contaminant sequences from our *de novo* assembled transcriptome using the Alien Index (Ryan, 2014). Target coral and Symbiodiniaceae ORFs were annotated based on the best BLAST hit (e-value < 1e-5) against a database containing 129,600 cnidarian (including corals and other cnidarians) and 44,114 Symbiodiniaceae amino acid (protein) sequences (Supplementary Table S3) obtained from the UniProt database (Bateman et al., 2017).

Benchmarking Universal Single-Copy Orthologs (BUSCO) v5.1.2 (Simão et al., 2015) was used to estimate the completeness of the taxonomically filtered *P. lobata* and Symbiodiniaceae transcriptomes. The transcriptome assemblies for *P. lobata* and Symbiodiniaceae were compared against the metazoan and alveolate BUSCO gene sets, respectively. For *de novo* assembled transcriptomes, it is expected that multiple predicted isoforms map to the same BUSCO gene, which can lead to high inferred gene duplication rates. To account for this potential artifact, multiple isoforms of the same gene model that mapped to the same BUSCO gene were counted as a single hit.

Identification of Symbiodiniaceae clades

RNA sequence reads from each sample (Supplementary Table S2) were mapped against publicly available Symbiodiniaceae transcriptomes (Bayer et al., 2012; Ladner et al., 2012) using a custom Perl script (zooxType3. pl; Manzello et al., 2019). The number of high-quality reads (MAPQ >40) mapped to representative Symbiodiniaceae transcriptome assemblies was used to calculate the proportions of *Symbiodinium*, *Breviolum*, *Cladocopium*, and *Durusdinium* in the sampled *P. lobata* colonies (Manzello et al., 2019). PERMANOVA from the R package, pairwise Adonis (version 0.4.1), was used to test for significant differences in Symbiodiniaceae community composition between sites, zones, and seasons.

Read abundance estimation

Transcriptomes assembled *de novo* usually generate more gene models and transcripts than predicted from whole-genome sequences, with the read coverage frequently not being uniform across inferred transcripts (*cf.* Hayer et al., 2015). This is often addressed by collapsing inferred transcripts using clustering based on a similarity cutoff chosen prior to differential gene expression analysis. Rather than reducing the size of our transcriptome through transcript clustering based on an arbitrarily chosen cutoff, we followed the "analysis first, aggregation second" approach proposed by Yi et al. (2018), which addresses the issue of uneven read coverage across transcripts by aggregating *p*-values from transcript-level differential expression analysis to identify differentially expressed genes (DEGs). Transcript abundances were estimated using the fast k-mer hashing and pseudo-alignment algorithm implemented in Kallisto v0.46.2 (Pimentel et al., 2017), followed by differential gene expression analysis in R using the Sleuth v0.30.0 (Pimentel et al., 2017) package. Read counts for transcripts belonging to the same gene were aggregated (*p*-value aggregation (Pimentel et al., 2017) to infer differential expression at the gene level.

Differential gene expression and GO enrichment

Our analysis included several units of analysis to explore the variation in the data: comparisons between sampling sites (and zones of the bay), between the sides of the bay, and seasons. Note that comparisons across seasons include repeated measures of gene expression from the same individuals collected during dry and wet seasons. A likelihood ratio test was used to compare full and null (reduced) models to identify significant DEGs between sites, locations, and seasons while accounting for variation of other factors incorporated in the two models (full model: Site + Season + Side [N or S]; null model: Season + Side). All pairwise comparisons between sites (1 vs. 2, 2 vs. 3, *etc.*) were assessed for DEGs (*q*-value <0.05) with the side of Fouha Bay (N or S) and season used for the null model. Since comparisons 1 vs. 2 and 3 vs. 4 showed extremely low DEGs, sites 1 and 2 were combined into inner zones (closer to the river) and sites 3 and 4 into outer zones (closer to the opening of Fouha Bay) for further comparisons. Wald's tests were used within Sleuth to obtain log2 fold changes of DEGs between conditions. Genes identified as differentially expressed were separated into up and downregulated (enriched in the inner and outer zones, respectively; Figure 5) and used for GO enrichment analysis using R package GO_MWU using default parameters (Wright et al., 2015). The R packages pheatmap (version 1.0.12)

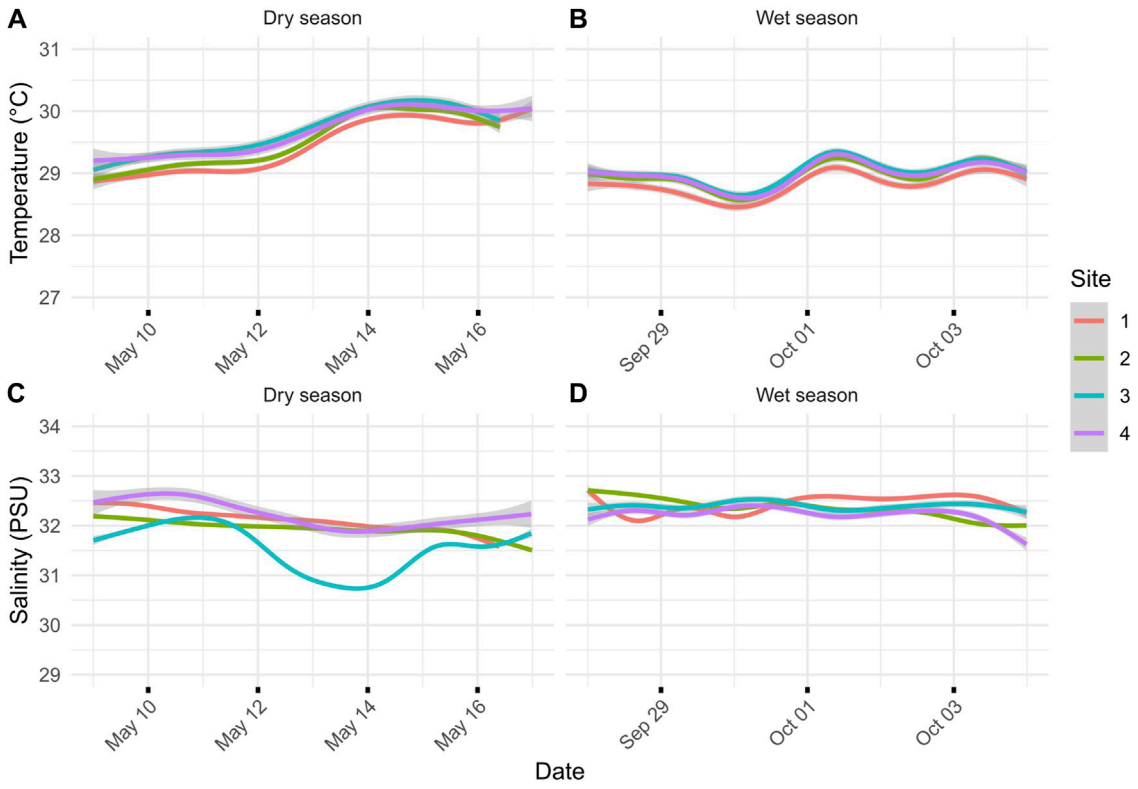

FIGURE 2
(A) Dry-season temperature for the sites during the 7 days leading up to transcriptomic sampling on 16 May 2018. **(B)** Wet-season temperature for the sites during the 7 days leading up to transcriptomic sampling on 4 October 2018. **(C)** Salinity (ppt) during the dry season leading up to transcriptomic sampling. **(D)** Salinity (PSU) during the wet season leading up to transcriptomic sampling. Lines represent the average of two loggers, and gray areas represent 95% confidence intervals: one for the north and south sides of the river channel.

and ggplot2 (version 3.4.2) were used to visualize the heatmap and GO enrichment plots, respectively.

Results

Seasonal sedimentation patterns

During the dry season, sedimentation rates showed a gradient from severe sedimentation, exceeding rates of 135 mg cm^{-2} day^{-1} near the river mouth at sites N1 and S1 to moderate rates of 36 mg cm^{-2} day^{-1} at sites N4 and S4 (Figures 1C,D). Comparison of the inner (sites 1 and 2) and outer (sites 3 and 4) zones showed statistically significant differences in sedimentation rates for the dry season (p-value = 0.029). The side of the river channel was not significantly different for sedimentation rates (p-value = 0.091). During the wet season, sedimentation rates converged, being extremely severe across all sites (p = 0.993; Figure 1D). Average sedimentation rates did not differ between seasons for sites N1 and S1, but sedimentation increased for the remaining sites during the wet season compared to the dry season (Figure 1D). These seasonal differences in sedimentation rates were mirrored by differences in rainfall, with precipitation recorded at the Humåtak rain gauge being almost twice as high during the wet season from 21 September 2018 to 22 October 2018 (~15 mm day^{-1}) compared to the dry season from 2 May 2018 to 1 June 2018 (~8 mm day^{-1}) (US Geological Survey monitoring site 131729144393766; USGS, 2023). The only significant difference in salinity and temperature on sampling days was the temperature when comparing between seasons. The maximum temperature difference between seasons on the sampling days at any site was 1.02°C (S4 dry season vs. S4 wet season; p-value <0.001). The temperature was very similar for all sites for the 7 days leading up to sampling during both the dry (Figure 1A) and wet (Figure 1B) seasons and not significantly different across sites (wet season p-value = 0.123 and dry season p-value = 0.549). While salinity varied by site for the 7 days leading up to sampling, the variation in salinity was not significant on the day of sampling for different sites, i.e., <1 and <0.7 PSU for dry (p-value = 0.7644) and wet seasons (p-value = 0.943), respectively. Salinity comparisons between seasons on the sampling day were not significant (p-value = 0.494).

Species identification, sample selection, and RNA sequencing

Massive *Porites* species are morphologically cryptic (Forsman et al., 2015). Using a DNA barcoding approach, we assigned 20 tagged coral colonies to *P. lobata*, forming a well-supported monophyletic clade, while 4 colonies were assigned to *P. lutea* (Figure 3A) and excluded from further analyses. RNA was extracted from the 20 coral colonies identified as *P. lobata*. For

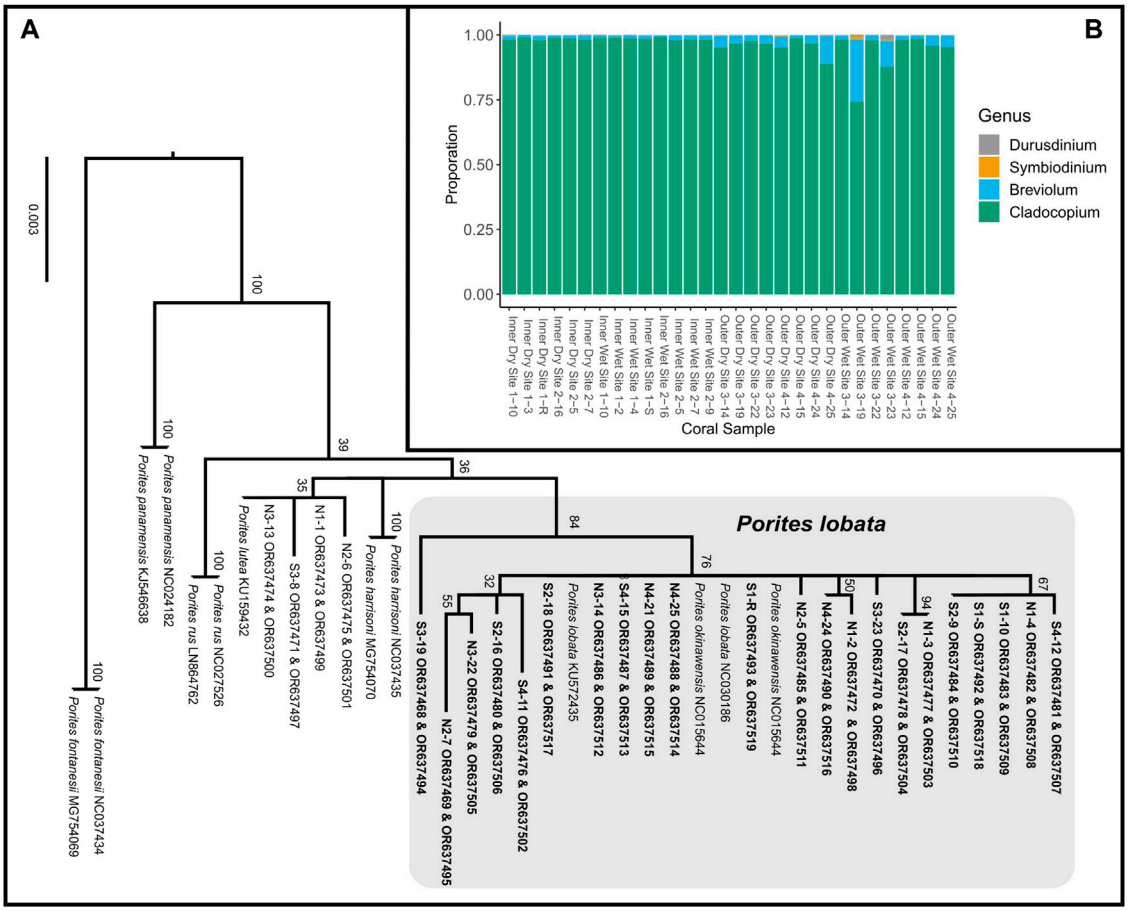

FIGURE 3
(A) Maximum likelihood phylogeny of concatenated mitochondrial COX3-COX2 and ND5-tRNA-Trp-ATP8-COX1 inferred under the GTRCAT model implemented in RAxML (Stamatakis, 2014). Node support was evaluated using 1,000 non-parametric bootstrap replicates. Tagged *Porites* colonies indicated by site, followed by specimen number (e.g., N2-6 represents specimen tag 6 from site N2); colonies in bold were sampled for transcriptome sequencing. ORXXXXXX are the GeneBank accession numbers for that sample. **(B)** Proportionate contributions of Symbiodiniaceae clades contained in each *P. lobata* sample based on read mapping to reference transcriptomes.

each site (N1 to N4 and S1 to S4; Figure 2C), samples that produced the best-quality RNA extracts (RIN >6) were chosen for sequencing, yielding a total of 30 samples (Supplementary Table S1, 2; Figure 2C) for differential gene expression analysis.

RNA sequencing generated 81,379,001 ± 55,399,881 (mean ± SD) reads, with 73,696,495 ± 51,328,889 reads retained after quality trimming. After *de novo* transcriptome assembly of the filtered reads, removal of contaminants, and taxonomic binning, the resulting *P. lobata* and Symbiodiniaceae transcriptomes contained 72,813 putative gene models (105,623 transcripts) and 57,891 putative gene models (72,428 transcripts), respectively. The transcriptome of *P. lobata* was relatively complete, with almost 90% of BUSCO genes complete (C: 88.5% [S: 78.2%, D: 10.3%], F: 5.0%, M: 6.5%, n: 954); the Symbiodiniaceae transcriptome contained close to 70% of complete BUSCO genes (C: 67.8% [S: 44.4%, D: 23.4%], F: 6.4%, M: 25.8%, n: 171). Relatively higher levels of BUSCO gene duplication are expected in transcriptome assemblies than in genome assemblies, as multiple transcripts (isoforms) may map to the same BUSCO gene. Mapping of Symbiodiniaceae transcripts to publicly available Symbiodiniaceae transcriptomes revealed that all *P. lobata* colonies predominately harbored (>74% relative abundance) *Cladocopium* spp., with most samples showing >95% abundance of *Cladocopium* spp. (Figure 3B; Supplementary Table S4). This is consistent with the findings obtained by Fifer et al. (2022), who showed that *P. lobata*-associated Symbiodiniaceae communities in Fouha Bay were dominated by *Cladocopium* C15. PERMANOVA tests revealed that the site (p-value = 0.0750), zone (p-value = 0.0518), and season (p-value = 0.5649) were not significantly different in Symbiodiniaceae community composition.

Differential gene expression and GO term enrichment

Likelihood ratio tests of the pairwise comparisons (see *Methods* "Differential gene expression and GO enrichment") between the sides of the river channel (N vs. S) produced few differentially expressed genes (42 in *P. lobata* and 0 in Symbiodiniaceae; Table 2). Comparisons between sites produced similar results for *P. lobata* and Symbiodiniaceae: fewer than two genes were differentially expressed when comparing between sites 1 and 2 and 3 and 4

TABLE 1 Number of differentially expressed genes for each pairwise comparison between sites using likelihood ratio model comparisons; factors included in null models given in brackets. Sites were merged into inner (sites 1 and 2) and outer (sites 3 and 4) zones based on the low gene expression between those sites.

Porites lobata: inner versus outer zone [side (N/S) + season]					Symbiodiniaceae: inner versus outer zone [side (N/S) + season]				
Site	1	2	3	4	Site	1	2	3	4
1	-				1	-			
2	2	-			2	0	-		
3	736	499	-		3	825	97	-	
4	873	1,333	0	-	4	435	488	0	-

TABLE 2 Number of differentially expressed genes identified for *Porites lobata* and its Symbiodiniaceae endosymbionts using likelihood ratio model comparisons; factors included in null models given in brackets. The comparison of inner and outer zones yielded the largest number of differentially expressed genes. Arrows in the last row indicate the number of genes upregulated (↑) and downregulated (↓) in the inner zone, which all subsequent analyses are based on.

Comparison	*Porites lobata*	Symbiodiniaceae
Season: dry versus wet [side (N/S) + zone]	5	0
Season (inner zone): dry versus wet [side (N/S)]	11	0
Season (outer zone): dry versus wet [side (N/S)]	0	0
Side: north (N) versus south (S) [season + site]	42	0
Zone: inner versus outer [season + side (N/S)]	1,702 (↑ 433; ↓ 1,259)	1,514 (↑ 319; ↓1,195)

(Table 1). Given these results, sites were combined into an inner zone (sites 1 and 2) and an outer zone (sites 3 and 4) that correspond to the transition between moderate and severe sedimentation. Taking the variation between zones (inner versus outer) and sides (N or S) into account, the season produced five DEGs for *P. lobata* and none for Symbiodiniaceae (Table 2). Additionally, comparisons of the wet versus dry seasons for only the inner and outer zones revealed between 0 and 11 DEGs for *P. lobata* and none for the Symbiodiniaceae (Table 2). The side of Fouha Bay (north versus south) produced 42 differentially expressed genes for *P. lobata* and none for Symbiodiniaceae.

The zone (inner versus outer) produced the largest number of DEGs for both *P. lobata* (1,702 DEGs; 433 upregulated and 1,259 downregulated in the inner zone) and Symbiodiniaceae (1,514 DEGs; 319 upregulated and 1,195 downregulated in the inner zone) (Table 1; Supplementary Table S5). These results mirror the patterns of gene expression profile similarity that largely group samples by zone rather than season, differentiating between the inner zone affected by severe sedimentation and the outer zone impacted by moderate sedimentation (Figure 4). GO enrichment analysis (Supplementary Table S7) identified 38 biological processes enriched ($p < 0.01$) in *P. lobata* (Figures 5A, B) and 10 biological processes enriched ($p < 0.01$) in Symbiodiniaceae (Figures 5C, D), which were separated into GO categories enriched in the inner and outer zones. It is worth noting that gene annotation and subsequent GO enrichment analysis are based on gene homology with mostly vertebrate model organisms that possess immune responses that differ from the innate immune responses of cnidarians. However, we identified the most similar homologs across publicly available cnidarian sequence data that provide our current best understanding of non-model cnidarian genes.

Discussion

Severe sedimentation in Fouha Bay began in the 1980s because of improper soil management during road construction, which has led to a decrease in coral cover when comparing coral community surveys prior to construction (Randall and Birkeland, 1978) with more recent surveys (Rongo, 2004; Minton et al. 2022). During our sampling periods, sedimentation ranged from moderate (37 mg cm^{-2} day^{-1}) to severe (136 mg cm^{-2} day^{-1}) during the dry season along the environmental gradient sampled in Fouha Bay (Figure 1D). During the wet season, all sites were inundated with extremely severe levels of sedimentation (>200 mg cm^{-2} day^{-1}; range: 199–245 mg cm^{-2} day^{-1}) (Figure 1D). Our observations are consistent with those of previous studies that documented and modeled sedimentation rates at times exceeding 200 mg cm^{-2} day^{-1} in Fouha Bay (Randall and Birkeland, 1978; Wolanski et al., 2003; Rongo, 2004; Minton et al., 2022). Rongo (2004) proposed a model of annualized sedimentation rates (N1/S1 = 102.5 mg cm^{-2} day^{-1}, N2/S2 = 65.2 mg cm^{-2} day^{-1}, N3/S3 = 53.4 mg cm^{-2} day^{-1}, and N4/S4 = 22.5 mg cm^{-2} day^{-1}), which closely mirrors our sampling period in the dry season and shows a gradient of sedimentation rates decreasing from the river mouth toward the outer parts of Fouha Bay (Figure 1D), with the transition from moderate to severe sedimentation between the inner and outer zones representing a significant difference in sedimentation rates. However, wet season sedimentation documented by us, albeit with limited sampling, showed that the sedimentation gradient in Fouha Bay broke down during the wet season, with all sites becoming impacted by severe sedimentation. Nonetheless, decreases in coral coverage and species richness documented over the last 40 years in Fouha Bay, linked to long-term chronic sedimentation stress, followed the

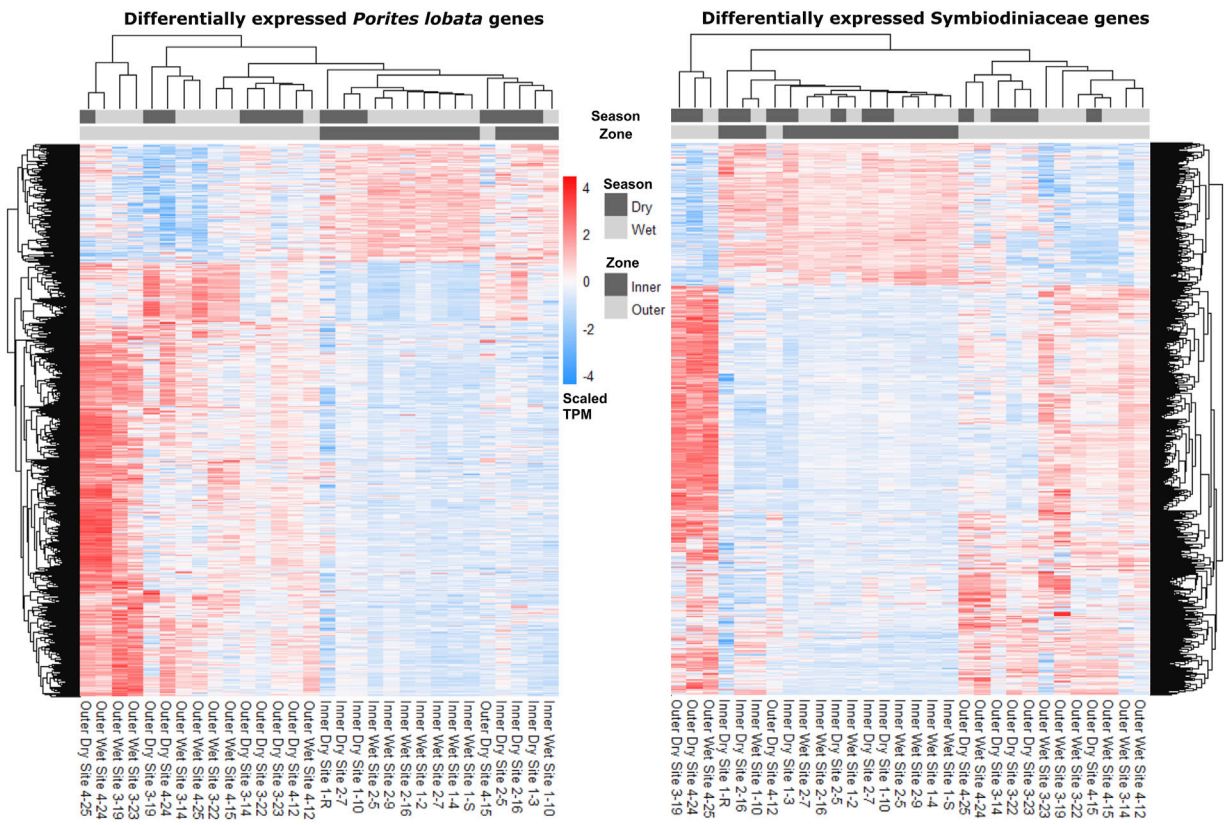

FIGURE 4
Heatmaps depicting read counts in transcripts per million (TPM) for each differentially expressed gene (rows) for *P. lobata* and Symbiodiniaceae. Samples (columns) are ordered by gene expression similarity. For both *P. lobata* and Symbiodiniaceae, samples cluster by zone rather than season (see *Results* for more information).

patterns of the dry-season sedimentation gradient, with the lowest coral diversity and abundance near the river mouth, where sedimentation is severe, and coral diversity and abundance increasing as sedimentation decreases to moderate or light levels further from the river mouth (Randall and Birkeland, 1978; Minton et al., 2022). The stark decrease in coral diversity and cover in Fouha Bay linked to the transition from moderate to severe sedimentation has previously been identified as a critical sedimentation threshold (Minton et al., 2022). Sedimentation is the result of a freshwater influx carrying suspended sediments. Considering that freshwater plumes float atop seawater due to their low specific gravity, it is not surprising that salinity at the depths where corals grow in Fouha Bay showed little variation (<1 PSU) across sites (Figure 2). While drastic reductions in salinity (~10 PSU) have been shown to elicit specific transcriptomic responses (Aguilar et al., 2019), the corals sampled in this study were not exposed to salinity levels significantly below 32–33 PSU, close to the ambient salinity in Guam (34–35 PSU). Given these considerations, the transcriptomic signatures described below are likely and primarily attributable to sedimentation stress.

Despite a large difference in sedimentation rates between dry and wet seasons (Figure 1D), gene expression profiles were more similar across samples within zones than those within seasons (Figure 4; Table 2). Indeed, differential gene expression analysis comparing dry and wet seasons yielded a minimal number of differentially expressed genes in both *P. lobata* and its Symbiodiniaceae endosymbiont community (Table 2). The lack of detectable gene expression differences between seasons may be linked to the chronic nature of the sedimentation stress experienced by *P. lobata* in Fouha Bay, consistent with significant reductions in coral cover and diversity between the outer and inner zones (Minton et al., 2022). The outer zone of Fouha Bay is more exposed to wave action than the inner zone, which would allow for a more expedient dissipation of turbidity and accumulated sediments. Despite this, the larger outer colonies still have significant energetic requirements to remove sediment from their large colonies, especially since the sedimentation rates even for the outer colonies are at the limits of survival for many coral species (Figure 1D; Erftemeijer et al., 2012; Tuttle and Donahue, 2022). Shifts in Symbiodiniaceae communities could theoretically contribute to the mitigation of sedimentation stress, but we found these communities to be largely homogenous and stable (Figure 3B), consistent with the previously reported dominance of *Cladocopium* C15 and lack of spatial structuring of symbiont subclades in *P. lobata* across Fouha Bay (Fifer et al., 2022).

Given that sampling during the wet season occurred following significant rain events, sedimentation rates may have increased temporarily in the outer zone of Fouha Bay, temporarily obscuring the well-described sedimentation gradient of Fouha Bay (Rongo, 2004; Minton et al., 2022). The lack of differentially expressed genes between sites N3/S3 and N4/S4 in the outer zone and N1/S1 and N2/S2 in the inner zone points to an environmental

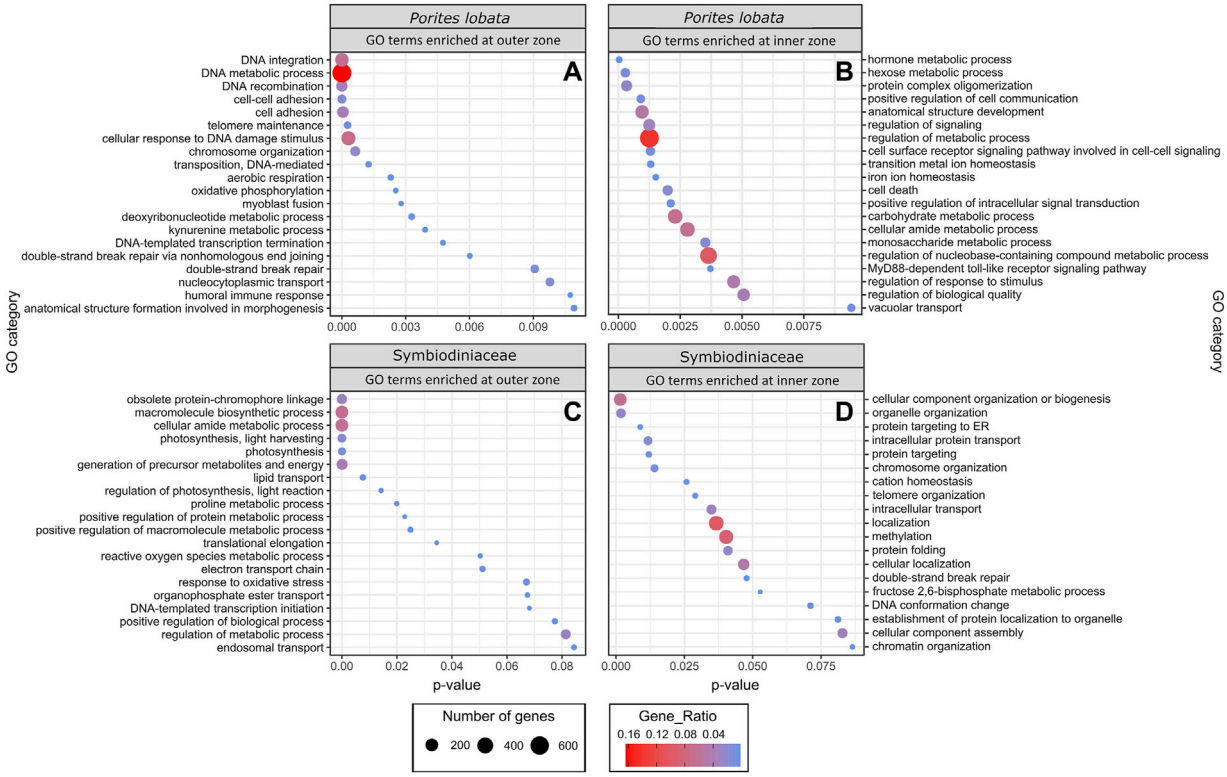

FIGURE 5
GO terms identified as enriched when comparing inner and outer zones for both *P. lobata* and Symbiodiniaceae. Up and downregulated genes were separated into "enriched in the inner zone" and "enriched in the outer zone." Gene ratio (color of circles) indicates the number of genes represented by a GO term relative to the total number of differentially expressed genes, whereas the number of genes (size of circle) is the total number in that GO category.

break between zones, consistent with a transition from moderate to severe sedimentation rates (Figure 1D) (Minton et al., 2022). The large number of differentially expressed genes identified when comparing the inner and outer zones using differential gene expression analysis (Table 2), in conjunction with the clustering of inner and outer zones based on gene expression similarities (Figure 4), suggests a strong metabolic threshold associated with the transition from moderate (~57 mg cm^{-2} day^{-1} during the dry season) to severe (~85 mg cm^{-2} day^{-1} during the dry season) sedimentation in *P. lobata*. These results are consistent with those obtained by Minton et al. (2022), who identified a critical sedimentation threshold of 48 mg cm^{-2} day^{-1} at which the abundance and diversity of corals significantly decrease in Fouha Bay, with massive *Porites* spp. being one of the few taxa able to persist. Chronic sedimentation affects the metabolism of persisting corals and likely reduces coral recruitment. Limited recruitment and high metabolic costs to survive at the inner site likely led to the observed small, average colony sizes. Furthermore, many of the colonies in this inner zone have perished since the sampling in 2018.

Taken together, coral community survey data (Minton et al., 2022) and our gene expression analysis suggest that *P. lobata* and their Symbiodiniaceae endosymbionts are chronically stressed due to severe sedimentation in the Fouha Bay inner zone. Through comparisons of gene expression patterns (Figure 4; Table 2), annotation of differentially expressed genes, and GO term enrichment analysis (Supplementary Table S3-5), we identified the putative signatures of sedimentation on the energy metabolism and immune response of *P. lobata* and its endosymbiotic Symbiodiniaceae community discussed below. Messenger RNA (mRNA) and protein expression are often poorly correlated (e.g., due to variations in mRNA stability and translational efficiency [Payne, 2015; Liu et al., 2016]), including in corals and their symbionts (Mayfield et al., 2016). While this has led to concerns about interpreting differential gene expression patterns, the correlation of differentially expressed mRNAs with protein expression may be significantly better than for non-differentially expressed genes (Koussounadis et al., 2015). Transcriptomics allows for rapidly profiling tens of thousands of potential biomarkers at once, which we used to provide a framework for the coral sedimentation stress response under field conditions that can guide multi-omics approaches aimed at linking genes to protein expression and their enzymatic and metabolic products to untangle the regulation and complexity of this system.

Energy metabolism

GO terms associated with oxidative phosphorylation (GO: 0006119) and aerobic respiration (GO:0009060) were enriched for *P. lobata* in the outer zone, exposed to moderate sedimentation (Figure 5A). For Symbiodiniaceae, photosynthesis (GO:0015979), generation of precursor metabolites and energy (GO:

0006091), electron transport chain (GO:0022900), and lipid transport (GO:0006869) were enriched in the outer zone (Figure 5C). Photosynthesis-associated genes coding for fucoxanthin–chlorophyll a–c binding proteins A, F, B, and E and photosystem I/II reaction center proteins were downregulated in Symbiodiniaceae from the inner zone (Supplementary Table S6), suggesting that the maintenance of the photosynthetic machinery is reduced under severe sedimentation, likely attributable to depleting energy stores (Sheridan et al., 2014), reallocation of energy due to crucial stress responses (Riegl and Branch, 1995), reduced light, and/or decreased oxygen availability (Jones and Hoegh-Guldberg, 2001; Weber et al., 2012). Other studies have reported a significant reduction in the maximum quantum yield (F_v/F_m) of photosystem II in response to sedimentation stress from a variety of coral species (Philipp and Fabricius, 2003), consistent with the decreased rates of photosynthesis and a significant reduction in the lipid stores of corals (Sheridan et al., 2014). The upregulation of lipid catabolic and transport enzymes (lipases and apolipoprotein L domain-containing protein 1; Supplementary Table S6) and downregulation of fat storage-inducing transmembrane protein 2 (Supplementary Table S6) in *P. lobata* indicate that corals in the inner zone of Fouha Bay likely deplete their lipid reserves to maintain antioxidant production, an innate immune response, and increased cilia action and mucous production to persist under chronic and severe sedimentation stress that requires the removal of sediment deposits, mitigation of pathogens, and elimination of increasing reactive oxygen species (ROS) that are the result of decreased dissolved oxygen available for metabolic processes in a turbid environment. Reduction in photosynthesis, as suggested by the downregulation of photosystem genes in Symbiodiniaceae observed in this study, may be offset by increased heterotrophic feeding, which has been suggested as an adaptive strategy for corals persisting in turbid environments (Bay et al., 2009; Pacherres et al., 2013), a possible strategy for *P. lobata* that is a mixotroph (Conti-Jerpe et al., 2020). Taken together, our results of GO term enrichment (Figure 5) and differential gene expression (Table 2; Supplementary Table S6) analyses indicate that *P. lobata* in the inner zone showed a decrease in energy generation, likely due to a depletion of energy reserves (Sheridan et al., 2014), and decreased photosynthetic activity of Symbiodiniaceae due to reduced light availability and/or lack of oxygen availability for aerobic respiration (Jones and Hoegh-Guldberg, 2001; Philipp and Fabricius, 2003).

GO terms associated with aerobic energy generation for *P. lobata* were enriched in the outer zone compared to the inner zone (Figure 5A), further indicating that corals in the inner zone experienced hypoxic stress as can be expected under conditions of severe sedimentation (Weber et al., 2012; Bollati et al., 2021). In *ex situ* sedimentation experiments, Bollati et al. (2021) found genes associated with an anaerobic glycolytic pathway upregulated in two coral species. Similarly, we find glyceraldehyde-3-phosphate dehydrogenase (GAPDH) (Supplementary Table S6) upregulated within Symbiodiniaceae in the inner zone and GO terms for aerobic respiration (GO:0009060) and oxidative phosphorylation (GO:0006119) of *P. lobata* enriched in the outer zone (Figure 5A), pointing to a reduction in aerobic respiration in corals of the inner zone to mitigate oxygen limitations caused by severe sedimentation. Furthermore, we found a hypoxia-inducible factor (aryl hydrocarbon receptor nuclear translocator in *P. lobata*; Supplementary Table S6) upregulated in *P. lobata* colonies from the inner zone. While not intuitive at first glance, the observed enrichment of the GO term response to oxidative stress (GO:0006979) and reactive oxygen species metabolic process (GO:0072593) in Symbiodiniaceae of the outer zone (Figure 5C) is consistent with the metabolic differences between inner and outer zones. In particular, increased photosynthetic activity in the less turbid outer zone compared to the inner zone likely elevated photosynthetic rates and increased ROS production in Symbiodiniaceae, which required mitigation. Similarly, antioxidant-associated genes (HSP-70, thioredoxin domain-containing proteins, superoxide dismutase, DnaJ-like proteins, and peroxidase; Supplementary Table S6) were upregulated in *P. lobata* in the outer zone. Our results are consistent with a switch from aerobic to anaerobic-dominated respiration in *P. lobata* from the outer to the inner zone. Quantifying the impacts of such metabolic switching on the health of *P. lobata* using appropriate assays (Murphy and Richmond, 2016) would provide additional insights into the adaptive capacity of this resilient coral species to chronic sedimentation stress and resulting hypoxia.

Immune response

Corals are known to possess a diverse repertoire of genes involved in innate immunity, with many being unique to *Scleractinia* and specific to certain coral taxa, which helps explain their variable responses to bacterial challenges (Cunning et al., 2018). This includes genes involved in pathogen recognition, signal transduction, and apoptosis pathways. In the marine environment, pathogenic bacteria are often associated with sediment influx and require corals to rapidly respond to these challenges to persist in turbid environments (Weber et al., 2012). In this study, we found GO terms associated with the positive regulation of cell communication (GO:0007267), positive regulation of signal transduction (GO:0009967), MyD88-dependent Toll-like receptor signaling pathway (GO:0002755), cell surface receptor signaling pathway involved in cell–cell signaling (GO:0007166), and regulation of the response to the stimulus (GO:0048583) overrepresented in *P. lobata* growing in the inner zone impacted by severe sedimentation (Figure 5B). The MyD88-dependent Toll-like receptor signaling pathway is involved in the innate immune response of corals to many different stressors (van de Water et al., 2015a; van de Water et al., 2015b; Anderson et al., 2016; Mydlarz et al., 2016; Young et al., 2020), stimulating the expression of pro-inflammatory cytokines (Poole and Weis, 2014). In sponges, this signaling pathway is strongly upregulated in response to bacterial endotoxin lipopolysaccharides, effectively eliminating Gram-negative bacteria through the formation of a recombinant protein (Wiens et al., 2005). Gram-negative pathogenic bacteria, such as *Vibrio* spp., are associated with marine sediments (Franco et al., 2020), and bacterial communities associated with heavy sediment loads are known to exacerbate mortality in corals (Hodgson, 1990; Weber et al., 2012). Indeed, microbiome metabarcoding previously revealed that *P. lobata* colonies growing in the inner zone of Fouha Bay, close to the river

mouth, harbored higher abundances of Vibrionaceae than colonies in the outer zone (Fifer et al., 2022).

Although corals are thought to only possess an innate immune system (Palmer and Traylor-Knowles, 2012), the presence of the MyD88-dependent Toll-like receptor signaling pathway is an example of an adaptive-like immune response system that may help corals mitigate bacterial infections (Wiens et al., 2005; Poole and Weis, 2014) associated with severe sedimentation. Only recently, coral immune cells and their gene expression have been characterized using single-cell transcriptomics (Levy et al., 2021). Interestingly, we found genes associated with immune functions in coral immune cells upregulated in the inner zone (interferon regulatory factor 2, tyrosinase, and homeobox genes coding for Meis2 and Nkx-2.2a; Supplementary Table S6). In summary, we observed the enrichment of cell signaling GO terms (Figure 5B) and upregulation of genes previously identified as molecular signatures of the immune function (Palmer and Traylor-Knowles, 2012; Poole and Weis, 2014; Mydlarz et al., 2016; Levy et al., 2021) in *P. lobata* colonies growing in the inner, severely sedimentation-impacted zone, suggesting that coral colonies in the inner zone rely on their immune response to mitigate the impacts of severe sedimentation.

Despite environmental sensing and resulting metabolic and immune responses, cell damage under severe stress is expected to increase. The initiation of apoptosis is a critical process that allows organisms to maintain tissue homeostasis by eliminating damaged cells that, for example, pose a risk for infection by pathogens (Ameisen, 2002). Various programmed cell death pathways have been identified in the cnidarian stress response, but the destabilization of cellular adhesion seems to be a crucial component in apoptosis initiation, given that changes in cell adhesion proteins have been associated with the response to coral bleaching (Gates et al., 1992; DeSalvo et al., 2012; Traylor-Knowles and Connelly, 2017), disease (Daniels et al., 2015), and heat plus sedimentation stress (Poquita-Du et al., 2019). Consistent with these prior studies, we found GO terms for cell death (GO:0008219) enriched in the inner zone (Figure 5B), as well as the enrichment of cell adhesion terms (GO:0007155, GO:0098609) in the outer zone (Figure 5A). This pattern suggests that *P. lobata* from the inner zone modified the extracellular matrix of part of its population of cells in conjunction with elevated rates of apoptosis initiation to remove cells damaged by severe sedimentation stress in an attempt to survive in this turbid, marginal habitat.

Conclusion

Transcriptomics provide a valuable insight into the rapid physiological response of an organism, but differential gene expression analysis may fail to capture longer-term responses such as seasonal differences, which may be more appropriately investigated with methods such as epigenomics. Nevertheless, in this study, we sampled corals along an established sedimentation gradient and provide a framework of the metabolic acclimation response of *P. lobata* colonies and its Symbiodiniaceae endosymbionts to varying sedimentation rates under *in situ* field conditions.

We identified processes that may allow for sedimentation-tolerant corals, such as *P. lobata*, to persist in habitats impacted by chronic and severe sedimentation. Switching between energy generation pathways may help corals living in sedimentation-impacted, turbid reefs maintain a stress response to survive when the availability of light and oxygen is diminished. Rapid environmental sensing and cell–cell communication allow corals to respond to freshwater influx, sedimentation stress, and bacterial challenges associated with terrestrial runoff. Given the cellular damage associated with environmental stress, the removal of damaged cells through programmed cell death pathways is crucial to maintaining coral colony integrity and closing entryways to pathogens. While many of these implicated pathways are involved in a range of coral stress responses, from bleaching to contamination from anthropogenic chemicals, here we observe these responses of *P. lobata* colonies to increasing sedimentation along a gradient in Fouha Bay, Guam. These putative mechanisms identified by us using transcriptomics ought to be further investigated and tested using additional approaches, in particular those that capture persistent and heritable modifications of traits under field and controlled conditions, to gain a better understanding of sedimentation stress-tolerance mechanisms in corals. Coastal development activities continuously increase sedimentation and turbidity in near-shore reefs, and a more in-depth understanding of the metabolic plasticity of diverse corals will facilitate predicting the acclimation and adaptation limits of near-shore reef ecosystems in the Anthropocene.

Data availability statement

The datasets presented in this study can be found in online repositories. The names of the repository/repositories and accession number(s) can be found in the article/Supplementary Material.

Author contributions

CL: data curation, formal analysis, investigation, methodology, visualization, writing–original draft, and writing–review and editing. MG: conceptualization, data curation, formal analysis, investigation, methodology, and writing–original draft. BB: conceptualization, data curation, formal analysis, funding acquisition, investigation, methodology, project administration, resources, supervision, and writing–review and editing.

Funding

The author(s) declare that financial support was received for the research, authorship, and/or publication of this article. This work was supported through the National Science Foundation EPSCoR awards OIA-1457769 and OIA-1946352.

Acknowledgments

The authors thank Constance Sartor for assisting with genetics laboratory work and Edriel Aquino for processing sediment samples.

Conflict of interest

The authors declare that the research was conducted in the absence of any commercial or financial relationships that could be construed as a potential conflict of interest.

Publisher's note

All claims expressed in this article are solely those of the authors and do not necessarily represent those of their affiliated organizations, or those of the publisher, the editors, and the reviewers. Any product that may be evaluated in this article, or claim that may be made by its manufacturer, is not guaranteed or endorsed by the publisher.

Supplementary material

The Supplementary Material for this article can be found online at: https://www.frontiersin.org/articles/10.3389/fphys.2024.1303681/full#supplementary-material

References

Aguilar, C., Raina, J.-P., Foret, S., Hayward, D. C., Lapeyre, B., Bourne, D. G., et al. (2019). Transcriptomic analysis reveals protein homeostasis breakdown in the coral *Acropora millepora* during hypo-saline stress. *BMC Genmics* 20, 148. doi:10.1186/s12864-019-5527-2

Altschul, S. F., Gish, W., Miller, W., Myers, E. W., and Lipman, D. J. (1990). Basic local alignment search tool. *J. Mol. Biol.* 215 (3), 403–410. doi:10.1016/S0022-2836(05)80360-2

Ameisen, J. C. (2002). On the origin, evolution, and nature of programmed cell death: a timeline of four billion years. *Cell Death Differ.* 9 (4), 367–393. doi:10.1038/sj.cdd.4400950

Anderson, D. A., Walz, M. E., Weil, E., Tonellato, P., and Smith, M. C. (2016). RNA-Seq of the Caribbean reef-building coral Orbicella faveolata (Scleractinia-Merulinidae) under bleaching and disease stress expands models of coral innate immunity. *PeerJ* 2016 (2), e1616. doi:10.7717/peerj.1616

Anthony, K., and Larcombe, P. (2000). "Coral reefs in turbid waters: sediment-induced stresses in corals and likely mechanisms of adaptation," in Proceedings of the 9th International Coral Reef Symposium, I, Bali, 23-27 October 2000, 239–244.

Barshis, D. J., Ladner, J. T., Oliver, T. A., and Palumbi, S. R. (2014). Lineage-specific transcriptional profiles of Symbiodinium spp. Unaltered by heat stress in a coral host. *Mol. Biol. Evol.* 31 (6), 1343–1352. doi:10.1093/molbev/msu107

Barshis, D. J., Ladner, J. T., Oliver, T. A., Seneca, F. O., Traylor-Knowles, N., and Palumbi, S. R. (2013). Genomic basis for coral resilience to climate change. *Proc. Natl. Acad. Sci.* 110 (4), 1387–1392. doi:10.1073/pnas.1210224110

Bateman, A., Martin, M. J., O'Donovan, C., Magrane, M., Alpi, E., Antunes, R., et al. (2017). UniProt: the universal protein knowledgebase. *Nucleic Acids Res.* 45 (D1), D158–D169. doi:10.1093/nar/gkw1099

Bay, L. K., Nielsen, H. B., Jarmer, H., Seneca, F., and van Oppen, M. J. H. (2009). Transcriptomic variation in a coral reveals pathways of clonal organisation. *Mar. Genomics* 2 (2), 119–125. doi:10.1016/j.margen.2009.07.004

Bayer, T., Aranda, M., Sunagawa, S., Yum, L. K., DeSalvo, M. K., Lindquist, E., et al. (2012). Symbiodinium transcriptomes: genome insights into the dinoflagellate symbionts of reef-building corals. *PLoS ONE* 7 (4), e35269. doi:10.1371/journal.pone.0035269

Bessell-Browne, P., Fisher, R., Duckworth, A., and Jones, R. (2017). Mucous sheet production in Porites: an effective bioindicator of sediment related pressures. *Ecol. Indic.* 77, 276–285. doi:10.1016/j.ecolind.2017.02.023

Bollati, E., Rosenberg, Y., Simon-Blecher, N., Tamir, R., Levy, O., and Huang, D. (2021). Untangling the molecular basis of coral response to sedimentation. *Mol. Ecol.* 2021, 884–901. doi:10.1111/mec.16263

Burdick, D., Brown, V., Asher, J., Gawel, M., Goldman, L., Hall, A., et al. (2008). The state of coral reef ecosystems of Guam. *Secr. Pac. Regional Environ. Programme*, 465–510. doi:10.13140/RG.2.1.2183.8960

Conti-Jerpe, I. E., Thompson, P. D., Wai, C., Wong, M., Oliveira, N. L., Duprey, N. N., et al. (2020). Trophic strategy and bleaching resistance in reef-building corals. *Sci. Adv.* 6, eaaz5443. doi:10.1126/sciadv.aaz5443

Cunning, R., Bay, R. A., Gillette, P., Baker, A. C., and Traylor-Knowles, N. (2018). Comparative analysis of the Pocillopora damicornis genome highlights role of immune system in coral evolution. *Scientific Reports*, 8 (1) doi:10.1038/s41598-018-34459-8

Daniels, C. A., Baumgarten, S., Yum, L. K., Michell, C. T., Bayer, T., Arif, C., et al. (2015). Metatranscriptome analysis of the reef-building coral Orbicella faveolata indicates holobiont response to coral disease. *Front. Mar. Sci.* 2 (SEP). doi:10.3389/fmars.2015.00062

DeSalvo, M. K., Estrada, A., Sunagawa, S., and Medina, M. (2012). Transcriptomic responses to darkness stress point to common coral bleaching mechanisms. *Coral Reefs* 31 (1), 215–228. doi:10.1007/s00338-011-0833-4

Ensminger, M. (2016). *Analysis of whole sample suspended sediments in water*.

Erftemeijer, P. L. A., Riegl, B., Hoeksema, B. W., and Todd, P. A. (2012). Environmental impacts of dredging and other sediment disturbances on corals: a review. *Mar. Pollut. Bull.* 64 (9), 1737–1765. doi:10.1016/j.marpolbul.2012.05.008

Fabricius, K. E. (2005). Effects of terrestrial runoff on the ecology of corals and coral reefs: review and synthesis. *Mar. Pollut. Bull.* 50 (2), 125–146. doi:10.1016/j.marpolbul.2004.11.028

Fifer, J. E., Bui, V., Berg, J. T., Kriefall, N., Klepac, C., Bentlage, B., et al. (2022). Microbiome structuring within a coral colony and along a sedimentation gradient. *Front. Mar. Sci.* 8. doi:10.3389/fmars.2021.805202

Flores, F., Hoogenboom, M. O., Smith, L. D., Cooper, T. F., Abrego, D., and Negri, A. P. (2012). Chronic exposure of corals to fine sediments: lethal and sub-lethal impacts. *PLoS ONE* 7 (5), e37795. doi:10.1371/journal.pone.0037795

Forsman, Z., Wellington, G. M., Fox, G. E., and Toonen, R. J. (2015). Clues to unraveling the coral species problem: distinguishing species from geographic variation in Porites across the Pacific with molecular markers and microskeletal traits. *PeerJ* 2015 (2), e751. doi:10.7717/peerj.751

Foster, S., and Ballendorf, D. A. (2023). Guam | history, geography, and points of interest | britannica. Available at: https://www.britannica.com/place/Guam.

Franco, A., Rückert, C., Blom, J., Busche, T., Reichert, J., Schubert, P., et al. (2020). High diversity of Vibrio spp. associated with different ecological niches in a marine aquaria system and description of Vibrio aquimaris sp. nov. *Syst. Appl. Microbiol.* 43 (5), 126123. doi:10.1016/j.syapm.2020.126123

Gates, R. D., Baghdasarian, G., and Muscatine, L. (1992). Temperature stress causes host cell detachment in symbiotic Cnidarians: implications for coral bleaching. *Biol. Bull.* 182 (3), 324–332. doi:10.2307/1542252

Gault, J. A., Bentlage, B., Huang, D., and Kerr, A. M. (2021). Lineage-specific variation in the evolutionary stability of coral photosymbiosis. *Sci. Adv.* 7, eabh4243. doi:10.1126/sciadv.abh4243

Golbuu, Y., van Woesik, R., Richmond, R. H., Harrison, P., and Fabricius, K. E. (2011). River discharge reduces reef coral diversity in Palau. *Mar. Pollut. Bull.* 62 (4), 824–831. doi:10.1016/j.marpolbul.2010.12.015

Grabherr, M. G., Haas, B. J., Yassour, M., Levin, J. Z., Thompson, D. A., Amit, I., et al. (2013). Trinity: reconstructing a full-length transcriptome without a genome from RNA-Seq data. *Nat. Biotechnol.* 29 (7), 644–652. doi:10.1038/nbt.1883

Haas, B. J., Papanicolaou, A., Yassour, M., Grabherr, M., Blood, P. D., Bowden, J., et al. (2013). *De novo* transcript sequence reconstruction from RNA-seq using the Trinity platform for reference generation and analysis. *Nat. Protoc.* 8 (8), 1494–1512. doi:10.1038/nprot.2013.084

Hayer, K. E., Pizarro, A., Lahens, N. F., Hogenesch, J. B., and Grant, G. R. (2015). Benchmark analysis of algorithms for determining and quantifying full-length mRNA splice forms from RNA-seq data. *Bioinformatics* 31 (24), 3938–3945. doi:10.1093/bioinformatics/btv488

Hodgson, G. (1990). Tetracycline reduces sedimentation damage to corals. *Mar. Biol.* 104 (3), 493–496. doi:10.1007/BF01314355

Hughes, T. P., Baird, A. H., Bellwood, D. R., Card, M., Connolly, S. R., Folke, C., et al. (2003). Climate change, human impacts, and the resilience of coral reefs. *Science* 929 (2003), 929–933. doi:10.1126/science.1085046

Hughes, T. P., Barnes, M. L., Bellwood, D. R., Cinner, J. E., Cumming, G. S., Jackson, J. B. C., et al. (2017). Coral reefs in the Anthropocene. *Nature* 546 (7656), 82–90. doi:10.1038/nature22901

Ishibashi, H., and Takeuchi, I. (2023). "Effects of anthropogenic chemicals on hermatypic corals with special reference to gene expression," in *Coral reefs of eastern asia under anthropogenic impacts*, 153–166. doi:10.1007/978-3-031-27560-9_9

Jones, R., Giofre, N., Luter, H. M., Neoh, T. L., Fisher, R., and Duckworth, A. (2020). Responses of corals to chronic turbidity. *Sci. Rep.* 10 (1), 4762. doi:10.1038/s41598-020-61712-w

Jones, R. J., and Hoegh-Guldberg, O. (2001). Diurnal changes in the photochemical efficiency of the symbiotic dinoflagellates (Dinophyceae) of corals: photoprotection, photoinactivation and the relationship to coral bleaching. *Plant, Cell Environ.* 24 (1), 89–99. doi:10.1046/j.1365-3040.2001.00648.x

Koussounadis, A., Langdon, S. P., Um, I. H., Harrison, D. J., and Smith, V. A. (2015). Relationship between differentially expressed mRNA and mRNA-protein correlations in a xenograft model system. *Scientific Reports* 5. doi:10.1038/srep10775

Ladner, J. T., Barshis, D. J., and Palumbi, S. R. (2012). Protein evolution in two co-occurring types of Symbiodinium: an exploration into the genetic basis of thermal tolerance in Symbiodinium clade D. *BMC Evol. Biol.* 12 (1), 217. doi:10.1186/1471-2148-12-217

Levy, S., Elek, A., Grau-Bové, X., Menéndez-Bravo, S., Iglesias, M., Tanay, A., et al. (2021). A stony coral cell atlas illuminates the molecular and cellular basis of coral symbiosis, calcification, and immunity. *Cell* 184 (11), 2973–2987.e18. doi:10.1016/j.cell.2021.04.005

Liu, Y., Beyer, A., and Aebersold, R. (2016). On the Dependency of Cellular Protein Levels on mRNA Abundance. *Cell* 165 (3), 535–550. doi:10.1016/j.cell.2016.03.014

Lock, C., Bentlage, B., and Raymundo, L. J. (2022). Calcium homeostasis disruption initiates rapid growth after micro-fragmentation in the scleractinian coral Porites lobata. *Ecol. Evol.* 12 (9), e9345. doi:10.1002/ece3.9345

Manzello, D. P., Matz, M. V., Enochs, I. C., Valentino, L., Carlton, R. D., Kolodziej, G., et al. (2019). Role of host genetics and heat-tolerant algal symbionts in sustaining populations of the endangered coral Orbicella faveolata in the Florida Keys with ocean warming. *Glob. Change Biol.* 25 (3), 1016–1031. doi:10.1111/gcb.14545

Martin, M. (2011). Cutadapt removes adapter sequences from high-throughput sequencing reads. *EMBnet J. Tech. Notes* 17 (10), 10–2809. doi:10.14806/ej.17.1.200

Mayfield, A. B., Wang, Y. B., Chen, C. S., Chen, S. H., and Lin, C. Y. (2016). Dual-compartmental transcriptomic + proteomic analysis of a marine endosymbiosis exposed to environmental change. *Molecular Ecology* 25 (23), 5944–5958. doi:10.1111/mec.13896

Minton, D., Burdick, D., and Brown, V. (2022). Changes in coral reef community structure along a sediment gradient in Fouha Bay, Guam. *Mar. Pollut. Bull.* 181, 113816. doi:10.1016/j.marpolbul.2022.113816

Murphy, J. W. A., and Richmond, R. H. (2016). Changes to coral health and metabolic activity under oxygen deprivation. *PeerJ* 2016 (4), e1956. doi:10.7717/peerj.1956

Mydlarz, L. D., Fuess, L., Mann, W., Pinzón, J. H., and Gochfeld, D. J. (2016). Cnidarian immunity: from genomes to phenomes. *Cnidaria, Past, Present Future*, 1–855. doi:10.1007/978-3-319-31305-4

National Academies of Sciences, Engineering, and Medicine (2019) *A research review of interventions to increase the persistence and resilience of coral reefs*. Washington, DC: The National Academies Press. doi:10.17226/25279

Pacherres, C. O., Schmidt, G. M., and Richter, C. (2013). Autotrophic and heterotrophic responses of the coral Porites lutea to large amplitude internal waves. *J. Exp. Biol.* 216 (23), 4365–4374. doi:10.1242/jeb.085548

Palmer, C. V., and Traylor-Knowles, N. (2012). Towards an integrated network of coral immune mechanisms. *Proc. R. Soc. B Biol. Sci.* 279 (1745), 4106–4114. doi:10.1098/rspb.2012.1477

Paz-García, D. A., Galván-Tirado, C., Alvarado, J. J., Cortés, J., García-De-León, F. J., Hellberg, M. E., et al. (2016). Variation in the whole mitogenome of reef-building Porites corals. *Conserv. Genet. Resour.* 8 (2), 123–127. doi:10.1007/s12686-016-0527-x

Payne, S. H. (2015). The utility of protein and mRNA correlation. *In Trends in Biochemical Sciences* 40 (1), 1–3. doi:10.1016/j.tibs.2014.10.010

Philipp, E., and Fabricius, K. (2003). Photophysiological stress in scleractinian corals in response to short-term sedimentation. *J. Exp. Mar. Biol. Ecol.* 287 (1), 57–78. doi:10.1016/S0022-0981(02)00495-1

Pimentel, H., Bray, N. L., Puente, S., Melsted, P., and Pachter, L. (2017). Differential analysis of RNA-seq incorporating quantification uncertainty. *Nat. Methods* 14 (7), 687–690. doi:10.1038/nmeth.4324

Poole, A. Z., and Weis, V. M. (2014). TIR-domain-containing protein repertoire of nine anthozoan species reveals coral-specific expansions and uncharacterized proteins. *Dev. Comp. Immunol.* 46 (2), 480–488. doi:10.1016/j.dci.2014.06.002

Poquita-Du, R. C., Huang, D., Chou, L. M., Mrinalini, and Todd, P. A. (2019). Short term exposure to heat and sediment triggers changes in coral gene expression and photo-physiological performance. *Front. Mar. Sci.* 6 (MAR), 1–15. doi:10.3389/fmars.2019.00121

Randall, R. H., and Birkeland, C. (1978). *Guam's reefs and beaches, Part II, sedimentation studies at Fouha bay ad ylig bay.*

Reynolds, T., Burdick, D., Houk, P., Raymundo, L. J., and Johnson, S. (2014). Unprecedented coral bleaching across the Marianas archipelago. *Coral Reefs* 33 (2), 499. doi:10.1007/s00338-014-1139-0

Riegl, B., and Branch, G. M. (1995). Effects of sediment on the energy budgets of four scleractinian (Bourne 1900) and five alcyonacean (Lamouroux 1816) corals. *J. Exp. Mar. Biol. Ecol.* 186 (2), 259–275. doi:10.1016/0022-0981(94)00164-9

Rogers, C. S. (1990). Responses of coral reefs and reef organisms to sedimentation. *Mar. Ecol. Prog. Ser.* 62, 185–202. doi:10.3354/meps062185

Rogers, C. S., and Ramos-Scharrón, C. E. (2022). Assessing effects of sediment delivery to coral reefs: a caribbean watershed perspective. *Front. Mar. Sci.* 8. doi:10.3389/fmars.2021.773968

Rongo, T. (2004). Coral community change along a sediment gradient in Fouha Bay, Guam. Available at: http://onlinelibrary.wiley.com/doi/10.1002/cbdv.200490137/abstract.

Ryan, J. (2014) *Alien Index: identify potential non-animal transcripts or horizontally transferred genes in animal transcriptomes*. doi:10.5281/zenodo.21029

Scheman, N., Khosrowpanah, S., Golabi, M. H., and Leroy, H. (2002). Identification of erosion processes and sources of exposed patches in the La Sa Fua Watershed of Southern Guam. Available at: https://www.researchgate.net/publication/253992920.

Schulz, F., Eloe-Fadrosh, E. A., Bowers, R. M., Jarett, J., Nielsen, T., Ivanova, N. N., et al. (2017). Towards a balanced view of the bacterial tree of life. *Microbiome* 5 (1), 140. doi:10.1186/s40168-017-0360-9

Sheppard, C. R. C., Davy, S. K., and Pilling, G. M. (2009). "The biology of coral reefs," in *The biology of coral reefs*, 1–352. doi:10.1093/ACPROF:OSO/9780198566359.001.0001

Sheridan, C., Grosjean, P., Leblud, J., Palmer, C. V., Kushmaro, A., and Eeckhaut, I. (2014). Sedimentation rapidly induces an immune response and depletes energy stores in a hard coral. *Coral Reefs* 33 (4), 1067–1076. doi:10.1007/s00338-014-1202-x

Simão, F. A., Waterhouse, R. M., Ioannidis, P., Kriventseva, E. V., and Zdobnov, E. M. (2015). BUSCO: assessing genome assembly and annotation completeness with single-copy orthologs. *Bioinformatics* 31 (19), 3210–3212. doi:10.1093/bioinformatics/btv351

Stafford-Smith, M. G. (1993). Sediment-rejection efficiency of 22 species of Australian scleractinian corals. *Mar. Biol.* 115 (2), 229–243. doi:10.1007/BF00346340

Stamatakis, A. (2014). RAxML version 8: a tool for phylogenetic analysis and post-analysis of large phylogenies. *Bioinformatics* 30 (9), 1312–1313. doi:10.1093/bioinformatics/btu033

Storlazzi, C. D., Field, M. E., and Bothner, M. H. (2011). The use (and misuse) of sediment traps in coral reef environments: theory, observations, and suggested protocols. *Coral Reefs* 30 (1), 23–38. doi:10.1007/s00338-010-0705-3

Terraneo, T. I., Benzoni, F., Arrigoni, R., Baird, A. H., Mariappan, K. G., Forsman, Z. H., et al. (2021). Phylogenomics of Porites from the arabian peninsula. *Mol. Phylogenetics Evol.* 161, 107173. doi:10.1016/J.YMPEV.2021.107173

Traylor-Knowles, N., and Connelly, M. T. (2017). What is currently known about the effects of climate change on the coral immune response. *Curr. Clim. Change Rep.* 3 (4), 252–260. doi:10.1007/s40641-017-0077-7

Tuttle, L. J., and Donahue, M. J. (2022). Effects of sediment exposure on corals: a systematic review of experimental studies. *Environ. Evid.* 11 (1), 4–33. doi:10.1186/s13750-022-00256-0

USGS (2023). National water information system data available on the world wide web – USGS water data for the nation. Available at: https://waterdata.usgs.gov/nwis. (Accessed February 10, 2023)

van de Water, J. A. J. M., Ainsworth, T. D., Leggat, W., Bourne, D. G., Willis, B. L., and Van Oppen, M. J. H. (2015a). The coral immune response facilitates protection against microbes during tissue regeneration. *Mol. Ecol.* 24 (13), 3390–3404. doi:10.1111/mec.13257

van de Water, J. A. J. M., Leggat, W., Bourne, D. G., van Oppen, M. J. H., Willis, B. L., and Ainsworth, T. D. (2015b). Elevated seawater temperatures have a limited impact on the coral immune response following physical damage. *Hydrobiologia* 759 (1), 201–214. doi:10.1007/s10750-015-2243-z

Weber, M., De Beer, D., Lott, C., Polerecky, L., Kohls, K., Abed, R. M. M., et al. (2012). Mechanisms of damage to corals exposed to sedimentation. *Proc. Natl. Acad. Sci. U. S. A.* 109 (24), E1558–E1567. doi:10.1073/pnas.1100715109

Wiens, M., Korzhev, M., Krasko, A., Thakur, N. L., Perović-Ottstadt, S., Breter, H. J., et al. (2005). Innate immune defense of the sponge *Suberites domuncula* against bacteria involves a MyD88-dependent signaling pathway: induction of a perforin-like molecule. *J. Biol. Chem.* 280 (30), 27949–27959. doi:10.1074/jbc.M504049200

Wolanski, E., Richmond, R. H., Davis, G., and Bonito, V. (2003). Water and fine sediment dynamics in transient river plumes in a small, reef-fringed bay, Guam. *Estuar. Coast. Shelf Sci.* 56 (5–6), 1029–1040. doi:10.1016/S0272-7714(02)00321-9

Wright, R. M., Aglyamova, G. V., Meyer, E., and Matz, M. V. (2015). Gene expression associated with white syndromes in a reef building coral, Acropora hyacinthus. *BMC Genomics* 16 (1), 371. doi:10.1186/s12864-015-1540-2

Yi, L., Pimentel, H., Bray, N. L., and Pachter, L. (2018). Gene-level differential analysis at transcript-level resolution. *Genome Biol.* 19 (1), 53. doi:10.1186/s13059-018-1419-z

Young, B. D., Serrano, X. M., Rosales, S. M., Miller, M. W., Williams, D., and Traylor-Knowles, N. (2020). Innate immune gene expression in Acropora palmata is consistent despite variance in yearly disease events. *PLoS ONE* 15 (10), e0228514. doi:10.1371/journal.pone.0228514

frontiers | Frontiers in Physiology

TYPE Original Research
PUBLISHED 17 June 2024
DOI 10.3389/fphys.2024.1339907

OPEN ACCESS

EDITED BY
Davide Seveso,
University of Milano-Bicocca, Italy

REVIEWED BY
Adán Guillermo Jordán-Garza,
Universidad Veracruzana, Mexico
Rachel Alderdice,
University of Technology Sydney, Australia

*CORRESPONDENCE
Toshiyuki Suzuki,
suzuki.toshiyuki@shizuoka.ac.jp

†These authors have contributed equally to this work and share first authorship

RECEIVED 17 November 2023
ACCEPTED 16 April 2024
PUBLISHED 17 June 2024

CITATION
Suzuki T, Casareto BE, Yucharoen M, Dohra H and Suzuki Y (2024), Coexistence of nonfluorescent chromoproteins and fluorescent proteins in massive *Porites* spp. corals manifesting a pink pigmentation response.
Front. Physiol. 15:1339907.
doi: 10.3389/fphys.2024.1339907

Coexistence of nonfluorescent chromoproteins and fluorescent proteins in massive *Porites* spp. corals manifesting a pink pigmentation response

Toshiyuki Suzuki[1*†], Beatriz E. Casareto[1†], Mathinee Yucharoen[2†], Hideo Dohra[3] and Yoshimi Suzuki[1]

[1]Graduate School of Science and Technology, Shizuoka University, Shizuoka City, Japan, [2]Faculty of Environmental Management, and Coastal Oceanography and Climate Change Research Center, Prince of Songkla University, Songkhla, Thailand, [3]Research Institute of Green Science and Technology, Shizuoka University, Shizuoka City, Japan

Introduction: Several fluorescent proteins (FPs) and chromoproteins (CPs) are present in anthozoans and play possible roles in photoprotection. Coral tissues in massive corals often display discoloration accompanied by inflammation. Incidences of the pink pigmentation response (PPR) in massive *Porites*, described as inflammatory pink lesions of different shapes and sizes, has recently increased worldwide. FPs are reported to be present in PPR lesions, wherein a red fluorescent protein (RFP) appears to play a role in reducing reactive oxygen species. However, to date, the biochemical characterization and possible roles of the pigments involved are poorly understood. The present study aimed to identify and characterize the proteins responsible for pink discoloration in massive *Porites* colonies displaying PPRs, as well as to assess the differential distribution of pigments and the antioxidant properties of pigmented areas.

Method: CPs were extracted from PPR lesions using gel-filtration chromatography and identified via genetic analysis using liquid chromatography-tandem mass spectrometry. The coexistence of CPs and RFP in coral tissues was assessed using microscopic observation. Photosynthetic antivity and hydrogen peroxide-scavenging activitiy were measured to assess coral stress conditions.

Results: The present study revealed that the same CP (plut2.m8.16902.m1) isolated from massive *Porites* was present in both the pink spot and patch morphologies of the PPR. CPs were also found to coexist with RFP in coral tissues that manifested a PPR, with a differential distribution (coenosarc or tip of polyps' tentacles). High hydrogen peroxide-scavenging rates were found in tissues affected by PPR.

Discussion and Conclusion: The coexistence of CPs and RFP suggests their possible differential role in coral immunity. CPs, which are specifically expressed

in PPR lesions, may serve as an antioxidant in the affected coral tissue. Overall, this study provides new knowledge to our understanding of the role of CPs in coral immunity.

KEYWORDS

chromoprotein, fluorescent protein, non-fluorescent chromoprotein, *Porites* spp., oxidative stress, pink pigmentation response, innate immune response

1 Introduction

Global climate change and anthropogenic disturbances have led to an increased incidence of coral diseases and bleaching during the last 3 decades, particularly in corals inhabiting tropical regions in the Caribbean and Indo-Pacific Ocean (Beeden et al., 2008; Aeby et al., 2011; Weil et al., 2012; 2016; Hughes et al., 2018; Johnson et al., 2022). In the last decade, heat-susceptible genotypes may have declined and/or adapted to such conditions; therefore, the remaining coral populations could have a higher thermal threshold for bleaching (Sully et al., 2019). Despite the increasing risk of climate change affecting coral health, studies have revealed that corals can improve their resilience through certain innate physiological mechanisms that involve chaperones and antioxidative enzymes, particularly heat shock proteins (Hsp70, Hsp60, and Hsp32) (Arya et al., 2007; Lanneau et al., 2008; Jin et al., 2016; Seveso et al., 2018; 2020; Montalbetti et al., 2021; Thummasan et al., 2021).

Massive *Porites* spp. are reef-building corals commonly found in reefs of the Indo-Pacific region, including the Ryukyu Islands in southern Japan (Veron, 1992; Nishihira, 2004). The health compromised coral tissues in massive corals such as *Porites* spp. often display non-normal pigmentation and develop some discoloration, such as pink, purple, and blue, that potentially represent an inflammation-like response (Palmer et al., 2009a). Among these, the pink pigmentation response (PPR) in massive *Porites* spp. colonies, a generalized inflammatory response characterized by the formation of pink lesions of different shapes and sizes, has been reported to increase in the Ryukyu Islands (Kubomura et al., 2021), with chronic seasonal variations (Yucharoen, 2016). In general, PPRs in corals develop swollen areas with pink discoloration, described as “pink lines” (Ravindran and Raghukumar 2002; 2006; Kenkel, 2008; Mohamed et al., 2012; Kritsanapuntu and Angkhananukroh, 2014; Séré et al., 2015), “pink spots” (Willis et al., 2004; Benzoni et al., 2010; Thinesh et al., 2011; Putchim et al., 2012; Kumar et al., 2014), and “pink pigmentation” (Raymundo et al., 2005; Palmer et al., 2009a).

Discoloration in PPRs is a phenomenon frequently observed in *Porites* spp. corals, but there are some reports regarding similar pigmentation phenomenon in other genera, such as *Acropora* (Bongiorni and Rinkevich, 2005; D’Angelo et al., 2012) and *Montipora* (D’Angelo et al., 2012; Aeby 1992; 2003 found that corals manifesting pink spots were infected by the trematode *Podocotyloides stenometra*. However later in the literature; Benzoni et al., 2010; Yucharoen 2016, found that the pink spots and other pink swollen lesions observed in massive corals, may not always be the result of tissue inflammation caused by the trematodes, but also injuries caused by other organisms penetrating the coral tissues, bites of fishes and the response to environmental stressors like high sea-surface temperature, strong illumination, low salinity, and desiccation. Therefore, the PPR is linked with an immune response of corals to those stresses mainly promoting the formation of reactive oxygen species (ROS) and the coral innate immune response through the production of antioxidant enzymes and FP (fluorescent proteins) (Palmer et al., 2009a; Palmer et al., 2009b; Bridges et al., 2020). Palmer et al. (2009)a and Palmer et al. (2009)b reported the presence of a red fluorescent protein (RFP) that plays an important role in photoprotection and the reduction of ROS. Bridges et al. (2020) reported that RFP expression in pink-pigmented lesions of *Porites lobata* is an innate immune response. Moreover, green fluorescent proteins (GFPs) in scleractinian corals play an important role in the removal of ROS (Bou-Abdallah et al., 2006).

To date, several FPs and chromoproteins (CPs) have been reported in anthozoans with possible roles in photoprotection (Matz et al., 1999; Miyawaki, 2002; Verkhusha and Lukyanov 2004; Bollati et al., 2022). The CPs present in anthozoans are highly homologous to FPs, such as GFPs. FPs and FP-like CPs are classified into four groups: cyan, green, and red that are fluorescent, and nonfluorescent CPs (Labas et al., 2002). Apart from the normal green-brown color of anthozoans from their symbiotic algae, CPs are also responsible for the nonfluorescent coloration (Lukyanov et al., 2000; Wiedenmann et al., 2000). Since the discovery of GFPs in the crystal jelly, *Aequorea victoria*, CPs and FPs have been extensively studied. Alieva et al. (2008) revealed for the first time that several CPs are present in some scleractinian coral genomes. Similarly, Shinzato et al. (2012) reported the presence of fluorescent and nonfluorescent CPs in a whole-genome analysis of *Acropora* corals. In recent years, it has become clear that diverse FPs are present with complex expression in corals of the genus *Acropora* (Kashimoto et al., 2021; Satoh et al., 2021). However, it is not clear what condition will promote the expression of these proteins in *Porites* spp. corals. Therefore, this study aimed to identify and characterize the CPs expressed in the discolored tissues of massive *Porites* spp. colonies manifesting PPRs, by extracting and purifying their proteins and further identifying the genes involved in their expression. In addition, microscopic observations of coral tissues under normal and ultraviolet light were conducted to clarify differences in the localization of CPs and RFP.

2 Materials and methods

2.1 Coral sampling

Colonies of massive *Porites* spp. were sampled from a coral reef at Sesoko Beach in Sesoko Island, Okinawa, Japan (26°39′N 127°51′E), at low tide (depth 0.5–1 m) on 18 September 2018

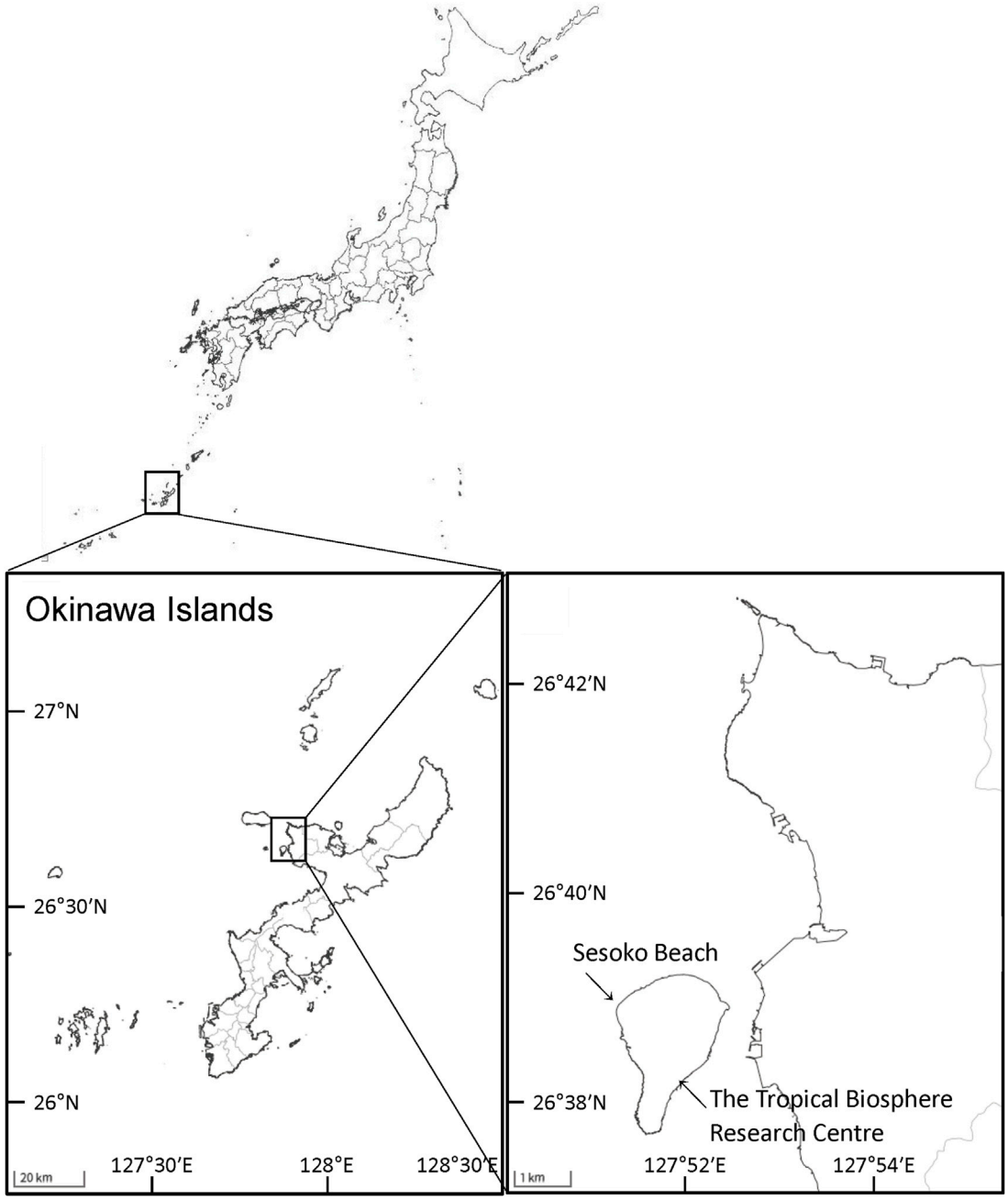

FIGURE 1
Study area and sampling sites in Okinawa, Japan. Maps were obtained from The Geospatial Information Authority of Japan (https://www.gsi.go.jp/).

(sampling permit No. 30–55, granted by the Okinawa Prefectural Government) (Figure 1). For protein analysis, a hammer and chisel were used to collect coral pieces from three colonies of *Porites* spp., two displaying PPRs as pink spots (Ps) and pink patches (Pp), and one healthy colony (H) (Figure 2). For microscopic observation, the coral pieces displaying Pp and the healthy-appearing colony were used. Sampled fragments of each colony (10–20 cm^2) were kept in sterilized tagged bags with surrounding seawater and transported to the laboratory at the Tropical Biosphere Research Centre (University of The Ryukyus, Okinawa, Japan) at Sesoko Island. Samples were maintained in an aquarium for 24 h with natural running seawater, temperature fluctuating between 26.5°C and 27.5°C, and attenuated natural illumination with a maximum of 200 μmol photons cm^{-2} s^{-1} to avoid the formation of ROS until treatment.

2.2 Extraction and concentration of chromoproteins

Tissue solutions were obtained from the pink-pigmented area of the colonies displaying Ps and Pp, as well as from H as a control.

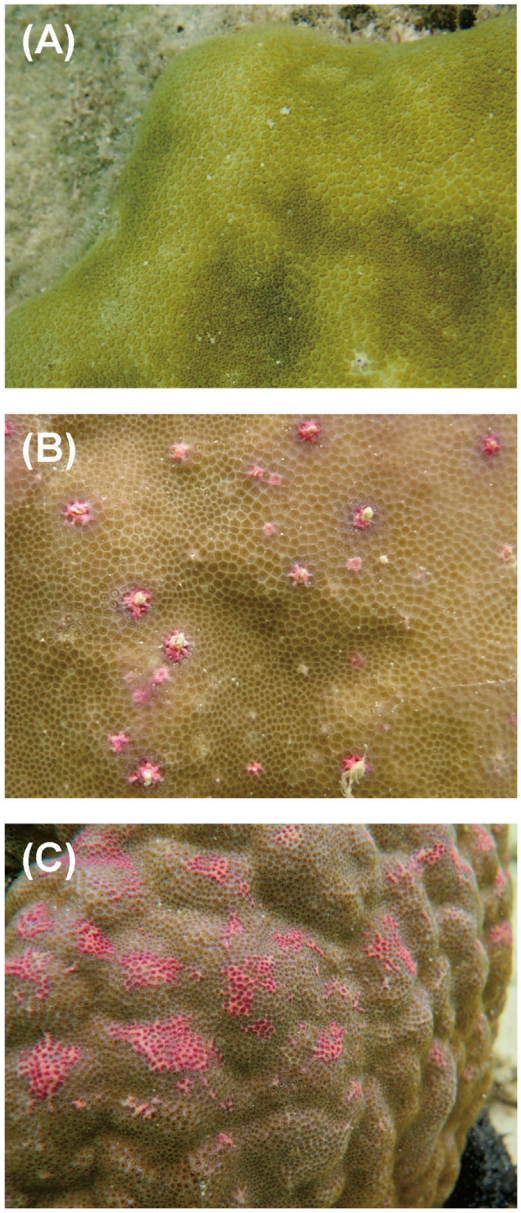

FIGURE 2
Aspects of different types of PPRs in massive *Porites* colonies: **(A)** healthy-appearing colony, **(B)** colony exhibiting pink spots, and **(C)** colony exhibiting pink patches.

Coral tissues of 0.8–1.6 cm^2 (Ps), 3–5 cm^2 (Pp), and 4 cm^2 of H were removed from the skeleton with a Waterpik dental flosser (DENTREX; Ricoh Elemex, Aichi, Japan) (Johannes and Wiebe, 1970) using 3.5% NaCl solution and 10 mM sodium phosphate buffer (pH 7.5). Crude tissue solutions were homogenized using a glass homogenizer and filtered through Whatman glass microfiber filters (Grade GF/F, pore size 0.7 μm; GE Healthcare Life Sciences, Buckinghamshire, United Kingdom) to remove the endosymbiotic algae Symbiodiniaceae cells and coral tissue debris. The soluble fractions were centrifuged at 3,000 × *g* using Amicon Ultra centrifugal filters (Merck KGaA, Darmstadt, Germany) to concentrate molecules with masses greater than 10,000 Da to retain proteins. Concentrated extracts were transferred to microtubes using Pasteur pipettes. The Amicon meshes were then washed three times with 200 μL of 10 mM sodium phosphate buffer (pH 7.5) for complete recovery of the samples. The final volume of the extract was approximately 1.5 mL. Approximately 50 μL of the protein extracts were used for separation through electrophoresis, and the remaining used for purification. A scheme of the experimental flow is shown in Figure 3.

2.3 Purification and characterization of chromoproteins

Partial purification of CPs from the protein extracts was performed via successive gel-filtration chromatography (Superdex 200 HR 10/30 column; GE Healthcare Life Science) on a fast protein liquid chromatography (FPLC) system (ÄKTA prime; GE Healthcare Life Science). The samples were eluted with 10 mM sodium phosphate buffer (pH 7.5) containing 0.15 M NaCl at a flow rate of 0.5 mL/min. Forty elution products were collected in 1-mL fractions each, and their optical properties and enzymatic activity measured. Absorbance at 280 and 580 nm was measured for each fraction using a spectrophotometer (model UV-2450; Shimadzu, Kyoto, Japan). Molecular weights were estimated using a Gel Filtration Standard molecular marker (Bio-Rad Laboratories, Hercules, California, United States of America).

2.4 Amino acid sequence identification

2.4.1 Protein concentration

The total protein content was determined using a Bio-Rad Protein Assay Kit (Bio-Rad Laboratories) based on the Bradford method (Bradford, 1976) with bovine serum albumin as a standard. The Bradford method quantifies proteins using Coomassie Brilliant Blue G-250, a triphenylmethane blue dye that binds to proteins in acidic solutions and shifts the maximum absorption wavelength from 465 to 595 nm. Absorbance at 595 nm was measured using a Shimadzu spectrophotometer (model UV-2450) at 25°C.

2.4.2 Electrophoresis

Sodium dodecyl polyacrylamide gel electrophoresis (SDS-PAGE) was performed using a RAPIDAS AE-6500 apparatus (ATTO, Tokyo, Japan) with 1-mm thick precast slab gels containing 10%–20% gradient acrylamide (e-PAGEL E-T1020L; ATTO), according to the procedure described by Laemmli (1970). 100 μg of each protein extract (Pp, Ps, and H) were loaded onto the gel. Electrophoresis was performed at 40 mA for 80 min. After electrophoresis, the gel was stained with a CBB-250 solution (Wako Pure Chemical Industries, Osaka, Japan). The applied molecular mass standard (Precision Plus Protein Standards; Bio-Rad Laboratories) contained protein bands of 10, 20, 25, 37, 50, 75, 100, 150, and 250 kDa in size. Gel photographs were taken with a Panasonic DMC-GF3 camera (Panasonic, Osaka, Japan), and the molecular weights of the protein sample bands calculated using ImageJ software (http://imagej.net/) after the exposure and contrast were adjusted.

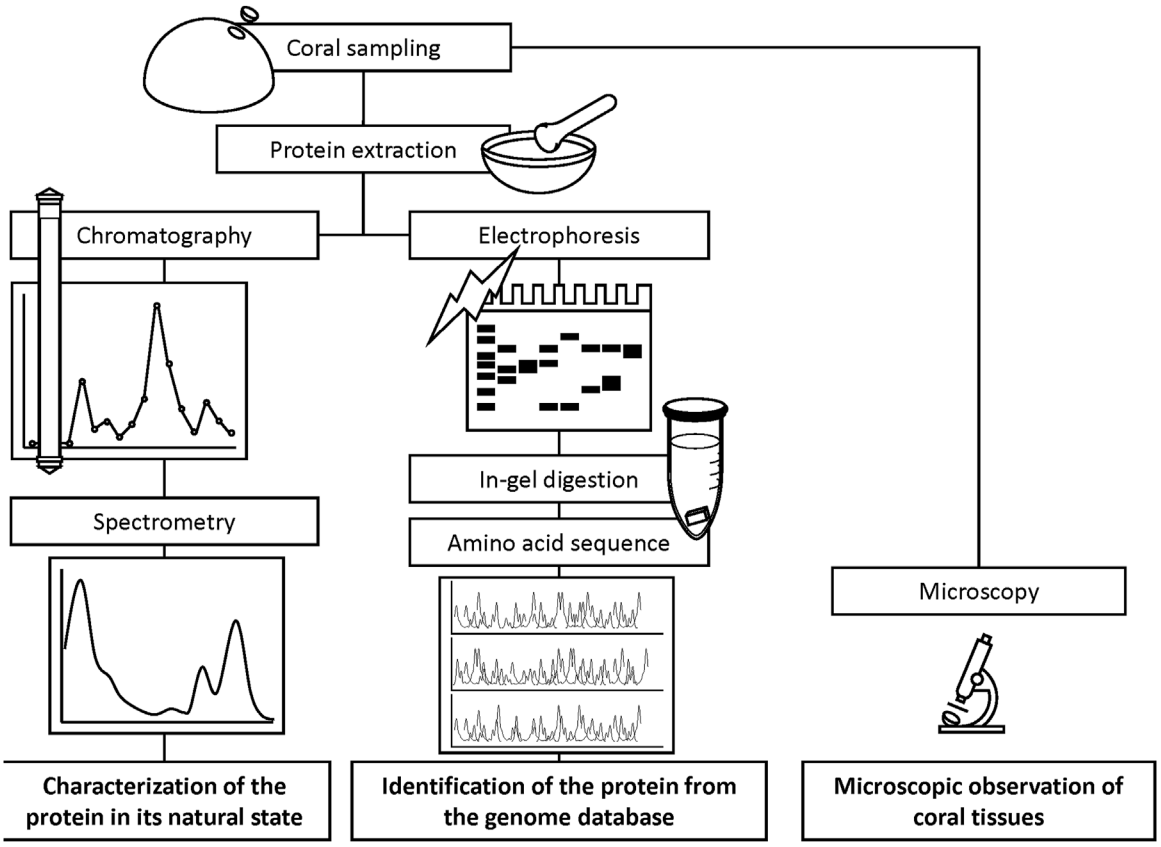

FIGURE 3
Schematized experimental flow for the characterization of chromoprotein.

2.4.3 In-gel tryptic digestion

The protein bands obtained from the CBB-stained SDS-PAGE gel were sliced into small pieces (approximately 1 mm^3) and faded with 50 mM NH_4HCO_3/50% acetonitrile. Proteins in the sliced gel fragments were reduced and alkylated with 10 mM dithiothreitol/50 mM NH_4HCO_3 for 45 min at 56°C and 55 mM iodoacetamide/50 mM NH_4HCO_3 at 25°C for 30 min in the dark. After being washed with acetonitrile, the proteins were digested in 10 µL trypsin (Sequencing Grade; Promega, Madison, WI, United States of America) at 37°C overnight. Tryptic peptides were extracted from the gel fragments using 50% acetonitrile containing 3% formic acid, and the peptide extracts centrifuged at 10,000 × *g* for 20 min in a vacuum centrifuge.

2.4.4 Liquid chromatography-tandem mass spectrometry analysis

Liquid chromatography-tandem mass spectrometry analysis was performed using a linear ion trap time-of-flight mass spectrometer (LIT–TOF MS; NanoFrontier eLD; Hitachi High-Technologies Corporation, Tokyo, Japan) coupled to a nanoflow HPLC (NanoFrontier nLC; Hitachi High-Technologies Corporation) at the Instrumental Research Support Center of the Research Institute of Green Science and Technology, Shizuoka University (Shizuoka, Japan). Peptides extracted from the gel were trapped and desalted using a C18 monolith trap column (0.05 mm ID × 150 mm long; Hitachi High-Technologies Corporation) and thereafter loaded onto a MonoCap C18 Fast-flow column (0.05 mm ID × 150 mm long; GL Sciences, Inc., Tokyo, Japan). Elution was done using a linear gradient from 5% to 40% solvent B for 60 min at a flow rate of 200 nL/min. Solvent A comprised 2% acetonitrile and 0.1% formic acid, and solvent B contained 98% acetonitrile and 0.1% formic acid. The eluent was ionized using a nanoelectrospray ionization source equipped with an uncoated silica tip (New Objective, Woburn, MA, United States of America) and analyzed using LIT–TOF MS. Mass spectra were obtained by scanning in the positive ion mode in the mass range of *m/z* 200–2000. MS/MS spectra were generated by using collision-induced dissociation in a linear ion trap. The proteins were identified by analyzing the MS/MS data via *de novo* sequencing and with the protein identification software, PEAKS Studio (version 7.0; Bioinformatics Solutions, Inc., Waterloo, ON, Canada) (Ma et al., 2003). A protein identification database was generated using the protein sequences of *P. astreoides*, *P. australiensis*, and *P. lobata* obtained from Reef Genomics (http://reefgenomics.org/) (Liew et al., 2016). Reliability of the protein identification results obtained via PEAKS was increased through further analysis of the sequences using MASCOT MS/MS Ions Search (http://www.matrixscience.com/) (Cottrell, 2011) and the sequence tag search tool, SPIDER (Han et al., 2004). The detected proteins were identified through a similarity search of amino acid sequences using the Basic Local Alignment Search Tool (BLAST) on

the National Center of Biotechnology Information database (https://blast.ncbi.nlm.nih.gov/), the DNA Data Bank of Japan (DDBJ) (http://blast.ddbj.nig.ac.jp/), and Reef Genomics.

2.4.5 Phylogenetic analysis

A phylogenetic tree of the proteins identified in this study, together with other FPs described previously (Alieva et al., 2008), was constructed using an online program (http://www.phylogeny.fr/) developed by Dereeper et al. (Dereeper et al., 2008; Dereeper et al., 2010). Phylogenetic analysis was performed using the following programs: MUSCLE 3.8.31 for multiple alignments, Gblocks 0.91b for alignment refinement, PhyML 3.1 for phylogeny using maximum likelihood, and TreeDyn for tree rendering.

2.5 Microscopic observation of *in vivo* fluorescence in corals

Overview photographs of corals manifesting PPR and healthy-appearing corals were taken in the laboratory with an OLYMPUS E-PL6 camera under a white light-emitting diode (LED) and processed using Adobe Lightroom (Adobe, San Jose, CA, United States of America) with the following settings: exposure, +0.5; highlight, −75; shadow, −20; white level, +65; black level, −40. The fluorescence levels of each sample were observed using a stereoscopic microscope (Nikon SMZ-1000; Nikon, Tokyo, Japan), and photographs obtained using an OLYMPUS E-PL6 camera equipped with a mount conversion ring. Visible images were obtained under environmental light and an exposure of one-fifth of a second with a sensitivity of ISO 400. Fluorescence images were obtained through excitation with a blue LED with a wavelength range of 380–550 nm (KR93SP; Eco-lamps Inc., Kowloon, Hong Kong), exposure for 13 s with a sensitivity of ISO 100, and filtering through a 600-nm bandpass filter (BPB-60; Fujifilm, Tokyo, Japan). The bandpass filter was attached to the objective lens of the microscope. All images were processed using Adobe Lightroom software.

2.6 Maximum quantum yield of photosystem II

The photosynthetic activity of Symbiodiniaceae under each coral condition was evaluated using the maximum quantum yield of photosystem II (*Fv*/*Fm*), and the minimum fluorescence yield (*F0*) measured using Junior-PAM (Walz, Effeltrich, Germany). Coral nubbins were subjected to dark acclimation for 30 min (Krause and Weis, 1991). The *Fv*/*Fm* and *F0* values measured at 10 different points in every coral nubbin were used to estimate averages and standard errors (Supplementary Table S1).

2.7 Hydrogen peroxide-scavenging activity

Enzyme samples were prepared by removing excess water from the collected coral pieces and excavating nine points (1.0–1.5 cm^2) on each coral colony surface (Pp and H) using whetstone drilling. The excavated areas were rinsed with 1 mL of 50 mM Tris-HCl buffer (pH 7.6) to collect the coral tissue, and the extract centrifuged at 10,000 × *g* for 3 min to remove debris. The supernatant was used to measure the protein concentration and hydrogen peroxide-scavenging activity (HSA), following the method described in Palmer et al., 2009a. To measure HSA, each 50 µL of the sample (coral tissue in buffer solution) and 50 µL of 50 mM hydrogen peroxide solution were mixed on 96-wells microplate. The absorbance at 240 nm was measured every 81 s for 30 min, and the data converted using a standard curve of hydrogen peroxide (serial dilutions: 0, 6.25, 12.5, 25, and 50 mM). HSA was normalized to the protein concentration (Supplementary Table S2).

2.8 Statistical analysis

Independent-samples *t*-test analysis was carried out to determine significant differences between the *Fv*/*Fm* and HSA data from Pp colony and H colony. Normality of the data was tested using Anderson–Darling test. Significant differences were evaluated at $p < 0.01$.

3 Results

3.1 Purification and characterization of chromoproteins

The soluble fraction of coral tissues manifesting Pp was separated into 40 elution fractions using FPLC. Of these, elution product 18 (18 mL elution volume) showed the highest absorbance at a wavelength of 580 nm (Figure 4A). Using a marker protein, the molecular weight of the main peak fraction (18) was estimated to be 49 kDa. The absorption spectrum of the main fraction is shown in Figure 4B.

3.2 Identification of chromoproteins from corals manifesting pink pigmentation responses

Three notable bands on the SDS-PAGE gel were found in the Ps and Pp coral tissues (Figure 5; bands 1–3). PEAKS analysis showed that the proteins extracted from bands 1 and 2 (Protein A) had the same alignment as that of the candidate protein (Porites_australiensis_11250) that was detected in the protein sequences of *P. australiensis* with high coverage (75%). The amino acid sequence of Protein A was queried on Reef Genomics with the protein database "Porites lutea gene models (ReFuGe 2020)," which identified 20 homologous proteins. Reanalysis of the Protein A was performed with these 20 proteins using PEAKS, where the database identified six proteins with high scores and coverage values with respect to the proteins synthesized by *P. lutea*. The amino acid sequences of these six proteins are shown in Figure 6. Among the six proteins, plut2.m8.16902.m1 with a GFP domain had the highest coverage (81%). Alignment of plut2.m8.16902.m1 using the BLAST search

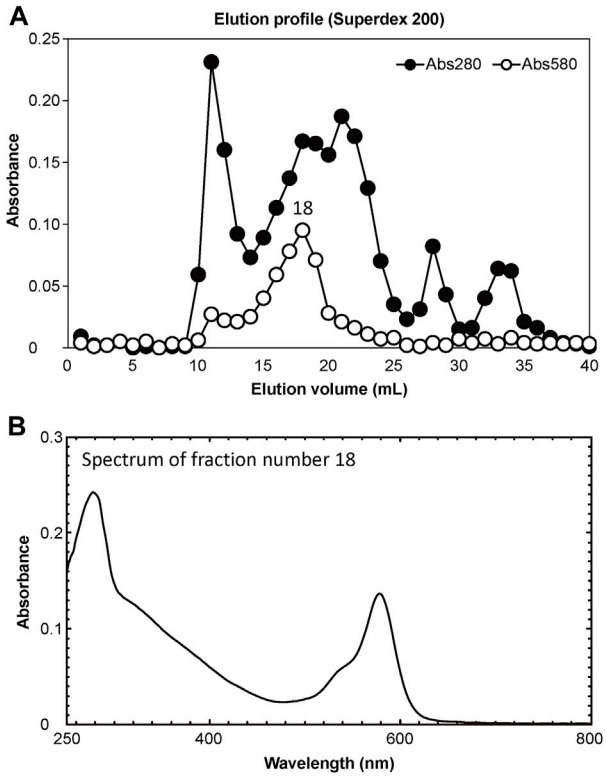

FIGURE 4
Results of purification of extracted proteins. **(A)** Separation of pink-coloured protein by Superdex 200 gel filtration column chromatography. Solid and open circles indicate protein fractions measured at 280 nm (estimate protein content) and 580 nm (estimate CP content), respectively. **(B)** Absorption spectrum of peak fraction number 18 in the elution profile.

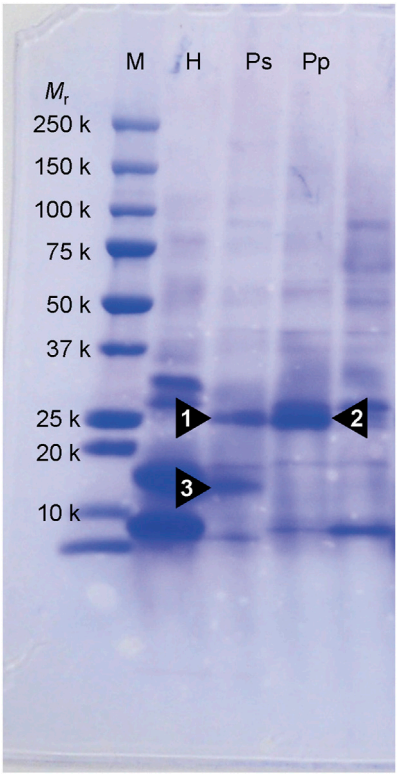

FIGURE 5
SDS-PAGE on 10% polyacrylamide gel of partially purified protein extracts from corals. Proteins were stained by coomassie brilliant blue R-250. Numerals under *Mr* denote the molecular masses of marker protein. Arrowhead (1, 2 and 3) indicates a protein that appears specifically in the pink lesions of Ps and Pp. M, molecular weight markers; H, healthy-appearing colony; Ps, pink spot exhibiting colony; Pp, pink patch exhibiting colony.

program in the DDBJ database revealed high similarities with other CPs and FPs from *Acropora aculeus*, *A. digitifera*, *Goniopora tenuidens*, *Galaxea fascicularis*, *A. millepora*, and many other coral species (Table 1). Using electrophoresis and amino acid sequence analyses (in-gel trypsin digestion and liquid chromatography-tandem mass spectrometry analysis), its molecular weight was determined to be 25 kDa (Figure 5; Table 1). The protein in band 3 (Protein B) was also analyzed using the same methods and showed a high similarity with thioredoxin-like proteins from several marine organisms (Table 1). On the other hand, no remarkable band in the electrophoresis result near 25 kDa (CPs and GFP) was found for the healthy colony: the greenish appearance of the healthy colony (Figure 2A) was due to the reflection from the green band of the endolithic community that was well developed underneath the coral tissue and not to the presence of GFP. Moreover, the molecular weight of GFP in *Porites lutea* is 24.8 kDa (*Porites lutea* database in Reef Genomics) but, from the electrophoresis study, the healthy coral did not show high expression of protein in the band corresponding to GFP's molecular weight. Phylogenetic analysis revealed that the six identified proteins were nonfluorescent, similar to that of other CPs in several coral species (Figure 7).

3.3 Localization of chromoproteins and red fluorescent protein in corals displaying pink pigmentation responses

Figure 8 shows the aspect of the colony manifesting Pp (Figure 8A,C,E) and healthy-appearing coral colony (Figure 8B,D,F) under visible light, and their fluorescence under a stereoscopic microscope using the bandpass filter transmitting light at 600 nm wavelength. Under visible light, the entire surface of the corals was purple and the tentacles a pale pink (Figure 8C). Conversely, under blue LED light and bandpass filter, red fluorescence was observed only at the tip of the tentacles (Figure 8E), and slight fluorescence was observed in healthy-appearing corals (Figure 8F).

3.4 Evaluation of the coral stress state

The stress conditions of the studied corals and their Symbiodiniaceae were estimated by measuring the *Fv*/*Fm* and *F0* (Table 2), as well as the HSA (Table 3). The *Fv*/*Fm* and *F0* values of the corals with pink pigmentation were 0.434 and

10.3389/fphys.2024.1339907

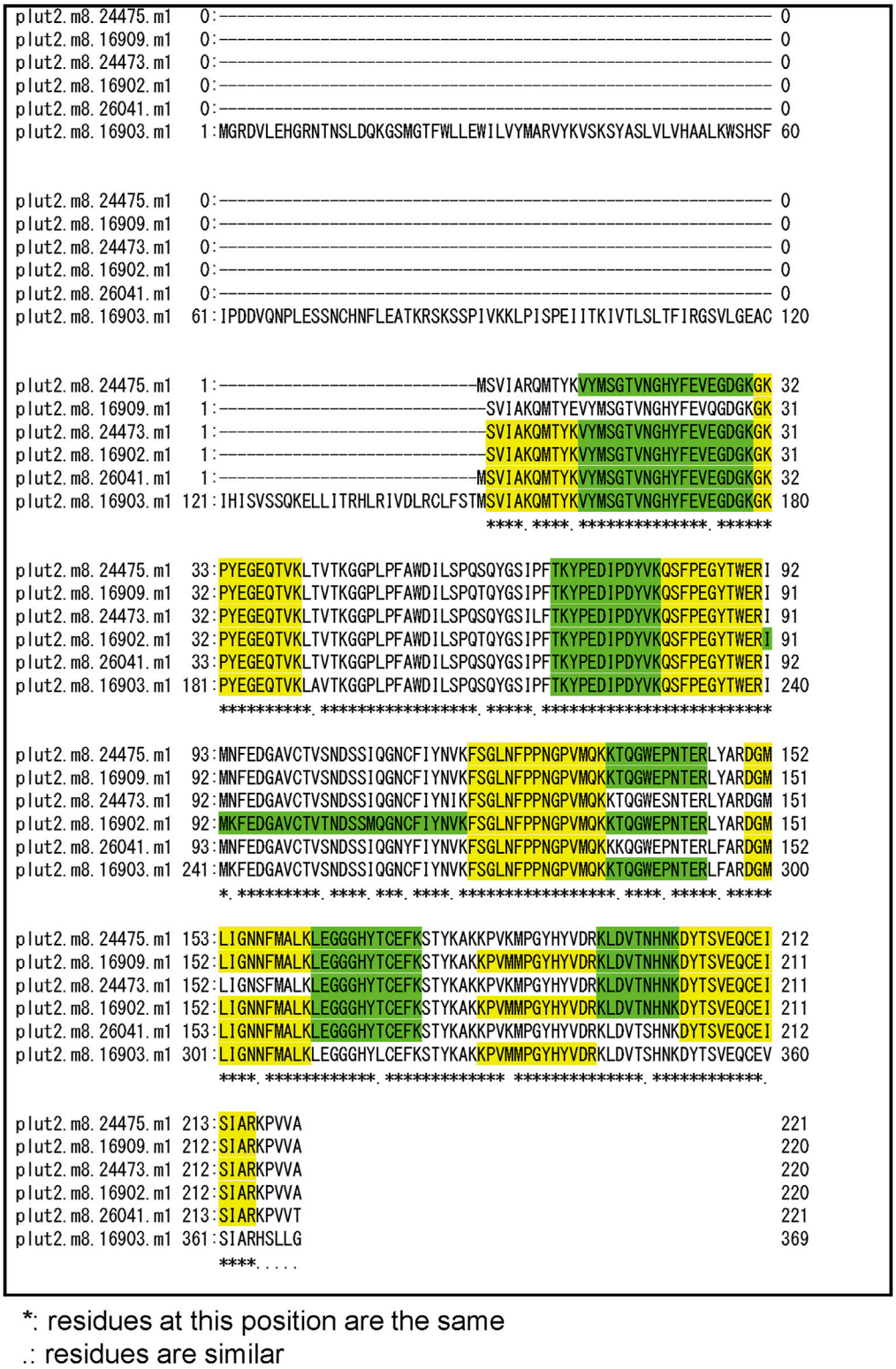

FIGURE 6
Alignment of amino acid sequence of 6 candidate proteins that hitted with high coverage values for peptide fragments of bands 1 and 2 (Protein A) in Figure 5. Peptide fragments detected by PEAKS Software were indicated as green and yellow.

369.5, respectively, which were significantly lower than those of healthy-appearing corals (0.521 and 597.3, respectively) ($p < 0.01$). Furthermore, the HSA value of corals manifesting pink pigmentation (1.88 nmol min^{-1} mg^{-1} protein) was 4.3 times significantly higher than that of healthy-appearing corals (0.44 nmol min^{-1} mg^{-1} protein) ($p < 0.01$).

TABLE 1 Amino acid sequences and homologues of protein that were specific for corals manifesting Ps and Pp. Alignments were determined by BLAST search from database of *P. lutea* on Reef Genomics. Putative conserved domains and similar proteins were determined by BLAST search from UniProtKB/Swiss-Prot + TrEMBL database on DDBJ.

[Bands 1 and 2; protein A]				[Band 3; Protein B]			
Alignment				Alignment			
Name: plut2.m8.16902.m1 Alignment: SVIAKQMTYKVYMSGTVNGHYFEVEGDGKGKPYEGEQTVKLTVTKGGPLPFAWDILSPQTQYGSIPFT KYPEDIPDYVKQSFPEGYTWERIMKFEDGAVCTVTNDSSMQGNCFIYNVKFSGLNFPPNGPVMQKKTQGWEPNTE RLYARDGMLIGNNFMALKLEGGGHYTCEFKSTYKAKKPVMMPGYHYVDRKLDVTNHNKDYTSVEQCEISIARKPVVA				Name: plut2.m8.16752.m1 Alignment: QDDFDAFLKEAGSTLVVVDFYADWCGPCKMIAPKIKGFAEEFSG KVYFAKVNVDENDEVAGKEGISAMPTFNLYKNGAKVDELTGANEAKLRELIEKRI			
Average mass: 24,870				Average mass: 10,957			
Putative conserved domains: GFP superfamily				Putative conserved domains: TRX_family, thioredoxin and thioredoxin_like superfamily			
Similar proteins				Similar proteins			
Accession number	Protein name	Species	Identity	Accession number	Protein name	Species	Identity
Q66PU8	Chromoprotein	*Acropora aculeus*	211/220 (95%)	A0A2B4SRX0	Thioredoxin	*Stylophora pistillata*	61/94 (64%)
A0A1S7IWH7	Fluorescent protein	*Acropora digitifera*	211/220 (95%)	A0A1X7VQB2	Thioredoxin	*Amphimedon queenslandica* (sponge)	56/97 (57%)
Q95P04	GFP-like non-fluorescent chromoprotein	*Goniopora tenuidens*	211/220 (95%)	A0A3S3QB26	Thioredoxin	*Dinothrombium tinctorium* (red velvet mite)	58/98 (59%)
A8CLV6	GFP-like chromoprotein	*Galaxea fascicularis*	211/220 (95%)	A0A1D2NA26	Thioredoxin-2	*Orchesella cincta* (springtail)	61/98 (62%)
A0A1S7IWI5	Fluorescent protein	*Acropora digitifera*	210/220 (95%)	L7XAL0	Thioredoxin	*Scylla paramamosain* (mud crab)	58/97 (59%)
Q66PV0	Chromoprotein	*Acropora millepora*	210/220 (95%)	Accession number	Protein name	Species	Identity
B5T1L1	Chromoprotein CP584	*Acropora pulchra*	210/220 (95%)	A0A2B4SRX0	Thioredoxin	*Stylophora pistillata*	61/94 (64%)
M4R4D0	Chromoprotein 580	*Acropora millepora*	211/220 (95%)	A0A1X7VQB2	Thioredoxin	*Amphimedon queenslandica* (sponge)	56/97 (57%)
A0A1S7IWI6	Fluorescent protein	*Acropora digitifera*	209/220 (95%)	A0A3S3QB26	Thioredoxin	*Dinothrombium tinctorium* (red velvet mite)	58/98 (59%)
A8CLL3	GFP-like chromoprotein	*Goniopora djiboutiensis*	209/220 (95%)	A0A1D2NA26	Thioredoxin-2	*Orchesella cincta* (springtail)	61/98 (62%)

10.3389/fphys.2024.1339907

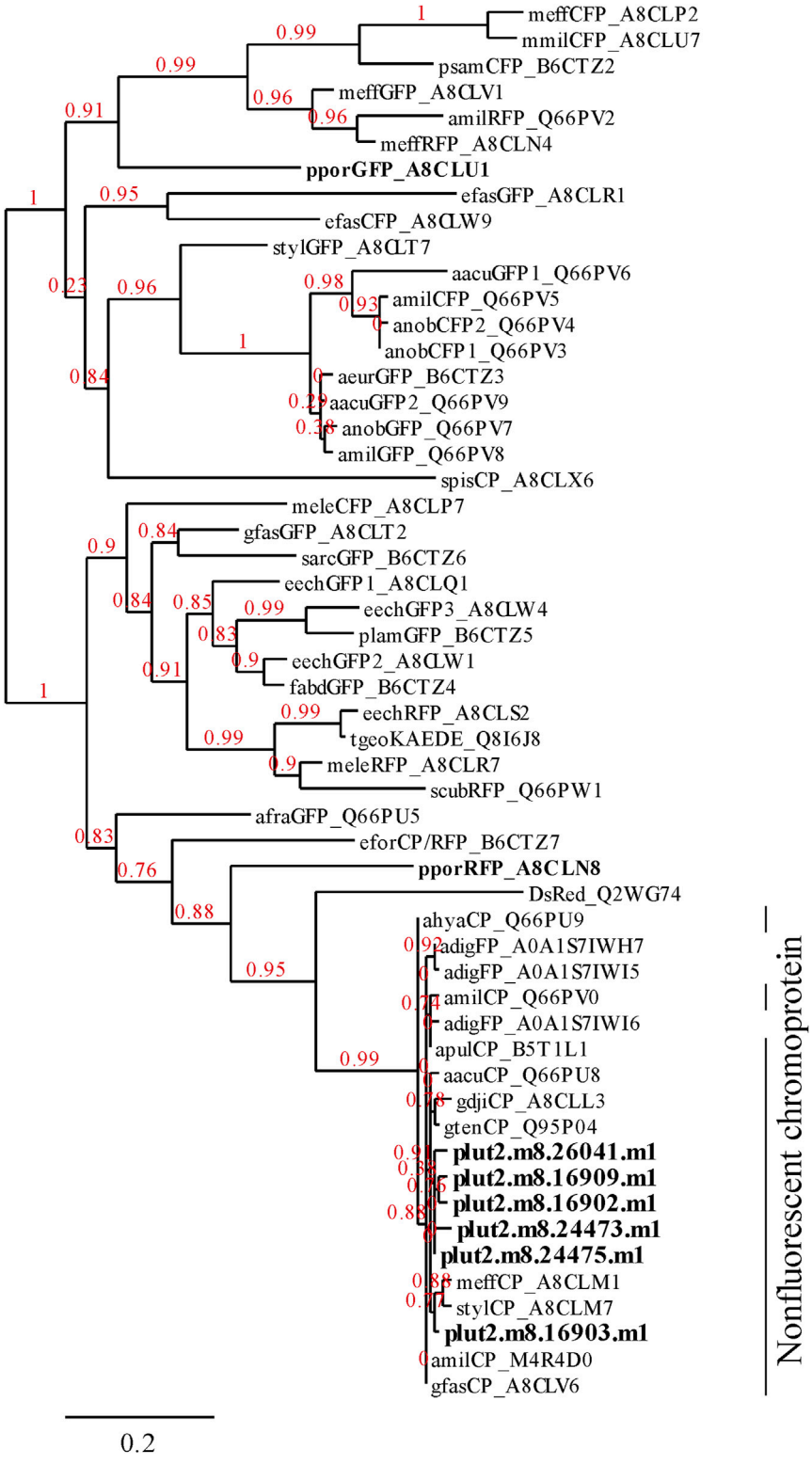

FIGURE 7
Phylogenetic tree showing the relationships among 6 proteins found in the present research (Figure 6) and FPs and CPs of corals. The alignments of *P. lutea* protein were identified using PEAKS analysis. Other FPs listed in Alieva et al. (Alieva et al., 2008) were obtained from the database of UniProt (http://www.uniprot.org/). The 6 proteins identified in this study and other FPs of *Porites* spp. are indicated in bold text.

10.3389/fphys.2024.1339907

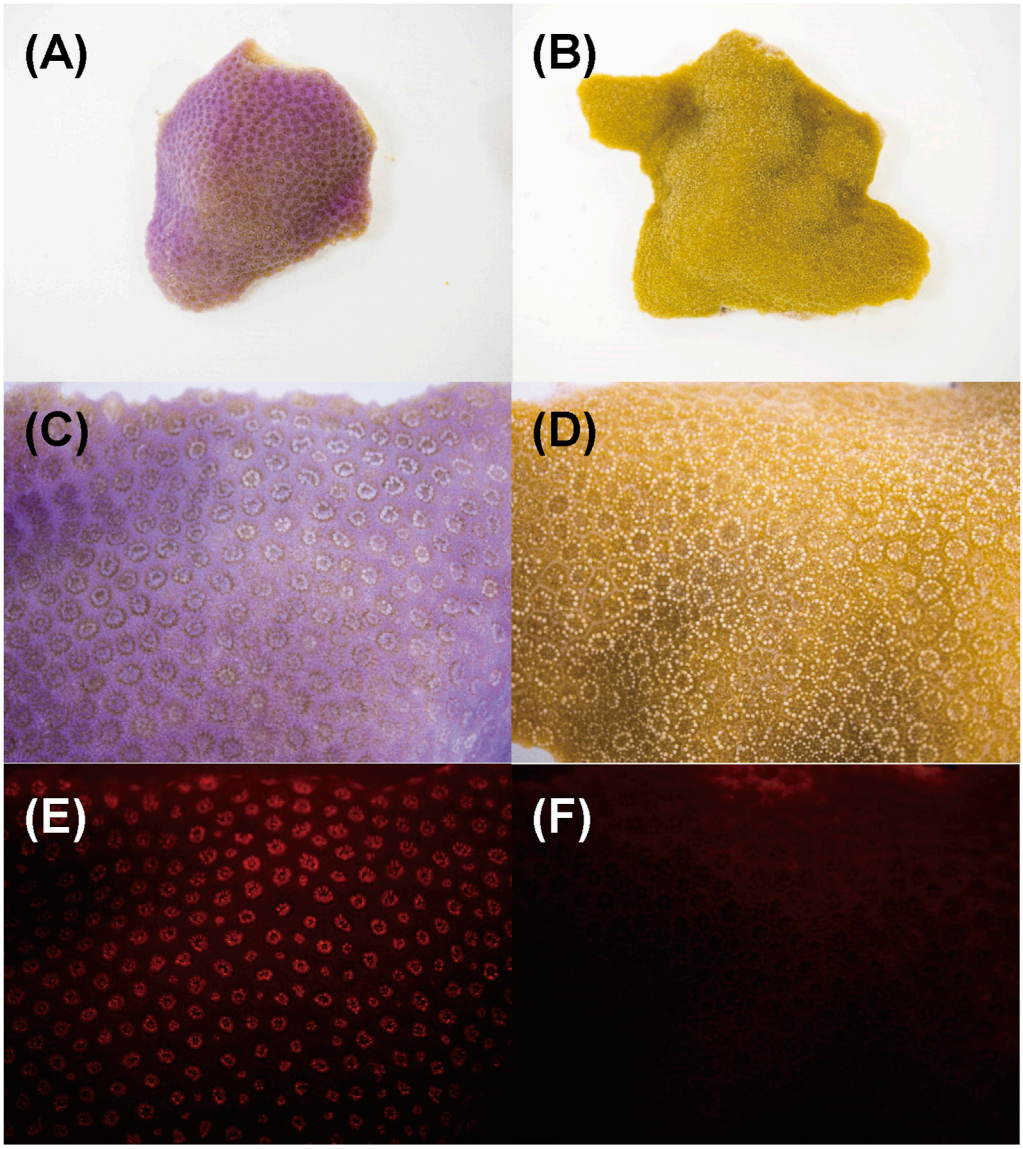

FIGURE 8
Aspects of *Porites* nubbins and fluorescence image that were taken under microscope. Images of **(A, B)** are overview of corals nubbins and **(C–F)** are magnified images (10X). **(A, C, and E)** Coral manifesting pink patch (Pp), **(B, D and F)** healthy-appearing colony **(H)**. The **(E and F)** are fluorescent image under blue LED light.

TABLE 2 Comparison of maximum quantum yield of photosystem II (*Fv*/*Fm*) and minimum fluorescence yield (*F0*) of each coral colony (Pp and H). Means ± s.e. (n = 10). Asterisks mean significant differences with healthy-appearing coral by t-test at $p < 0.01$.

	Fv/*Fm*	s.e.	*F0*	s.e.
Pp colony	0.434*	±0.036	369.5*	±44.8
H colony	0.521	±0.016	597.3	±25.4

4 Discussion

The pink pigment produced by corals manifesting PPRs was found to be a type of nonfluorescent CP. Our results also revealed that the CP was common in Ps and Pp lesions and homologous to other nonfluorescent CPs that have been reported in other corals (Alieva et al., 2008; Shinzato et al., 2012; Takahashi-Kariyazono et al., 2018). Furthermore, Protein A in this study showed high similarity to the six nonfluorescent CPs that are encoded in the genome of *P. lutea*, especially plut2.m8.16902.m1 (plutCP)

TABLE 3 Comparison of hydrogen peroxide scavenging activity (HSA) of each coral colony (Pp and H). Means ± s.d. (n = 9). Asterisks mean significant differences with healthy-appearing coral by t-test at $p < 0.01$.

	HSA (decrease of nmol H_2O_2 min^{-1} mg $protein^{-1}$)	
Pp colony	1.88*	±0.05
H colony	0.44	±0.06

(Figure 6). In particular, the fragments from I91–K118 were not detected in proteins other than plutCP. In addition, proteins other than nonfluorescent CPs were detected with low coverage and intensity using PEAKS analysis. These results indicate that plutCP expressed in the PPR lesions was a major protein present in the bands 1 and 2. As only plutCP was detected with the highest degree of similarity, we assumed that only this protein could be responsible for the pink-colored tissue. A BLASTP search of the plutCP protein identified several CPs and FPs with high similarities, including CPs of *A. aculeus* (accession number Q66PU8), *A. millepora* (Q66PV0 and M4R4D0), *A. pulchra* (B5T1L1), *G. tenuidens* (Q95P04), *G. djiboutiensis* (A8CLL3), and *G. fascicularis* (A8CLV6), and FPs of *A. digitifera* (A0A1S7IWH7, A0A1S7IWI5, and A0A1S7IWI6). Although these CPs have a maximum absorbance at a wavelength of approximately 580 nm, they did not produce any fluorescence (Alieva et al., 2008). Furthermore, the amino acid sequences of plutCP and the other five proteins were compared with those of several known FPs, DsRed (Q2WG74), KAEDE (Q8I6J8), asFP595 (Q9GZ28), and other proteins listed in Table 1 by Alieva et al., 2008 (Figure 7). Surprisingly, all six proteins found in this study were identified as nonfluorescent CPs, unlike other RFPs, confirming that plutCP is a type of nonfluorescent CP that belongs to clade B in Alieva's classification. Clade B mainly consists of purple and blue nonfluorescent CPs, and their genes have been found in Acroporidae, Pocilloporidae, Poritidae, Faviidae, Pectinidae, Oculinidae, and Dendrophyliidae. In this study, novel CP genes from *P. lutea* were added to this clade, and plutCP isolated from coral tissue. Finally, to confirm that the protein was indeed a nonfluorescent CP, we examined the corals using optical and fluorescence microscopy (Figure 8). A red-purple color was found throughout the coenosarc, and was particularly intense in color, whereas the tips of the tentacles were pale. In contrast, fluorescence observations revealed strong red fluorescence at the tips of the tentacles and almost no fluorescence in the coenosarc. Fluorescence images were obtained by filtering through a 600-nm bandpass filter attached under the objective lens of the microscope. Therefore, the red fluorescence of chlorophyll that is predominantly detected at a wavelength of 680 nm was removed; thus, the red fluorescence detected was most likely because of RFP, which emits fluorescence at wavelengths below 600 nm. As a reference, similar observations in healthy corals showed almost no fluorescence, suggesting that the detected fluorescence was a result of RFP and not chlorophyll. Thus, the protein responsible for the reddish-purple discoloration found in PPR was different from a RFP and confirmed to be an independent, nonfluorescent CP. These results indicate that CPs were distributed uniformly across the surface of the coral colonies mainly in the coenosarc, and the localization of the CPs was different from that of RFP. The molecular weight of plutCP extracted from massive *Porites* spp. manifesting PPRs was different in the SDS-PAGE (25 kDa), amino acid sequence (24,870 Da), and gel-filtration chromatography (49 kDa), and this result can be attributed to the formation of a dimer under native conditions, similar to that observed for GFP (Ward and Cormier, 1979). Ahmed et al. (2022) also reported that other CPs (gfasPurple, amilCP, spisPink, and eforRed) form dimers in solution, based on X-ray crystal structure analysis.

The present study demonstrated that CPs were encoded in the genome of *Porites* corals (*P. astreoides*, *P. australiensis*, and *P. lobata*), and the same CP expressed in different morphologies of PPRs (Ps and Pp), associated with the pink pigmentation response of inflamed tissues. Three presumed CP sequences were also identified in *A. digitifera* (Shinzato et al., 2012). These sequences were also included in the same clade as the six *Porites* sequences obtained in our study, which supports the present results as the 6 detected proteins beat similar properties as non-fluoresce and the formation of dimers. Moreover, in addition to plutCP synthesized by *Porites* spp. corals, a thioredoxin-like protein that is linked to redox signaling was expressed at high levels in the Ps lesions (Figure 5, Band 3).

The CP of *Porites* spp. was detected only in tissues that manifested PPRs. In relation to other types of CPs, Shinzato et al. (2012) reported that the three CPs of *A. digitifera* were highly expressed in the developmental stages but very poorly in adults. Studies by Takahashi-Kariyazono et al. (2018) also showed that FPs in middle-/long-wavelength emissions (519, 606, and 613 nm) and CPs were important for *Acropora* larvae, but were not expressed in adults. However, Smith et al. (2013) and Gittins et al. (2015) reported that high-level expression of CPs in adult corals (*Acropora nobilis* and *A. millepora*) was correlated with the reduction of photodamage under acute light stress, confirming the photoprotective function of CPs. This, together with the results of electrophoresis in the present study, show *Porites* spp. corals manifesting PPR lesions expressed high levels of CPs rather than in healthy tissues.

The PPRs in *Porites* spp. corals are highly distributed in the apical area of the colony, which is impacted by light in the shallow reefs of Okinawa during the low-tide period, in contrast to those medial and basal areas of the colony which are self-shaded (Yucharoen, 2016). The high production of CPs in the restricted PPR lesions reflects a focalized immune response of these corals to environmental stressors: biotic as the penetration of boring organisms, and more importantly, abiotic factors such as the salinity, the height of low tide, the time of exposure to air, and nutrient concentration, among others (In Yucharoen, 2016, pg.41, Table 5). In addition, RFPs and CPs coexist in the PPR lesions, but their distribution differs within the coral tissue, mainly coenosarc for CPs and tip of polyps' tentacles for RFPs. CPs and their homologs have been suggested to serve as coral health indicators, as they usually protect cells against free radicals, and CPs likely also play important roles in the coral immune system and photoprotection, similar to that of RFPs. Palmer et al. (2009a) demonstrated that various CPs may act as antioxidants in coral hosts, showing a greater ability to scavenge hydrogen peroxide in inflamed tissues than

healthy tissues. Correspondingly, the current study found high hydrogen peroxide-scavenging rates in *Porites* spp. corals tissues affected by PPR confirming this hypothesis. Several cases, such as dark-blue pigment in *A. hemprichii* (Rinkevich et al., 1994), pink-blue spot syndrome in *A. eurystoma* (Bongiorni and Rinkevich, 2005), dark spot syndromes in *Porites*, *Siderastrea*, and *Montastraea* (Cervino et al., 2001; Borger, 2005), and purple pigment in octocorals (Mullen et al., 2006), have been reported, but information about the presence and roles of CPs in *Porites* corals is scarce. D'Angelo et al. (2012) proposed that coloration changes in hosts expressing GFP-like proteins in response to wounding and infestation. Yucharoen (2016) reported a remarkable increase in CPs in relation to high HSA. Taken together, these studies indicate that massive *Porites* may produce CPs as an immune response against oxidative stress promoted by several environmental disturbances (biotic and abiotic), resulting in PPR lesions. Therefore, it can be concluded that the CP isolated from *Porites*. in the present study might possess antioxidant activity, contributing to the coral defense mechanism against ROS induced by various stresses (Yucharoen, 2016), and opportunistic infection in coral tissues displaying PPRs.

Although *Porites* corals are tolerant species that can adapt to various environments (Cantin and Lough, 2014), they occasionally show sensitivity to environmental stresses (Raymundo et al., 2005). Our results indicate that PPRs on *Porites* spp. in the area of Sesoko Lagoon could be promoted by environmental stressors and/or mechanical injuries caused by fish bites or boring organisms. CP, which is specifically expressed in PPR lesions, may serve as an antioxidant in the affected coral tissue. Furthermore, CP and RFP showed differential distribution within the PPR lesion, suggesting that CP, which is uniformly distributed in the coenosarc and covers a wide surface area, may have a more important role as an antioxidant than that of RFP, which is present only at the tips of tentacles.

This is the first study to report the role and distribution of CPs in corals manifesting PPR lesions. We believe that these findings will aid our understanding of PPR formation mechanism, which is an important subject in coral disease research. In addition, we describe, for the first time, the coexistence of nonfluorescent proteins and FPs in massive *Porites* spp. manifesting PPRs. Despite the PPR morphology (Ps or Pp) of *Porites* spp., the corals expressed the same type of CP. CPs have potential applications as genetic markers and cellular biosensors because of their ease of detection (Liljeruhm et al., 2018). The protocol used in this study, including genome analysis and microscopic observation using different filters, could be applied in future studies of pigments that commonly manifest in corals affected by other diseases. Therefore, this method opens the possibility to a deeper understanding of coral disease mechanisms in response to changing environment.

5 Compliance

Permission for coral sampling was obtained from Okinawa Prefecture (permit No. 30–55). The permit period was from 20 July 2018 to 19 July 2019.

Data availability statement

The original contributions presented in the study are included in the article/Supplementary Material, further inquiries can be directed to the corresponding author.

Ethics statement

The manuscript presents research on animals that do not require ethical approval for their study.

Author contributions

TS: Writing–original draft, Investigation, Conceptualization, Methodology, Formal Analysis, Visualization, Validation, Data curation, Writing–review and editing. BC: Writing–original draft, Writing–review and editing, Validation, Supervision, Resources, Project administration, Methodology, Funding acquisition. MY: Writing–original draft, Writing–review and editing, Formal Analysis, Validation, Data curation. HD: Writing–review and editing, Methodology, Formal Analysis, Data curation. YS: Writing–review and editing, Supervision, Project administration.

Funding

The author(s) declare that financial support was received for the research, authorship, and/or publication of this article. Grant-in-Aid for Fund for the Promotion of Joint International Research [Fostering Joint International Research (B)] from the Japanese Ministry of Education, Culture, Sports, Science and Technology (MEXT) (No. 18KK0298), and by the 50th Anniversary Grant from the Mitsubishi Corporation on "Global Coral Reef Conservation Project (GCRCP). The funders were not involved in the study design, collection, analysis, interpretation of data, the writing of this article, or the decision to submit it for publication.

Acknowledgments

We are grateful to the staff at Sesoko Station, Tropical Biosphere Research Center (University of the Ryukyus, Japan), for providing the necessary facilities during this study, and to Mr. Sunao Uehara for his assistance with coral sampling.

Conflict of interest

The authors declare that the research was conducted in the absence of any commercial or financial relationships that could be construed as a potential conflict of interest.

The author(s) declared that they were an editorial board member of Frontiers, at the time of submission. This had no impact on the peer review process and the final decision.

Publisher's note

All claims expressed in this article are solely those of the authors and do not necessarily represent those of their affiliated organizations, or those of the publisher, the editors and the reviewers. Any product that may be evaluated in this article, or claim that may be made by its manufacturer, is not guaranteed or endorsed by the publisher.

Supplementary material

The Supplementary Material for this article can be found online at: https://www.frontiersin.org/articles/10.3389/fphys.2024.1339907/full#supplementary-material

References

Aeby, G. S. (1992). The potential effect the ability of a coral intermediate host to regenerate has had on the evolution of its association with a marine parasite. Proceeding of the Seventh International Coral Reef Symposium, Guam, 1992, 2.

Aeby, G. S. (2003). Corals in the genus *Porites* are susceptible to infection by a larval trematode. *Coral Reefs* 22, 216. doi:10.1007/s00338-003-0310-9

Aeby, G. S., Williams, G. J., Franklin, E. C., Kenyon, J., Cox, E. F., Coles, S., et al. (2011). Patterns of coral disease across the Hawaiian Archipelago: relating disease to environment. *PLoS ONE* 6, e20370. doi:10.1371/journal.pone.0020370

Ahmed, F. H., Caputo, A. T., French, N. G., Peat, T. S., Whitfield, J., Warden, A. C., et al. (2022). Over the rainbow: structural characterization of the chromoproteins gfasPurple, amilCP, spisPink and eforRed. *Acta Crystallogr. D. Struct. Biol.* 78 (Pt 5), 599–612. doi:10.1107/S2059798322002625

Alieva, N. O., Konzen, K. A., Field, S. F., Meleshkevitch, E. A., Hunt, M. E., Beltran-Ramirez, V., et al. (2008). Diversity and evolution of coral fluorescent proteins. *PLoS ONE* 3, e2680. doi:10.1371/journal.pone.0002680

Arya, R., Mallik, M., and Lakhotia, S. C. (2007). Heat shock genes - integrating cell survival and death. *J. Biosci.* 32, 595–610. doi:10.1007/s12038-007-0059-3

Beeden, R., Willis, B., Raymundo, L., Page, C., and Weil, E. (2008). *Underwater cards for assessing coral health on indo-pacific reefs - Resources - CCRES.*

Benzoni, F., Galli, P., and Pichon, M. (2010). Pink spots on *Porites*: not always a coral disease. *Coral Reefs* 29, 153. doi:10.1007/s00338-009-0571-z

Bollati, E., Lyndby, N. H., D'Angelo, C., Kühl, M., Wiedenmann, J., and Wangpraseurt, D. (2022). Green fluorescent protein-like pigments optimise the internal light environment in symbiotic reef-building corals. *eLife* 11, e73521. doi:10.7554/eLife.73521

Bongiorni, L., and Rinkevich, B. (2005). The pink-blue spot syndrome in *Acropora eurystoma* (Eilat, Red Sea): a possible marker of stress? *Zoology* 108, 247–256. doi:10.1016/j.zool.2005.05.002

Borger, J. L. (2005). Dark spot syndrome: a scleractinian coral disease or a general stress response? *Coral Reefs* 24, 139–144. doi:10.1007/s00338-004-0434-6

Bou-Abdallah, F., Chasteen, N. D., and Lesser, M. P. (2006). Quenching of superoxide radicals by green fluorescent protein. *Biochimica Biophysica Acta - General Subj.* 1760, 1690–1695. doi:10.1016/j.bbagen.2006.08.014

Bradford, M. M. (1976). A rapid and sensitive method for the quantitation of microgram quantities of protein utilizing the principle of protein-dye binding. *Anal. Biochem.* 72, 248–254. doi:10.1006/abio.1976.9999

Bridges, M. C., Woodley, C. M., Peters, E. C., May, L. A., and Galloway, S. B. (2020). Expression and characterization of a bright far-red fluorescent protein from the pink-pigmented tissues of *Porites lobata*. *Mar. Biotechnol.* 22, 67–80. doi:10.1007/s10126-019-09931-9

Cantin, N. E., and Lough, J. M. (2014). Surviving coral bleaching events: *Porites* growth anomalies on the Great Barrier Reef. *PLoS One* 9, e88720. doi:10.1371/journal.pone.0088720

Cervino, J., Goreau, T. J., Nagelkerken, I., Smith, G. W., and Hayes, R. (2001). Yellow band and dark spot syndromes in Caribbean corals: distribution, rate of spread, cytology, and effects on abundance and division rate of zooxanthellae. *Hydrobiologia* 460, 53–63. doi:10.1023/A:1013166617140

Cottrell, J. S. (2011). Protein identification using MS/MS data. *J. Proteomics* 74, 1842–1851. doi:10.1016/j.jprot.2011.05.014

D'Angelo, C., Smith, E. G., Oswald, F., Burt, J., Tchernov, D., and Wiedenmann, J. (2012). Locally accelerated growth is part of the innate immune response and repair mechanisms in reef-building corals as detected by green fluorescent protein (GFP)-like pigments. *Coral Reefs* 31, 1045–1056. doi:10.1007/s00338-012-0926-8

Dereeper, A., Audic, S., Claverie, J. M., and Blanc, G. (2010). BLAST-EXPLORER helps you building datasets for phylogenetic analysis. *BMC Evol. Biol.* 10, 8. doi:10.1186/1471-2148-10-8

Dereeper, A., Guignon, V., Blanc, G., Audic, S., Buffet, S., Chevenet, F., et al. (2008). Phylogeny.fr: robust phylogenetic analysis for the non-specialist. *Nucleic acids Res.* 36, W465–W469. doi:10.1093/nar/gkn180

Gittins, J. R., D'Angelo, C., Oswald, F., Edwards, R. J., and Wiedenmann, J. (2015). Fluorescent protein-mediated colour polymorphism in reef corals: multicopy genes extend the adaptation/acclimatization potential to variable light environments. *Mol. Ecol.* 24, 453–465. doi:10.1111/mec.13041

Han, Y., Ma, B., and Zhang, K. (2004).SPIDER: software for protein identification from sequence tags with *de novo* sequencing error. Proceedings - 2004 IEEE Computational Systems Bioinformatics Conference, CSB 2004. IEEE Computer Society, 206–215.

Hughes, T. P., Kerry, J. T., Baird, A. H., Connolly, S. R., Dietzel, A., Eakin, C. M., et al. (2018). Global warming transforms coral reef assemblages. *Nature* 556 (7702), 492–496. doi:10.1038/s41586-018-0041-2

Jin, Y. K., Lundgren, P., Lutz, A., Raina, J. B., Howells, E. J., Paley, A. S., et al. (2016). Genetic markers for antioxidant capacity in a reef-building coral. *Sci. Adv.* 2 (5), e1500842. doi:10.1126/sciadv.1500842

Johannes, R. E., and Wiebe, W. J. (1970). Method for determination of coral tissue biomass and composition. *Limnol. Oceanogr.* 15, 822–824. doi:10.4319/lo.1970.15.5.0822

Johnson, J. V., Exton, D. A., Dick, J. T. A., Oakley, J., Jompa, J., and Pincheira-Donoso, D. (2022). The relative influence of sea surface temperature anomalies on the benthic composition of an Indo-Pacific and Caribbean coral reef over the last decade. *Ecol. Evol.* 12 (9), e9263. doi:10.1002/ece3.9263

Kashimoto, R., Hisata, K., Shinzato, C., Satoh, N., and Shoguchi, E. (2021). Expansion and diversification of fluorescent protein genes in fifteen *Acropora* species during the evolution of acroporid corals. *Genes.* 12 (3), 397. doi:10.3390/genes12030397

Kenkel, C. D. (2008). Coral disease: baseline surveys in the andaman sea and gulf of Thailand. *Phuket Mar. Biol. Cent. Res. Bull.* 53, 43–53.

Krause, G. H., and Weis, E. (1991). Chlorophyll fluorescence and photosynthesis: the basics. *Annu. Rev. Physiol. Plant Mol. Biol.* 42, 313–349. doi:10.1146/annurev.pp.42060191.001525

Kritsanapuntu, S., and Angkhananukroh, P. (2014). Coral disease prevalence in samui Island and the adjacent islands, southern part of the gulf of Thailand | international network for natural Sciences INNSPUB - academia.edu. *J. Biodivers. Environ. Sci.* 5, 158–165.

Kubomura, T., Wee, H. B., and Reimer, J. D. (2021). Investigating incidence and possible causes of pink and purple pigmentation response in hard coral genus *Porites* around Okinawajima Island, Japan. *Regional Stud. Mar. Sci.* 41, 101569. doi:10.1016/j.rsma.2020.101569

Kumar, J. S. Y., Geetha, S., Satyanarayana, C., Venkataraman, K., and Kamboj, R. D. (2014). Observations on coral diseases in marine national park, gulf of kachchh. *Scholars Acad. J. Biosci.* 2, 370–373. doi:10.36347/sajb.2014.v02i06.002

Labas, Y. A., Gurskaya, N. G., Yanushevich, Y. G., Fradkov, A. F., Lukyanov, K. A., Lukyanov, S. A., et al. (2002). Diversity and evolution of the green fluorescent protein family. *Proc. Natl. Acad. Sci. U. S. A.* 99, 4256–4261. doi:10.1073/pnas.062552299

Laemmli, U. K. (1970). Cleavage of structural proteins during the assembly of the head of bacteriophage T4. *Nature* 227, 680–685. doi:10.1038/227680a0

Lanneau, D., Brunet, M., Frisan, E., Solary, E., Fontenay, M., and Garrido, C. (2008). Heat shock proteins: essential proteins for apoptosis regulation. *J. Cell. Mol. Med.* 12, 743–761. doi:10.1111/j.1582-4934.2008.00273.x

Liew, Y. J., Aranda, M., and Voolstra, C. R. (2016). Reefgenomics.Org - a repository for marine genomics data. *Database J. Biol. databases curation* 2016, baw152. doi:10.1093/database/baw152

Liljeruhm, J., Funk, S. K., Tietscher, S., Edlund, A. D., Jamal, S., Wistrand-Yuen, P., et al. (2018). Engineering a palette of eukaryotic chromoproteins for bacterial synthetic biology. *J. Biol. Eng.* 12, 8. doi:10.1186/s13036-018-0100-0

Lukyanov, K. A., Fradkov, A. F., Gurskaya, N. G., Matz, M. V., Labas, Y. A., Savitsky, A. P., et al. (2000). Natural animal coloration can be determined by a nonfluorescent green fluorescent protein homolog. *J. Biol. Chem.* 275, 25879–25882. doi:10.1074/jbc.C000338200

Ma, B., Zhang, K., Hendrie, C., Liang, C., Li, M., Doherty-Kirby, A., et al. (2003). PEAKS: powerful software for peptide *de novo* sequencing by tandem mass spectrometry. *Rapid Commun. Mass Spectrom.* 17, 2337–2342. doi:10.1002/rcm.1196

Matz, M. V., Fradkov, A. F., Labas, Y. A., Savitsky, A. P., Zaraisky, A. G., Markelov, M. L., et al. (1999). Fluorescent proteins from nonbioluminescent Anthozoa species. *Nat. Biotechnol.* 17, 969–973. doi:10.1038/13657

Miyawaki, A. (2002). Green fluorescent protein-like proteins in reef anthozoa animals. *Cell. Struct. Funct.* 27, 343–347. doi:10.1247/csf.27.343

Mohamed, A. R., Ali, A.-H. A. M., and Abdel-Salam, H. A. (2012). "Status of coral reef health in the northern Red Sea, Egypt," in *12th international coral reef symposium*, 5.

Montalbetti, E., Biscéré, T., Ferrier-Pagès, C., Houlbrèque, F., Orlandi, I., Forcella, M., et al. (2021). Manganese benefits heat-stressed corals at the cellular level. *Front. Mar. Sci. 29 June 2021 Sec. Aquat. Physiol.* 8–2021. doi:10.3389/fmars.2021.681119

Mullen, K. M., Harvell, C. D., Alker, A. P., Dube, D., Jordán-Dahlgren, E., Ward, J. R., et al. (2006). Host range and resistance to aspergillosis in three sea fan species from the Yucatan. *Mar. Biol.* 149, 1355–1364. doi:10.1007/s00227-006-0275-7

Nishihira, M. (2004). "Hermatypic corals of Japan," in: *Coral Reefs of Japan, eds. Ministry of the Environment and The Japanese Coral Reef Society* (Tokyo, Japan: Ministry of the Environment), 10–13.

Palmer, C. V., Modi, C. K., and Mydlarz, L. D. (2009a). Coral fluorescent proteins as antioxidants. *PLoS ONE* 4, e7298. doi:10.1371/journal.pone.0007298

Palmer, C. V., Roth, M. S., and Gates, R. D. (2009b). Red fluorescent protein responsible for pigmentation in trematode-infected *Pontes compressa* tissues. *Biol. Bull.* 216, 68–74. doi:10.1086/BBLv216n1p68

Putchim, L., Yamarunpattana, C., and Phongsuwan, N. (2012). Observations of coral disease in *Porites lutea* in the Andaman Sea following the 2010 bleaching. *Phuket Mar. Biol. Cent. Res. Bull.* 71, 57–62.

Ravindran, J., and Raghukumar, C. (2002). Pink line syndrome (PLS) in the scleractinian coral *Porites lutea*. *Coral Reefs* 21, 252. doi:10.1007/s00338-002-0247-4

Ravindran, J., and Raghukumar, C. (2006). Histological observations on the scleractinian coral *Porites lutea* affected by pink-line syndrome. *Curr. Sci.* 90, 720–724. doi:10.2307/24089122

Raymundo, L. J., Resell, K. B., Reboton, C. T., and Kaczmarsky, L. (2005). Coral diseases on Philippine reefs: genus *Porites* is a dominant host. *Dis. Aquatic Org.* 64, 181–191. doi:10.3354/dao064181

Rinkevich, B., Frank, U., Bak, R. P. M., and Müller, W. E. G. (1994). Alloimmune responses between *Acropora hemprichi* conspecifics: nontransitive patterns of overgrowth and delayed cytotoxicity. *Mar. Biol.* 118, 731–737. doi:10.1007/BF00347522

Satoh, N., Kinjo, K., Shintaku, K., Kezuka, D., Ishimori, H., Yokokura, A., et al. (2021). Color morphs of the coral, *Acropora tenuis*, show different responses to environmental stress and different expression profiles of fluorescent-protein genes. *G3* 11 (2), jkab018. doi:10.1093/g3journal/jkab018

Séré, M. G., Chabanet, P., Turquet, J., Quod, J. P., and Schleyer, M. H. (2015). Identification and prevalence of coral diseases on three Western Indian Ocean coral reefs. *Dis. Aquatic Org.* 114, 249–261. doi:10.3354/dao02865

Seveso, D., Arrigoni, R., Montano, S., Maggioni, D., Orlandi, I., Berumen, M. L., et al. (2020). Investigating the heat shock protein response involved in coral bleaching across scleractinian species in the central Red Sea. *Coral Reefs* 39, 85–98. doi:10.1007/s00338-019-01878-6

Seveso, D., Montano, S., Maggioni, D., Pedretti, F., Orlandi, I., Galli, P., et al. (2018). Diel modulation of Hsp70 and Hsp60 in corals living in a shallowreef. *Coral Reefs* 37, 801–806. doi:10.1007/s00338-018-1703-0

Shinzato, C., Shoguchi, E., Tanaka, M., and Satoh, N. (2012). Fluorescent protein candidate genes in the coral *Acropora digitifera* genome. *Zoological Sci.* 29, 260–264. doi:10.2108/zsj.29.260

Smith, E. G., D'Angelo, C., Salih, A., and Wiedenmann, J. (2013). Screening by coral green fluorescent protein (GFP)-like chromoproteins supports a role in photoprotection of zooxanthellae. *Coral Reefs* 32, 463–474. doi:10.1007/s00338-012-0994-9

Sully, S., Burkepile, D. E., Donovan, M. K., Hodgson, G., and van Woesik, R. (2019). A global analysis of coral bleaching over the past two decades. *Nat. Commun.* 10 (1), 1264–1265. doi:10.1038/s41467-019-09238-2

Takahashi-Kariyazono, S., Sakai, K., and Terai, Y. (2018). Presence–absence polymorphisms of highly expressed FP sequences contribute to fluorescent polymorphisms in *Acropora digitifera*. *Genome Biol. Evol.* 10, 1715–1729. doi:10.1093/gbe/evy122

Thinesh, T., Mathews, G., and Edward, J. K. P. (2011). Coral disease prevalence in the Palk Bay, Southeastern India – with special emphasis to black band. *Indian J. Geo-Marine Sci.* 40, 813–820.

Thummasan, M., Casareto, B. E., Ramphul, C., Suzuki, T., Toyoda, K., and Suzuki, Y. (2021). Physiological responses (Hsps 60 and 32, caspase 3, H_2O_2 scavenging, and photosynthetic activity) of the coral *Pocillopora damicornis* under thermal and high nitrate stresses. *Mar. Pollut. Bull.* 171, 112737. doi:10.1016/j.marpolbul.2021.112737

Verkhusha, V. V., and Lukyanov, K. A. (2004). The molecular properties and applications of Anthozoa fluorescent proteins and chromoproteins. *Nat. Biotechnol.* 22, 289–296. doi:10.1038/nbt943

Veron, J. E. N. (1992). Conservation of biodiversity: a critical time for the hermatypic corals of Japan. *Coral Reefs* 11, 13–21. doi:10.1007/BF00291930

Ward, W. W., and Cormier, M. J. (1979). An energy transfer protein in coelenterate bioluminescence. Characterization of the Renilla green-fluorescent protein. *J. Biol. Chem.* 254 (3), 781–788. doi:10.1016/S0021-9258(17)37873-0

Weil, E., Irikawa, A., Casareto, B., and Suzuki, Y. (2012). Extended geographic distribution of several Indo-Pacific coral reef diseases. *Dis. Aquatic Org.* 98, 163–170. doi:10.3354/dao02433

Weil, E., Rogers, C. S., and Croquer, A. (2016). "Octocoral diseases in a changing ocean," in *Marine animal forests*. Editors S. Rossi, L. Bramanti, A. Gori, and C. Orejas Saco del Valle (Springer International Publishing), 1–55.

Wiedenmann, J., Elke, C., Spindler, K. D., and Funke, W. (2000). Cracks in the β-can: fluorescent proteins from *Anemonia sulcata* (anthozoa, actinaria). *Proc. Natl. Acad. Sci. U. S. A.* 97, 14091–14096. doi:10.1073/pnas.97.26.14091

Willis, B. L., Page, C. A., and Dinsdale, E. A. (2004). *Coral disease on the great barrier reef. Coral health and disease*. Berlin Heidelberg: Springer, 69–104.

Yucharoen, M. (2016). Pink pigmentation response during recovery period after coral bleaching. *dissertation/PhD Thesis*. Shizuoka (Japan): Shizuoka University. doi:10.14945/00009914

Frontiers in Physiology

Understanding how an organism's components work together to maintain a healthy state

The second most-cited physiology journal, promoting a multidisciplinary approach to the physiology of living systems - from the subcellular and molecular domains to the intact organism and its interaction with the environment.

Discover the latest Research Topics

See more →

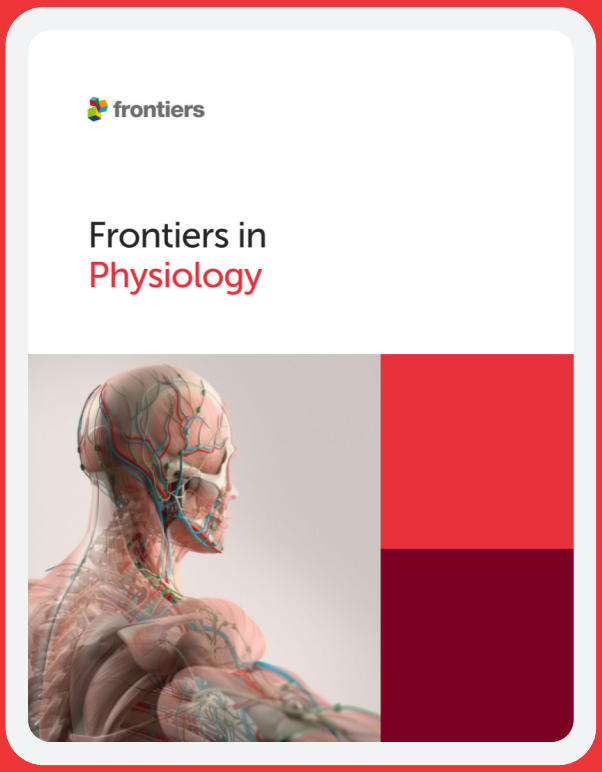

Frontiers

Avenue du Tribunal-Fédéral 34
1005 Lausanne, Switzerland
frontiersin.org

Contact us

+41 (0)21 510 17 00
frontiersin.org/about/contact